INFLUENCE OF BUS RAPID TRANSIT (BRT) ON MIXED-TRAFFIC CAPACITY UTILIZATION AND ITS TIME HEADWAY IMPLICATIONS

By

Abayomi Emmanuel MODUPE

Student No: 219091761

Submitted in fulfillment of the academic requirements for the degree of

Doctor of Philosophy in Civil Engineering

College of Agriculture, Engineering, and Science,

The University of KwaZulu-Natal,

Howard College Campus, Durban

MARCH 2024

Supervisor: Prof. Johnnie Ben-Edigbe

PREFACE

The research contained in this thesis was completed by the candidate whilst based in the Discipline of Civil Engineering, School of the College of Agriculture, Engineering and Science, University of KwaZulu-Natal, Howard Campus South Africa.

The contents of this work have never been submitted in any form to another University and, except where the work of others is acknowledged in the text, the results reported are due to investigations by the candidate.

Signed: Prof. Johnnie Ben-Edigbe
Date: March 4, 2024.

DECLARATION 1: PLAGIARISM

I, **Mr. Abayomi Emmanuel MODUPE** declare as follows that:

(i) the research reported in this dissertation, except where otherwise indicated or acknowledged, is my original work.

(ii) this dissertation has not been submitted in full or in part for any degree or examination to any other university.

(iii) this dissertation does not contain other persons' data, pictures, graphs, or other information unless specifically acknowledged as being sourced from other persons.

(iv) this dissertation does not contain other persons' writing unless specifically acknowledged as being sourced from other researchers. Where other written sources have been quoted, then:

a) their words have been re-written, but the general information attributed to them has been referenced.

b) where their exact words have been used, their writing has been placed inside quotation marks, and referenced.

(v) where I have used material for which publications followed, I have indicated in detail my role in the work.

(vi) this dissertation is primarily a collection of material, prepared by me, published as journal articles, or presented as a poster and oral presentations at conferences. In some cases, additional material has been included.

(vii) this dissertation does not contain text, graphics, or tables copied and pasted from the internet, unless specifically acknowledged, and the source is detailed in the dissertation and in the references sections.

Signed by Candidate: Abayomi Emmanuel MODUPE
Date: March 1, 2024.

DECLARATION 2: PUBLICATIONS AND TRAINING

Details of publications that form part and/or include research presented in this thesis.

Journal Publications

1. Modupe, A., & Ben-Edigbe, J. (2023). Modelling Mixed Traffic Time Headway Distribution Induced by Bus Rapid Transit (BRT) in Cape Town, South Africa. *The Open Transportation Journal*, *17*(1).

2. Modupe, A. E., and Ben-Edigbe, J. (2023). Comparative Analysis of BRT Roadway Level of Service (LOS) and Level of Capacity Utilization (LCU). ICE – Transport Journal. (Manuscript Submitted for Publication).

3. Modupe, A. E., and Ben-Edigbe, J. (2023). Assessment of BRT dedicated lane road capacity utilization and service quality equilibrium. Promet-Traffic and Transportation. (Abstract/Indexed in SCI and Scopus; impact factor 0.43, DHET Accredited Journal, (Manuscript Submitted for Publication).

4. Modupe, A. E., and Ben-Edigbe, J. (2023). Influence of BRT on mixed traffic functional service quality differentials. Transportation Planning and Technology. (Abstract/Indexed in SCI and Scopus; impact factor 1.845, DHET Accredited Journal, Manuscript Submitted for Publication).

Conference Papers

5. Modupe, A. E., & Ben-Edigbe, J. (2022). Influence of Bus Rapid Transit (BRT) on Anomalous Road Capacity Utilization. In ASCE *International Conference on Transportation and Development 2022* (pp. 88-97). https://doi.org/10.1061/9780784484371.009.

6. Modupe A. E., & Ben-Edigbe J. (2023). Extent of Bus Rapid Transit (BRT) Travel Time Differentials Caused by Mixed Traffic Flow in Cape Town, South Africa. Being Paper Accepted for Presentation at the Canadian Society for Civil Engineering (CSCE) Annual Conference (Changing Tides and Ingenuity), Moncton, Canada, May 24 – 27, 2023 (Presented by Modupe, A. E.).

The study is an analysis of data collected at four different sites or road segments along route R27, situated on major BRT trunk route **T02 (Atlantis – Table View – Civic Centre)**, in Cape

Town, South Africa. It precisely involved the examination of three traffic flow scenarios in the vicinity of BRT viz: BRT dedicated lane scenario, 'without BRT' scenario, and 'with BRT' scenario, under steady flow conditions. The 'with BRT' scenario was created by adding BRT dedicated lane hourly traffic flows to the 'without BRT hourly traffic flows with PCEs applied and subsequently analyzing it to determine the influence of BRT on mixed traffic capacity utilization and its time headway implications. From the study, the Influence of Bus Rapid Transit (BRT) on anomalous road capacity utilization under mixed traffic conditions was investigated in conference paper 1. In conference paper 2, the extent of BRT travel time differentials caused by mixed traffic flow was evaluated. The stochastic nature of the time headway of traffic flows induced by BRT on the adjoining lanes was investigated in journal paper 1 by modelling the inherent time headway distribution of the 'without BRT' scenario. The best-fitted distribution provided a guide towards determining the safest minimum mixed traffic time headway that would maximize capacity utilization, while journal paper 2 presented a comparative analysis of BRT Roadway Level of Service (LOS) and Level of Capacity Utilization (LCU). In journal paper 3, an assessment of BRT dedicated lane road capacity utilization and service quality equilibrium was carried out, while journal paper 4 investigates the influence of BRT on mixed traffic functional service quality differentials.

Training

(i) Invitation to attend the 32nd Annual International Course on Transportation Planning and Traffic safety (Road Safety, Road Safety Audit, Vehicle Safety Technology, Pre-Hospital care, and Trauma) at the Indian Institute of Technology), New Delhi, India, from 5th – 19th December 2022.

(ii) Volvo Research and Education Foundation (VREF) - Study Visit Grants (SVG) 2022. Visiting Research Scholar to Lagos State University (LASU), Ojo, Lagos State Nigeria, 1st – 30th November 2022.

[redacted]

Signed by Candidate: Abayomi Emmanuel MODUPE
Date: March 1, 2024.

As the candidate's supervisor, I agree to the submission of this thesis.

[redacted]

Signed by Supervisor: Prof. Johnnie Ben-Edigbe
Date: March 4, 2024.

DEDICATION

This Thesis is dedicated firstly to:

God Almighty, the Alpha and the Omega who made this dream a reality.

and secondly,

My beloved family,

Mrs. Oyeyemi Christiana Modupe (Wife)

David Ayodeji Modupe (First Son)

Daniel Ojurereoluwa Modupe (Second Son)

ACKNOWLEDGEMENTS

Firstly, I thank the Almighty God, the Alpha, and Omega, my creator who kept me alive and in good health, provided for my financial needs when I had nothing, and favoured me all through the course of my research.

I immensely appreciate Prof. Johnnie Ben-Edigbe, my PhD supervisor, for his mentorship throughout my study. I freely drew from his deep well of knowledge and intelligence, and benefited greatly from his vast experience, both in academics and research. I am grateful to God I finally got the opportunity to study under his supervision. Sir, I appreciate your willingness to share knowledge at all times, as well as your generosity, sage counsel, and fatherly encouragement while the research was being conducted., in you I have found a life coach and permanent academic mentor, thanks, coach.

I acknowledge my phenomenal and beautiful wife (Oyeyemi), as amazing children (David and Daniel) for their sacrifice, prayers, fortitude, perseverance, and motivation throughout the course of my studies. I cannot forget what you all went through for my sake, having to temporarily leave the serene and comfortable environment of Landmark University Nigeria, for an uncomfortable one. Thank you for believing in me, I love you all eternally.

I appreciate the efforts of the Academic Leader (Prof. Mostafa Mohamed Hassan), Prof. Dillip Kmar Das, Dr. Joy Adu, Dr. Frank Aneke, Mrs. Ooma Chetty, Mr. Logan Govender, Mr. Ishan, and all the other faculties and staff of the Civil Engineering Department of the University of KwaZulu-Natal in promoting environmental friendliness. Special appreciation to Dr. Benedict Olalusi, for your financial support when the going was tough, you are one of a kind, and may God bless you richly.

To my parents, Rev. David Olawale Modupe and Evangelist (Mrs.) Ebunola Modupe, you are immensely appreciated for your constant financial support for my family's upkeep and prayers, to keep me focused on my studies and not worry about their survival and wellbeing, God bless you richly. I appreciate all my siblings for their moral and financial support to me and my family during my study. Special appreciation goes to my Head of Department, Department of Civil Engineering of Landmark University, Nigeria, Prof. A. J. Gana, thank you, sir, for being a father, and for your immense support for my family, while I was away, I am grateful for your kindness sir.

I want to appreciate one of my graduated senior colleagues from the same supervisor, my big brother, and my friend, Engr. Dr. S. O. Ibijola. You brought all my application documents to South Africa and processed my admission for me ahead. Thank you for initiating the plan sir and for your motivating spirit, God bless your kind heart forever. Special appreciation also goes to my academic mentor from TUT, Pretoria, Prof. W. K. Kupolati, thank you for your counsel, support, and encouragement when I needed them the most.

I want to appreciate Prof. B. F. Bakare and his wife Mrs. Mercy Bakare, thank you so much for your support even before I left Nigeria for South Africa. Thank you for initially signing an undertaking to be my guardian during my visa processing. Special appreciation goes to my graduated senior colleagues and friends from the same supervisor, Dr. Mrs. Yemisi Makinde, and Dr. Janet Oyaro, thank you for all the research experiences you shared, they were all helpful. Special appreciation also goes to Dr. and Mrs. Adegun, for always checking on me to make sure I was alright in spirit, soul, and body and wasn't stranded. Special thanks to you my Zulu friend and course mate, Mr. Sibusiso Ndebele from Petroza, thank you brother for all the time you sacrificed during the survey. You even put a roof over my head free of charge, I am immensely grateful.

The University of KwaZulu-Natal is highly appreciated for its three-year fee-remission scholarship, travel awards for conferences and fieldwork, funding for publications, and other benefits enjoyed during the study period. Many thanks for making it available to pursue my degree without worrying about finances.

I appreciate my Nigerian and foreign housemates (Tosin, Emmanuel, Wole, Grace, Nathan, Chege, Chemweno, Yinka, Folarin, Regina, Dr. Rilwan, and Lone), thanks for making my stay at Jukumu Residence fun filled. I appreciate my Departmental colleagues and friends (Adekunle, Abayomi, Chukwuemeka, Daniel, and Temesgen), thank you guys for all the academic assistance rendered during my study period. How can I forget my co-labourers and friends in God's vineyard, the Choir members of Winners Chapel International Durban, thank you all for your prayers. Special thanks to Pastor and Dcns Samuel David, Pastor and Dcns Femi Adeoye, Pastor and Dcns Tony Obute, Prof. and Dcns. Olatunji, thank you all for all your prayers. Pastor and Dcns Samuel Ilupeju and Izzy Aigbokhaebho, you are all just ministering angels packaged before I arrived in South Africa, thank you so much for all God used you to do for me throughout my study period. To everyone who's name I haven't mentioned, your contributions and support are immensely appreciated.

ABSTRACT

Bus Rapid Transit (BRT) systems are sustainable mobility interventions that provide commuters with fast, safe, and efficient mobility. Unfortunately, they have been characterized by fundamental traffic flow parameter anomalies, especially speed changes, with attendant consequences on capacity utilization, capacity differentials, and time headway implications. Consequently, this study was carried out to determine the influence of Bus Rapid Transit (BRT) on mixed traffic capacity utilization and implications for time headways. The overarching objective was to develop a capacity utilization criteria table for assessing roadway performance and determining the Level of Capacity Utilization (LCU) with and without the influence of BRT. Criteria tables serve as standards by which the performance of a roadways in terms of capacity utilization is decided. Traffic data at peak and off-peak periods were collected for a '*with and without' BRT* impact study at four selected road segments along route R27, located on BRT major trunk route T02 which connects Atlantis, Table View, and Sunset City. Data were logged for 12 weeks continuously using an Automatic Traffic Counter (ATC). The study assumed that density was a function of speed and flow and hence was not directly impacted by BRT infrastructure based on the conditions at the time of the survey. It suggests that capacity utilization is triggered by variations in speed, and the attendant variations in density, capacity, and time headways were used to estimate capacity utilization rates and determine the LCU. Traffic data on speed, vehicle classes, and volumes were collected, and the results were analyzed. The collected traffic volumes were converted to flow using the South African passenger car equivalent (PCE) values. The results showed speed reductions with attendant differentials in other parameters such as capacity, density, travel time, and time headways. From the developed criteria table, the estimated capacity utilization rates for the BRT dedicated lanes scenario showed poor LCU at E (9% and 36%) across the four sites SS001 to SS004, under steady flow conditions. The capacity utilization rates of the mixed traffic 'without BRT' scenario showed fair utilization within the range of 37% and 79%, with average LCU at C across the four sites, whilst the capacity utilization rates of mixed traffic 'with BRT' scenario also showed fair utilization (between 40% and 75%), with average LCU C. The time headway implications induced by the capacity utilization and its differentials were also modelled, and the empirical time headway data were fitted to continuous probability distribution models. The Burr continuous probability distribution model, which is known for its compatibility, flexibility and appropriateness in modelling headway data under different traffic conditions, provided the best fit, having emerged with the largest Log-likelihood, and the smallest Akaike Information Criterion (AIC) values at 95% confidence and 0.05

significance levels across the four sites. At sites SS002, SS003, and SS004, it ranked first with the lowest AIC values of 3623.33, 4002.73, 3857.44, and corresponding largest LLH values of -1807.64, -1997.35, and -1924.70, respectively, while the Gaussian distribution performed best at site SS001, with the lowest AIC value of 4356.01 and largest LLH value of -2176.00, closely followed by the Generalized Extreme Value (GEV) distribution with the lowest AIC and largest LLH values of 4368.09 and -2181.03, respectively at off-peak traffic period. The Burr distribution however performed second best at peak traffic with the lowest AIC and largest LLH values of 4352.49 and -2172.23. The P-values, which ranged between 0.65 and 0.81 across the four sites showed the likelihood of the occurrence of the data sets under the null hypothesis. Hence the null hypothesis was accepted. In conclusion, the study showed that mixed traffic operations 'with BRT' and its associated minimized time headways, could significantly enhance capacity utilization. In view of the mixed traffic scenarios considered with and without BRT, it is hereby recommended for future research consider analysing traffic capacity through the development and application of microscopic fundamental diagrams, and a simulation of the time headway distribution of the mixed traffic scenario with BRT should also be considered. In traffic engineering practice, the curbside and mixed traffic designs are therefore recommended for implementation in future BRT infrastructure as the way forward for the South African BRT system for enhanced capacity utilization and sustainable mobility.

TABLE OF CONTENTS

LIST OF FIGURES

Figure No. **Title** **Page**

LIST OF TABLES

Table No. **Title** **Page**

LIST OF ABBREVIATIONS USED

A-D	Anderson-Darling
ADT	Average/Annual Daily Traffic
AIC	Akaike Information Criterion
ARX	Modification of AustRoads94
ATC	Automatic Traffic Counter
BIC	Bayesian Information Criterion
BRT	Bus Rapid Transit
CDF	Cumulative Density Function
C-S	Chi-Squared
DOT	Department of Transport
EDM	Empirical Distribution Method
F-D	Flow-Density
FDM	Fundamental Diagram Method
FQOS	Functional Quality of Service
GEV	Generalized Extreme Value
HCM	Highway Capacity Manual
HCMTRB	Transportation Research Board's Highway Capacity Manual
HQIC	Hannan Quinn Information Criterion
HV	Heavy vehicle
ICU	Intersection Capacity Utilization
IRT	Integrated Rapid Transport
K-S	Kolmogorov-Smirnoff
LCU	Level of Capacity Utilization
LLH	Log likelihood
LOS	Level of Service
LV	Light vehicle
MLE	Maximum Likelihood Estimation
MV	Medium vehicle
N	National
NDOT	National Department of Transport
NGC	Northern Growth Corridor

P	Provincial
PDF	Probability Density Function
PLM	Product Limit Method
P-P	Probability Plot
PC	Passenger car
PCE	Passenger car equivalent
PCU	Passenger car unit
QOS	Quality of Service
R^2	Coefficient of determination
RCU	Roadway Capacity Utilization
RSA	Republic of South Africa
RSU	Roadside Unit
R27	Regional 27
SANRAL	South African National Roads Agency Limited
S-D	Speed-Density
SQ	Service Quality
SS	Study site
SIC	Schwarz Information Criterion
SSD	Stopping Sight Distance
TCQSM	Transit Capacity and Quality of Service Manual
TRB	Transport Research Board
US-BPR	United State Bureau of Public Road
WCDTPW	Western Cape Department of Transport and Public Works

LIST OF SYMBOLS USED & UNITS

Q	capacity / maximum flow	pce/hr
k_{crt}	critical density	pce/km
u_Q	speed at capacity	km/hr
k_Q	density at capacity	pce/km
T_h	Tip-to-tip Headway	sec
u_f	free-flow speed	km/hr
%	percentage	
u	speed	km/hr
X^2	Chi-Squared	
h	headway	sec
t_f	travel time at free-flow speed	sec
$\propto$	ratio of free flow to speed at capacity	
μ	abrupt drop of curve from the free-flow speed	
v/Q	volume – capacity ratio	
x	degree of saturation	
S	spacing	km/veh
Δ	differential	
Q_u	capacity utilization	
k_j	jam density	pce/km
q_p	prevailing flow	pce/hr
Q_1	capacity ‘with BRT’	pce/hr
Q_2	capacity ‘without BRT’	pce/hr
Q_3	BRT dedicated lane capacity	pce/hr
k_1	density at capacity ‘with BRT’ influence	pce/km
k_2	density at capacity ‘without BRT’ influence	pce/km
k_{31}	density at capacity ‘with BRT’ influence	pce/km
k_{32}	density at capacity ‘without BRT’ influence	pce/km
d	distance	km
k_τ	density at constrained region	pce/km

CHAPTER 1

INTRODUCTION

1.1 Overview

Bus Rapid Transit (BRT) is a mass transit system that transports large volumes of commuters along a transit corridor and offers a bus service that is swifter, more efficient, appealing, and boosts transit usage than a regular bus line (Wirasinghe *et al*., 2013). According to the definition by (Levinson, Zimmerman, Clinger, Bast, *et al*., 2003), "It is a flexible, rubber-tired kind of rapid transit that incorporates cars, BRT stations, transit services, dedicated lanes, and information technologies to create an integrated system, which can be strongly identified". All over the World, BRT systems have been reputably identified as a cost-effective alternative, even more than investments in urban rail transportation (Scorcia & Munoz-Raskin, 2019). Moreover, BRT systems have been introduced and funded in most developed countries of the world, and they have on the one hand resulted in significantly reduced travel times and improved travel speeds on the BRT lanes. On the other hand, it frequently causes abnormalities in other traffic stream characteristics such as capacity, density, time headways and reduced speed on the adjoining lanes, with consequential increase in travel time. (Chengula & Kombe, 2017).

The advent of BRT systems in South Africa has spurred increased demand for public transit ridership and provided swift mobility for commuters in all the provinces they are located and constructed (Adewumi & Allopi, 2014b). The Rea Vaya BRT system (phase 1) in Johannesburg, South Africa was the first to be established in the country in 2009, followed by the MyCiTi BRT system in Cape Town which was established in 2012 (Adewumi & Allopi, 2014a; Wirasinghe *et al*., 2013). Traffic operations on roadway segments with or without BRT are characterized by stream flows similar to the blood flow in the veins and arteries of the human body (Vilakazi & Govender, 2014). The stream flows are further characterized by speed, volume, density, and time headways which are fundamental traffic flow parameters that define the fundamental diagram method of capacity analysis and performance evaluation of a roadway (Alhassan *et al*., 2012a).

Based on the prevalent traffic conditions, these parameters are employed to evaluate the average capacity of the roadway and the quality of service delivery using travel time as the perception variable from the users' standpoint (Alhassan *et al*., 2012b; Ben-Edigbe &

Ferguson, 2005). However, on some roadway segments with BRT lanes, BRT buses are assigned to transit on dedicated or separate right-of-way lanes at the median section, thus affecting the heterogeneous vehicular traffic flows on adjoining lanes with respect to the capacity utilization and attendant time headways at large. The type of mixed traffic flow which is the focus of this study is that which involves a mix of BRT buses (single or articulated), and other vehicles of different classes and characteristics together in a stream. This can be demonstrated by removing the lane separator between the BRT lanes and adjoining lanes, thereby coalescing the two traffic flows.

In terms of the characteristics of other vehicles, mixed traffic refers to cars that have many different physical and performance traits. Among these vehicles are cars, buses, lorries, auto-rickshaws (three-wheelers), motorized two-wheelers, and different non-powered ones including bicycles, and human- and animal-powered carts. Because these vehicles have a shared right of way, they have several distinguishing characteristics that are not present in homogeneous traffic flows. These characteristics include variations in the driving styles of the various types of vehicles and their effects on the flow of traffic, in addition to the most conspicuous weak lane-discipline conduct. Due to the peculiarities mentioned above, the theory of traffic flow created for homogeneous traffic cannot be applied to mixed traffic settings without considerable changes. However, much of the latter's present theory and models are based on principles that were developed primarily for homogeneous traffic (Mallikarjuna, 2007). There have recently been doubts raised about the applicability of these ideas, and several initiatives have been made to put forth fresh or modified concepts that are more suitable for mixed traffic circumstances. (Khan & Maini, 1999) made the most recent attempt, however, their study focused mostly on macroscopic flow correlations and micro-simulation models (Verma, 2016). Since then, there has been significant progress in our understanding of mixed traffic dynamics. Understanding the characteristics of each vehicle type and how they behave in the traffic stream is crucial for studying heterogeneous or mixed traffic (Patel & Joshi, 2012), hence a unique vehicle type that is the focus of this study is BRT.

1.2 Background to the Research Problem

Bus Rapid Transit (BRT) mixed traffic operations have been shown in previous studies by (Chen *et al*., 2015; HCM, 2010; Mohan & Ramadurai, 2013; Wirasinghe *et al*., 2013), to reduce travel speed and time headways, increase capacity, density, and travel time, among other influences or consequences. Considering these, it can be argued that these anomalous capacity utilization and time headway differentials, can result from traffic flows in the presence

of BRT. *Capacity Utilization is the ratio of operating traffic flowrate and roadway capacity. It is a quantitative measure of road space used by traffic flow.* According to (Oyaro & Ben-Edigbe, 2020; TCQSM, 2013) and (Alhassan *et al*., 2012a), roadway capacity is the maximum number of transit vehicles, commuters, or both, expected to pass a specific point or section of a roadway in a specific amount of time (typically one hour), given the current roadway, ambient, environmental, control, and traffic conditions. This definition shows that capacity is influenced by many variables or factors (Oyaro & Ben-Edigbe, 2020), and is valid for the focus of this research. Other factors that affect traffic flow are: rainfall, both on road links (Alhassan & Ben-Edigbe, 2010, 2012c) and at roundabouts, (Ben-Edigbe & Ibijola, 2020), on-street parking, on/off ramps, work zone activities, pavement distress (Ben-Edigbe & Ferguson, 2005), heavy trucks, road humps (Ben-Edigbe & Mashros, 2012), as well as BRT dedicated lanes along road segments.

Furthermore, a road's capacity per lane is specified during design; as a result, the total capacity of the roadway may be calculated from the total number of lanes. For example, if the capacity of a two-lane road must be evaluated, and a lane's capacity is 3000veh/hr/lane, 3000 is multiplied by two to get the capacity of the entire route. Due to the uniformity in segment length and breadth, regardless of whether there is BRT or not, capacity estimates are projected to be equal on all lanes. Most BRT-operating cities across the globe did not build their roadways with the intention of introducing BRT in their minds from the start, thus adding BRT lanes means superimposing BRT there. In other words, one lane is removed and dedicated to BRT, reducing capacity and its utilization, meaning that capacity has not been fully utilized or optimized. For instance, in South Africa, in the year 2010, the Rea Vaya and MyCiTi BRT systems were designed and constructed only for the fast-approaching World cup at the time, hence the Curitiba median configuration design was just adopted without any plan or assessment of its shortfalls with respect to capacity utilization, safe time headways and speed, accessibility and by extension, the functional quality of service.

Service providers have tried to address this issue by introducing articulated buses, but given the geometry of the roadway segment, this will only increase passenger capacity and not roadway capacity. According to certain arguments, BRT can carry more passengers per lane than heterogeneous traffic. Although they are not intended for persons per lane or person capacity, roadways are constructed for mixed vehicular traffic volume. In other words, it can be argued that the removal of 200 passengers for example from a roadway by BRT, does not necessarily mean that 200 cars have been taken off the same roadway, as it cannot be

ascertained whether all the 200 passengers are private cars. Given the aforementioned setbacks, it has therefore become expedient to investigate the impact of BRT on mixed-traffic capacity utilization and time headway implications, as well as the quality of service (QOS), bearing in mind that the concept of service quality (SQ) on roadways refers to the qualitative appraisal of how well they deliver good operational performance that conforms with the stipulations in their geometric and structural designs (Mashros & Ben-Edigbe, 2014). Given the foregoing, the study described in this thesis was intended to fill the gap in research on the current BRT infrastructure's dedicated lane influence on anomalous mixed traffic capacity utilization and the time headway implications. It is discussed in seven chapters and each chapter is discussed in a way to address the problems spelled out by the topic. This chapter, therefore, has been divided into six sections. Section 1.2 discusses the study's aim and objectives. The method of study is discussed in section 1.3. The significance of the study is discussed in section 1.4, while the organization of the thesis is presented in section 1.5.

1.3 Aim and Objectives of the Study

1.3.1 Aim

The study investigated the influence of Bus Rapid Transit (BRT) on road capacity utilization and its time headway implications.

1.3.1 Objectives

The objectives were to:

i. develop a level of capacity utilization (LCU) criteria table and use it to assess road capacity utilization under different traffic flow scenarios.
ii. estimate capacity utilization of BRT dedicated lane and determine the level of capacity utilization.
iii. estimate capacity utilization of mixed traffic without BRT influence and determine the level of capacity utilization.
iv. estimate capacity utilization of mixed traffic with BRT influence and determine the level of capacity utilization.
v. compare the capacity utilization outcomes in sections ii, iii, and iv.
vi. model the mixed traffic without BRT time headway distribution, and
vii. determine the best-fitted continuous probability distribution model for capacity utilization.

The study is based on the following hypotheses:

Hypothesis 1 (Null Hypothesis):

- The presence of a BRT dedicated lane on a roadway segment causes anomalous lane capacity utilization, with attendant time headway variabilities.

Hypothesis 2 (Alternative Hypothesis):

- The presence of a BRT dedicated lane on a roadway segment does not cause anomalous lane capacity utilization, with no significant time headway variabilities.

Hypothesis 3:

If hypothesis 1 exists, the associated time headway distribution is fitted to probability distribution models and its compatibility with the models is rejected if ($P - value < \alpha$) or accepted if ($P - value > \alpha$). Additionally, the distribution which gives the smallest AIC, SIC, and HQIC values, as well as the largest log-likelihood value is considered the best-fitted model (Das & Maurya, 2018, 2020). The information criterion that determines the overall best-performing distribution is the AIC.

1.4 Method of the Study

The investigation was conducted using both empirical and analytical methods. The empirical approach which refers to a 'with and without BRT' impact assessment was employed because primary and secondary data were obtained. The primary data were collected through observations and field sample surveys on the selected BRT sites to elicit traffic information such as speed, headways, traffic volume, gap, etc. The secondary data was sourced from the Western Cape Department of Transport and Public Works (WCDTPW). Traffic data parameters obtained from the survey were used to calibrate models to analyze the influence of the incorporation of BRT lanes on mixed traffic capacity utilization 'with or without' BRT Different methods exist for estimating the capacity of a roadway section, estimation with headways, estimation with traffic volumes and speeds, and estimation with the fundamental diagram of traffic flow. Two main groups can be distinguished as follows: in the first group, capacity is measured directly from the roadway where the bottleneck is frequently reached. In the second group, road capacity is estimated by extrapolating free-flow observations. Investigation into the acceptability of passenger car equivalent values was done, and where necessary, values were changed. The main criteria for site selection were the presence of BRT dedicated lanes on both sides of the carriageway with median configuration and traffic moving in opposite directions, flat terrain or straight BRT segments void of circular and reverse curves and with sufficient distance from the influence of intersections, in compliance with the principle of Safe Stopping Distance (SSD). The site selection also required a road section or

segment with three existing lanes, with the median lane taken away or dedicated to BRT. The automatic traffic counter installed on the roadway segments recorded all classes of vehicles in the traffic stream.

By way of exploring a variety of alternative methodologies to be compared with the 'with and without' BRT empirical approach, the study attempted to determine the influence of BRT on mixed traffic capacity utilization and time headway implications using a 'before and after' BRT approach. To apply the 'before and after' BRT approach, and due to the pandemic in the year 2020, the study identified the need for pre-BRT 2009, and pre-lockdown 2019 (after BRT) traffic volume data. Consequently, two analytical steps were distinguished and applied as follows: in the first step, traffic data for the post-lockdown year 2021 (after BRT), was collected directly from the roadway under steady flow conditions and analyzed. In the second step, the post-lockdown 2021 traffic data was extrapolated or compounded backward to obtain the pre-BRT 2009 and pre-lockdown year 2019 (after BRT) traffic volumes.

Due to similarities in terminologies, the 'before and after' BRT approach must not be misconstrued with the 'with and without' BRT empirical approach. In the 'with and without' Bus Rapid Transit (BRT) approach, the contribution of BRT to roadway capacity utilization was particularly emphasized. The principal aim of the investigation is to look into the question of capacity utilization in the presence of Bus Rapid Transit and establish whether a strong relationship exists between the variables.

1.5 Research Scope and Limitations

The first part of this study, herewith referred to as part A, is centered on obtaining empirical data of mixed traffic characteristics such as flow, speed, density, and time headways on a multilane roadway adjoining a BRT dedicated lane, with the view of determining its capacity utilization in the presence of BRT. The R27, a BRT corridor located along the major trunk route T02 (Atlantis – Table View – Civic Centre) in Cape Town, South Africa fits this geometric characteristics' description. The traffic data collected is restricted to the uninterrupted flow on selected road segments along the main study site. The main study site is selected based on appropriate site location and selection criteria that would ensure that the data collected is unbiased and void of errors. Furthermore, the study is limited to the exploration of roadway capacity utilization with respect to vehicles moving on it and their relationship with the geometric features of the roadway, and not person or passenger capacity. The second part of this study focused on modelling the empirical time headway data collected at each site in part A, by fitting them to continuous probability distribution models and

analyzing the outcomes. The study is generally limited by manpower and funding. Limited funding, in addition to satisfying the site location and selection criteria, compelled the researcher to finally pitch a research tent in Cape Town, against the initial intention of investigating the Rea Vaya and Areyeng BRT systems in Johannesburg and Pretoria respectively. This research was also limited by the non-availability of pre-built design traffic volumes before the advent of BRT, intended to serve as traffic information for the 'without' BRT survey period. Besides, the pandemic and lockdown prevented the researcher from launching into the field early enough. Consequently, no traffic data was collected during the pandemic period in the year 2020. However, traffic data for the pre-BRT 2009 and pre-lockdown 2019 periods were determined by backward extrapolation using identified traffic growth rates from the literature. Even though the traffic loggers were secured at the sites, frequent visits were made to the sites to avoid any theft and to ascertain that the ATC machines were actively logging data.

1.6 Significance of the Study

Firstly, vital to the socio-economic development of the South African population is the provision of urban transport infrastructure as well as a sustainable and integrated BRT system that is affordable, accessible, safe, and with optimum traffic capacity utilization and good quality of service delivery especially a reduced travel time (Aropet, 2017). According to (Mashros & Ben-Edigbe, 2014), good transportation systems are anticipated to produce an operational performance that is consistent with their design specifications. Route R27 in Cape Town South Africa is a very important road in Cape Town as it connects the north at Atlantis to the south at Cape Town Civic centre.

Secondly, according to (Stone, 2009), on the regional route R27 in Cape town South Africa, the main justification adduced for the adoption or selection of a dedicated median bus lane configuration with central BRT stations over the curb side design was that the latter model would not be practicable. He further argued that the whole point of BRT is to have a dedicated bus lane that enables speedy transportation and that the kerbside design would cause commuters to stop or park in the lane where the BRT is supposed to drive, disrupting the smooth operation of the BRT vehicle, and forcing it into the middle or right lane, which contradicts the objective of a speedy and easy-to-use public transportation system in the end. This justification, although true in terms of its attendant travel time savings is however not strong enough from the standpoint of the importance of the route R27, and the need for commuter ridership attraction. In other words, the commercial importance of route R27

requires that more people be moved from their origin to destinations of their choice within the corridor, hence the need to fully utilize or maximize capacity.

The road system is a capital-intensive investment, requiring a thorough schematic framework and structured maintenance programme. In passing, although the level of service is a common measure of road traffic effectiveness, however, the tests of road investment justification would require roadway capacity utilization. Nevertheless, given the homogeneity in segment length and width, road capacity estimates are anticipated to be the same on all lanes (Ben-Edigbe, 2016). Most cities with BRT schemes did not design their roads with BRT in mind when they were being built, thus adding BRT lanes meant imposing BRT there. To put it another way, one lane is removed and set aside for BRT, which has an impact on the macroscopic traffic stream characteristics, capacity, and ultimately, capacity utilization. As indicated, assuming uniform length and width and regardless of whether there is BRT, a roadway's capacities per lane should be similar. If this is not so, then road capacity has yet to be fully utilized. Therefore, the findings from this study are expected to provide more insight into the merits of adopting a BRT mixed traffic infrastructure design, which could attract ridership and increase capacity utilization of the BRT corridor.

Thirdly, previous literature by (Alhassan *et al*., 2012b; Ben-Edigbe, 2003; Ben-Edigbe, 2010; Ben-Edigbe *et al*., 2013; Ben-Edigbe & Ferguson, 2005; Ben-Edigbe & Mashros, 2012) had evaluated capacity and its attendant differentials, including other traffic characteristics anomalies. These studies looked at the effect of traffic flow inhibitors such as pavement distress, road humps, rainfall (Oyaro & Ben-Edigbe, 2020), on-street parking, and many more to mention a few. This study, therefore, evaluates the underutilization effect of introducing BRT dedicated lanes on mixed traffic characteristics and implications on time headway distribution. The overarching objective of its findings is to maximize capacity and ensure optimum traffic management through the assessment of its attendant time headway distribution.

Fourthly, the time headway distribution on the adjoining lanes, occasioned by the presence of BRT dedicated lanes was modelled by way of fitting continuous probability distribution functions to data and determining which distribution provided the best fit. The purpose of this was to provide an in-depth understanding of the induced heterogeneous traffic flow and behaviour of motorists as well as determine the safest headway for commuters and pedestrians.

Finally, this study is significant because the evaluation of the influence of BRT on mixed traffic capacity utilization and its time headway implications through the fundamental diagram approach and time headway distribution modelling is a relatively new undertaking in South Africa. Since the implementation of BRT in South Africa, previous research works of literature have only focused on the effectiveness of the BRT buses and the justification for the adoption of the median BRT configuration.

1.7 Organization of Thesis

This section shows how the thesis is organized into chapters. Each chapter is organized to address concerns about the topic of the research. Figures, tables, and equations are presented in a logical order and designated by the chapter in which they appear. Figure 3.3, for example, is the third figure in Chapter 3, equation 2.6 is the sixth equation in Chapter 2, and table 4.4 is the fourth table in Chapter 4. The remainder of this thesis is in six chapters as follows:

Chapter 2: Review of previous literature on roads and traffic characteristics in South Africa, BRT in Cape Town, South Africa, and road capacity utilization concepts. The review provided a background on the hypothesis underpinning the concept of capacity utilization and time headway.

Chapter 3: The research methodology is presented. It outlines the design of the study, the location of the sites, and the criteria for selection.

Chapter 4: Results of empirical surveys are presented and discussed for each study site, including site figures and photos.

Chapter 5: Effects of BRT on mixed traffic capacity utilization are discussed.

Chapter 6: BRT implications for time headway are presented, and continuous probability distribution models were fitted to the time headway data.

Chapter 7: The conclusions drawn, and the way forward are presented.

CHAPTER 2

LITERATURE REVIEW

2.1 Overview

The focus of this study is on the influence of Bus Rapid Transit (BRT) on mixed traffic capacity utilization and its implications on the time headway distributions. The objectives were established in the previous chapter. In this chapter, a review of previous literature to support arguments in the subsequent chapters is presented. As defined in the previous chapter, BRT refers to mass transit and high-capacity public transportation system that transports commuters from one location to another within a transit corridor and provides a bus service that is faster, more attractive, increases transit ridership, and more efficient than an ordinary bus line (Agarbattiwala & Bhatt, 2016; Hashem *et al*., 2016; Krüger *et al*., 2021; Wirasinghe *et al*., 2013).

By this definition, BRT is expected to attract more commuters, as well as reduce their travel time from their origin to destination by using the BRT corridor, and these two service attributes are consequently considered as benefits or merits of introducing the dedicated lane infrastructure, in line with the adopted design configuration. BRT is homogeneous on its dedicated lane and the heterogeneous vehicles on the adjoining lanes experience changes in traffic characteristics. Besides, the resulting traffic flow scenario on the adjoining lanes is characterized by bottlenecks and differentials in traffic stream characteristics such as speed, volume, density, and time headways. These differentials result in capacity disparities as well as time headway variations at reduced magnitudes, which leads to increased travel times, and anomalous capacity utilization.

In passing, the concept of service delivery in highway engineering studies involves the interaction between the road providers or operators and users or commuters, where a service is rendered by the provider and the road user either derives or loses time value from it (Devasurendra *et al*., 2020). Road users benefit from an increase in the value of time when services are delivered extremely well, which in turn affects the economy positively and boosts the daily productivity of every commuter. However, capacity utilization which is the focus of this study is *a measure of the extent to which the capacity of a roadway is being used*. It is the relationship between the maximum flowrate per lane per hour that the roadway can carry, and

the operating flowrate that the road produced under prevailing conditions. Capacity utilization rate measures the percentage of total capacity that is being achieved in a given period. It can be argued that the resulting time headway distribution is continuous, capable of aligning or fitting some existing continuous probability distributions, that can best describe its characteristics and provide the best data fit for capacity estimations. Hence, in addition to the development of a capacity utilization criteria table as stated in the objectives in chapter 1 for the evaluation of traffic flow performance, this study analyses the mixed traffic 'without BRT' time headways by fitting them to suitable continuous probability distribution models. In view of the aforementioned, the remainder of this chapter is divided into six sections. Section 2.2 describes roads and traffic characteristics in South Africa, whilst section 2.3 provides insights into Bus Rapid Transit in Cape town South Africa. Section 2.4 gives a background on roadway capacity, while section 2.5 addresses roadway capacity utilization. Section 2.6 describes the time headway concepts and continuous probability distribution models, whilst section 2.7 discusses the effect of BRT time headway distribution modelling on capacity utilization. Section 2.8 gives a summary of the chapter.

2.2 Roads and Traffic Characteristics in South Africa

Roads are components of the transportation system infrastructure that primarily support cycling, vehicular (both motorized and non-motorized), and pedestrian traffic on the ground (Kutz, 2011). According to (Lay, 2009), roads comprise segments, nodes or intersections, and junctions, each with its own set of features that might influence traffic flow rates and capacity with associated capacity utilization effects. Some geometric features of roads include lanes, walkways, carriageways, medians, shoulders, verges, and cycle paths (Lilley, 2012). The individual characteristics of these road features make vehicles more vulnerable to events like reductions in speed, delays, queues, accidents, and traffic congestion. This can happen at any time of day, regardless of the type of road or its location. In South Africa, roads are the most popularly used modes of transportation, other modes are railways, airports, water, and petroleum oil pipelines (Fedderke & Garlick, 2008; Tchanche, 2019). The majority of South Africans travel by informal minibus taxis (Vilakazi & Govender, 2014). In 2009, BRT was implemented to make public transportation more structured and secure (Gauthier & Weinstock, 2010; van Rensburg & Krygsman, 2020; Venter, 2013; Wood, 2014a, 2014b). South Africa has the tenth-longest road system in the world, according to the South African National Roads Agency Limited (SANRAL), with a total length of 750 000 kilometres. (Smith & Visser, 2001; van Rensburg & Krygsman, 2020). SANRAL currently oversees a total of 21, 403 kilometres, with 84 percent of them not tolled while only 16 percent are tolled. Municipalities oversee 51,682 kilometres, whereas provinces oversee 47,348 kilometres. The national road

infrastructure budget is anticipated to be R197 billion. Table 2.1 provides a summary of the South African road system as released by the Republic of South Africa's Department of Transport (DoT).

Table 2. 1: An overview of the South African Road Network

Authority	Paved (km)	Gravel (km)	Total
SANRAL	21 403	0	21 403
Provinces - 9	47 348	226 273	273 621
Metros - 8	51 682	14 461	66 143
Municipalities	37 691	219 223	256 914
Sub Total	158 12	459 957	618 081
Un-Proclaimed (Estimate)	-	131 919	131 919
Estimated Total	162 124	591 876	754 000

Source: South African National Roads Agency Limited (SANRAL)

In terms of road system hierarchy and ease of communication between the three major stake holders in roadway infrastructure viz engineers, road administrators, and the general public (Acai & Amadi-Echendu, 2018). South African roads are classified using three criteria into administrative, functional, and design type based on roadway traffic capacity (Pasindu *et al*., 2020). In South Africa, in terms of administrative responsibilities, the three different government levels each have road functions assigned to them. Bearing in mind that no relationship exists with the functional and design types of roads classification, the administrative strategy employed separates the South African road network into national, provincial, and local government roadways. (Atkinson, 2007; Heggie, 1995). The nation's main thoroughfares and freeways connect the largest cities therein. They account for the highest category in the South African route numbering scheme, with route numbers beginning with the letter "N." and ranging from N1 to N18. The South African National Roads Agency SOC Ltd (SANRAL) maintains the majority of the national route network, but other segments are maintained by provinces or municipalities (Mitchell, 2014). The system was largely constructed during the 1970s by South Africa's National Party government, while new roads and repairs to old segments have continued to this day. The system was designed after the transport system operated in the US for Interstate Highways, which was first adopted in the 1950s by US President Dwight D. Eisenhower and was inspired by the German Autobahn, which he observed while touring Germany during World War II (Falkner, 2012). Although the

terms "national road" and "national route" are sometimes interchanged, they have distinct meanings. National Roads are not all national highways, and only some "R" - numbered routes are recognized as such. Some road segments of the national route network are not maintained by SANRAL and are hence not National Roads. The second category of roads in the South African route-numbering scheme is provincial roads (sometimes known as major regional routes). In contrast to the letter "P" followed by a number ranging from 66 as indicated earlier for national roads, they are designated by the letter "R" followed by a number ranging from 21 to 82. They function as feeders to national routes and as trunk highways in locations where no national routes exist. Some elements of the provincial route network are maintained by the National Roads Agency (SANRAL), and parts of towns may be regular streets managed by municipal road departments (SANDoT, 2007). From gravel roads (such as the R31 between Askham and Hotazel in the Northern Cape) to freeways, provincial routes range in condition (for example the R59 between Vereeniging and Johannesburg).

In the South African route numbering scheme, regional routes (sometimes known as minor regional routes) are the third category of roads. The letter "R" is followed by a three-digit number to identify them (Falkner, 2012). They act as feeders for smaller communities, connecting them to national and provincial highways. A regional road can be anything from a gravel road (such as the R340 between Plettenberg Bay and Uniondale) to a multi-lane highway (like the R300 near Cape Town). Although most regional roads are maintained by provincial road authorities, this is not always the case; some may be under the supervision of the National Roads Agency (SANRAL) in provinces with insufficient capacity. They may also be conventional streets under the supervision of the municipal roads department in metropolitan areas. Similarly, rather than SANRAL, some national (N) highways, and motorways are under the supervision of provincial or municipal agencies (Stone, 2009). Furthermore, the roads are classified by function mainly for transportation planning purposes. The functional classification scheme used for the South African road network is illustrated in Table 2.2. This was employed in the early 1980s for the South African Rural Road Needs Study. There are two functions of roads: they allow people to move around, and they allow people to access land. These functions are, however, incompatible from the standpoint of design. Fast or consistent speeds are useful for mobility, while variable or low speeds are undesirable; low speeds are desirable for land access, while high speeds are bad.

Table 2. 2: Functional Classification of Roads in South Africa

Functional Classification	Description of Road Function or Type
1	Roads that form the principal avenues of communication between: * Major regions of the RSA and/or, * Defined or proposed metropolitan areas and/or * Major regions of the RSA and other countries which are declared National roads or extensions of these.
1a*	Roads which comply with the above, but which are not declared National roads or extensions of these.
2	Roads not being Class 1 or 1a, which form the main avenues of communication between * Importation centers** and Class 1 and 1a roads and/or *Important centers and/or of an arterial nature within a town in a rural area.
3	All other surfaced roads for which the road authorities are responsible, and which are not Class 1, 1a, 2 or 5 roads.
4	All Gravel Roads for which the road authorities are responsible, excluding class 5 roads.
5***	Special Purpose Roads: Roads that provide for some activity or function, and which are not assigned to Classes 1 to 4, e.g.: *For minerals development, *For strategic or defense purposes *For social need, or *For agricultural or other development.
NOTES:	*Class 1a roads include declared National roads that do not follow an 'N' route.
	** Important centers are centers with a population of 5000 or more.
	*** Class 5 roads may be either surfaced or gravel roads

***SOURCE**: SANRAL*

Freeways, for example, provide a high level of mobility, with access granted only at spaced interchanges to maintain the facility's high-speed, high-volume features. Local, low-speed roads that primarily give local access are the opposite. Figure 2.1 depicts the overall interdependence of functionally classed systems in serving mobility and land access. Traffic Characteristics in South Africa follow the design and dimensions of the geometric features of the country's roadways. The primary purpose of traffic management is to enable safe, comfortable, effective, and economical mobility. For traffic engineers to develop and improve mobility and the quality of transportation services, they need to fully understand the status quo of traffic patterns and accurately forecast future traffic conditions.

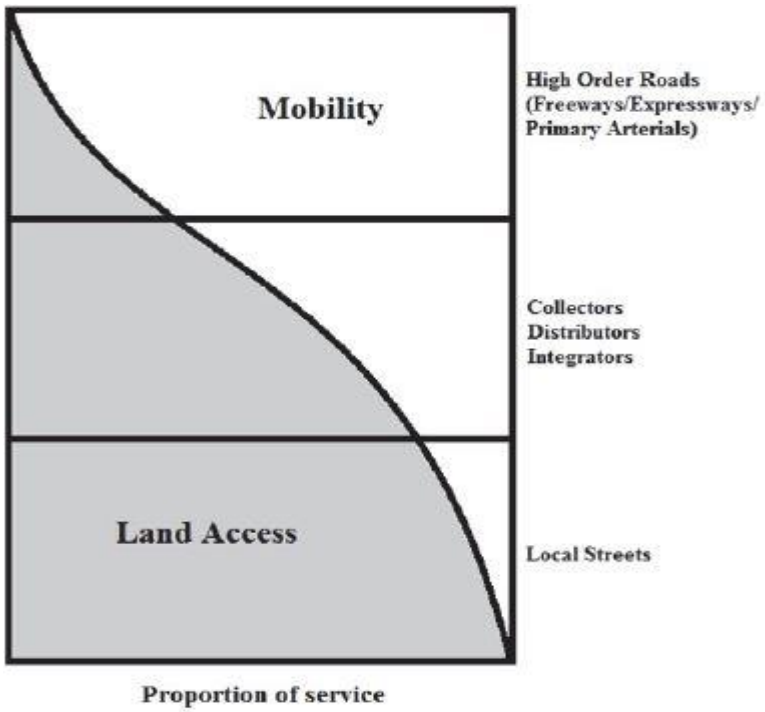

Source: (Ross & Townshend, 2018; Veramoothea *et al*., 2015)

Figure 2. 1: Relationship of Functional Road Classes

Although seasonal and daily traffic patterns differ, however, for design, the traffic engineer is expected to be aware of the magnitude of these alternations to estimate patterns of flow. The bi-directional or unidirectional distribution of traffic and how its composition changes are additional crucial elements to consider, hence, any genuine design must have a full understanding of how they all interact. At this juncture, traffic flow can be defined as the number of cars or vehicles passing through a particular point or section of roadway in each period. The Average Daily Traffic (ADT) is the flow of interest in most cases. Evaluating existing traffic conditions can be extremely complex due to the constant change in the movement patterns of people. It is this continuous variation that causes the natural patterns observed in traffic flow over time. Understanding the patterns of the movement of people is crucial for the effective quantification of the variation in traffic flow, as well as for forecasting representative traffic volumes for facility design purposes. Traffic variation patterns include a variation of traffic over a day (hourly variation), a week (daily variation), months of the year (monthly variation), and annual growth (annual variation). Vehicular traffic flows can also be estimated and given per hour, such as "hourly observed traffic volume," "thirtieth-highest hour," or "hundredth hour," which are standard design metrics. Studies of signalized junctions often utilize flows with relatively short duration, such as for five-minute periods. In rural locations, it is typical to design for the thirtieth greatest hourly flow, i.e., the flow that is

surpassed for just 29 hours of the year. This is because rural roads have very high seasonal peaks, and it is not cost-effective to keep a route free of traffic every hour of the year. Seasonal peaks are less noticeable in metropolitan settings, and for design purposes, the 100th-greatest hourly flow is regarded as a realistic flow level. It is required to know the ADT and the peaking factor to anticipate hourly flows. The parameter, β is a description of traffic flow on a certain route that is affected by factors such as the percentage and frequency of holiday traffic, the relative sizes of daily peaks, and so on. The peaking factor might range from -0,1 to -0,4. A score of -0,1 denotes the absence of seasonal peaks. In urban planning, this value of peaking factor should be employed. A rating of -0,4 denotes extremely high seasonal peaks and is typically applied to highways like the N3. Usually, a value of -0.2 is considered typical as a rule, hence the flows between the highest and 1020th highest hour can be computed using equation 2.1.

$$Q_N = 0.072ADT(N/1030)^{\beta} \quad 2.1$$

Where Q_N = two directional flows in the N-th hour of the year (veh/h), ADT = average daily traffic (veh/day), N = hour of the year, and β = peaking factor.

Flows beyond the 1030th hour can be calculated using a straight-line relationship from the 1030th flow to zero veh/hr at the 8760th or last hour of the year, albeit this is not a particularly good model. It's worth noting that the Highway Capacity Manual's peak hour factor, K, is frequently considered to be 0,15 for design purposes. The design hour is generally referred to as the 30th-highest hour of the year. Using a value of -0,2 for β and a value of 30 for N, Q_N equals 0,146 x ADT for the thirty-first highest hour, according to Equation 2.1. When designing sections or planning for the development of new infrastructures, designers need to estimate future traffic flows. For future planning, it is suggested that a 20-year design term be adopted. The flow that occurs in the design year, which is normally twenty years away, is the 30th or 100th largest flow employed in the design. Over this period, staged building or road widening might be a part of a cost-effective design. The flow referred to in this context is also known as capacity, usually estimated by various methods. Capacity is one of the most germane traffic characteristics of roadways. The capacity of both rural and urban road sections is affected by certain key characteristics viz: road configuration – e.g., two-lane two-way, multilane divided or undivided; operating speed; terrain; lane and shoulder width; traffic composition, and gradients. In the case of road configuration, and by extension the development of new infrastructure, the introduction of BRT with median configuration is also an important factor that influences capacity, which is the focus of this research.

Besides, vehicles are directionally dispersed on two-lane two-way roads, particularly in urban centres, where morning peak traffic is often in bound into the core district (with relatively low outward-bound flows), but afternoon peak traffic is in the opposite direction. Vehicles of various sizes and masses, as well as diverse operational characteristics, can be found on South African roads. Trucks have a larger mass-to-power ratio than passenger cars and take up more road space. As a result, they obstruct traffic flow more than passenger vehicles, resulting in a situation where one truck is comparable to numerous passenger cars. The percentage of truck traffic during peak hours must be estimated for design purposes. As a common practice in other countries, traffic studies in South Africa are used to identify the composition of traffic for the design of a specific highway. In the case of a two-lane road, truck traffic is often expressed as a percentage of total traffic during the design hour, and in the case of a multi-lane road, as a percentage of total traffic in the prevailing direction of travel. Trucks are converted to equivalent Passenger Car Units (PCUs) since it is impractical to plan for a heterogeneous traffic stream, the number of PCUs linked with a single truck is a measure of the impedance it poses to the passenger cars in the traffic stream. This subject is further discussed in section 2.4 and covered in depth in the Highway Capacity Manual (HCM). The following section describes BRT in Cape town, South Africa.

2.3 Bus Rapid Transit in Cape Town, South Africa

The provision of transportation to and from cities is very important because they are centres for economic growth and development. Like other developing countries of the world, South Africa also finds difficulty in providing mobility for its people in urban areas. Coming to the rescue, the Bus Rapid Transit (BRT) was introduced in 2009 and became part of the National Development Plan initiatives of the South African government which seeks to make transport to be one of the main drivers of the economy and aims at bringing value to various stakeholders, the commuters and the country's economy at large. Fortunately, in 2010, South Africa was chosen to host the World cup and this international event encouraged national-level transportation improvement. Twelve (12) cities were selected to enhance the bus system development viz Johannesburg, Cape town, Nelson Mandela Bay Metropole, and so on. The focus of this study is on Cape town due to its many advantages over the other provinces, which are discussed in detail in the next chapter. Development has spread to some areas in Cape town termed low-density areas, which results in the movement of people in the pursuit of their daily chores over a long distance. However, a larger percentage of about three (3) million residents of Cape Town rely solely on public transport as their means of movement. Considering the topography of Cape Town, there is no more space for the expansion or building of new roads

for private automobiles that might carry one person at a time because it is surrounded by two oceans and Table Mountain at the center. Traffic congestion increases year by year (Cape Town Transport Integrated Rapid System, 2012).

Besides, studies have revealed that building or expansion of road networks does not ease congestion because commuters often opt for automobiles instead of using public transport, hence the need for a great investment in high-class public transport to encourage private car users to use it and alleviate congestion. This was what prompted the BRT/IRT system in Cape Town named "MyCiTi" (Cape Town Transport Integrated Rapid System, 2012). The first phase of the Integrated Rapid Transport (IRT) system stretched from the Civic Centre (CBD) to Table View as the trunk route coupled with a series of interim feeder services. Some of the routes are intersected while all the routes are connected to the Civic Centre station. Numerous design combinations have been used in 177 cities across the world that have BRT-dedicated lanes (Levinson, Zimmerman, Clinger, & Gast, 2003). They are selected based on the benefits and drawbacks of their service quality, as well as the arrangements for the kerbside, segregation lanes, and geometry (Adewumi & Allopi, 2014b). The most common designs, with associated benefits and drawbacks for the capacity utilization of the roadway, are the median and kerbside arrangements as shown in Figure 2.2(a) and (b). As illustrated in figure 2.3, the MyCiTi BRT system adopted the use of a median BRT lane configuration that is situated in the center of the road in a two-way direction. It has an exclusive right-of-way with pavement/lane markings, and intersection road markings, and is a few meters away from the main station (Civic Centre). Some locations allow for its operation in mixed traffic and at grade, eliminating the need for lane markers, dividers, or a segregated lane.

(a) Kerbside Dedicated Lane (b) Median Dedicated Lane

Figure 2. 2: BRT Dedicated Lane Configurations

To prevent vehicle manoeuvres, the lane marking acts as a barrier to other vehicles. A few meters from the Civic Centre to Table View is a fully coloured bus route. It stands out from other forms of public transportation thanks to its distinctive branding, identifiable identity, and colour of the vehicle. In addition to having multiple entrances for boarding and alighting,

regular and articulated low-emission vehicle technology buses with bi-fold doors on both sides are also used. The stations are built at the median of the road, just like the lanes, and have maps, automatic doors on both sides of the station, an elevator for commuters with disabilities, an improved station environment, full weather protection on all the station platforms, security, CCTV, an information desk, and a phone booth (only at the main station). The locations of the stations follow a predictable pattern, and only a few locations adopt the kerbside bus stops currently used by other public transportation systems. Except for a few locations with mixed traffic (at Table View, for example) and a segregated lane throughout the Woodstock to Zoarvlei corridor, the lane layout and design are nearly the same throughout.

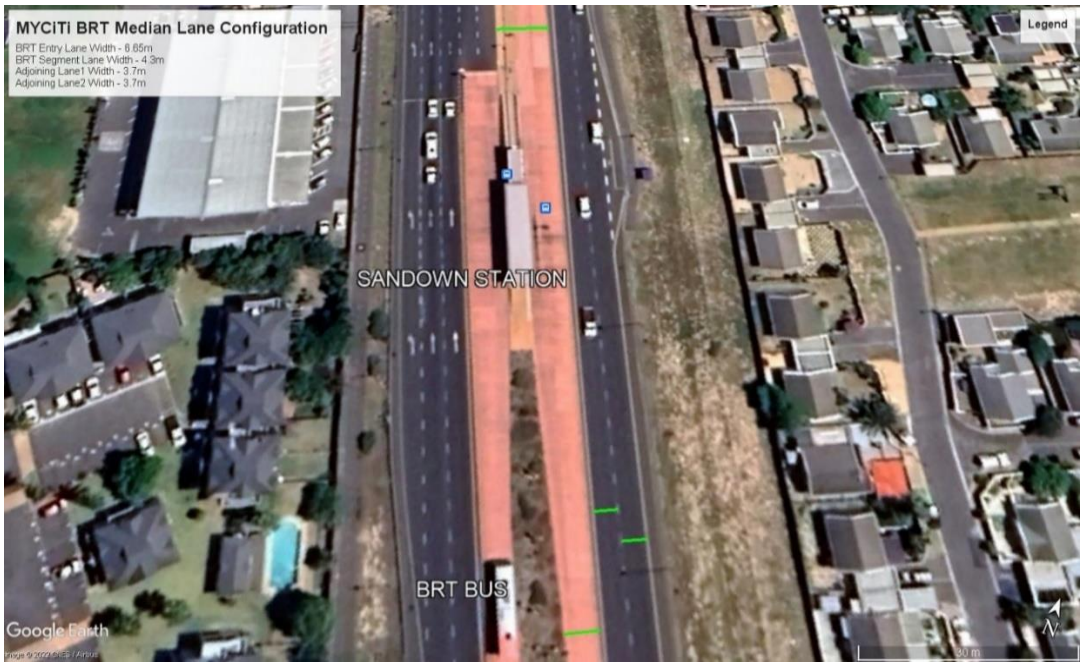

Figure 2. 3: R27 MyCiTi BRT Segment with Median Lane Configuration and Lane Widths

Adding to the road's median is a footpath. When waiting for the next bus, travellers can wait in more efficient shelters with less comfortable seats and real-time information displays, but the station also features CCTV, maps, a distinctive paint job, a trademark, and security. There is a display showing the destination in front of the bus, the destination is located within the bus, and staff members can help. From 5h10 to 21h20 on weekdays and 6h10 to 20h00 on weekends, BRT buses are supposed to run every 20 minutes. They use the CCTV that has been put in the hallways to keep an eye on the performance and theft of the buses. The BRT buses use audio announcements and maps to educate passengers about the current and the next bus stop, especially for those who are unsure about which station to exit at. It only uses smart cards, which operate at a flat rate, and only the card's monetary value can be refunded upon its return;

the money loaded onto the card is not reimbursed and in-bus fare verifications are usually carried out. The operation of BRT buses is not the focus of this study but on roadway capacity and its utilization with implications for time headways under mixed traffic conditions. The following sections give an understanding of these concepts *vis – a – vis* the quality-of-service delivery of a roadway, including other factors that can trigger their differentials in later sub-sections such as travel speed, volume-capacity ratio, and density.

2.4 Roadway Capacity Concepts

Roadway capacity is the maximum number of vehicles passing a specific uniform section or link of a roadway in a certain amount of time (often one hour), given prevailing traffic, environmental, and road conditions (Oyaro & Ben-Edigbe, 2020). Even though there has been much research carried out on roadway capacity, numerous experts have taken notice of its definition since it has been generally called into question and demonstrated to be inadequate and unworkable. Minderhoud, in 1996 argued that only traffic flow scenario on a roadway can best describe the term capacity (Minderhoud *et al*., 1996). On second thought, (Hall & Agyemang-Duah, 1991) believed that the definition did not include all circumstances in which capacity was required for roadway traffic.

However contrary to Minderhoud's assertion, (Elefteriadou & Lertworawanich, 2003) argued that the definition of capacity for freeway capacity is inadequate because the roadway becomes crowded and "breaks down" when demand exceeds the capacity value. According to (Jia *et al*., 2000) and (Sugiarto & Saleh, 2015), capacity estimations made using the HCM (2000)'s physical capacity approach may be deceptive. Similar to this, (Homan, 2012) noted that the HCM 2000 definition's use of the word "reasonable expectation" denotes a discrepancy in the maximum number of vehicles' numerical value. The HCM 2000's definition of roadway capacity according to (Ben-Edigbe, 2009), suggests section measurement under certain conditions, i.e., sections with different conditions will have different capacities, proving that capacity is stochastic (Minderhoud *et al*., 1997). It can be argued that the inability to provide a clear and acceptable definition is due to the stochastic characteristics of roadway capacity, which results from variations in driver behaviour, as well as road and weather conditions. Traffic characteristics such as density, speed, and flow are therefore the variables used to calculate roadway capacity. The analysis of traffic studies for quantity and quality reasons requires the assessment of roadway capacity. According to (Umadevi & Suresh, 2014), capacity is viewed as a prediction and a probabilistic evaluation since variations might happen

randomly and at different locations within the same facility. Despite this, the differences cannot be precisely accounted for.

In the design of highways and traffic control signals, the concept of capacity has become a central phenomenon as it can predict the possibility of traffic congestion and places where it can occur, determine the traffic volumes expected at bottle necks, and estimate the magnitude of delay involved in transiting from one location to another. While the HA note TA 79/99, seems to give a clear and understandable description of capacity, a lot of misconceptions have risen in its interpretation, owing to the different ways by which scholars have been expressing it. Consequently, for proper modelling and the purpose of making accurate operational decisions, is imperative to define roadway capacity properly and clearly. The following are various definitions of roadway capacity according to the purpose for which they were determined (Technote10, 2013):

*Design Capacity***:** The design capacity of a road link or segment refers to a single capacity value, maybe computed from a distribution of capacity, that indicates the maximum volume of traffic that may cross a road section with related probabilities under predetermined environmental, weather, and road conditions**.**

*Strategic Capacity***:** The term "strategic capacity" refers to a capacity value (perhaps generated from a capacity distribution) expressing the highest traffic volume a road section can accommodate. It is assumed that this capacity value is a valuable one for monitoring circumstances in road networks (e.g., traffic flow assignment and assimilation). Static capacity models use observed traffic flow data to determine the capacity value or distribution.

Operational Capacity: Operational capacity is a capacity value that represents a roadway's actual maximum flow rate and is thought to be a helpful measure for short-term traffic forecasts and for performing traffic flow management procedures. This value is determined based on direct empirical capacity methodologies and dynamic capacity models.

As discussed in chapter one, roadway capacity is usually affected by both physical and environmental barriers to traffic flow such as road humps (Ben-Edigbe & Mashros, 2012) and rainfall (Ben-Edigbe & Ibijola, 2020). However, the focus of this study is on inhibitions or flow disturbances caused by physical factors and not environmental or weather situations. Other physical factors that have been investigated and shown to affect traffic flow are pavement distresses (Ben-Edigbe & Ferguson, 2005), median openings (Ben-Edigbe, 2016), side friction

(Biswas *et al*., 2021; Gulivindala & Mehar, 2018; Rao *et al*., 2017), and highway consistency (Gibreel *et al*., 1999). Others are referred to as traffic conditions such as anomalous traffic volume variations (Salisu et al., 2020b), and severe freeway traffic conditions (Berechman, 1984; Salisu et al., 2020b). The physical factor investigated in this study is Bus Rapid Transit (BRT) dedicated lanes and their impact on capacity and capacity utilization of the BRT corridor.

Concerning the misconceptions around roadway capacity in the vicinity of BRT dedicated lanes, it has been generally misconstrued that the main goal of designing BRT lanes and running BRT buses in countries that have them is to eliminate captive commuters by increasing passenger capacity. Consequently, it has erroneously created an impression that a substantial number of cars owned by the number of persons in a BRT bus have been automatically taken away from the roadway, making road providers believe that more people have been transported in this way. It can be argued that not all the passengers in the BRT bus ~~may~~ own a private vehicle. However, it must be stressed, or counter-argued that mixed vehicular traffic carries more people per lane than BRT buses only. This is the main reason why roads are designed, for vehicular movements, not people. It is on this premise that this study investigates how well the MyCiTi BRT corridor R27 is being utilized in terms of road space and determines whether the capital investment in its construction has been worthwhile.

With respect to the design and design configuration adopted by road providers for BRT, it can be argued that the type of design adopted can affect the capacity utilization on both the BRT lane and its adjoining lanes. The design of the BRT (red line) in London for example is with the kerbside (left side) configuration with bus parking bays located at specific locations off the dedicated lane (Modupe & Ben-Edigbe, 2022), where the BRT buses can conveniently park and pick commuters, while mixed traffic movements continues on the BRT lane. This approach has substantially helped in maximizing capacity by the reduction of headways between vehicles. The design configuration of the BRT in this study is the median configuration, and the possible demerits in terms of capacity usage have been identified.

Studies on how BRT affects lane capacity differentials on the BRT and adjacent lanes are either scarce or non-existent. However, using the VISSIM simulation model software, the impact of BRT on "microscopic" traffic stream features was examined in a closely related study by (Sipos, 2019). To determine how BRT would affect total travel time and totally stopped delays, he studied a "with and without" BRT scenario.

Various scholars and methodologies have also estimated capacity. It can be calculated using various empirical data, based on, among other factors, the location, the type of data, the traffic situation, the observation duration, and the headways. Some of the techniques used include headway estimation, utilizing traffic flow (chosen highest method, predictable extreme value method, and bi-modal distribution method), using traffic flow and speed (Product Limit Method), and using traffic flow, speed, and density (fundamental diagram) (Minderhoud *et al*., 1997), the sections that follow cover each of these in further detail. In a mixed traffic flow, not only do vehicles interact amongst themselves but also with the environmental and geometric characteristics of the roadway (Ben-Edigbe & Ferguson, 2005). Traffic flow hence refers to the movement of people and their cars between two points, as well as their interactions with one another. The variety of features displayed by the vehicles using the road under varied driving styles is what causes the operation to be complex. To take care of this challenge, quantify the impact of different characteristics on driving behaviour, a conversion term called "passenger car equivalent" was created as a common base in achieving uniformity for all classes of vehicles in a traffic stream flow. This is discussed in detail in the next section.

2.4.1 Passenger Car Equivalent (PCE) Values

The term "passenger car equivalent" (PCE), sometimes known as "passenger car unit" (PCU), is used to translate various types of vehicles in a mixed traffic volume into a comparable number of passenger cars to assess the traffic flow rate on a roadway. Passenger car equivalence according to (Shalini & Kumar, 2014), is a measurement of how a single heavy vehicle affects traffic characteristics (such as speed and headway) when compared to a number of passenger vehicles. The term "passenger car equivalency" was originally used in the HCM (1965) to explain how the presence of trucks and buses in a traffic stream can cause passenger cars to be dislodged from their normal positions.

According to The HCM (2010, p. 9–13), a passenger car equivalent is defined as "*the number of passenger cars that will produce the same operational conditions as a single heavy vehicle of a specific kind under specified highway, traffic, and control conditions*," (HCM, 2010). As a result, PCE is typically used to assess how a traditional mode of transportation compares to a car in terms of elements like speed, headway, and density of traffic. The amount and quality of traffic flow on roads are impacted by this. To calculate the impact of heavy vehicles on a traffic stream's behaviour under mixed traffic conditions, the (HCM, 2010) employs passenger car equivalent factors. Considering that both are employed in defining the volume and flow rates of traffic, the passenger car equivalent also represents the capacity of a roadway. Passenger car units can be used to express the concept of capacity (Ben-Edigbe *et al*., 2013).

In a traffic flow, passenger car equivalency values and capacity measures can thus be linked. One could counter that while capacity may be expressed in terms of PCEs, hence, the parameters impacting road capacity may also affect passenger car counterparts. Since heavy vehicles are larger than passenger cars, it is logical to expect that they will take up more space in a traffic flow. Heavy vehicles need longer and wider turning distances than passenger vehicles because they have more limited and worse operational capabilities (Ahmed, 2010). Numerous studies have looked at how heavy cars affect the capacity of a roadway. According to (Mehar *et al*., 2014), passenger car equivalence is a complicated parameter that depends on the traffic and geometric conditions in place at the time of the survey. While (Suhas Vijay Patil, 2015) claimed that variables including traffic flow, road conditions, environmental, meteorological, and control conditions have an impact on passenger car equivalency, (Ben-Edigbe, 2009) stressed that the varied levels of instability on roads that affected the quantity and quality of traffic flow were caused by variations in the flow of traffic. To account for differences in the traffic stream, all traffic vehicles are translated into the acceptable passenger car equivalent (PCE), which is represented as "pce per hour," "pce per hour per lane," or "pce per kilometre" of the road's length. In general, as demonstrated in Table 2.3, passenger car equivalents have been computed from observations and they vary with respect to the type of vehicles and roads. The values provided are simply a guide, and designers should consult the Highway Capacity Manual for the computation of PCUs for various settings and scenarios.

Table 2. 3: South Africa Passenger Car Equivalent Values

Vehicle type	Passenger Car Units			
	Rural roads	Urban streets	Roundabouts	Traffic signals
Cars and light vans	1,0	1,0	1,0	1,0
Heavy vehicles	3,0	1,75	2,8	1.75
Buses and coaches	3,0	3.0	2,8	2,25
Motorcycles	1,0	0,75	0,75	0,33
Pedal cycles	0,5	0,33	0,5	0,2

Source: SANRAL

Based on information from the South African National Roads Agency Limited (SANRAL), the passenger car equivalent values provided in table 2.3 are with respect to favourable weather, daylight, and level roadway conditions. However, due to the introduction of the BRT infrastructure with median dedicated lanes configuration and the conditions under which this study was conducted, including the presence and operation of BRT buses, assessing if the PCE values are suitable is therefore necessary. Due to variations in estimation techniques, the

calculation of passenger car equivalent values continues to be a contentious issue. It's easy to use the headway method. It is calculated as the difference between the target vehicle's average headway and the passenger car's average headway. It is mathematically expressed as:

$$pce_i = \frac{H_i}{H_C} \quad 2.2$$

Where pce_i = passenger car equivalent of vehicle class *I*, H_i = average headway of vehicle class *i* (s) and H_C = average headway of passenger car (s)

The headway method has the merit of being simple to use and the ease with which empirical headway data can be calculated. The headway method could also be used to distinguish between the effects of congested and free-flowing traffic. The headway approach will be used in the latter stages of this study to reassess the passenger car equivalent values based on these benefits. The (Chandra & Sikdar, 2000) speed approach method is another technique that measures vehicle occupancy on the road surface using the actual size of the vehicle. Equation 2.3 is a mathematical expression for the speed approach technique. The approach is appropriate for mixed traffic situations.

$$pce_i = \frac{V_c/V_i}{A_c/A_i} \quad 2.3$$

where pce_i = vehicle class i 's passenger car unit

V_c = mean speed of passenger car.

V_i = mean speed of vehicle class i

A_c= estimated rectangular car area on the road (length x width)

A_i = estimated rectangular area of vehicle class *i* on the road (length x breadth)

Equation 2.4, which is used in the approach based on delay, is expressed as follows:

$$pce_{ij} = (D_{ij} - D_{base})/D_{base} \quad 2.4$$

where pce_{ij} depicts *pce* values of vehicle class i under conditions *j*

D_{ij} denotes delay to passenger cars due to vehicle class i under conditions *j*.

D_{base} denotes delay to standard passenger cars due to slower passenger cars.

An alternative method for calculating the passenger car equivalent based on density is to use equation 2.5:

$$E_T = \frac{1}{\sum_1^n P_i}\left[\frac{q_B}{q_M} - 1\right] + 1 \quad 2.5$$

where P_i depicts the proportion of trucks of type i out of all trucks

n = no of trucks in the traffic

q_B = base flow rate (passenger cars only)

q_M = the mixed flow rates

The following is another density-based method:

$$PCU_i = \frac{k_{car}/W_L}{k_i/W_L} \quad 2.6$$

where PCU_i = passenger car unit for *i* vehicle in a homogenous traffic behaviour

k_{car} = density of passenger cars in homogenous traffic (car/km)

k_i = density of *i* type of vehicle in a homogenous traffic

W_L = lane width of the lane in a homogenous traffic

Notably, equation 2.5 is only applied in the case of homogeneous traffic with strict lane discipline, automobile following, and a constant fleet of vehicles, with the assumption that the spatial mean speeds of passenger cars and other vehicle types are equal. The (HCM, 2010) approach adjusts the flow rate owing to the impact of heavy vehicles in a traffic stream by employing the expression indicated in equation 2.7 and the passenger car equivalent components.

$$f_{HV} = \frac{1}{1+P_T(E_T-1)+P_R(E_R-1)} \quad 2.7$$

where; f_{HV} = HV adjustment factor

E_T,E_R= PCE for trucks/buses and recreational vehicles (RVs) in the traffic stream, respectively.

P_T, P_R = Proportion of trucks/buses and RVs in the traffic stream, respectively.

According to (Keller & Saklas, 1984), the projected passenger car equivalents depend on the volume of traffic and the kind of vehicle, and they suggested that the capacity reduction is directly connected to the additional delay brought on by large vehicles in the traffic stream. Thus, it can be mathematically stated as:

$$PCE = \frac{TT_i}{TT_O} \quad 2.8$$

where TT_i = total travel time of vehicle type *i* over the network in hours

TT_O = total travel time of base vehicle over the network in hours

There are other methods employed to estimate capacity which are based on factors like the number of vehicle hours, travel time, platoon formation, etc. Generally, the methodologies used to determine a vehicle's passenger car equivalent values vary widely. The variation concerning heavy vehicles is the most significant, and numerous studies have been done on how large vehicles affect a traffic stream. (Ahmed, 2010) found that the presence of heavy vehicles in a traffic stream increased passenger car and heavy vehicle headways in his study of passenger car equivalents for a level motorway operating under moderate and congested

conditions. He added that for level urban freeway portions, the PCE ratio of 1.76 obtained was greater than the 1.5 indicated in the HCM (2010).

Other studies that have attempted to calculate passenger car equivalent values include saturation flows (Kimber *et al*., 1985), mixed traffic flow at signalized intersections (Adams *et al*., 2014), capacity and LOS (Ben-Edigbe & Ferguson, 2005; Ben-Edigbe & Johnson, 2014), Indian heterogeneous traffic scenarios' estimation techniques (Budhkar & Maurya, 2012), capacity LOS due to pavement distress (Ben-Edigbe, 2003; Ben-Edigbe & Ferguson, 2005), and development of passenger car equivalents (Suhas Vijay Patil, 2015). (Tanyel *et al*., 2013) investigated the impact of heavy vehicles on traffic circles and discovered that when calculating the rates of heavy vehicles, separate passenger car equivalent values should be used for small and major flows. When studying the effects of passenger car equivalents in work zones, (Sun *et al*., 2007) found that these vehicles each have their unique characteristics. Since capacity can be defined in terms of a passenger car equivalent, it is assumed that the claim that a passenger car equivalent depends on the condition of the road, the volume of traffic, and the surrounding environment is correct. As a result, it might be appropriate to calculate the passenger car equivalent values given the local environment, traffic, and road conditions. Therefore, it becomes logical to modify the South African passenger equivalent values for the prevailing conditions under which this study was investigated, which is the incorporation of BRT dedicated lanes for specialized buses. This will help to discover any possible effects caused by the introduced infrastructure.

2.4.1.1 Assessment of Passenger Car Equivalent Values

The measurement of the impact of the mode of transportation on traffic variables is called passenger-car equivalence. Under the current traffic and road circumstances, it is the displacement effect of passenger cars because of heavy and medium-weight vehicles in a traffic stream. Although the current road and traffic conditions for the passenger car equivalent (PCE) values stated in the SANRAL highway traffic manual are not dissimilar from the conditions considered in this study, a modification of the passenger car equivalent (PCE) value is still required, regardless of whether the values are significant or not. A variety of techniques are used to modify the PCE. Since the automatic traffic counter recorded the headway information of cars, the headway approach is used for this investigation. Two hypotheses were established to determine whether the modified passenger car equivalent (PCE) value is relevant. The following are the two hypotheses:

- Null hypothesis (H_0): No distinction between SANRAL PCE values and the modified values
- Alternative hypothesis (H_1): There is a distinction between SANRAL PCE values and the modified values.

A chi-square test with a 95% level of confidence is taken into consideration because the hypotheses call for a statistical test to ascertain the significance of the modified passenger car equivalent (PCE) values in comparison to the SANRAL passenger car equivalent values. Equation 2.9 is used to represent the chi-square test.

$$X^2 = \frac{(o-e)^2}{e} \quad 2.9$$

where X^2 = chi-square

o = observed value

e = expected value

2.4.2 Methods for Estimating Roadway Capacity

Two approaches to measuring capacity viz direct and indirect were identified by (Minderhoud *et al*., 1996). The direct empirical method, which is relevant to this study and whose nature is stochastic, analyses data to create models that forecast traffic flow and calculate road capacity. Data on headway, traffic volume, average speed, and density are used in empirical approaches to estimate capacity. The headway data applies the car-following theory with respect to time, whereas the speed data divides the traffic state into stable, unstable, and congested. Other estimation methods were created because of the drawbacks of traffic volume estimation techniques. One of these approaches uses data on traffic flow and speed to represent the state of the road's capacity. The upstream traffic situation of the observation point must be known to get a satisfactory value. The product limit method (PLM), the selection method (SM), and the empirical distribution method (EDM) are frequently used techniques. Figure 2.4 shows the methodology framework for the direct approach to estimating capacity, according to Minderhoud.

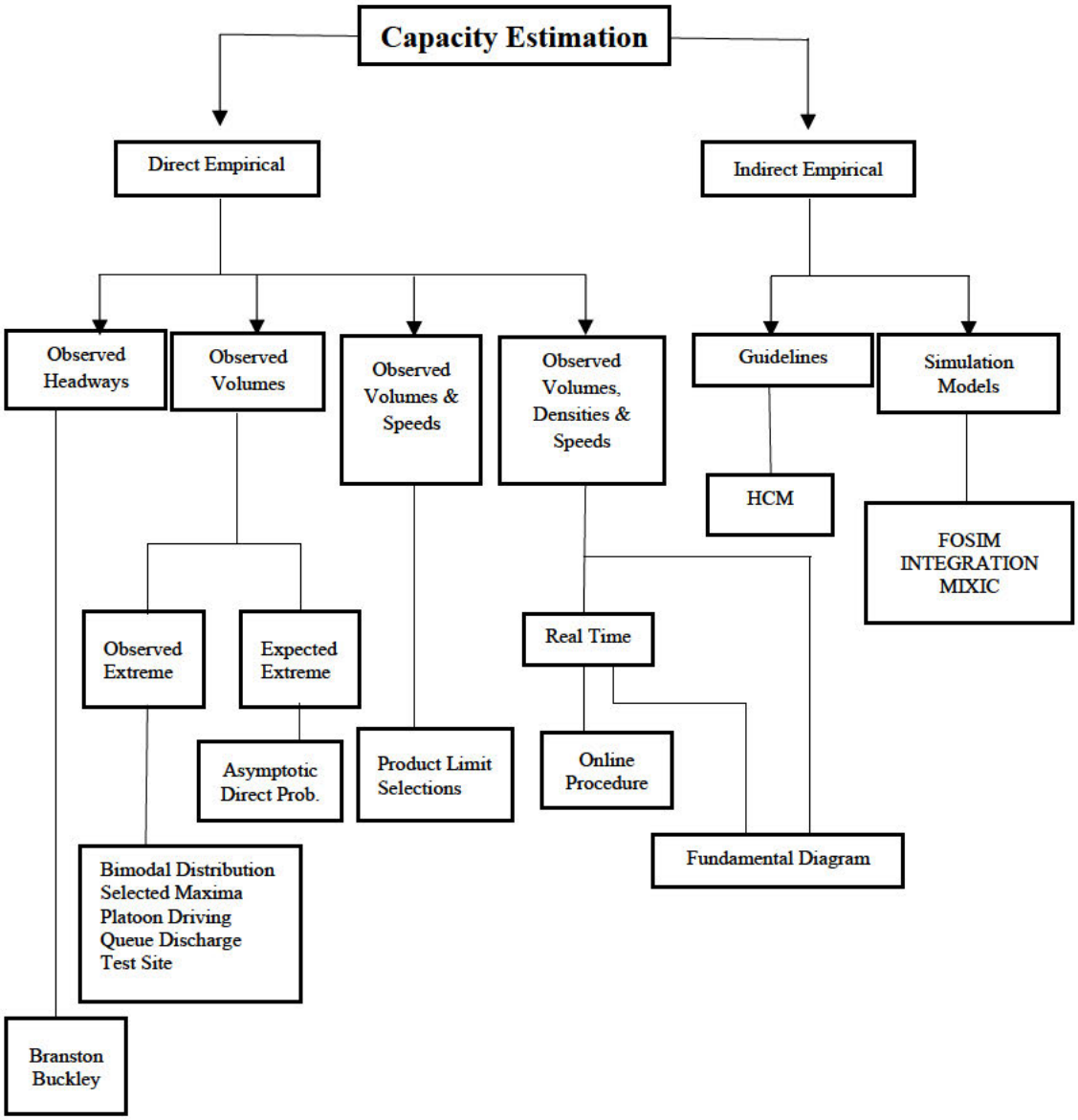

Source: (Minderhoud et al., 1998; Technote10, 2013)

Figure 2. 4: Roadway Capacity Estimation Methods

2.4.2.1 Product Limit Method (PLM)

Based on previous investigations by (Kaplan & Meier, 1958) (product limit approach) and van (Van Toorenburg, 1986) (distribution function), (Brilon *et al*., 2005) modified the capacity estimating method developed by (Minderhoud *et al*., 1997). The modification is as follows:

$$F_c(q) = 1 - \Pi_{i,q_i \leq q} \frac{k_i - d_i}{k_i}; i \in \{B\} \qquad 2.10$$

The empirical distribution approach and the product limit method are comparable in that both emphasize the separation of flow observations acquired over the observation period. The free-

flow and capacity measurements are both used in the product limit technique to obtain a more accurate image of the real capacity value. Be mindful that before breakdown and recovery can happen, the maximum observed volume must exist; otherwise, the entire distribution function cannot be achieved because it would terminate in a value lower than one. A complete capacity distribution function is typically difficult to model; even if it is, for a larger volume, it could not be as reliable as such unless a sizable amount of data is obtained. On the other hand, the product limit technique, according to (Brilon *et al*., 2005), does not necessitate the assumption of a particular kind of distribution function. A technique called maximum likelihood estimation is used to estimate the parameters of a model. The parameter settings for this approach are chosen to maximize the likelihood that the process envisioned by the model will result in the data that was seen. The success of the maximum likelihood method, as implied by its name, depends on how strongly the distributional assumptions used are held. The following is a description of a maximum likelihood method proposed by (Lawless, 2011) for estimating the distribution function parameters:

$$L = \prod_{i=1}^{n} f_c(q_i)^{\delta i}[1 - F_c(q_i)]^{1-\delta i} \qquad 2.11$$

Where $f_c(q_i)$ = statistical density function of capacity c

$F_c(q_i)$ = cumulative distribution function of capacity c

n = number of intervals

δi = 1, if uncensored (breakdown of classification B)

δi = 0, elsewhere

The Log-likelihood function is therefore converted into capacity analysis as:

$$\ln(L) = \sum_{i=1}^{n}\{\delta i \ln[f_c(q_i)] + (1 - \delta i)\} \ln[1 - F_c(q_i)] \qquad 2.12$$

The shortcomings of this method include the too many numbers of capacity measurements needed and its inadequacy for off-peak data collection. Besides, since no data on capacity distribution is provided by the product limit technique, the accuracy of the projected capacity is questionable. Furthermore, according to (Ben-Edigbe *et al*., 2013), the product limit is ineffective in estimating capacity because the cumulative distribution function's capacity values are randomly chosen, which leads to unreliable results. Whatever the case, according to (Minderhoud *et al*., 1996) p. 36), traffic capacity using the product limit method is a "location with features of the estimated capacity distribution". The mean, median, and percentile points are among the location features, and the estimated distribution is derived from the data on high-volume free-flow observations, which contains the empirical distribution of capacity observations. This approach needs a sizable database of volume and speed measurements, as

well as a bottleneck location to determine the road's capacity once upstream congestion is observed. The empirical distribution function is given by Equation 2.13:

$$G(q) = Prob(q_c > q) \qquad 2.13$$

Where $G(q)$ = the probability that capacity value > certain intensity q and $F(q)$ is defined as $1 - G(q)$. In general, equation 2.14 below represents the Product Limit Function:

$$G(q) = \Pi_{q_i} \frac{K_{qi-1}}{K_{qi}} \qquad q_i \in \{C\} \qquad 2.14$$

Where K_q = number of observation elements i in set $\{S\}$ with intensity $q_i \geq q)$

$\{C\}$ = set of observed congested flow intensities

$\{Q\}$ = set of observed free flow intensities

$\{S\}$ = $\{Q\} \cup \{C\}$, $\{S\}$ is set of all observations i

Table 2.4 below gives a straightforward illustration of the product limit approach using data that were changed from a 15–minute average interval to an hour. The hourly traffic flow observations are shown in column 1 of the table, while the flow rates, (q_i), at each interval i. are shown in column 2. The traffic types are shown in Column 3, with Q denoting open flow and C denoting congested flow. Column 4 displays the flows' ranking in ascending order. The flow intensities in column 5 that are equal to or higher than the threshold capacity values are treated as 1. Following that, the discrete functions $G(q)$ and $F(q) = 1 - G(q)$ were computed. However, as there is no information available regarding the quality (reliability, precision) of the projected capacity value, the efficacy of the product limit technique is in doubt.

Table 2. 4: Product Limit Method Estimation Example

1 interval i	2 q_i	3 Set	4 Order j	5 k_{q_i}	6 $G(q)$	7 $F(q)$
1. 15.30 - 15.45	3000	Q	2	-		
2. 15.45 - 16.00	2500	Q	1 lowest	-	1	0
3. 16.00 - 16.15	3500	C	3	6	5/6 = 0.83	0.17
4. 16.15 - 16.30	4000	Q	4	-		
5. 16.30 - 16.45	4000	C	6	3	5/6.3/4.2/3.0/1 = 0.41	0.59
6. 16.45 - 17.00	4500	Q	7	-		
7. 17.00 - 17.15	4600	C	8 highest	1	5/6.3/4.2/3.0/1 = 0	1
8. 17.15 - 17.30	4100	C	5	4	5/6.3/4.2= 0.62	0.38
2 hours	Average Flow 3775	Total I = 8 i in (Q) = 4 i in (C) = 4				

Source: (Minderhoud et al., 1997)

2.4.2.2 Empirical Distribution Method (EDM)

According to the empirical distribution approach, the distribution of capacity measurements can be used to determine the value of capacity. This approach relies on the clear separation of observed flows over the observation period. Figure 2.5 demonstrates the splitting of the observed flow rate into two portions as determined from the upstream site.

- free flow measurement or measurements that reflect traffic demand.
- measurement of congested flow

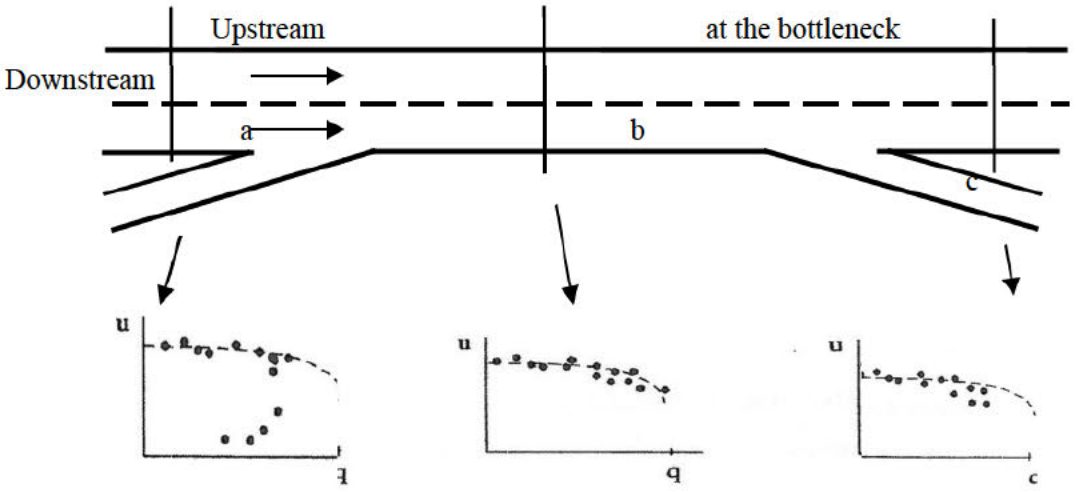

Figure 2. 5: Measurement Points for FDM, Product Limit, and Selection Method.

Source (Minderhoud et al., 1997)

Utilizing only the intensities that are components of the capacity set, C, equation 2.15 can be used to estimate the function of the empirical capacity distribution.

$$F(q) = Prob(q_c \leq q) \qquad q_i \in \{C\} \tag{2.15}$$

Rewriting equation 2.15 as equation 2.16.

$$F(q) = N_c/N \tag{2.16}$$

Where $F(q)$ = cumulative distribution function of capacity values

q_c = value of capacity

q_i = value of intensity counted at average interval i

N_c = number of observation elements i, in set $\{C\}$ with intensities q_i less than q

N = total number of observation elements i, in set $\{C\}$

$\{C\}$ = set of observed congested flow measurements

The acceptability of the capacity value derived from the equation above is dependent on the the variance of the intensities calculated using equation 2.17.

$$Var\big(F(q)\big) = F(q)\,.\,(1 - F(q))\;/N \qquad 2.17$$

One of the key benefits of this method, according to (Minderhoud *et al.*, 1997) is the unambiguous and unbiased capacity value with its distribution based on the intensity measurements taken during upstream congested situations. The technique, however, discourages the use of capacity values derived from free-flow measurements. According to the study by (Homan, 2012) on a few work zones in the Netherlands, the empirical distribution method (EDM) provides a more accurate capacity estimate when compared to the product limit method PLM values. In conclusion, the empirical distribution approach has an accurate estimate of the capacity distribution, however a good distribution requires that the road's frequent capacity level be reached.

2.4.2.3 Fundamental Diagram Method (FDM)

Traffic flow is the study of how different drivers travel between two points and interact with one another. Regrettably, because the behaviour of drivers cannot be accurately predicted, researching traffic flow becomes very challenging. Drivers however typically exhibit consistent behavioural tendencies which also result in some consistency in the way traffic flows, hence can be represented mathematically. The mathematical relationship, therefore, involves three major traffic characteristics viz: flow, speed, and density, which is referred to as the Fundamental Diagram Method (FDM), represented as:

$$q = u * k,\ hence\ u = \frac{q}{k}\ and\ k = \frac{q}{u} \qquad 2.18$$

It is possible to write the flow-density relationship as:

$$q = ku_f\left(1 - \frac{k}{k_j}\right) \qquad 2.19$$

In the flow – density relationship, the slope of the curve represents the speed, given by:

$$u = q/k$$

Where u = Speed; q = flow; k = density, u_f = free flow speed; k_j = jam density.

Figure 2.6 shows a typical flow-density curve, which describes a traffic flow. It is used in this study to explain the concept of roadway capacity and its Utilization. Note that $\boldsymbol{u_f \sim free\ flow\ speed}$, $\boldsymbol{u_Q \sim speed\ at\ capacity}$, k_Q ~ density at capacity, $k_{0.85}$ ~ density at threshold flowrate.

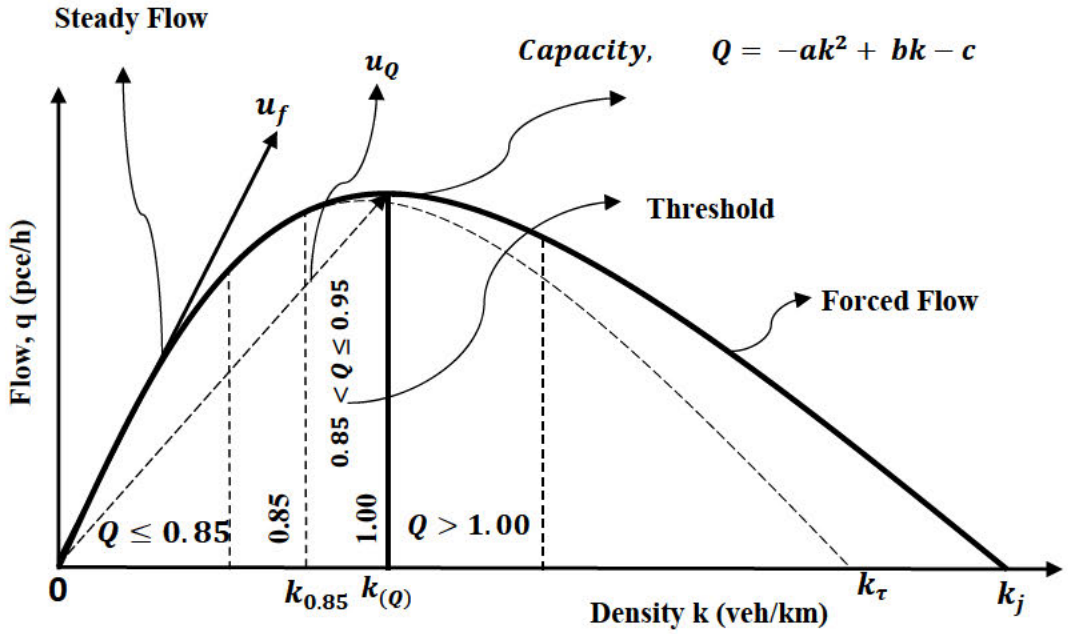

Figure 2. 6: Typical Flow–Density Curve

There are two sections to the flow-density curve: a steady flow section (left side) and a forced flow section (right side). In the steady flow section, the flow of vehicles is at free-flow speed, a situation where speed oscillates between the unconstrained and constrained ultimate points or points of critical density or density at capacity (k_Q) while in the forced flow section, flow contracts gradually. Four fundamental boundary conditions exist for the flow-density curve. These are:

- when density is zero, flow is also zero. i.e., $q = 0$ at $k = 0$
- flow is zero when density is at jam state. i.e., $q = 0$ at $k = k_j$
- when density is zero, speed equals free flow. i.e., $u = u_f$ at $k = 0$
- when density is at jam condition, speed is zero. i.e., $u = 0$ at $k = k_j$

During a traffic flow scenario, flow rises along with density until it reaches an optimum value under free flow known as the critical density (k_{cr}). Traffic flow then enters a constrained area beyond the critical density until the maximum value, under congested flow called jam density k_j is reached, which is about five times the critical density due to the asymmetric nature of the curve. The flow of vehicles is therefore hampered at this jam density because there is a complete breakdown. Speed then decreases as density in the confined segment increases, and it eventually reaches zero when there is no vehicle movement, or at a jam k_j. In other words

and according to (Ben-Edigbe, 2010; Ben-Edigbe & Ferguson, 2005), the density at capacity or critical density $K_{crt(Q)}$, is reached at the apex point of the curve as shown, and it may be argued that the relationship between density and flow ends there. Other associated traffic characteristics derivatives are the speed at capacity u_Q and time headway at capacity. In terms of road planning and design, speed is a key control parameter, as well as a measure of the effectiveness of vehicle operation.

The measures for control and management of traffic are based on density, which represents the volume of traffic on the road. According to (Greenshields *et al*., 1935), the first speed-density model was a negative linear model. In his postulation, the calculated speed-density connection deviates slightly from reality due to the linear model's overlap and classification of the observed data groupings, which is shown to be illogical, with a limited set of representations. Later, more in-depth research into the relationship between speed and density led to the development of various models, including the Pipes-Munjal model, a modified Greenshields model, the Newell model, the Greenberg logarithmic model, the Edie model, the Underwood exponent model, and so forth (Sharma *et al*., 2021). (Heydecker & Addison, 2011) looked at the relationship between density and speed using different speed limits and found that the speed of vehicles becomes zero at the jam state.

A broad logistic model of traffic flow features was developed by (Xiao-long *et al*., 2015) employing several traffic flow parameters with distinct physical interpretations. According to the analysis of the parameters' impacts on speed-density logistic curves and the experimental findings, the model is capable of accurately reflecting the traffic flow characteristics such as speed change rate and the supremum of speed in various stages. (Shao *et al*., 2015) suggested a speed-density model under clogged traffic situations paired with the minimum safety spacing constraint, and the experiment results showed that the absolute error of this model was lower than that of previous models fitting the traffic data of two highways. A family of speed-density models was suggested by (Wang *et al*., 2011) using a variety of factors with significant physical implications and they performed well in the experiment. There are two categories of travel speed-density models: single-regime and multi-regime models. The equation for the Greenshields speed-density model is given by equation 2.20:

$$u = u_f - \frac{u_f}{k_j}.k \qquad 2.20$$

Although the function expressions vary, they are essentially the same in the domains $k \in \langle 0, k_j \rangle$. Some of them, though, do not concurrently meet the two boundary criteria $v(0) = 0, and\ v_{f,}(k_j) = 0$. Multi-regime models often include two or three regimes to explain various traffic circumstances, while single-regime models only include one functional form to describe the relationship between flow, speed, and density. The Eddie model from 1961, the modified Greenberg model, and three regime models are examples of common multi-regime models. According to (Edie, 1961) the car-following model in equation 2.21 can be integrated to get the Greenberg model (1959) in equation 2.22.

$$w_{\ddot{x}_{n+1}}(t) = \lambda_i \frac{(\dot{x}_n\langle t+\Delta t\rangle - \dot{x}_{n+1}(t+\Delta t))}{(x_n\langle t+\Delta t\rangle - x_{n+1}(t+\Delta t))} \quad 2.21$$

$$v = V_m \ln\left(\frac{k}{k_j}\right) \quad 2.22$$

Where w = mass of vehicle; λ_i = character coefficient of driver's sensitivity; Δt = average time lag, a constant, for driver-car system $x_n(t)$, $x_{n+1}(t)$ = the coordinate of the front vehicle and the subjective vehicle with respect to the inertia coordinate system at time t, $x_m(t)$, $x_{n+1}(t)$ is the distance headway. It should be noted that the integration would not be affected by a constant Δt. Using the average distance headway and density relationship,

$$k = \frac{1}{y} = \frac{1}{x_n - x_{n+1}} \quad 2.23$$

The boundary condition $v(k_j) = 0$ and $V_m = \lambda_i / W$ is obtained.

Generally, the Greenberg model is obtained by adding parameters for data fitting flexibility:

$$v(k) = g_1 + g_2 \ln\langle\frac{k}{k_j}\rangle \quad 2.24$$

The following are identified as the weakness of the Greenberg model:

$$\mathrm{Lim}_{k\to 0} V_m \ln\frac{k_j}{k} = \infty$$

This indicates that the model is inappropriate for light traffic. Eddie then asserted that additional advancement is required by mentioning the microscopic car-following model for the uncongested traffic shown below.

$$w_{\ddot{x}_{n+1}}(t) = \lambda_i \dot{x}_{n+1}(t) \frac{(\dot{x}_n\langle t+\Delta t\rangle - \dot{x}_{n+1}(t+\Delta t))}{(x_n\langle t+\Delta t\rangle - x_{n+1}(t+\Delta t))^2} \quad 2.25$$

With the boundary condition $v(0) = v_f$ (free flow) if $\frac{1}{x_n - x_{n+1}} = \frac{1}{y} = 0$.

The speed that results when density and flow are both zero is known as free-flow speed. Naturally, seeing zero density and flow makes no sense since zero density implies that there isn't even a single vehicle. However, by observing the link between density and headway, one might arrive at the following model:

$$k = 1/y\,, k = k_m \ln\left(\frac{v_f}{v}\right); k_m = 1/y_m \qquad 2.26$$

Or $v = V_f\, exp\left(\frac{-k}{k_m}\right)$ which is exactly the Underwood model (1961) where y_m=

The pacing of maximum flow I estimated by minimizing the $q(v)$

k_m = the density of maximum flow

Parameters ω_1 and ω_2 are added for flexibility in the data fitting:

$$v = V(k) = \exp + \langle -\omega_1 \frac{k}{k_m} + \omega_2 \rangle \qquad 2.27$$

It is strictly concave for $k \in \langle 0, 2k_m \rangle$. These two can be combined in one model as:

$$v(k) = \begin{cases} \exp\left[-\omega_1 \frac{k}{k_j} + \omega_2\right] & k \le k_j \\ g_1 + g_2 \ln \langle \frac{k}{k_j} \rangle & k > k_j \end{cases} \qquad 2.28$$

Zhang (1999) described the following polynomial model as the one-parameter polynomial, and stated below:

$$v = v_f \left(1 - \langle \frac{k}{k_j} \rangle^n\right) \qquad 2.29$$

Where v_f = free–flow speed, k_j = jam density, n =1 is the Greenshields model (1934).

This model can be thought of as a particular instance of the exponential model utilized by Hegyi *et al* (2002).

$$v(k) = v_f\, exp\left(-\frac{1}{\varphi} \langle \frac{k}{k_c} \rangle^{\varphi}\right) \qquad 2.30$$

Where; v_f = free flow speed; φ = model parameter; k_c = critical density, is the same as the k_m used by Eddie. In each instance, it generalizes the Underwood model in some way. The simplest of all the models is the Greenshields model with useful parameters. Additionally, it

works across a wide variety of densities and statistically matches actual observations of road traffic. The limitations include the need for a specific model for data fitting and the inability to estimate speed at low densities. It results in the microscopic car-following model and the macro-traffic stream model being connected. According to Greenberg's model, speed was said to increase to infinity as density decreases. The Underwood's model however contends that speed is zero when density is at the level of infinity, to address the flaws of the Greenberg model. (Alhassan & Ben-Edigbe, 2012b), (Ben-Edigbe *et al*., 2013), (Alhassan & Ben-Edigbe, 2014), (Umadevi & Suresh, 2014), and (Ben-Edigbe & Ferguson, 2005) are some more research studies that used fundamental diagrams (2016). According to (Khanorkar *et al*., 2014), the fundamental diagram returns a futuristic value, making it appropriate for any road operating situation. (Ben-Edigbe & Ferguson, 2005) opined that equation 2.30 can be expressed as equation 2.31 and used to calculate the capacity of a road:

$$Q = -\frac{u_f}{k_j}\left(\frac{u_f}{2\left(\frac{u_f}{k_j}\right)}\right)^2 + (u_f)\frac{v_f}{2\left(\frac{v_f}{k_j}\right)} - c \qquad 2.31$$

Where; u = space mean speed; u_f = free flow space mean speed, k_j = jam density, c is constant, and Q is capacity.

2.4.3 BRT Dedicated Lane Capacity Estimation

Bus Rapid Transit (BRT) is a high-capacity bus-based public transport system that provides fast service than conventional bus systems. Typically, a BRT system includes roadways that are dedicated to buses and gives priority to buses at intersections where buses may interact with other traffic. BRT aims to combine the capacity and speed of a light rail or metro system (LRT, HRT) with the flexibility, lower cost, and simplicity of a bus system. The headway method is a primary consideration in the estimation of BRT route capacity (Ben-Edigbe *et al*., 2013). It is defined by the braking performance of vehicles and other factors like the sizes of blocks. It considers factors such as the number of vehicles per unit of time and the maximum safe speed of the vehicles (Dowling *et al*., 2004). The BRT time headway, defined by braking performance and measured tip-to-tail, is given by:

$$T_h = \frac{L}{V} + t_r + \frac{kV}{2}\left(\frac{1}{a_f} - \frac{1}{a_l}\right) \qquad 2.32$$

Where T_h – time headway (s); V – vehicle speed; L – Length of vehicle.

t_r – Reaction time and k – arbitrary safety factor (usually greater than or equal to 1)

a_f – Minimum braking deceleration of the following vehicle

a_l – Maximum braking deceleration of the lead vehicle

Note that for brick wall considerations, a_l is infinite and is usually eliminated. The capacity of vehicles on a single roadway lane is the inverse of the tip-to-tip headway. Hence the BRT lane capacity in vehicles per hour can be expressed as:

$$Q_{BRT} = \frac{3600}{\{\frac{L}{V} + t_r + \frac{kV}{2}\left(\frac{1}{a_f} - \frac{1}{a_l}\right)\}} \quad 2.33$$

2.5 Roadway Capacity Utilization (RCU)

In many cities of the world, BRT has emerged as a cost-effective mode of public transportation (Cervero & Kang, 2011). The introduction of and investments in BRT systems across the globe have yielded improvements in travel speed with an attendant significant reduction in travel time on the BRT lanes on the one hand. However, on the other hand, it often results in a decrease in travel speed on the adjoining lanes, which leads to an increase in travel time as well as other anomalies in traffic stream characteristics, and the capacity utilization on both the BRT dedicated lane and its adjoining lanes (Chengula & Kombe, 2017). The term 'capacity utilization' is a utility phenomenon with a derived equation from the flow-density relationship shown in Figure 2.8. It is a quantitative measure often used to describe the degree or extent to which the roadway is used. In other words, it is measured by volume-to-capacity (v/c) ratio, a dimension usually employed to measure the overall performance of a transportation system and mobility in addition to quality of service. The threshold value for (v/c) is 1, which relates traffic volumes captured at different road segments with their maximum operational capacities. The evaluation of roadway capacity utilization is not very common in literature, hence studies that are usually found are with respect to capacity loss. However, in a closely related transport logistics study by (Salisu et al., 2020a), the capacity utilization of selected highways viz Lagos – Ibadan, Lagos – Abeokuta, and Sagamu – Benin, in the vicinity of Ogun State, Nigeria was evaluated. The approach involved the estimation of roadway capacity by simply relating the total vehicle volume counts with the total period, and the capacity utilization rates were determined by relating the traffic flow rate against the prevailing capacity of the highways. In a study by (Neena *et al*., 2018), the efficiency of a road link in Kondotty town, India was evaluated to determine the shortfall of the roadway segment in maximizing capacity. In this study, capacity utilization was measured by volume-to-capacity (v/c) ratio, and findings revealed the deplorable operating condition of the road, as flow levels exceeded the design service volume at the desired level of service. Another familiar and closely related roadway characteristic that is commonly found in literature is Intersection Capacity Utilization (ICU), which is a quantitative assessment of an intersection's traffic flow in terms of the volume/capacity (v/c) ratio for important turning movements (Goodall *et al*., 2013). The ICU

is commonly used to determine the Level of Service (LOS) of intersections. For instance, an intersection with an ICU of "1.00" is an indication of maximum capacity. Even though the assessment of ICU from this definition conforms with the evaluation of capacity utilization, it erroneously considers capacity utilization as a qualitative measure of effectiveness of a roadway, whereas it is not, but rather a quantitative measure.

The highway capacity manual (concepts), also defined capacity utilization of a transportation system as "*the amount of congestion experienced by users of the system, the physical length of the congested system, and the number of hours that the congestion exists*" (HCM, 2010). This definition is arguably very superficial in the sense that it does not properly reflect the usage of a roadway or the number of traffic volumes per lane, in relation to the estimated maximum number of vehicles it is expected to carry. In view of the identified gaps in research, it can be confidently concluded that scientific contributions that have looked into the estimation of roadway capacity utilization, with BRT dedicated lanes, using the fundamental diagram approach, in which flow is related to density, and speed is the slope, are scarce or virtually non-existent. As illustrated in figure 2.6, the flow density relationship is not a parabolic curve, rather the application of polynomial is merely to determine the maximum flowrate (Q) as a function of optimum density $(\mathrm{k_Q})$. The resultant slope is the speed $(\mathrm{U_Q})$. The flow/density parabola terminates at $(\mathrm{k_\tau})$. and the extended density $(\mathrm{k_j})$, is derived from the speed-density relationship. Consequently, by evaluating the definite integral of the three regions under the the flow/density curve and substituting equation 2.31 in each integral, we obtain equation 2.34, which can be expressed as:

$$\int_0^{k_Q}\left\{-\frac{u_f}{k_j}\left(\frac{u_f}{2\left(\frac{u_f}{k_j}\right)}\right)^2+(u_f)\frac{v_f}{2\left(\frac{v_f}{k_j}\right)}-c\right\}\partial k+\int_{k_Q}^{k_\tau}\left\{-\frac{u_f}{k_j}\left(\frac{u_f}{2\left(\frac{u_f}{k_j}\right)}\right)^2+(u_f)\frac{v_f}{2\left(\frac{v_f}{k_j}\right)}-c\right\}\partial k+\int_{k_\tau}^{k_j}u_f-\left(\frac{u_f}{k_j}\,k\right)\partial k \qquad 2.34$$

In equation 2.34, the first part deals with steady flow whilst the second and third parts deal with forced flow. Since the study is based on steady flow, it will focus on the steady flow only, given as:

$$\int_0^{k_Q}\left\{-\frac{u_f}{k_j}\left(\frac{u_f}{2\left(\frac{u_f}{k_j}\right)}\right)^2+(u_f)\frac{v_f}{2\left(\frac{v_f}{k_j}\right)}-c\right\}\partial k \qquad 2.35$$

It can be mentioned in passing that apart from the capacity and zero points, any flow on the curve will produce two densities and speeds. That raises the question of vehicle volume on the

road and explains why volume/capacity ratio is not an exact replica of flow/capacity ratio (capacity utilization). It is important to know the difference between the volume and flow of vehicles. Note that volume and flow are variables that quantify demand. Whilst volume describes the sheer number of vehicles being used within the roadway, flow relates to the speed at which the vehicles are moving along the roadway. In context, traffic density is the volume of vehicles per kilometre per lane. The argument is that beyond the optimum density as shown in Figure 2.6, more vehicles are added to the stream, and flow experiences contraction and speed drops with a corresponding increase in density until vehicles come to a halt at a jam state where the flow becomes zero. Keep in mind that beyond optimum density, traffic congestion is triggered. In passing, when traffic demand is great enough that the interaction between vehicles slows the speed of the traffic stream, this results in congestion. Traffic congestion is a condition that is characterized by slower speeds, longer travel times, shorter time headways, and increased vehicular queueing, as well as increased attendant problems like increased driving anxiety, carbon emission, and environmental degradation. In many studies, a traffic flow ratio less than 0.85 generally indicates that adequate capacity is available, and vehicles are not expected to experience significant queues (Ben-Edigbe *et al*., 2013). It is often called the threshold flow rate, suggesting that spare capacity is available at a lower speed. In any case assuming a threshold value of 85%, equation 2.35 can be divided into free flow and capacity-constrained parts expressed as:

$$\text{Free flow, } \int_0^{0.85}\left\{-\frac{u_f}{k_j}\left(\frac{u_f}{2\left(\frac{u_f}{k_j}\right)}\right)^2+\left(u_f\right)\frac{v_f}{2\left(\frac{v_f}{k_j}\right)}-c\right\}\partial k \qquad 2.36$$

$$\text{Constrained flow, } \int_{0.85}^{k_Q}\left\{-\frac{u_f}{k_j}\left(\frac{u_f}{2\left(\frac{u_f}{k_j}\right)}\right)^2+\left(u_f\right)\frac{v_f}{2\left(\frac{v_f}{k_j}\right)}-c\right\}\partial k \qquad 2.37$$

Since capacity utilization is the ratio of prevailing flowrate against road capacity it can be expressed as:

$$Q_u=\frac{q_p}{\left(-\frac{u_f}{k_j}\left(\frac{u_f}{2\left(\frac{u_f}{k_j}\right)}\right)^2+\left(u_f\right)\frac{v_f}{2\left(\frac{v_f}{k_j}\right)}-c\right)}\times 100\% \qquad 2.38$$

Where q_p = Prevailing flow (veh/h), and Q = Capacity. (veh/hr) [See equation 2.31]

2.5.1 Determination of Road Capacity Utilization Criteria Table

Criteria tables are used in context as the standard by which capacity utilization is decided. Each row of the road capacity utilization criteria table represents an occurrence of a single entity

within that entity set whereas each column represents an attribute, whilst the intersection of the row and column represents a single data value. Due to its non-existence in the literature, this study developed a capacity utilization criteria table under the steady flow condition. In presenting it, the method of assessment for the Level of Capacity Utilization (LCU) uses steady flow q and capacity Q as control parameters to describe five possible capacity utilization levels on a roadway. LCU divides the flow-density curve shown in Figure 2.10 into five levels (A to E), where LCU A is the best roadway capacity utilization and LCU E, is the worst. In other words, LCU E denotes traffic operation at free flow but poor capacity utilization, while LCU A denotes traffic operation at capacity ($v/Q = 1$), indicating excellent capacity utilization but poor traffic flow. Keep in mind that capacity utilization is a measure of efficiency not effectiveness. The primary concern of capacity utilization is high traffic flow relative to road capacity. According to (Ben-Edigbe *et al*., 2014), the volume-capacity ratio, which is also known as a measure of roadway occupancy or usage, represents the percentage of traffic moving through a route. Although there are no fundamental rules for how volume-capacity ratios should be distributed, it is generally prudent to have an equal distribution. As shown in Figure 2.7 and Table 2.11, the greatest proportion is set at 100 percent or LCU A, and the remaining percentages are distributed as 85 (LCU B), 75 (LCU C), 50 (LCU D), and 25 (LCU E) percent respectively. An appropriate cut-off point of 85% ratio often called the threshold had been established by the Transport Research Board (Williams, 2003).

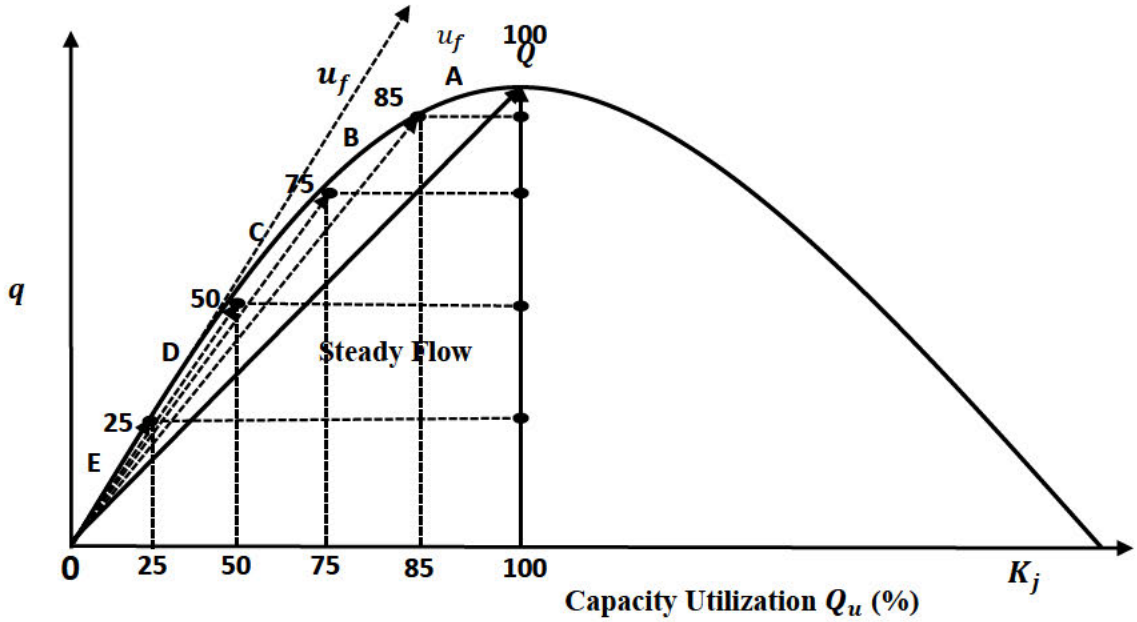

Note: $u_f \sim free\ flow\ speed,\ Q \sim capacity,\ q \sim flow,\ k_j \sim jam\ density$
Figure 2. 7: Hypothetical Capacity Utilization Curve

The proposed hypothetical capacity utilization criteria table is therefore presented in Table 2.5:

Table 2. 5: Proposed Hypothetical Capacity Utilization Criteria Table

LCU	(Q_u) %	Flow (Q) veh/hr	Density (k) veh/km/lane	Speed (u) km/hr	Time (s)
A	100	$100(Q_A)$	$100(Q_A) / u_A$	$100(Q_A)/ k_A$	$1/[100(Q_A) / k_A]$
B	85	$85(Q_B)$	$85(Q_B) / u_B$	$85(Q_B) / k_B$	$1/[100(Q_B) / k_B]$
C	75	$75(Q_C)$	$75(Q_C) / u_C$	$75(Q_C) / k_C$	$1/[100(Q_C) / k_C]$
D	50	$50(Q_D)$	$50(Q_D) / u_D$	$50(Q_D) / k_D$	$1/[100(Q_D) /k_D]$
E	25	$25(Q_E)$	$25(Q_E) / u_E$	$25(Q_E)/ k_E$	$1/[100(Q_E) / k_E]$

Note: LCU denotes the level of capacity utilization and Qu denotes capacity utilization

The following pertains to LCU criteria table interpretation. In Table 2.4, LCU standards using letters A through E, with A being the best and E being the worst capacity utilization. Most planning efforts in the context of capacity utilization typically use service flow rates at LCU B or C, to ensure an acceptable operating service for road users.

A: Capacity utilization is excellent even though traffic flow is unstable. At LCU A traffic flow is approaching or at capacity. Flow is irregular and speed varies rapidly because there are scanty usable gaps to manoeuvre in the traffic stream. Time headway and spacing reduced. Speeds are still at or near capacity. Any disruption to traffic flow will create a kinematic wave affecting traffic upstream and the incident will cause serious delays and queues. This is common in urban areas where road congestion is somehow inevitable.

B: Capacity utilization is very good even though flow tends to be erratic. At LCU B, speeds slightly decrease as traffic volume slightly increases. Although the choice of speed is free, the manoeuvrability has somewhat decreased. Time headway and spacing are also reduced. Low level of comfort for the driver.

C: Capacity utilization is good even though the flow is stable, at or near free flow. At LCU C, the ability to manoeuvre through lanes is noticeably restricted and lane changes require more driver awareness. Minimum vehicle spacing and time headway. Drivers are comfortable and posted speed limit is maintained. This is the target LCU for some urban and most rural highways.

D: Capacity utilization is poor even though traffic flow is operating near free flow. At LCU D, although posted speed limits are relatively maintained, manoeuvrability within the traffic stream is good. Motorists still have a high level of physical and psychological comfort.

E: Capacity utilization is very poor even though traffic flow is operating at free flow. At LCU E, Traffic is characterized by free flow, with low volumes and high speeds. The level of comfort is excellent as the driver needs minimal attention. Traffic flows at or above the posted speed limit and motorists have complete mobility on their lanes. Motorists have a high level of physical and psychological comfort. The effects of incidents or point breakdowns are easily absorbed. LCU E generally occurs late at night in urban areas and frequently in rural areas.

2.5.2 Hypotheses on Capacity Utilization Differentials

Consider the illustration shown in Figure 2.8 where roadway capacity for traffic scenarios with BRT (Q_1), without BRT (Q_2), and BRT dedicated lane capacity (Q_3), are estimated with relevant equations. Note that u_f denotes free flow speed, u_1 is the speed at capacity with the influence of BRT, u_2 is the speed at capacity without the influence of BRT, k_1 is the density at capacity with the influence of BRT, k_2 is the density at capacity without the influence of BRT, k_{31} is BRT dedicated lane density based on travel speed 'with BRT' influence, and k_{32} is BRT dedicated lane density based on travel speed 'without BRT' influence.

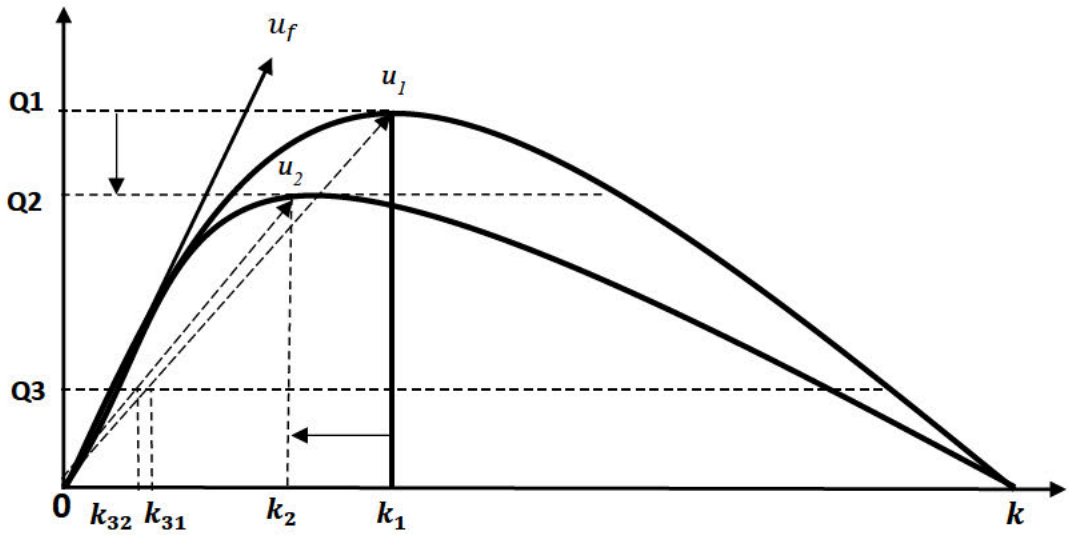

Figure 2. 8: Hypothetical Roadway Capacity Utilization Differentials

The three scenarios illustrated in Figure 2.8, show capacity utilisation loss due to BRT influence and dedicated BRT lane. BRT are buses that carry passengers throughout an entire BRT corridor and network using dedicated or shared lanes. Dedicated lanes are separated from

traffic congestion and conflicting movements, thus improving capacity and more dependable service to users. Whilst dedicated lane yields a good level of service for BRT, ultimately the downside is poor capacity utilization rate. As shown in Figure 2.7 capacity utilization is the extent to which the roadway capacity is productive. For example, a road with 2400veh per hour capacity is expected to carry about 85 percent of 2400 vehicles per hour or more during peak periods. A capacity utilization rate of about 70 percent at off-peak traffic periods is equally productive.

In context, with the influence of BRT, (Q_1) is the highest capacity hence the best utilization rate and where the influence of BRT is removed, (Q_2), is the next highest of the three scenarios whilst the BRT dedicated lane has the lowest capacity utilization. Not to be confused with the level of service, capacity utilization is inverse to the level of service. Level of service (LOS) is a qualitative measure used to relate the quality of traffic service. It is used to analyze roadways based on performance measures like traffic speed and flow. Whereas the level of capacity utilization (LCU) is a quantitative measure driven by flow and density. Since road infrastructure investments are costly and capital-intensive, their investment returns are measured in capacity utilization rate. Thus, the capacity utilization rate is the proportion of the production capacity of a road infrastructure that is currently in use. As shown in Figure 2.2, BRT dedicated lane ensures short travel time, the highest relative speed, and the lowest density compared to a shared carriageway lane. When lane dedication is not possible, BRT can be operated in mixed traffic. Based on the hypothesis that the BRT dedicated lane though useful in terms of service quality has an inbuilt low-capacity utilization rate, it is postulated that consideration be given to the mixed traffic flow concept devoid of traffic congestion and conflicts on BRT road network corridors. Capacity utilization of a roadway will experience shifts resulting from changes in the link traffic volumes or capacities and densities, causing inconsistencies in the rate at which traffic flows. The inconsistencies are caused by differentials in operational traffic volumes or operational capacities, and speed, which is the gradient of the flow-density curve is controlled by density. As previously mentioned, the concept of capacity utilization is underpinned by the fundamental diagram relationship between flow, speed, and density. As earlier mentioned, and in previous studies, a linear relationship exists between speed and density according to Greenshields. If the traffic flow and speed curves are related to a common independent variable, capacity utilization as illustrated in Figure 2.9, then a shift in flow along the speed axis will cause changes to capacity utilization. For example, where $q_{0.85}$ (threshold flowrate) is the control flow, the upward shift will trigger a decrease in capacity utilization and an increase in average speed. On the other hand, if the flow shift is downward,

capacity utilization will increase, and average speed will decrease. The utilization of a roadway is the ratio of the actual output to the maximum possible output. When capacity is fully utilized, flow and speed will be zero. During off-peak periods traffic flowrate is below the threshold of 85% or $q_{0.85}$ and at peak traffic flow rate is between; 0.85 to 1.0 or if you like between the threshold point and capacity. Keep in mind that the study is only interested in traffic flow under steady flow conditions, hence it terminates at capacity. The model technique of parabolic flow/density curve is an attempt to compute the maximum flow rate as a dependent variable and a function of the critical density. Moreover, the flow and density curves are skewed to the right and not entirely symmetrical. Note that the flow/density curve has three key points, 0, apex (Q), and jam density (k_j). The determination of the jam density on a skewed flow/density curve is based on speed/density linearity as shown in equation 2.20. Note that capacity utilization is a quantitative measure of efficiency that relies on density as the key independent variable. It should not be confused or interchanged with the level of service, a qualitative measure of effectiveness that relies on flow as the independent variable. Level of Service (LOS) defines how well vehicle traffic flows along a roadway whereas level of capacity utilization [LCU] determines how many vehicle traffic flows along a roadway.

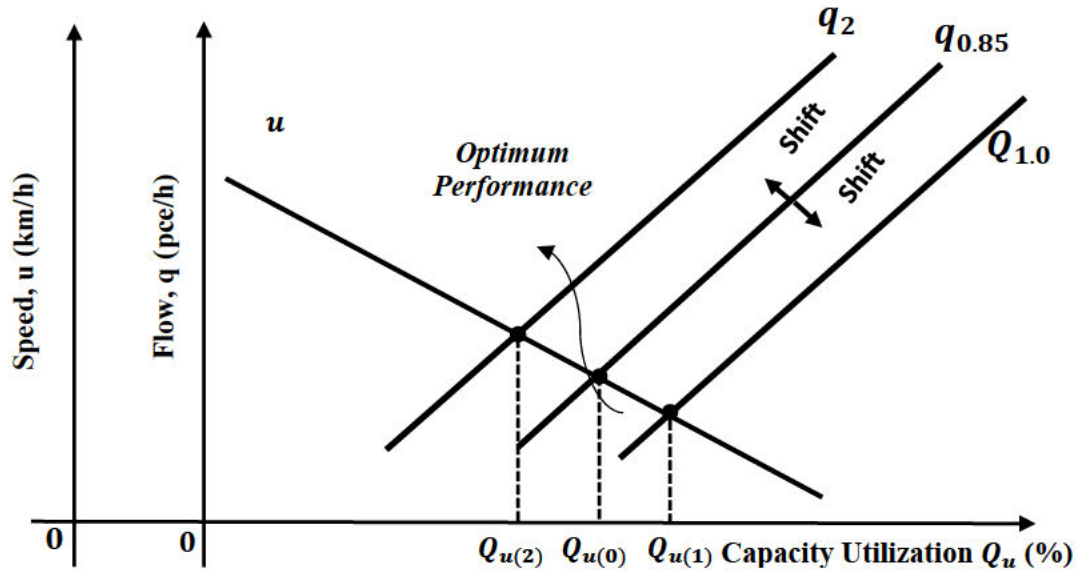

Figure 2. 9: Hypothetical Capacity Utilization Flow Shifts

Travel time, or the time required to traverse a route between any two points of interest, is a fundamental measure in transportation. As previously illustrated in Figure 2.9, speed is inversely proportional to flow, as well as capacity utilization, an increase in speed will cause a decrease in flow and capacity utilization and vice versa. However, travel time as illustrated in

figure 2.10, has a direct relationship with capacity utilization. In other words, an increase in road capacity utilization will also induce a travel time increase. According to (HCM, 2010), the average time spent by vehicles passing across a roadway segment is referred to as travel time. It is often considered by both road users and highway planners when evaluating road performance. The effectiveness of a roadway is measured by combining travel time with delay, and capacity (Ben-Edigbe & Mashros, 2012). Travel time is what most road users are concerned about and a useful guide for measuring the effectiveness of roadways when used in conjunction with delay and capacity utilization. Travel time is a key factor that travellers consider when making basic travel decisions. In this study travel time variability is presented as a generic term. It reflects a degree of variation in the travel time repeated over capacity utilization and asserted that increase in capacity utilization will trigger speed reduction and travel time increase.

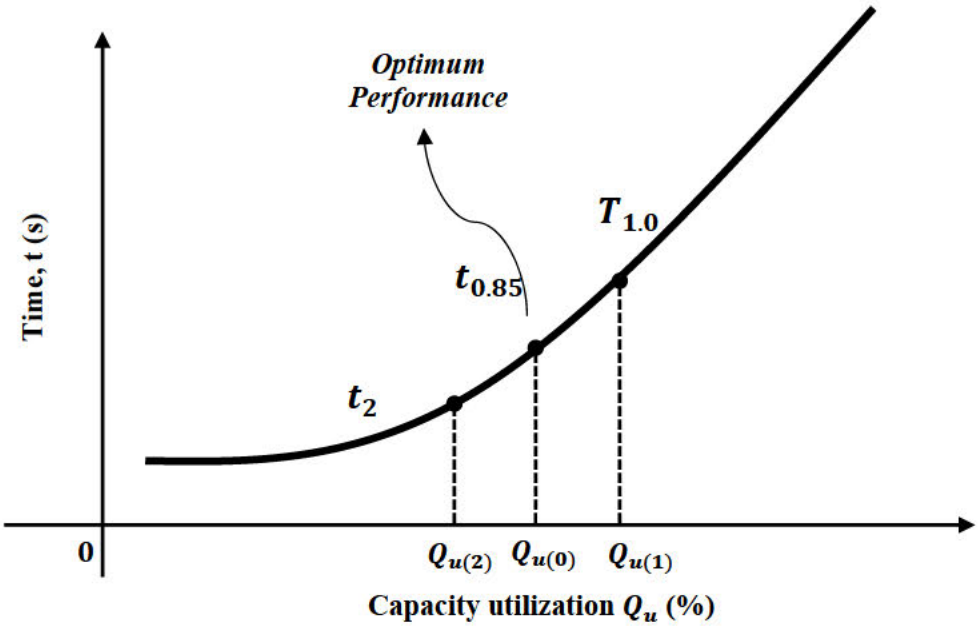

Figure 2. 10: Hypothetical Capacity Utilization Time Shifts

Generally, travel time over a roadway length can be predicted using the US Bureau of Public Roads (BPR, 1964) model equation given as:

$$T = t_f \left[1 + \propto \left(\frac{q}{Q}\right)^{\mu}\right] \tag{2.39}$$

Where T = travel time predicted over roadway length, t_f= travel time at free-flow speed Q = capacity, q/Q = degree of saturation (x), v = demand flow and $\propto$ = free-flow speed to the speed at capacity ratio.

BPR further stated that a high value of μ causes the speed to be unresponsive to "x" but as "x" tends to 1, the speed drops suddenly. The BPR 1965 version initially proposed the values 0.15 and 4 for "$\propto$" and "μ" respectively in the travel time equation. However, studies conducted on the BPR curve by (Dowling & Skabardonis, 1993) reported an underestimation of speed and re-plotted the BPR equation by proposing 0.2 for $\propto$ and 10 for μ. The new proposed values were later adopted and updated by BPR 1994.

For this study, the degree of saturation $q/Q < 0.9$, hence the values $\propto$ = 0.2, and μ = 10 are appropriate for off-peak traffic. The logic behind choosing off-peak is that peak travel data is distorted and skewed towards unsteady traffic flow. Nevertheless, the peak data is useful for constructing the criteria table discussed in the next section. Meanwhile, equation 2.40 is appropriate for mixed and non-mixed traffic conditions at off-peak conditions and can be re-written as

$$T = t_f[1 + 0.2(x)^{10}] \Longrightarrow \ T = t_f\left[1 + 0.2\left(\frac{v}{Q}\right)^{10}\right] \tag{2.40}$$

Travel time is crucial in determining traffic performance, where capacity is calculated using equation 2.31 then input equation 2.31 into equation 2.40 so that:

$$T = t_f[1 + 0.2(x)^{10}] \Longrightarrow \ T = t_f\left[1 + 0.2\left(\frac{v}{-c+(v_f)\frac{v_f}{2\left(\frac{v_f}{k_f}\right)}-\frac{v_f}{k_f}\left(\frac{v_f}{2\left(\frac{v_f}{k_f}\right)}\right)^2}\right)^{10}\right] \tag{2.41}$$

Equation 2.41 can therefore be used to calculate travel time in both mixed and non-mixed traffic conditions, taking advantage of the fundamental diagram's ability to determine traffic state at any point along the road section, regardless of whether capacity has been attained or not.

2.6 Time Headway Concepts

Time headway in traffic flow modelling and planning is considered a relevant control parameter that affects the behaviour of drivers, and it particularly plays a major role in the estimation of roadway capacity (Moridpour, 2014). According to the Highway Capacity Manual (HCM) 2010, time headway refers to "the time between two successive vehicles as they pass a point on a lane or roadway, measured in seconds from the same point on each vehicle (HCM, 2010). It is a microscopic characteristic of flow that has also found useful application in the estimation of Passenger Car Unit (PCU), Level of Service (LOS) evaluations,

analysis of safety, gap acceptance studies, and delay studies (J. Ben-Edigbe *et al*., 2014) It is a fundamental characteristic of the quality and quantity of traffic flow (Alhassan & Ben-Edigbe, 2012a), that describes the pattern of arrival of the leading vehicle and the one following it, at selected points on a roadway (Das & Maurya, 2017). Its analysis is one of the most important methods in traffic engineering, employed to understand the position of one vehicle relative to the other in a mixed traffic flow (Das & Maurya, 2017). It is typically calculated from a shared characteristic (such as the front/rear bump) of both cars as shown in figure 2.11.

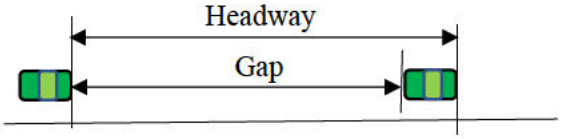

Figure 2. 11 Headway and Gap

In terms of quantitative applications, it is inversely proportional to capacity and traffic volumes. Furthermore, it has significant usage in traffic simulations, merge-diverge decisions of drivers at intersections, and traffic safety analysis (Das *et al*., 2019). Mixed traffic flows on roadways are characterized by incessant traffic manoeuvres, speed changes, and weak-lane discipline amongst other anomalous observations in the stream. The presence of vehicles of different sizes, varied manoeuvrability, and dynamic features often lead to differentials in-vehicle time headways varying from zero to several seconds (Das & Maurya, 2017), and then to minutes as in the case of BRT buses operating alone on dedicated lanes. On the adjoining lanes, these characteristics often result in transportation burdens such as delay, platooning, and ultimately traffic jams on as soon as jam density is reached, where all vehicles come to a stop.

The reciprocal of the minimum time headway determines the capacity of a roadway and the saturation flow rate of an intersection. Therefore, the time headways of vehicles in a traffic stream can be directly estimated using equation (2.42) which shows its simple basic relationship with traffic flow.

$$headway, h\ (s) = \frac{3600}{flow} \qquad 2.42$$

2.6.1 Time Headway Distribution Modelling

In traffic modelling and simulation, calibrating a suitable time headway distribution model is a vital step. Therefore, it is essential to statistically characterize the vehicle time headways using a distribution function (Roy & Saha, 2018). Thus, defining the headway distribution function is seen as being crucial to the study of traffic flow and the problems associated with its simulation. The production of inter-arrival times as an input into the simulation process is a

crucial step in establishing the performance of a simulation model (Gartner *et al*., 2002; Lieu, 1999; Roy & Saha, 2018). However, many earlier studies on this topic relied on homogeneous traffic and were thought to have low and medium traffic flows. Few studies have looked at modelling headways under heavy or congested traffic flow in the context of mixed traffic. Therefore, when making decisions on the development of transportation infrastructure, it is necessary to create a suitable headway model, especially in situations with mixed traffic (Gartner *et al*., 2002; Roy & Saha, 2018). In many developed Western countries, traffic congestion has also been a precarious issue, and transportation experts have been searching for effective solutions. They are thus looking for a uniform method of defining headways to characterize and model traffic in a congested condition of flow. This is since the typical strategy does not perform effectively in this circumstance, even when the traffic is homogeneous.

Conventionally, the headway data is typically described using the negative exponential distribution. However, for a traffic situation that is heterogeneous and car-following contact is frequent at higher flow levels, several studies have reported the use of several different models to explain the headway distribution pattern more clearly. Due to the presence of opposing flow, this is particularly bad on two-lane highways where it occurs fairly frequently. Mixed traffic, which consists of a wide variety of vehicles with different static and dynamic characteristics, makes the problem much worse. If the coefficient of variation is unity and the mean and standard deviation are plotted with an identical 45^0 angle, statistically speaking, the headway data can be regarded as exponential (Al-Ghamdi, 2001; Roy & Saha, 2018; Thamizh Arasan & Koshy, 2003). However, the exponential model has been found inadequate for characterizing headways according to research on the heterogeneity effect in traffic flows, as the coefficient of variation is likely to vary under such traffic, mostly due to complex traffic flow dynamics. A significant study has been done over the last few decades while recommending alternate distribution functions that are suitable for mixed traffic. For instance, at flow levels that correspond to peak hour traffic, the log-logistic and lognormal distributions were found to describe headway data better than off-peak hours, indicating a better approximation of congested traffic (Jang, 2012; Roy & Saha, 2018; Yin *et al*., 2009). Similarly, Pearson 5 and Pearson 6 distributions demonstrate their suitability at heavy flow and offer a respectable fit while describing the headways (Riccardo & Massimiliano, 2012). Almost a century later, the quest is still ongoing. Experts in the field of transportation are still attempting to develop accurate and useful descriptions of headways, especially where the predominant traffic is very heterogeneous and made up of a range of vehicles.

Using different approaches, many researchers have modelled the time headway distribution of mixed traffic flows on roadway segments and corridors. For instance, (Das & Maurya, 2017) examined vehicle time headway distributions on two-lane and four-lane roads for different flow levels in India using lognormal and log-Pearson statistical modelling methods. They further accessed the variations in vehicle time headways in morning and evening hours for different two-lane and four-lane roads under mixed traffic conditions. Their results not only captured the differences in headway distributions but also identified the headways of some types of vehicles, including the way vehicles maintain headways when headlights are turned on. In another study conducted in India by (Maurya *et al*., 2015), the distribution of speed and time headway of vehicles in a mixed vehicular flow on four two-lane bidirectional roads was examined using leader-follower vehicle pairs. Results show that the speed and time headway distributions varied significantly and were found to have useful applications in capacity estimations, level of service (LOS) analysis, and the development of micro-simulation models.

Time headway distributions were also modelled using three different probabilistic models (single, combined, and mixed) (Duy-Hung, 2012) in France. Results showed that the mixed models provided the best fits among several time headway samples. Using a traffic detector incorporated with laser sensors for sorting and analysis, (Jinhwan, 2012) developed theoretical traffic flow models to analyse time headway distributions. The results gave a better understanding of headway at signalized arterials. In another study conducted in Isfahan, Iran to assess driver behaviour at different highway lanes via headway distribution analysis, (Abtahi *et al*., 2012) investigated the lane position effects on time headway distributions through headway distribution models during high traffic flow levels. The results showed that the appropriate model for passing lanes differs from the one for middle lanes due to the different behavioural operations of drivers.

In a study conducted by (Ehsan *et al*., 2020), time headway, considering lateral distance was studied in a non-lane-based traffic flow using a novel approach, where time headways were divided into 5 intervals inform of measuring criteria to evaluate time headway values and implications as “Unsafe (0-0.7 sec), non-lane-based car-following (0.9 sec), lane-based car-following (1.0 sec), overtaking TH (1.3 sec), and free driving (larger than 2.5 sec)” (Ehsan *et al*., 2020). Results indicate that “the time headway of starting overtaking manoeuvre can be a good criterion to distinguish between following and free driving behaviour” Another closely related study conducted in China by (Chen *et al*., 2015) investigated traffic congestion and lane changing patterns involving interactions between BRT and general traffic flows at a typical

bottleneck along a BRT corridor. Results revealed abnormal lane violations resulted in a 16% reduction in the saturation rate of general traffic and 17% in bus travel time.

2.6.2 Time Headway Probability Distribution Models

Time headway probability distribution models, also known as statistical models, are widely employed in the field of traffic engineering because they effectively display the stochastic characteristics of traffic flows and reflect the inherent ambiguity in the car-following manoeuvres of drivers, under the prevailing traffic conditions. The empirical time headway data should be fitted using statistical models to identify a suitable headway distribution model. Typically, the distribution of time headways on highways is described by a negative exponential distribution. However, other studies have documented the usage of several additional models to explain the headway distribution pattern better fully. Furthermore, headway distributions for low and medium traffic flow rates were examined. Though all cars are in the car-following state, research that has been done on headway modelling at high flow is still minimal (Al-Ghamdi, 2001).

Thus, the underlying assumption of the current study considers the impact of heterogeneity on headway distribution models and, as a result, covers traffic flows ranging from mild to congested, wherein such an effect typically worsens due to frequent vehicle interactions. Therefore, to discover theoretical distribution models that suit headway data well, the present study considered the log-logistic, lognormal, log-logistic, Inverse Gaussian, Generalized Extreme Value (GEV), and Burr distributions. Using a methodology based on the goodness-of-fit tests viz the Akaike Information Criterion (AIC), the Schwartz or Bayesian Information Criterion (SIC or BIC), and the Hannan Quinn Information Criterion (HQIC), appropriate headway distribution models were chosen at 95% confidence level as well as 5% percent level of significance. These three goodness-of-fit test criteria are discussed in depth in the next chapter. The Kolmogorov-Smirnov (K-S), the Anderson Darling, and Chi-Square tests are the hypothesis testing methods frequently employed in traffic engineering, however, the AIC, SIC, and HQIC have been found to have advantages over the conventional three. Some probability distribution models are discussed below:

2.6.2.1 Lognormal Distribution

The well-known distribution model known as Lognormal is commonly employed in numerous research about headways. Additionally, modelling headways in instances where an automobile is following is suggested by (Greenberg 1966). The mathematical expression for the Lognormal distribution is:

$$f(t \mid \tau, \mu, \sigma) = \frac{1}{\sigma(t-\tau)\sqrt{2\pi}} \times \exp\left(-\frac{(\ln(t-\tau)-\mu)^2}{2\sigma^2}\right); t > \tau, \quad (2.43)$$

where: τ denotes the shift's value in seconds; μ and σ are the "location" and "scale" variables of the lognormal distribution, respectively. The following can be deduced from the observed data:

$$\hat{\mu} = \frac{\sum_{i=1}^{n} \ln(t_i-\tau)}{n}; \quad (2.44)$$

$$\hat{\sigma} = \left(\frac{\sum_{i=1}^{n} (\ln(t_i-\tau)-\hat{\mu}^2)}{n-1}\right)^{\frac{1}{2}} \quad (2.45)$$

$$f(x) = \frac{e^{\beta x} e^{-e^x/\alpha}}{\alpha^{\beta}\Gamma(\beta)} \qquad -\infty < x < \infty \quad (2.46)$$

2.6.2.2 Log Logistic Distribution

The log-logistic distribution is non-negative random variable probability distribution that is continuous and whose logarithm has a logistic distribution. Although it has heavier tails, it has a comparable shape to the log-normal distribution. Its cumulative distribution function can be expressed in closed form, unlike the log-normal distribution. The probability density function of a Log logistic distribution can be expressed as:

Probability Density Function:

$$f(x; \alpha, \beta) = \frac{(\beta/\alpha)(x/\alpha)^{\beta-1}}{\left(1+x/\alpha^{\beta}\right)^2} \quad (2.47)$$

and the Cumulative Distribution Function:

$$f(x; \alpha, \beta) = \frac{1}{1+(x/\alpha)^{-\beta}} \quad (2.48)$$

Where $x > 0, \alpha > 0, \beta > 0$.

2.6.2.3 Inverse Gaussian Distribution

The inverse Gaussian distribution is a family of continuous probability distributions with two parameters that has support on (0, ∞). It shares numerous characteristics with a Gaussian distribution. While the Gaussian represents a Brownian motion's level at a defined time, the inverse Gaussian defines the distribution of the time it takes a Brownian motion with positive drift to achieve a fixed positive level. The probability density function of the Inverse Gaussian Distribution is given by:

$$f(x; \mu, \lambda) = \sqrt{\frac{\lambda}{2\pi x^3}} \exp\left(-\frac{\lambda(x-\mu)^2}{2\mu^2 x}\right) \quad (2.49)$$

2.6.2.4 Generalized Extreme Value Distribution (GEV)

A family of continuous probability distributions known as the Generalized Extreme Value (GEV) was created from the extreme value theory. As a result, it serves as a limit distribution of correctly normalized maxima of a series of independent random variables with similar distributions. As a result, it is utilized as an approximation to describe the maxima of lengthy (finite) sequences of random variables. The distribution has a continuous scale parameter (k > 0) and a continuous shape parameter (k > 0). The PDF and CDF for this distribution are described as follows:

Probability Density Function (PDF):

$$f(x) = \begin{cases} \frac{1}{\alpha} exp\left(-(1+kz)^{-1/k}\right)(1+kz)^{-1-1/k}, & k \neq 0 \\ & k = 0 \\ \frac{1}{\propto}\exp(-z-\exp(-z)) & \end{cases} \quad (2.50)$$

Cumulative Distribution Function (CDF):

$$F(x) = \begin{cases} 1-\left(1+k\left(\frac{x-\mu}{\sigma}\right)\right)^{-1-1/k}, & k \neq 0 \\ \exp(-\exp(-z)), & \\ where & \\ z = \frac{x-\mu}{\sigma} & \\ & k = 0 \end{cases} \quad (2.51)$$

2.6.2.5 Burr Distribution

The Burr Distribution, also known as the generalized log-logistic distribution, is a continuous probability distribution for a non-negative random variable. To simulate household income, it is frequently utilized. Continuous shape parameters (k > 0; α > 0), continuous scale parameters (β > 0), and continuous location parameters (γ > 0) are present, and the PDF and CDF are given by:

Probability Density Function (PDF):

$$f(x) = \frac{\alpha k\left(\frac{x}{\beta}\right)^{\alpha-1}}{\beta\left(1+\left(\frac{x}{\beta}\right)^{\alpha}\right)^{k+1}} \quad (2.52)$$

Cumulative Distribution Function (CDF):

$$F(x) = 1-\left(1+\left(\frac{x}{\beta}\right)^{\alpha}\right)^{-k} \quad (2.53)$$

The Burr distribution is applied in this study to model traffic time headways due to its compatibility, flexibility, and appropriateness in modelling or fitting various types of headway

or frequency data. To decide which of the distributions is the most appropriate model for headway data on each road segment, six probability distributions viz: the Lognormal, Log Logistic, Inverse Gaussian, Generalized Extreme Value (GEV), and Burr distribution models were subjected to the goodness of fit tests also referred to as hypothesis testing.

2.6.3 Hypothesis Testing and Estimation of Model Parameters

The technique known as "goodness of fit" is used to confirm and determine whether a probability distribution is suitable for simulating a specific phenomenon. The Akaike Information Criterion (AIC), the Schwartz or Bayesian Information Criterion (SIC or BIC), and the Hannan Quinn Information Criterion (HQIC) were the methodologies used in this investigation. Although the Chi-Squared (C-S), Kolmogorov-Smirnoff (K-S), and Anderson-Darling (A-D) goodness of fit statistics are still widely used today, they are not theoretically the best ways to compare how well distributions fit data. They cannot include censored, truncated, or binned data and are also restricted to having accurate observations. The AIC, SIC or BIC, and HQIC however are statistical measures of fit generally known as information criteria. They are defined as follows:

- AIC (Akaike Information Criterion): The Akaike Information Criterion is defined by the following model equation:

$$\mathrm{AIC_c} = \left(\frac{2n}{n-k-1}\right)k - 2\ln[L_{max}] \tag{2.54}$$

- SIC (Schwarz Information Criterion, aka Bayesian Information Criterion BIC): The Schwarz Information Criterion, aka Bayesian Information Criterion, is defined as follows:

$$\mathrm{SIC} = \ln[n]k - 2\ln[L_{max}] \tag{2.55}$$

- HQIC (Hannan-Quinn Information Criterion): The Hannan-Quinn Information Criterion is defined as follows:

$$\mathrm{HQIC} = 2\ln\left[\ln[n]\right]k - 2\ln[L_{max}] \tag{2.56}$$

The objective is to identify the model with the given information criterion's lowest value. Each formula has the -2ln [Lmax] term, which is an estimation of the model fit's deviation. Each formula's first component contains coefficients for ‘k’ that indicate the severity of the penalty for the number of model parameters. When it comes to punishing the loss of a degree of freedom, SIC (Schwarz, 1978) and HQIC (Hannan & Quinn, 1979) are stricter than AIC

(Akaike, 1974). These three criteria are used to score each fitted model, whether it fits a copula, a time series model, or a distribution. Therefore, based on Maximum Likelihood Estimation (MLE), the model criterion with the lowest value each of AIC, SIC, or BIC, and HQIC, and the largest loglikelihood value provides the best fit. Amongst the three information criteria, the AIC ranking determines the best-fitted distribution.

2.7 Effect of BRT Time Headway Distribution Modelling on Capacity Utilization

In a similar manner to the behaviour of non-mixed heterogeneous traffic flows on the adjoining lanes discussed in the previous sections, BRT Mixed traffic flows on roadways or mixed traffic flows involving BRT buses are also characterized by traffic characteristics anomalies and time headway variations. BRT Mixed traffic flows also often lead to differentials in flow or capacity with attendant effects on time headways and capacity utilization at large. Other traffic parameters that are also affected are speed and density. However, there has been limited literature documented on these influences, to understand the attendant anomalous changes in traffic characteristics such as capacity utilization. Roadway capacity is very sensitive to the distribution time headways associated with it both in a non-mixed or a mixed traffic flow involving BRT vehicles (Ben-Edigbe & Johnson, 2014). He also opined in another study that roadways that deliver good operational services are expected to meet their attendant performance design standards (Mashros & Ben-Edigbe, 2014). However, the amount to which a good roadway service can be provided is consequent upon several influencing factors, including traffic, road, and environmental conditions (Makinde & Ben-Edigbe, 2019).

Furthermore, roadways according to their design must not only be able to withstand structural vehicular loads but also sustain functional mixed and non-mixed traffic flows over time. In this light, it is possible to argue that both structural and Functional Quality of Service (FQOS) can be important performance measures. The focus of this study is on mixed traffic capacity utilization caused by BRT dedicated lanes and the implications on time headways. Mixed traffic refers to cars that have a wide range of physical and performance qualities. Cars, buses, Lorries, auto-rickshaws (three-wheelers), motorized two-wheelers, and various non-powered vehicles such as bicycles, and human and animal-driven carts are among these vehicles. Because these vehicles share the same right of way, they have several distinguishing characteristics that are not present in homogeneous traffic situations. These characteristics include variances in driver behaviours of different types of vehicles and their impacts on the traffic stream, in addition to the most conspicuous weak lane-discipline conduct. Due to the peculiarities mentioned above, the traffic flow theory created for homogeneous traffic cannot be applied to mixed traffic settings without considerable changes. However, much of the latter's

present theory and time headway models are based on principles that were developed primarily for homogeneous traffic (Mallikarjuna, 2007). Indeed, the validity of these principles has recently been questioned, and efforts have been made to propose new or modified ideas that are more appropriate for mixed traffic scenarios. (Khan & Maini, 1999) made the most recent attempt, however, their study focused mostly on macroscopic flow correlations and micro-simulation models (Verma, 2016). Since then, there has been significant progress in our understanding of mixed traffic dynamics and is attendant time headways. To study heterogeneous or mixed traffic, it is essential to understand the characteristics of each vehicle type and their resulting behaviour in the traffic stream (Patel & Joshi, 2012), hence a unique vehicle type that is the focus of this study is BRT. Although BRT mixed traffic operations have been found in studies by (Chen *et al*., 2015; HCM, 2010; Mohan & Ramadurai, 2013; Wirasinghe *et al*., 2013), to reduce both BRT and mixed traffic travel speed, reduce time headways to unsafe values, reduce capacity, increase travel time as well as create bottlenecks on the adjoining lanes to the BRT dedicated lanes, and for which the increment in travel time may lead to a decline in the quality of service, the consideration or recommendation of a mixed traffic scenario involving the flow of vehicles on the adjoining lanes together with BRT buses is expected to result into slightly increased but safer headways, which would consequently enhance or maximize capacity utilization. These expected outcomes have been discussed in later chapters of this report.

2.8 Summary

So far it has become vital to review previous literatures that are germane to this study, including the attendant theoretical framework to support emerging assertions and findings in subsequent chapters. Eight significant and germane areas of discussion viz: Bus Rapid Transit (BRT), roadway capacity, passenger car equivalents (PCEs), Roadway Capacity Utilization (RCU), time headways, and time headway distribution modelling, were discussed in detail. Relevant works of literature on roads and traffic in South Africa were reviewed and it was opined that roadways with BRT dedicated lanes have attendant bottleneck traffic anomalies. According to the relevant literature on roads and traffic characteristics in South Africa, it was found that in all the provinces where BRT exists, most roads are multilane roads with three lanes and the median BRT configuration was adopted for the BRT infrastructure with BRT stations located in between segments. The road is the primary mode of transportation in South Africa designated as either N – National, R - Regional, or M – Municipal, depending on the government authority or agency overseeing its operations and maintenance.

Roadway traffic in South Africa is made up of various vehicle types which constantly interact with one another in a traffic stream displaying attendant macroscopic and microscopic attributes under different prevalent traffic conditions viz environmental, control, weather, and mixed traffic conditions involving BRT buses. BRT in Cape Town was also discussed, and the median configuration was identified as the main adopted design, with adjoining lanes supporting traffic flow in both directions. With the prior introduction of the concept of roadway capacity, the chapter further discussed the concept of road capacity utilization which refers to how well the roadway space is utilized or maximized. The chapter assessed roadway capacity utilization using the volume-to-capacity ratio as a performance measure. The LCU used five classes A to E for assessment in which class A indicates excellent capacity utilization, and E represents poor capacity utilization.

From the arguments hitherto, the chapter recognizes and supports the opinion that the capacity of roads is stochastic and based on their benefits and drawbacks in the evaluation of roadway capacity, several capacity estimation techniques were highlighted and evaluated in context. The headway and the fundamental diagram methods were identified the best due to their suitability and applicability for both peak and off-peak traffic conditions. However, the most preferred method for the evaluation of capacity and capacity utilization is the fundamental diagram method. This is because it enhances the understanding of roadway traffic operations through the application of the three fundamental traffic flow parameters viz, flow, speed, and density. These parameters are essential because the study is interested in their differentials under mixed traffic scenarios due to the introduction of BRT infrastructure.

Overall, research into the influence of BRT dedicated lanes on mixed traffic capacity utilization and time headway implications, and the development of a novel capacity utilization criteria table has not been previously embarked on prior to this study, as there is little or no evidence of existing literature on the subject matter. Perhaps the closest research hitherto has been on the effect of introducing BRT on existing major arterials in Addis Ababa, Ethiopia based on Level of Service (LOS) and delays only at intersections. This study will plug into this research gap in BRT studies and introduce the capacity utilization concept for road performance evaluations and improvements. The next chapter gives a methodological framework of the entire study.

CHAPTER 3

RESEARCH METHODOLOGY

3.1 Overview

Chapter three aims to set out the analytical and empirical background for the case studies discussed in Chapters Four, Five, Six, and Seven. Central to the impact of Bus Rapid Transit (BRT) on roadway capacity utilization study is the estimation of roadway capacity and the computation of critical density for free flow traffic conditions where capacity often occurs. In the conclusions reached in the literature review, the roadway capacity estimation method with traffic flows and density was considered suitable for the study. This study is focused on how BRT affects capacity utilization of the roadway under mixed traffic conditions and its implications on the attendant time headways. Recall as stated in Chapter 2, that the methodology employed for this study was empirical, based on survey data obtained directly from a 'with and without' BRT set-up of the four sites. In view of this, data on flow, speed, headway, of vehicles, and BRT flow rates are germane parameters. In addition to the BRT buses, the other vehicles surveyed in this study were passenger cars (PC), medium goods vehicles or medium vehicles (MV), and heavy goods vehicles or heavy vehicles (HV). However, to ensure the validity of the sample survey, the study sites must be representative of the local population.

With respect to time headway implication, which has a consequence on the capacity utilization of the roadways investigated, this thesis acknowledges that the time headway of vehicles in a mixed traffic flow scenario beside BRT dedicated lane is continuous and hence follows some stochastic probability distribution models. To confirm whether this hypothesis is true, the distributions are fitted to the time headway data. Visual inspection of the PDF, CDF, and P-P plots are three main determinants of how well the distribution model fits the data. Two additional performance indicators are the probability (P) and Log likelihood (LLH) values. The P value gives the probability or likelihood of finding a particular set of observations if the null hypothesis were true. The maximum LLH value shows the best-performed model. These will be discussed in detail in the subsequent sections of this chapter.

The mixed traffic on the adjoining lanes to BRT dedicated lanes is characterized by unsafe vehicle manoeuvres, unsafe overtaking, weak lane discipline, erratic driver behaviour, oscillatory movements, and platooning, especially towards intersections (Modupe & Ben-Edigbe, 2023). These anomalous traffic characteristics are consequently characterized by time

headway variabilities, which lead to traffic burdens such as longer travel time, reduced speed, etc., and affect the capacity utilization of the roadway (Roy & Saha, 2018). Hence as earlier mentioned the time-headway distributions in this study were analyzed using statistical probability distribution models. Given the foregoing, this chapter's goal is to lay forth the theoretical and empirical underpinnings for the data that was collected at the selected sites.

The study's main objectives were to estimate traffic characteristics of the anomalous flow generated by the presence of BRT dedicated lanes through flow-density models, using the fundamental diagram approach. According to the hypothesis mentioned in the method of the study section, that " BRT dedicated lane at the median of a roadway segment causes anomalous traffic stream characteristics, including time headway and lane capacity differentials, with attendant anomalous capacity utilization effects", the aim and objectives of this research would be achieved through a stepwise methodological framework, which is described in the next section. Considering this, the information gathered, and survey data are quantitative. Quantitative measurements were carried out at the four chosen sites.

This chapter is hereby organized as follows: the methodology framework adopted for the study is discussed in Section 3.2; Section 3.3 gives an exhaustive description of the study site, which includes its location and selection criteria. Other contents presented under this section are data collection method, sample size, survey team and equipment, the layout of the survey site, traffic and BRT survey data, and time headway distribution analysis. Appraisal of sample data and method of analysis are described in section 3.4, while section 3.5 gives the pilot study with attendant discussions. The chapter ends with a summary presented in section 3.6.

3.2 Research Methodology Framework

In this study, observations were made, and sample surveys were taken at the study sites in Cape Town, South Africa as part of the empirical research methodology. The study's methodology is represented by the framework in Figure 3.1. The empirical method was used in tandem with an analytical approach, where the empirical method entails set up, extraction, and evaluation of traffic data parameters including volume, and speed from the ATC, and the analytical approach involves the development of flow-density models to obtain the maximum flow i.e. capacity, and subsequently other related traffic parameters such as density, free-flow speed, etc. Before the application of the empirical ‘with and without BRT’ approach, the ‘before and after’ BRT approach, stated in chapter one was first experimented. Consequently, in the analysis that follows, the period before BRT is designated as the pre-BRT year 2009, while the periods after BRT are the pre-lockdown year 2019 and post-lockdown year 2020.

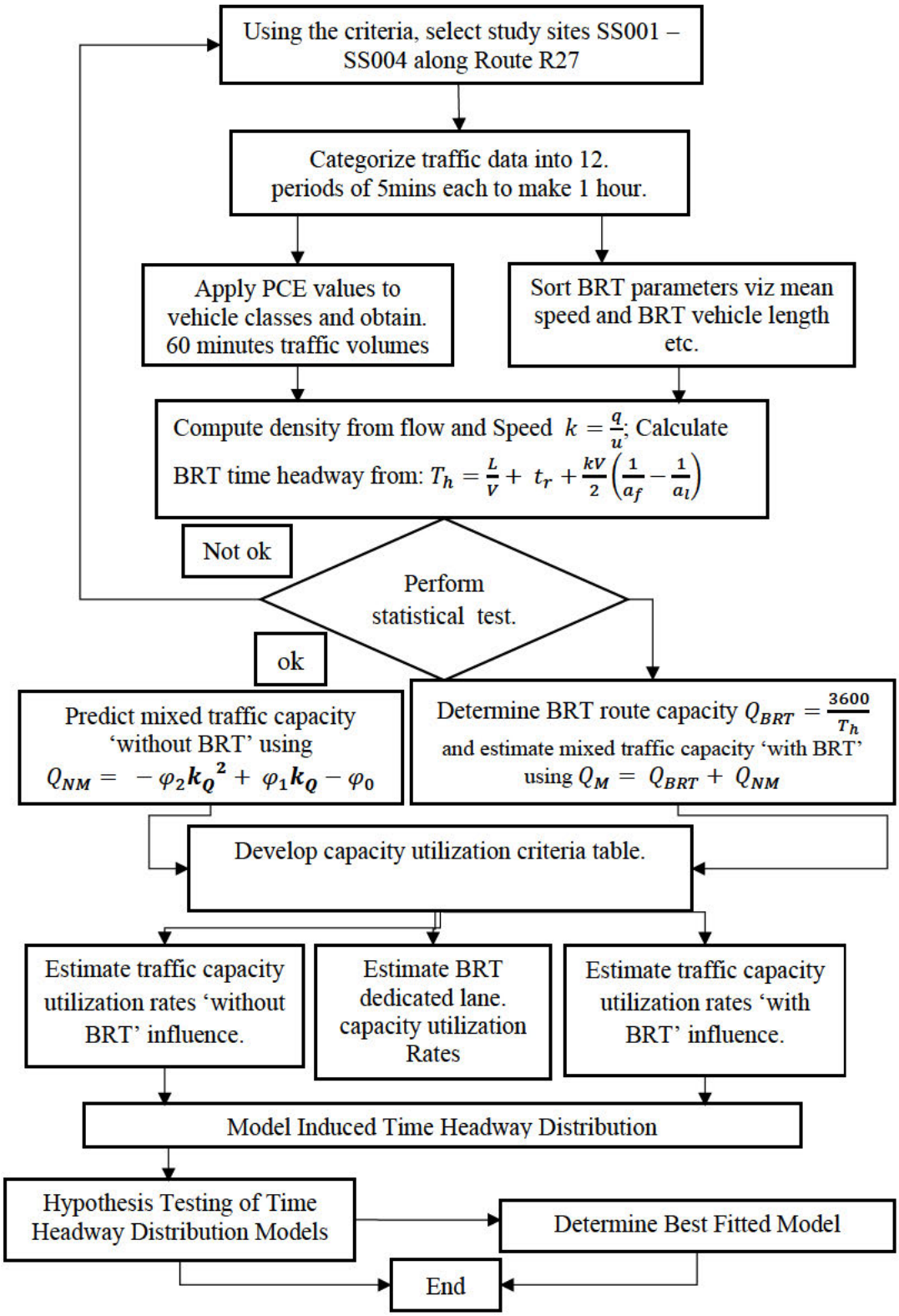

Figure 3. 1: Flowchart of Research Methodology Framework

The estimation of capacity as previously mentioned in chapter two is done using different techniques (Minderhoud *et al*., 1996). Empirical traffic data were collected at four chosen locations/segments along the BRT route R27 in Cape Town, South Africa for 12 weeks, during daylight hours and dry weather conditions. The data were collected using an Automatic Traffic Counter (ATC) that was installed at each of the four sites for 24 hours a day, during the period. Each location had two ATC loggers with one installed to log traffic data on the BRT dedicated lane and the other to record data on the adjoining lanes. Pneumatic tubes were installed and connected to the ATC loggers according to the specifications and configurations, where a pair of pneumatic sensor tubes each, was nailed parallel to each other onto both lanes at 1m apart. The data collected were sorted and processed. The loggers identified three types of vehicles: passenger cars (PC), medium vehicles (MV), and heavy vehicles (HV), and were investigated accordingly. The ATC recorded the following vehicle data: speed, volume, weight, headway, gap, class of vehicle, and date and time of sensor tube hits. Using the relevant passenger car equivalents (PCE) values recommended by SANRAL, the traffic volume in veh/hr was translated to traffic flow in pce/hr. To prevent skewed results, the PCE values were adjusted to match the study's actual circumstances. To maximize the likelihood of unbiased vehicle data gathering, the segment length (L) must be bigger than the stopping sight distance (SSD), hence this was ensured. Using the 'before and after BRT approach, the predicted capacity of traffic flows on the adjoining lanes was referred to as non-mixed traffic capacity Q_{NM}, while the capacity estimated by the summation of Q_{NM} and Q_{BRT} is referred to as mixed traffic Q_M. These parameters were determined for the pre-BRT year (2009), pre-lockdown year (2019), and post-lockdown year (2021).

3.3 Study Site

3.3.1 Location and Criteria for Selection

South African metropolitan roads are mainly constructed as three-lane roadways except for some national and regional roads under the administration of the National Department of Transport (NDOT). The study site is R27, situated along the major trunk route T02 (Atlantis – Table View – Civic Centre), as shown in Figure 3.2 is not an exception to this design. It is a provincial route in South Africa that belongs to the second category of roads in the South African route-numbering scheme and is referred to as a major regional route. It is made up of two parts that are not connected. The first leg, often known as the West Coast Highway, runs along the West Coast from Cape Town to Velddrif. The second stretches from Vredendal to Keimoes on the N14 at Upington, passing through Vanrhynsdorp, Calvinia, Brandvlei, and

Kenhardt. Although the route between Velddrif and Vredendal has never been built, it can be driven on gravel roads. The R27 designation used to extend from Upington to Pretoria, but this portion was eventually absorbed into the N14 and other roads. It begins at an interchange with the N1 Highway in Cape Town (east of the city center; next to Table Bay). It begins with a 13-kilometer journey north as Marine Drive through Milnerton to a junction with the M14 road. It then connects Table View and Bloubergstrand in the east and ends at a junction with the M12 road in the west. The R27 continues north as West Coast Road for 10 kilometres, passing through the Blouberg Nature Reserve until it reaches a crossroads in Melkbosstrand, where it meets the M14 and M19 roads again.

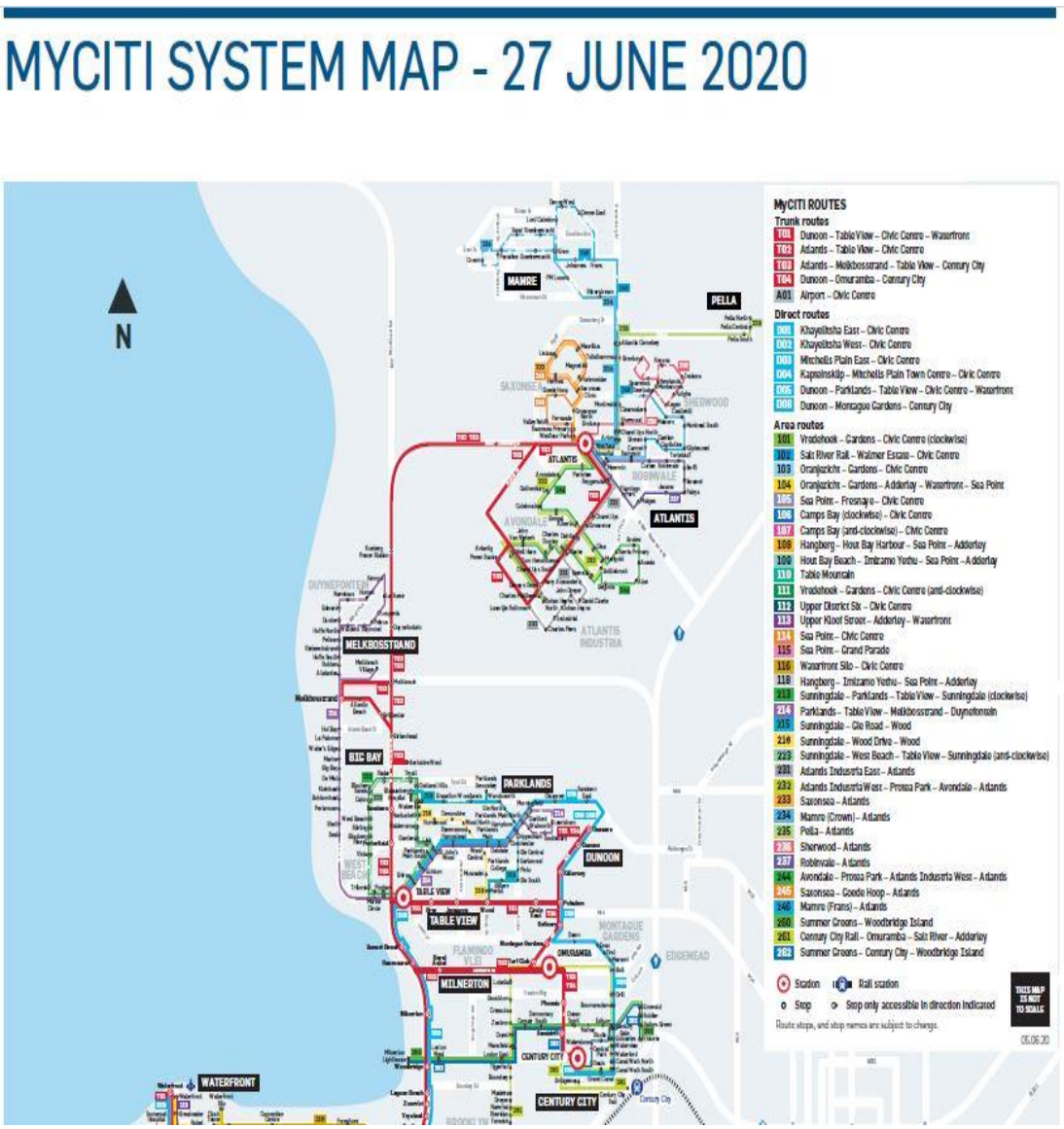

Figure 3.2: MyCiTi System Map Showing the Major Trunk Routes, Cape Town South Africa

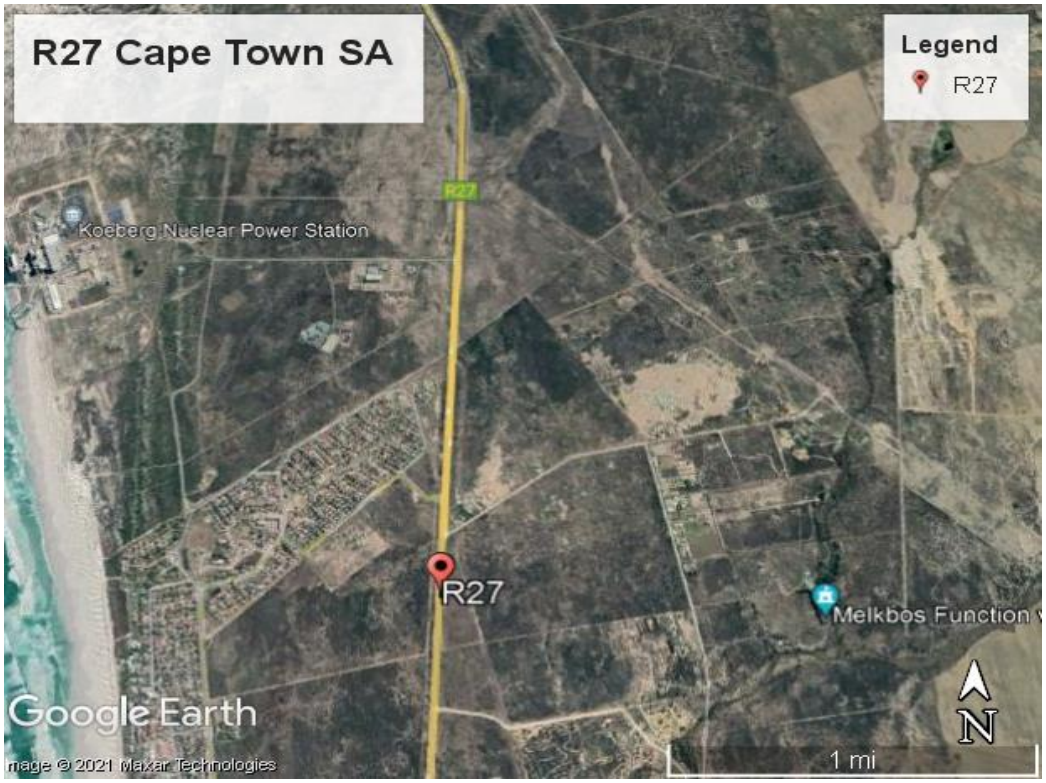

Figure 3. 3: R27, Cape Town, South Africa

It continues north for 49 kilometres until it reaches a connection with the R315 road east of Yzerfontein, where it leaves the City of Cape Town. The highway links with FW de Klerk Boulevard (N1) near Table Bay Harbor in Cape Town and then proceeds north along the coast for the Marine Drive portion. Many industrial warehouses line this stretch of road. The M14 eventually becomes the main coastal road as the road travels further inland. Before reaching Velddrif, the route continues north, passing through West Coast National Park. In terms of relevance, the Regional Main Road 27 is a sub-corridor of the Northern Growth Corridor (NGC) that is planned to facilitate the development and urban sprawl of the north of Cape Town through unrestricted commuter transit and tourism.

The NGC in Cape Town is a historically underdeveloped physical area that the South African government intends to turn into a mature activity corridor. Other elements identified as critical components to enhance developmental opportunities on this corridor, according to (Warnich & Verster, 2004), are economic potential, the natural environment, and the presence of a nuclear facility, the Koeberg Nuclear Power Station, which is Africa's only nuclear power station and the largest in the Southern Hemisphere. It has Africa's largest power station turbines, and the condensers are cooled by seawater, making it a one-of-a-kind facility. The picturesque R27 is a tourist destination in and of itself. The R27 is referred to as the "West

Coast experience" in tourism publications. People travel to the West Coast to attend flower displays, wine tastings at the district's different cellars, or simply to feel the landscape. More importantly, the R27, an existing route contributes to economic growth. Many visitors to the area like to utilize the R27 route because of its aesthetic appeal, and as a result, they are exposed to business activity along the way. The Bayside shopping center is in the Blaauwberg neighbourhood, close off the R27. It can be thought of as an economic centre that draws individuals from across the country. This is just one of the many shopping centres that have sprung up in recent years. Blaauwberg Century City, near the study area, is a regional shopping and entertainment complex. This retail centre houses 450 stores and is located near Ratanga Junction, Africa's first full-scale theme park, which is open from November to April. The regional route R27 was selected specifically because it met the expected and necessary geometric design criteria. A preliminary research visit was made to Johannesburg and Pretoria; however, the two sites did not meet the design criteria.

The BRT roadway at both sites had too many intersections and steep vertical alignments that could affect free flow speed data, the BRT route R27 in Cape Town was selected. Within the established research boundary, the study site was chosen based on the following criteria:

- The geometric feature of the roadway under investigation must include the presence of a BRT dedicated lane, precisely with a median configuration design and two adjoining lanes that run in parallel to it.
- The roadway segment must have a relatively flat topographical terrain void of too many steep vertical slopes that can affect the free flow speed data.
- Roadway segments must be free from the influence of road intersections, on-street parking, broken-down vehicles, traffic police checkpoints, roundabouts, and fuel filling stations along the route, which can also affect the free flow speed data.
- It must be ensured that survey equipment is set up at spots where there is sufficient free flow speed, and the segment length is greater than the stopping sight distance (SSD).
- The survey must be conducted under dry weather and not on a rainy day or period. Rain and wet pavement surfaces cause a reduction in free-flow speed.
- Roadway pavement surface must be free from surface defects viz, rutting, potholes, etc.

3.3.2 Site Coding and Assessment

It is crucial to detail the characteristics of each road section because the study locations were carefully chosen using the criteria. Therefore, to facilitate easy identification, the four selected

sites were assigned site codes. The preferred coding scheme is "SSyyy," where "yyy" stands for the sites' serial numbers and "SS" stands for the study site acronym. By way of illustration, "SS001" stands for "study site of serial number 001". While each site's specific evaluation is provided in the sections that follow, Table 3.1 displays the codes for all the study sites.

Table 3. 1**:** Study Site Identification Codes

Site Name	Site Code	Site Number
Sandown Station – Porterfield Station	SS001	001
Porterfield Station – Sandown Station	SS002	002
Table View Station – Sunset City Junction	SS003	003
Sunset City Junction – Table View Station	SS004	004

3.3.2.1 SS001 - Sandown Station – Porterfield Station

The Sandown Station – Porterfield Station roadway is a three-lane segment with one BRT dedicated lane running parallel to the median and two adjoining lanes also running parallel to it. It is a typical provincial road with an average daily traffic count of 12355 veh/day and a design speed of 80km/h. A speed limit of 70 km/h is posted on the asphalt-paved road, which has a 20-year pavement design life. The roadway is flat with minimal horizontal curves where it is situated. Vehicle traffic on this road is directed from Sandown Station – Porterfield Station. The two adjoining lanes are both 3.7 m wide and with a shoulder width of 2.5 m. The length of the road segment is 2120 m long and runs along the Atlantis axis to Sunset City route, precisely between Sandown Station – Porterfield Station. The length of the road exceeds the permitted stopping sight distances from Sandown Station and Porterfield Station, which are 210m and 550m, respectively. For twelve weeks, the road section's traffic data were continually recorded. There are a variety of vehicle kinds on this road, including motorcycles, lightweight, medium-weight, and heavy-weight automobiles, however, the proportions of each type of vehicle vary.

3.3.2.2 SS002 - Porterfield Station – Sandown Station

The Porterfield Station – Sandown Station roadway is in the opposite direction of the Sandown Station – Porterfield Station roadway. It has the same features as that of the Sandown Station – Porterfield Station roadway. Vehicle traffic on this road is directed from Porterfield Station – Sandown Station. The two adjoining lanes are both 3.7 m wide and with a shoulder width of 2.4m. The average daily traffic is about 12069 vehs/day with a design speed of 80km/hr. Due to a shift in the direction of vehicle travel as recorded by the ATC, the traffic statistics changed. Different vehicle types are present in different quantities in the traffic mix.

3.3.2.3 SS003 - Table View Station – Sunset City Junction

The Table View Station – Sunset City Junction roadway is also a three-lane segment with one BRT dedicated lane running parallel to the median and two adjoining lanes also running parallel to it. It is also a typical provincial road with an average daily traffic count of 14887 veh/day and a design speed of 80km/h. A speed limit of 70 km/h is posted on the asphalt-paved road, which has a 20-year pavement design life. The roadway is flat with minimal horizontal curves where it is situated. Vehicle traffic on this road is directed from the Table View Station towards Sunset City Junction. The two adjoining lanes are both 3.7 m wide and with a shoulder width of 2.1 m. The length of the road segment is 2120 m long and also runs along the Atlantis axis to the Sunset City route, precisely between Table View Station – Sunset City Junction. The length of the road exceeds the permitted stopping sight distances from Sandown Station and Porterfield Station, which are 210m and 550m, respectively. For twelve weeks, the road section's traffic data were continually recorded. There are a variety of vehicle kinds on this road, including motorcycles, lightweight, medium-weight, and heavy-weight automobiles, however, the proportions of each type of vehicle vary.

3.3.2.4 SS004 - Sunset City Junction – Table View Station

The Sunset City Junction – Table View Station roadway is located in the opposite direction of the Table View Station – Sunset City Junction roadway. It has the same features as that of the Table View Station – Sunset City Junction roadway. Vehicle traffic on this road is directed from the Sunset City Junction – Table View Station. The two adjoining lanes are both 3.7 m wide and with a shoulder width of 0.98m. The average daily traffic is about 14140 veh/day with a design speed of 70km/hr. Due to a shift in the direction of vehicle travel as recorded by the ATC, the traffic statistics changed. Different vehicle types are present in different quantities in the traffic mix.

3.3.2.5 Summary of Selected Study Sites

Table 3.2 contains a geometric overview of the sites based on the evaluation of the chosen sites as described in sections 3.3.2.1 through 3.3.2.4. It is clear from Table 3.2 that all study sites satisfy the requirements mentioned in section 3.3.1 and are therefore suitable for the study. The data collection techniques and equipment are covered in section 3.4 since empirical data must be gathered from the chosen road.

Table 3. 2**:** Summary of Geometric Features of Selected Study Sites

Site Features	SS001	SS002	SS003	SS004
Name of Road	SS to PS	PS to SS	TVS to SCJ	SCJ to TVS
Type of road	R27	R27	R27	R27
Terrain Type	Level Terrain	Level Terrain	Level Terrain	Level Terrain
Annual Daily Traffic (ADT)	12355 veh/day	12069 veh/day	14887 veh/day	14140 veh/day
BRT Lane	Yes	Yes	Yes	Yes
Number of Adjoining Lanes	2	2	2	2
Width of Adjoining Lanes	3.7m/ln	3.7m/ln	3.7m/ln	3.7m/ln
Pavement Surfacing	Asphalt	Asphalt	Asphalt	Asphalt
Length of Road Segment	1250	1250	1200	1200
Presence of Shoulder	Yes	Yes	Yes	Yes
Width of Shoulder	2.5m	2.4m	2.1m	0.98m
Width of BRT Lane	4.3m	4.3m	4.3m	4.3m
Posted Speed	70km/hr	70km/hr	70km/hr	70km/hr

SS ~ Sandown Station, PS ~ Porterfield Station, TVS ~ Table View Station, SCJ ~ Sunset City Junction

3.3.3 Data Collection – Survey Method and Equipment

3.3.3.1 Sampling

The survey period during which data was collected was a time when Cape Town was experiencing relatively dry weather, precisely from September to November 2021, hence the data was void of the influence of rainfall or wet pavement surface. Traffic data collected on the selected segments during the week were carefully sorted. They were separated from the data logged during the weekend, as there were low traffic volumes during the weekend. It was decided that sample size was required to make conclusions about population estimates. The population size was determined to be 2000 vehicles per hour in accordance with the international standard specification of (HCM7, 2022; HCMTRB, 2012; Salisu et al., 2020a), for multilane roads. Thus, using equation 3.1 and a 95 percent confidence interval with a 5 percent margin of error, the sample size was obtained for this population size.

$$s = \frac{X^2\, NP(1-P)}{d^2(N-1) + X^2 P(1-P)} \qquad 3.1$$

Where s = required size

X^2 = 3.84 (chi-square value for 1 degree of freedom at desired confidence level)

N = population size

P = population proportion (taken as 0.5 to provide maximum sample size)

d = degree of accuracy or margin of error expressed as proportion = 0.05

The minimal sample size needed for a population of 2000 vehicles per hour is 322 vehicles per hour, according to equation 3.1 when combined with its table, shown in (Appendix II). To accurately represent traffic statistics for all traffic situations under consideration, the sample size of 322 vehicles per hour is sufficient. However, the ATC continually gathered traffic statistics for twelve weeks. The period's continuous traffic data collection made it possible to collect enough data that was far larger than the population size predicted earlier.

3.3.3.2 Survey Team and Equipment

Sequel to obtaining permission from the Western Cape Department of Transport and Public Works (WCDTPW), the survey team, made up of the lead researcher and an assistant, moved to the site and initialized the commencement of the survey by first installing the ATCs at the selected road segments. The researcher carried out all aspects of the survey from the control of moving vehicles to the end of the installation of tubes and ATC setup. The ATC and its attachments viz a hammer, a metre rule, a laptop computer, road cones, a measuring wheel, reflective jackets, nails, a padlock, a security chain, a digger, and measuring tape are among the tools used. Before installing the ATC, the road section's stopping sight distance was first calculated, as shown below. First, operational speed was measured using stopwatches, two red cones labelled "c_1" and "c_2," and during the free-flow time. The two cones (c_1 and c_2) were positioned 20 meters apart along particular road segments. The first and second cones each had a time of passage (t_{c1} and t_{c2}) that was noted and recorded as the vehicles drove by. The time required to travel the distance between the two cones is represented by the difference between the first observed time, t_{c1}., and the second observed time, t_{c2}. During the free flow phase, this process was repeated at random for varied numbers of cars. Equation 3.2 was used to compute each vehicle's speed.

$$s_{osi} = \frac{D}{t_i} \qquad 3.2$$

where s_{osi} = operating speed of individual vehicle

D = distance between cones = 20m

t_i = time taken by *ith* vehicle to cover distance D given as

t_{c1} = time at cone 1

t_{c2} = time at cone 2

The 85th percentile of the recorded operating speeds was then calculated, and this was used as the road operating speed of the roadway. It was discovered that the operating speed was less than the posted speed when they were compared. Equation 3.3 was used to determine the stopping sight distance (SSD) based on this information, and by adopting the calculated operating speed.

$$SSD = \frac{u^2}{2gf} + ut \qquad 3.3$$

where SSD = stopping sight distance

t = perception-reaction time taken as 2.5s

u = design speed; g = acceleration

the stopping sight distance that was calculated was employed. The automatic traffic counter was set up so that the length of each road section from the automatic traffic counter to the end of the road section exceeded the measured stopping sight distance.

3.3.3.3 Layout of typical survey site:

Figure 3.4 shows a typical layout of the study site:

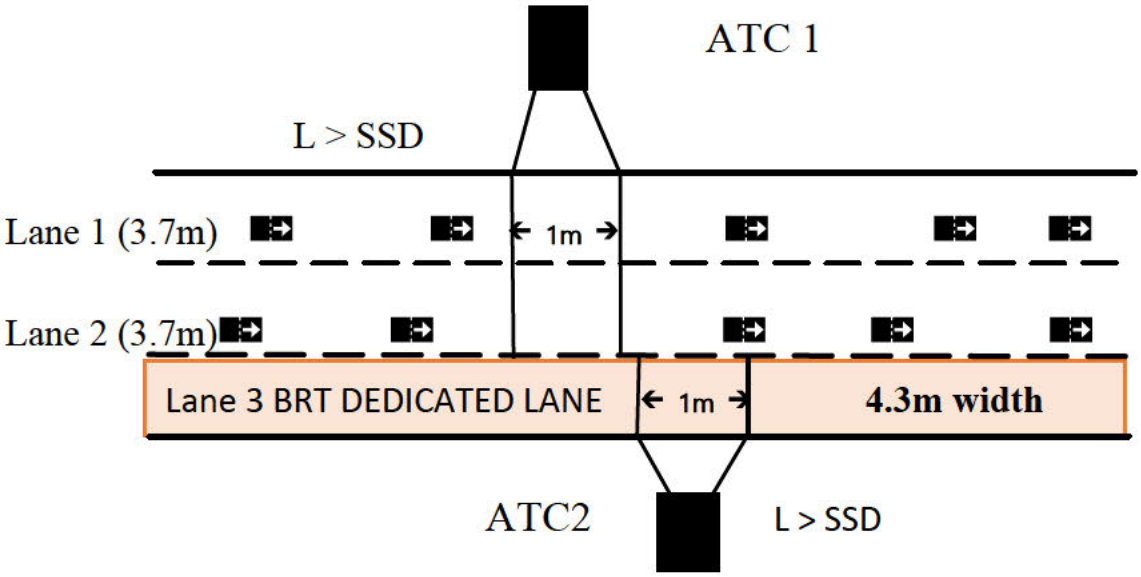

Figure 3. 4: Typical Set-Up of a BRT Impact Study Site

3.3.3.4 Traffic Survey Data

Data on Traffic characteristics is often utilized in describing the characteristics of vehicles with respect to the way they operate on the roadway. An Automatic Traffic Counter (ATC), 5900 series, designed by MetroCount was used to collect traffic characteristics data of the vehicles moving on the roadway within one hour. The ATC performs accurate and reliable data collection by logging in the information on the individual vehicles into itself. The vehicles' data collected include speed, traffic volume, gap, headway, vehicle classification, and vehicle type. The traffic data collected were used in the estimation of roadway capacity which at this juncture is non-mixed capacity. The ATC is described in the next section 3.3.3.4.1 while the procedure for the installation of the ATC and its accessories is described in section 3.3.3.4.2. The unloading of data from the ATC and its setup is as shown in sections 3.3.3.4.3 and 3.3.3.3.4 respectively. Typical traffic generated by the ATC is presented in section 3.3.3.4.5.

3.3.3.4.1 The Automatic Traffic Counter (ATC)

The Automatic Traffic Counter (ATC), also known as the logger is a rectangular dual-sensor traffic data logging unit used for short-term or long-term data logging operations. The ATC from MetroCount, also called the RoadPod VT or black box device, is housed in a standard steel road case, which provides mechanical protection for the device. As shown in Figure 3.4, the dual air sensors on the front are labelled A and B. The counter uses a user-replaceable alkaline battery pack for short-term operations, which can support up to 4 years of continuous data recording. An extra solar panel and SLA battery can power the device when it is being used for semi-permanent applications. The main system component has complete weatherproofing. Using the sealed circular connector, a USB communication cable provided by MetroCount, and the MTE software, a traffic surveyor can communicate with the device. The ATC logger's LED lights continuously provide information about the unit's status and the operation of the air sensors. The idle state is the unit's standby mode, which means the counter just keeps track of the data it already has without logging any new information. A setup places the device in the active logging state. The counter records axle hits in this condition and performs numerous maintenance operations. The device will keep doing this until a data unload is carried out or its memory space is exhausted. For a maximum of 10 days, the logging start time can be delayed. The device will be operational but not logging sensor hits during this period. The ATC also offers a Zombie Mode option that maintains the counter's complete inertness between axle impacts. Near the air sensors, the ATC has three status LEDs. Each sensor is matched by an A light and a B light, which can function in either of the active modes. A sensor's associated Status LED will flash when an air pulse activates it. Users can now

readily identify problems, such as obstructions, by checking the installation of their sensors. The unit's present state is shown by the Status LED, as shown in Table 3.3.

Table 3. 3: RSU's LED Status Indications

LED	State
Idle	Idle
Flashing every 2 seconds	Active Deferred
Flashing every second	Active Logging
On Continuously	Communications Active
Off Continuously	Data Transfer

Source:(Koorey, 2007)

The ATC is operated using replaceable alkaline batteries that can run for 290 days at 250C in continuous run mode. The machine has 2M RAM capable of logging all types of axle loads. It is however important at this point to bring up a description of the ATC and all its accompanying accessories, and they are presented as follows:

- Pneumatic tube: The pneumatic tube is shown in Figure 3.5. It is approximately 29.9m long, 31mm wide, and black. Its inner and outer diameters range from 5.3 to 5.7 and 12.7 to 13.5 millimeters, respectively. The automatic traffic counter receives air pulses generated by a car striking the tube through the tube.
- Stainless steel case: The stainless-steel case is shown in Figure 3.6. It helps to safeguard the device. It has dimensions of 350mm x 124mm x 95mm and is made of steel.
- Data communication cable: This is shown in Figure 3.7. The USB cable enables the communication between the computer system and the automatic traffic counter during the ATC setup and unloading of data.
- Bitumen road marking tape, cleats, nails, and flap: These fasteners are used to secure pneumatic tubes when installing them on the road. They are shown in Figure 3.8.
- There are other fittings which include a 6-volt welded battery, a protective dust lid to cover the USB port on the counter, a 4 mm ball driver for screwing and unscrewing, and a tube vent plug to seal the pneumatic tube end to prevent air leakage as shown in figure 3.9.

Figure 3. 5: Pneumatic Tube

Figure 3. 6: Automatic Traffic Counter

Figure 3. 8:Standard Steel Case

Figure 3. 7:Communication Cable

Figure 3. 10:Other Accessories

Figure 3. 9: Fasteners

3.3.3.4.2 ATC and Pneumatic Tube Installation

Two pneumatic tubes of equal lengths were laid parallel to each other, spaced one meter apart on the selected road segment. They were fastened to the pavement at a right angle to the flow of traffic. The ends of the tube that would be attached to the ATC were left free, while the other ends were tightly knotted to seal them off from air. For the tube to remain airtight while a vehicle passes over it, the knotting was done twice or three times. For ultimate airtightness within the tubes, vent plugs were additionally put into the knotted ends of the tubes. This prevents the loss of air from the tube, which would reduce the counter's sensitivity and result in a loss of high-quality data. By driving road nails through the eyelet of flaps positioned across the tubes, the double-knotted ends of the tubes were firmly fastened to the ends of the road surface.

The slack ends of the pneumatic tubes were similarly secured to the side of the road before being connected to the ATC. Before securing the loose ends tightly to the road and to ensure correct installation, the 1m gap between the tubes was again checked at various spots along the installed parallel tubes. To improve the accuracy of the data to be collected, consistency in tube spacing must be maintained. Bitumen tape was used to secure the tubes firmly to the pavement surface at regular intervals while the tubes were stretched between 10 and 15 percent after fastening for tensioning. This was done to minimize lateral movement in the tube positions as vehicles pass over it and prevent the tubes from shifting. The steel casing slots were made to accommodate the tubes, which were then properly attached to the two air-sensor holes A and B. Vehicles traveling in the same direction on the adjoining lanes hit tube A first due to the

connection convention in use. Later, a laptop was added to the Roadside Unit (RSU) configuration for data logging via the software driver. The ATC was then covered with a stainless-steel casing cover, chained, and locked with a padlock before being buried about 300mm below the ground by the side of the road. Figures 3.11 and 3.12, respectively show the pneumatic tubes that were installed over a road stretch, a vehicle moving over the pneumatic tubes after hitting A and B, and the ATCs logging data.

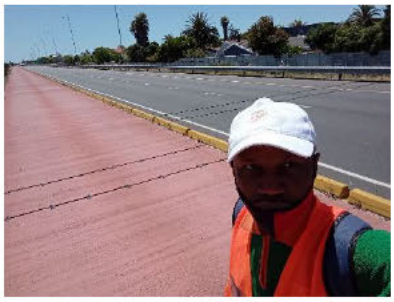

Figure 3. 11: Installed Pneumatic Tubes

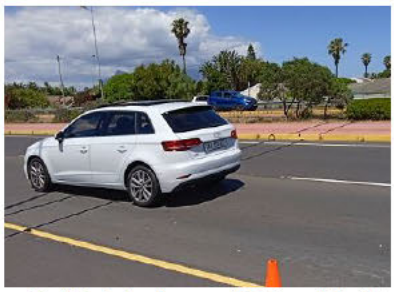

Figure 3. 12: Moving vehicle with data being logged.

3.3.3.4.3 ATC Set-Up

Before the commencement of data logging, the automatic traffic counter (ATC) is set up using the software driver that has been loaded on a laptop after the installation of the tubes.

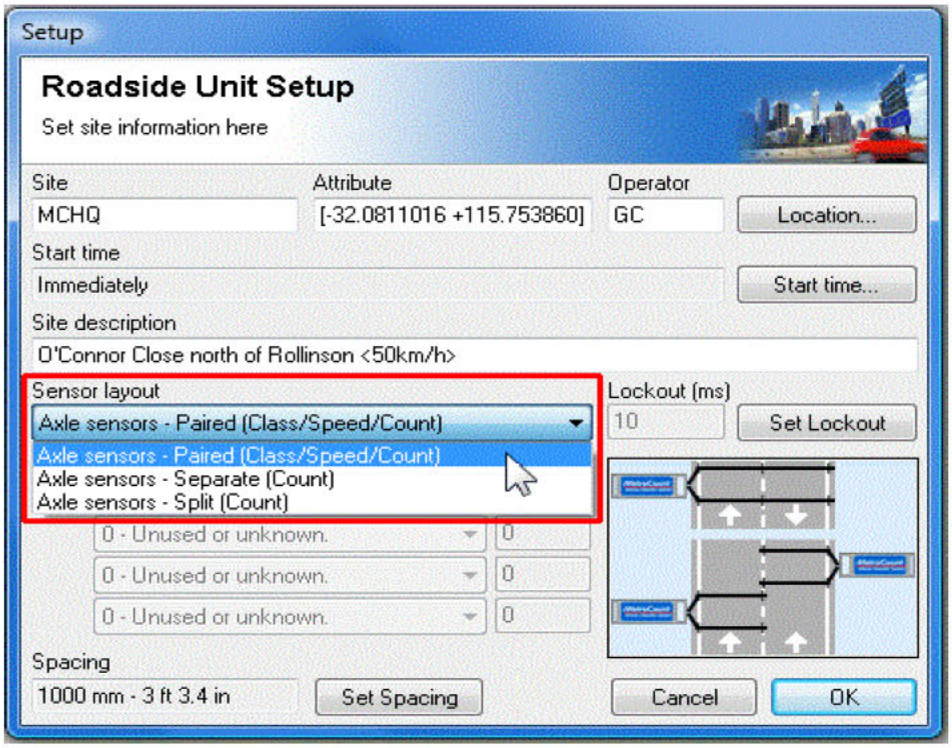

Figure 3. 13: RSU Set-up Dialogue Box

The Roadside Unit Setup is the first page that appears when you launch the automatic traffic counter software application. The automatic traffic counter software's typical interactive Set-page is shown in Figure 3.13.

Site data was logged on the interactive page for identifying reasons. The site details recorded include the name of the site, its attributes, lanes, operators, location, direction, debounce A, spacing, debounce B, start time, site description, and sensor configuration. Some of the information sections' drop-down menus offer additional potential choices. Data logging started after setup based on the start time entered during setup. The view (4) icon in Figure 3.13's left-hand pane was used to check the live traffic logging. This was required to verify that the counter was functioning. The options for rolling time, vehicle list, and axle timing are available under the view (4) icon.

3.3.3.4.4 Unloading Data from the ATC

Based on the scheduled time and memory of the automatic traffic counter, logged traffic data were downloaded into a computer system. Figure 3.14 depicts the interactive page for downloading data. The first page's left-hand pane includes the following information:

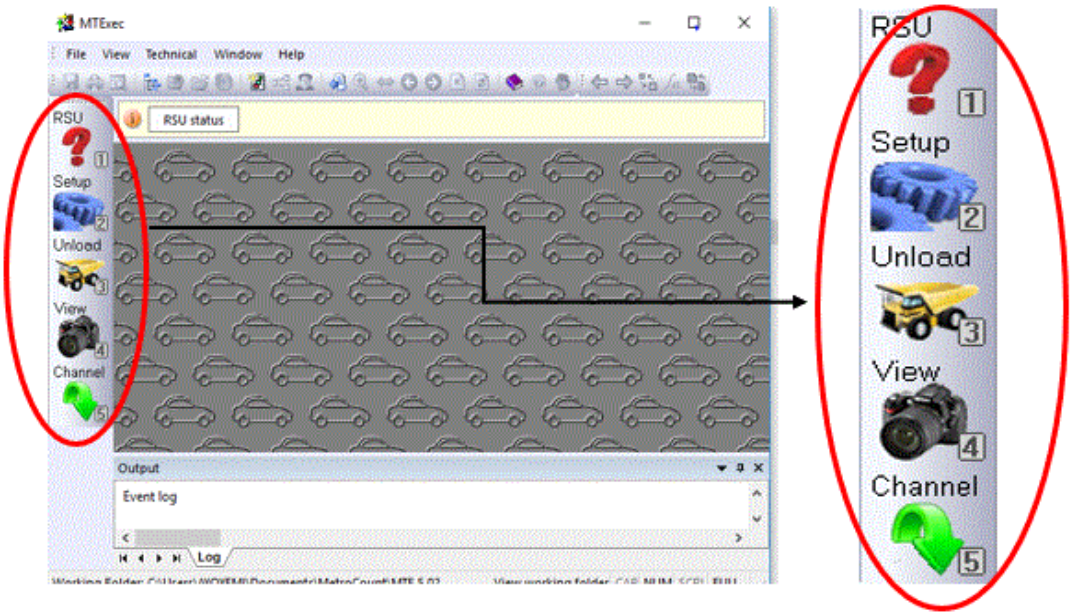

Figure 3. 14: MetroCount Executive Software Interactive Page

A brief description of the icons is presented below:

- RSU (1) – The RSU is the acronym for Roadside Unit and it gives the identity and status of the ATC in terms of data, serial number, battery, number of hits, and memory.
- Setup (2) – used to configure the ATC for data logging.
- Unload (3) – is used to download or unload logged data from the ATC into a laptop.
- View (4) – used to verify the sensor hits that the ATC has recorded.

Using the supplied USB communication cable, the ATC was connected to a laptop to download data. The RSU symbol (1) in the setup toolbar on the screen was used to verify the device status after connecting the connection. Before uploading data, the ATC battery and memory status were checked using the RSU icon (1). After the check, data was downloaded by clicking the unload button icon (3). Typically, there are two alternatives for unloading: "unload data and continue" or "unload data and stop." The option to "unload data and continue" enables data to be retained in the ATC even after downloading, in contrast to the option to "unload data and stop," which does not retain downloaded data and necessitates a new setup for each download. Unload data and stop' was employed for this study. This enables a check of the device's status, the data's quality, and any data loss that may have occurred. Remarkably, the screen shows the stored data graphically while data is being downloaded, utilizing the two-coloured lines A and B. When the lines overlap to form a blue line, the traffic data quality is acceptable; however, when the lines appear as mismatched red and blue lines, the traffic data quality is poor. The installed tubes were examined for any flaws including leaks in the case of mismatched lines. Downloaded data were kept in accordance with the data used during the automatic traffic counter setup mentioned in section 3.3.3.4.3 to facilitate easy identification.

3.3.3.4.5 ATC-Generated Traffic Information

The automatic traffic counter records data on a variety of characteristics, including the volume of traffic, speed, headway, and vehicle passing time. The number of vehicles passing the study site during the time considered is referred to as the traffic volume. During the data logging process, an air pulse is produced and supplied to the counter's air sensors as vehicles pass over the pneumatic tubes. A count and log are kept for each air sensor. The automatic traffic counter records headway based on the provided criteria, which defines headway as the time difference between succeeding cars as they pass a particular spot. The headway is the differential between how long it takes the front axles of the leading and following vehicles to contact the tube. One of the characteristics necessary for this study is speed, which is defined as the distance travelled

in a unit of time. By dividing the distance travelled through the tubes by the time required, the counter calculates the speed of a moving vehicle. It is noteworthy that the tubes are 1 m apart. The speeds recorded are referred to as spot speeds. The vehicle type produced by the automatic traffic counter is another piece of traffic information. The counter's capability to categorize automobiles into different classes is a crucial application. No matter the time or place, vehicles of all sizes, from small to large, are always moving on the highways, making the understanding of their classification very crucial. Additionally, using passenger car equivalent values, vehicle classification is crucial for transforming heterogeneous traffic into homogeneous traffic. SANRAL recognizes a variety of vehicle classifications, including heavy vehicles with 2, 3, 4, and 5 or more axles, motorbikes, cars, vans, pick-up trucks, minibuses, and buses.

The automatic traffic counter system has roughly twenty-two different types of vehicle classifications, with the ARX vehicle classification system being the most similar to the vehicle description used in South Africa. The ARX system was therefore chosen for this study. The AustRoads 94 was been modified to create the ARX. Figure 3.15 lists the properties of the ARX classification.

Axles	Groups	Description	Class		Parameters	Dominant Vehicle	Aggregate
2	1 or 2	Very Short - Bicycle or Motorcycle	MC	1	d(1)<1.7m & axles=2		1 (Light)
2	1 or 2	Short - Sedan, Wagon, 4WD, Utility, Light Van	SV	2	d(1)>=1.7m, d(1)<=3.2m & axles=2		
3, 4 or 5	3	Short Towing - Trailer, Caravan, Boat, etc.	SVT	3	groups=3, d(1)>=2.1m, d(1)<=3.2m, d(2) >=2.1m & axles=3,4,5		
2	2	Two axle truck or Bus	TB2	4	d(1)>3.2m & axles=2		2 (Medium)
3	2	Three axle truck or Bus	TB3	5	axles=3 & groups=2		
>3	2	Four axle truck	T4	6	axles>3 & groups=2		
3	3	Three axle articulated vehicle or Rigid vehicle and trailer	ART3	7	d(1)>3.2m, axles=3 & groups=3		3 (Heavy)
4	>2	Four axle articulated vehicle or Rigid vehicle and trailer	ART4	8	d(2)<2.1m or d(1)<2.1m or d(1)>3.2m axles = 4 & groups>2		
5	>2	Five axle articulated vehicle or Rigid vehicle and trailer	ART5	9	d(2)<2.1m or d(1)<2.1m or d(1)>3.2m axles=5 & groups>2		
>=6	>2	Six (or more) axle articulated vehicle or Rigid vehicle and trailer	ART6	10	axles=6 & groups>2 or axles>6 & groups=3		
>6	4	B-Double or Heavy truck and trailer	BD	11	groups=4 & axles>6		
>6	>=5	Double or triple road train or Heavy truck and two (or more) trailers	DRT	12	groups>=5 & axles>6		

Figure 3. 15: ARX vehicle classification system

Source: ATC 5900 MetroCount Manual

Figure 3.14 shows three groups of vehicles known as light vehicles (LV), also called passenger cars (PC), two groups of three different types of vehicles known as medium vehicles (MV), and three groups of six different types of vehicles known as heavy vehicles (HV). Individual vehicles each have their data that was transferred from the ATC logs into a laptop computer

system. The individual reports of four vehicles as seen in Figure 3.16 were gathered by the automatic traffic counter.

DS	Trig Num	Ht	YYYY-MM-DD	hh:mm:ss	Dr	Speed	Wb	Hdwy	Gap	Ax	Gp	Rho	Cl	Nm	Vehicle	
00	00000031	04	2021/11/06	11:06:00	N0	86.31	2.59	3.4	3.3	2	2	1	2	20	SV	oo
00	00000035	04	2021/11/06	11:06:03	N0	71.09	2.51	2.6	2.5	2	2	1	2	20	SV	oo
00	00000039	04	2021/11/06	11:06:05	N0	70.33	2.53	1.7	1.6	2	2	1	2	20	SV	oo
00	0000003d	04	2021/11/06	11:06:06	N0	71.06	2.5	1.5	1.4	2	2	1	2	20	SV	oo
00	00000041	04	2021/11/06	11:06:08	N0	68.73	3.12	2.2	2.1	2	2	1	2	20	SV	oo
00	00000045	04	2021/11/06	11:06:10	N0	65.04	2.83	1.5	1.4	2	2	1	2	20	SV	oo
00	00000049	04	2021/11/06	11:06:11	N0	74.25	2.6	1.1	0.9	2	2	1	2	20	SV	oo
00	0000004d	04	2021/11/06	11:06:12	N0	64.28	2.84	0.8	0.7	2	2	1	2	20	SV	oo
00	00000051	04	2021/11/06	11:06:14	N0	71.46	3.02	2.3	2.1	2	2	1	2	10	SV	oo

Figure 3. 16: A typical ATC captured individual vehicle report for adjoining lanes of traffic. Source: ATC Software

The following details are logged for each vehicle:

- DS – Tagged dataset index.
- Trig Number – Dataset axle number
- Ht – Number of axle hits in the vehicle
- YYYY-MM-DD – Date of the first axle in the vehicle
- Hh: mm: ss – Time of the first axle in the vehicle
- Dr – Direction of travel of the vehicle
- Speed – Speed of vehicle
- Wb – Wheelbase of vehicle
- Hdwy – Headway time since the first axle of the last vehicle travelling in the same direction.
- Gap – Gap time since the last axle of the last vehicle travelling in the same direction.
- Ax – Number of axles in the vehicle
- Gp – Number of axle groups in the vehicle
- Rho – Sensor correlation factor
- Cl – Class of vehicle
- Vehicle – Class name and scaled wheel picture of the vehicle.

The vehicles' sorting and analysis were conducted based on the specific details of the cars that make up the traffic stream for the period under consideration.

3.3.3.5 BRT Survey Data

In this study, the BRT traffic data was also collected the same way the adjoining lanes' traffic data was collected. As previously mentioned in the research methodology framework section, while one logger captured data on the adjoining lanes, the other one, installed and secured at the median of the carriageway, collected the BRT traffic data on the dedicated lanes as shown in Figure 3.10. The same setup was done in all the four sites investigated. Traffic flow parameters such as volume speed, headway, etc, were captured by the ATC and sorted accordingly. Figure 3.17 shows the individual BRT vehicle data captured by the ATC. Since only BRT buses use the dedicated lane and not competing with any other vehicle(s), the researcher considered the estimation of the BRT route capacity as germane for this study. The route capacity was calculated using the mean speed of the buses and other bus dimensions like the bus length. The procedure employed for obtaining the BRT route capacity and other parameters using the headway method is as follows:

DS	Trig Num	Ht	YYYY-MM-DD	hh:mm:ss	Dr	Speed	Wb	Hdwy	Gap	Ax	Gp	Rho	Cl	Nm	Vehicle	
02	4	4	2021/11/06	09:25:58	N0	67.44	6.51	97.8	97.8	2	2	1	4	10	TB2	oo
02	8	4	2021/11/06	09:45:41	N0	68.15	6.51	11.3	1182.6	2	2	1	4	10	TB2	oo
02	0c	4	2021/11/06	09:46:04	N0	69.11	6.44	23.7	23.4	2	2	1	4	10	TB2	oo
02	10	4	2021/11/06	10:06:50	N0	59.96	6.53	1245.5	1245.1	2	2	1	4	10	TB2	oo
02	14	4	2021/11/06	10:09:53	N0	68.29	6.58	182.7	182.3	2	2	1	4	10	TB2	oo
02	18	7	2021/11/06	10:28:00	N0	64.14	4.17	1087.7	1087.3	2	2	0.5	2	19a	SV	oo
02	1f	4	2021/11/06	10:28:21	N0	70.16	6.48	20.9	18.4	2	2	1	4	10	TB2	oo
02	23	4	2021/11/06	10:47:46	N0	34.98	2.5	1164.8	1164.4	2	2	1	2	10	SV	oo
02	27	4	2021/11/06	10:50:03	N0	55.12	6.52	136.7	136.4	2	2	1	4	10	TB2	oo

Figure 3. 17: A typical ATC captured individual vehicle report for BRT.
Source: ATC Software

3.3.3.5.1 BRT Traffic Flowrates and Mixed Traffic Characteristics

The capacity of a roadway is very sensitive to the distribution of headways in a mixed traffic stream situation (Ben-Edigbe *et al*., 2013; J. Ben-Edigbe *et al*., 2014). In BRT mixed traffic conditions which were examined in this study, time headway represents the spacing between a leading BRT and a following vehicle(s), or vice versa, hence the time headway of BRT under mixed or heterogeneous traffic situations is the inter-arrival time difference between two successive vehicles (BRT and others) as they pass a reference line taken along the entire width of the roadway (Maurya *et al*., 2015). It considers factors such as the number of vehicles per unit of time and the maximum safe speed of the vehicles (Dowling *et al*., 2004). Normally, time headways of vehicles in a traffic stream can be directly estimated using equation (3.4) which shows the simple basic relationship between traffic flow and headway:

$$headway, h = \frac{3600}{flow} \quad 3.4$$

Alternatively, and for BRT mixed traffic situations, BRT time headway, defined by braking performance and measured tip-to-tip, can be estimated using equation (3.5), and is given by:

$$T_h = \frac{L}{V} + t_r + \frac{kV}{2}\left(\frac{1}{a_f} - \frac{1}{a_l}\right) \quad 3.5$$

Where T_h – tip-to-tip time headway (s).

V – vehicle speed.

L – Length of vehicle.

t_r – reaction time

k – arbitrary safety factor (usually greater than or equal to 1)

a_f – minimum braking deceleration of the following vehicle

a_l – maximum braking deceleration of the lead vehicle

Note that for brick wall considerations, a_l is infinite and is usually eliminated.

The capacity of a designated route such as that for BRT can also be easily estimated using equation (3.6) if the time headway is known, as shown below:

$$Q_{BRT} = \frac{3600}{T_h} \quad 3.6$$

Where T_h = time headway.

By plugging equation (3.5) in equation (3.6), the BRT route capacity becomes:

$$Q_{BRT} = \frac{3600}{\frac{L}{V} + t_r + \frac{kV}{2}\left(\frac{1}{a_f} - \frac{1}{a_l}\right)} \quad 3.7$$

When the estimated BRT dedicated lane capacity is mixed with the adjoining lanes' capacities for the three survey periods considered, the capacity of mixed traffic 'with BRT' Q_M is determined by summing up the BRT dedicated lane capacity Q_{BRT} and the non-mixed traffic capacity as shown in equation (3.8), while equation (3.9) can then be used to estimate the BRT mixed traffic time headways as shown:

$$Q_M = Q_{BRT} + Q_{NM} \quad 3.8$$

hence

$$T_{h(M)} = \frac{3600}{Q_M} \quad 3.9$$

Given the estimated non-mixed traffic capacities and densities, as well as the mixed traffic capacities, the corresponding mixed traffic speeds and densities can thus be calculated by simple proportion. The mixed traffic critical density is calculated using equation 3.10 as shown below:

$$k_{Q(M)} = \frac{Q_M \times k_{Q(NM)}}{Q_{NM}} \quad 3.10$$

With that obtained, the mixed traffic speed at capacity can be estimated by simply dividing the mixed traffic capacity Q_M by the mixed traffic critical density $k_{Q(M)}$.

3.4 Appraisal of Sample Data and Proposed Analytical Methods

In this study, two analytical techniques viz a '*before and after BRT'* approach and an empirical *'with and without BRT'* approach were evaluated through a preliminary investigation known as a pilot study. The purpose of a pilot study is to assess and verify the effectiveness of the data collection strategy and the analytical techniques that will be applied to the study. Additionally, it assesses how beneficial the acquired data is for the methods used. The pilot study also aids in minimizing issues while providing remedies to any issues that might develop and influence the primary study. Besides, the findings of the pilot study enabled a statistical evaluation of the produced model's dependability. Due to the significance of a pilot study, as mentioned above, a two-week study was conducted at four pilot sites along the route R27 where speed samples were taken using cones and stopwatches to determine the traffic volume and density on the road. Further analysis was carried out to determine the capacity at peak and off-peak periods, and for the mixed and non-mixed conditions, and evaluate the time headway distribution to assess their influence on the capacity utilization of the roadway. Furthermore, due to the pandemic in the year 2020 and imposed lockdown, there were little or no vehicular movements, which consequently affected the year 2020 traffic data. Consequently, using the 'before and after BRT approach, the pilot study considered the backward extrapolation of flows for the periods 'before BRT' (*pre-BRT year 2009)*, and 'after BRT' (*pre-lockdown year 2019).* The traffic data collected in 2021 was also considered an after-BRT period, hence designated as the *post-lockdown year 2021* traffic data which the flows were extrapolated from. This was done to understand the traffic situation before and after the advent of BRT during those periods. Figure 3.18 illustrates the steps of the analytical methods used in this investigation.

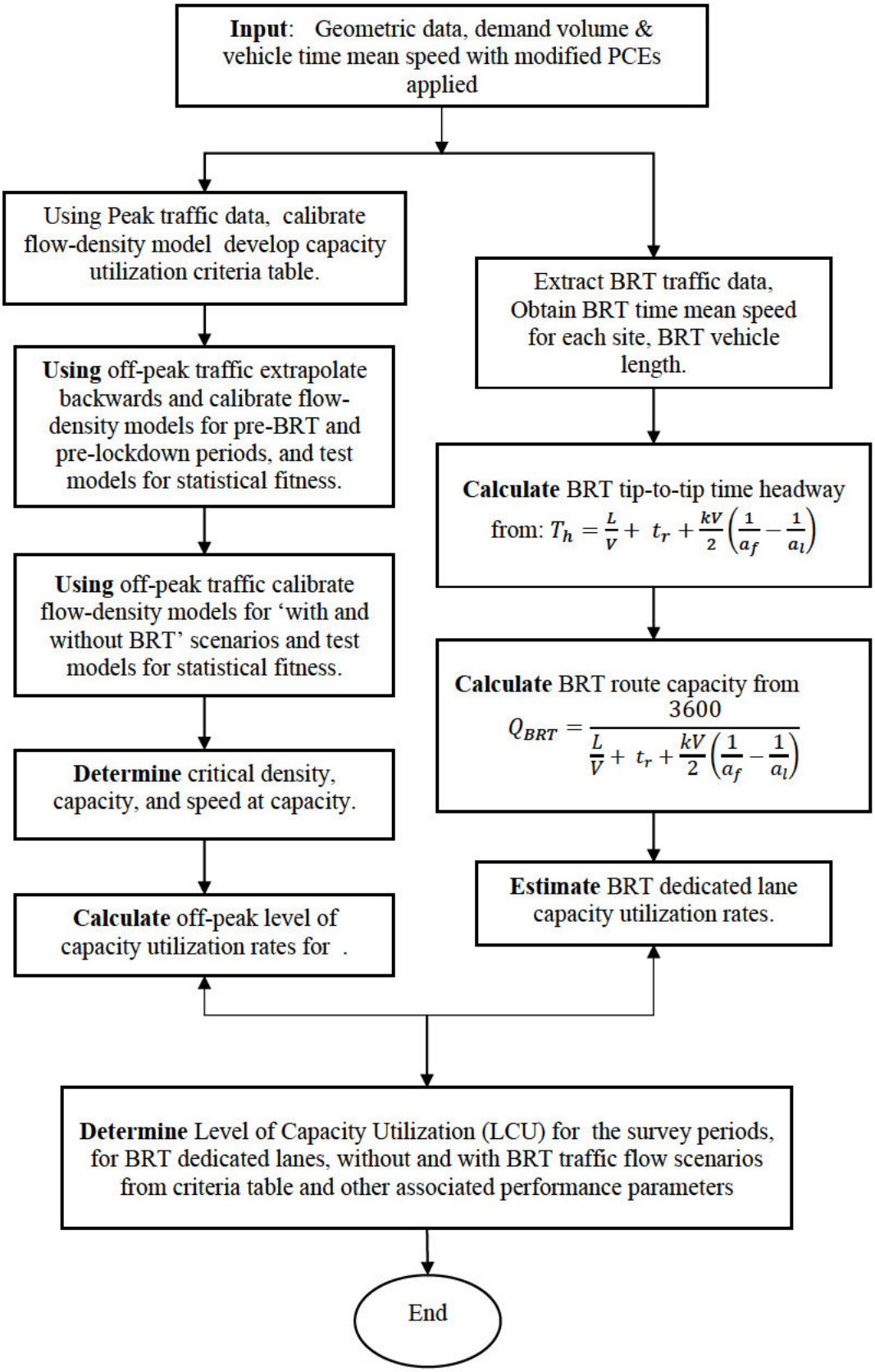

Figure 3. 18: Proposed Level of Capacity Utilization (LCU) Assessment Methodology

The empirical method, which considered a 'with and without' BRT situation consequently evaluated traffic performance using three flow scenarios as mentioned in Chapter 2 viz: BRT dedicated lane scenario, 'without BRT' scenario, and 'with BRT' scenario. The analytical steps are applicable for both methods and the LCU criteria table was set up using the peak traffic data for each site, while the off-peak data was analyzed and used for the evaluation of capacity utilization and traffic performance under the prevalent and assumed conditions. Section 3.4.1 presents the pilot study first, using the 'before and after' BRT approach, and subsequently using the empirical approach, by the criteria for the selection of the sites listed in section 3.3.1.

3.4.1 Pilot Study

The following outlined analytical procedures were employed for the extraction and sorting of the empirical data:

i. BRT and adjoining lanes traffic data were unloaded into a laptop computer from the ATCs 1 and 2 respectively, as shown in figure 3.3. Microsoft Excel was used to retrieve and properly save individual vehicle data from both the BRT lane and adjoining lanes. It should be noted that the traffic information extracted is referred to as an "individual vehicles report," whether it relates to BRT or the adjoining lanes.
ii. Both the BRT dedicated lane and adjoining lanes' traffic data were unloaded and separated into different folders in the laptop computer. Subsequently, traffic characteristics such as volume of vehicles (according to the identified classes), and speed were extracted for analysis. For this study only the peak and off–peak periods data between 5.00 am - 7.00 pm were used for analysis. Traffic data beyond 11 pm was not applicable as the period is usually characterized by long headways, low volumes, and a high percentage of heavy vehicles. Besides data within that period is outside the scope of this study.
iii. All traffic data was filtered to remove motorcycles. This is because commercial motorcycles are not in operation in Cape Town, and their population is very low, hence they were not readily found except for a few personal power bikes that owners ride on weekends for recreational purposes and exercise.
iv. For each vehicle classification the ATC identified, passenger car equivalent (PCE) values were applied. This converted the unit of the heterogeneous traffic volumes from vehicles per hour to passenger car unit per hour, making them appear homogeneous. As a result, the traffic became uniform. PCE was not applied to BRT vehicles as they don't compete with any vehicle on their dedicated lane, hence PCE application was not necessary.

v. Data were separated into 5mins intervals, the attendant volume counts and speed values for each interval were summed up, and the mean speed was calculated. It is necessary to know the mean values for traffic characteristics like speed and volume, hence they were separated on another Excel sheet for processing. It should be noted that the volume obtained is measured in $PCE/5min$. By multiplying by 12, the traffic volume was changed from PCE/5min to PCE/hr.

vi. Density, which is the third parameter in the equation of traffic flow was calculated using the same. Columns A, B, C, and D in the Excel spreadsheet shown in Figure 3.19 represent the tagged dataset index, serial number, dataset axle number, and the number of axle hits in the vehicle, respectively. The dates and times of the vehicle axle hits are shown in columns D and E. Column G indicates the direction of travel, column H the speed, column I the wheelbase,

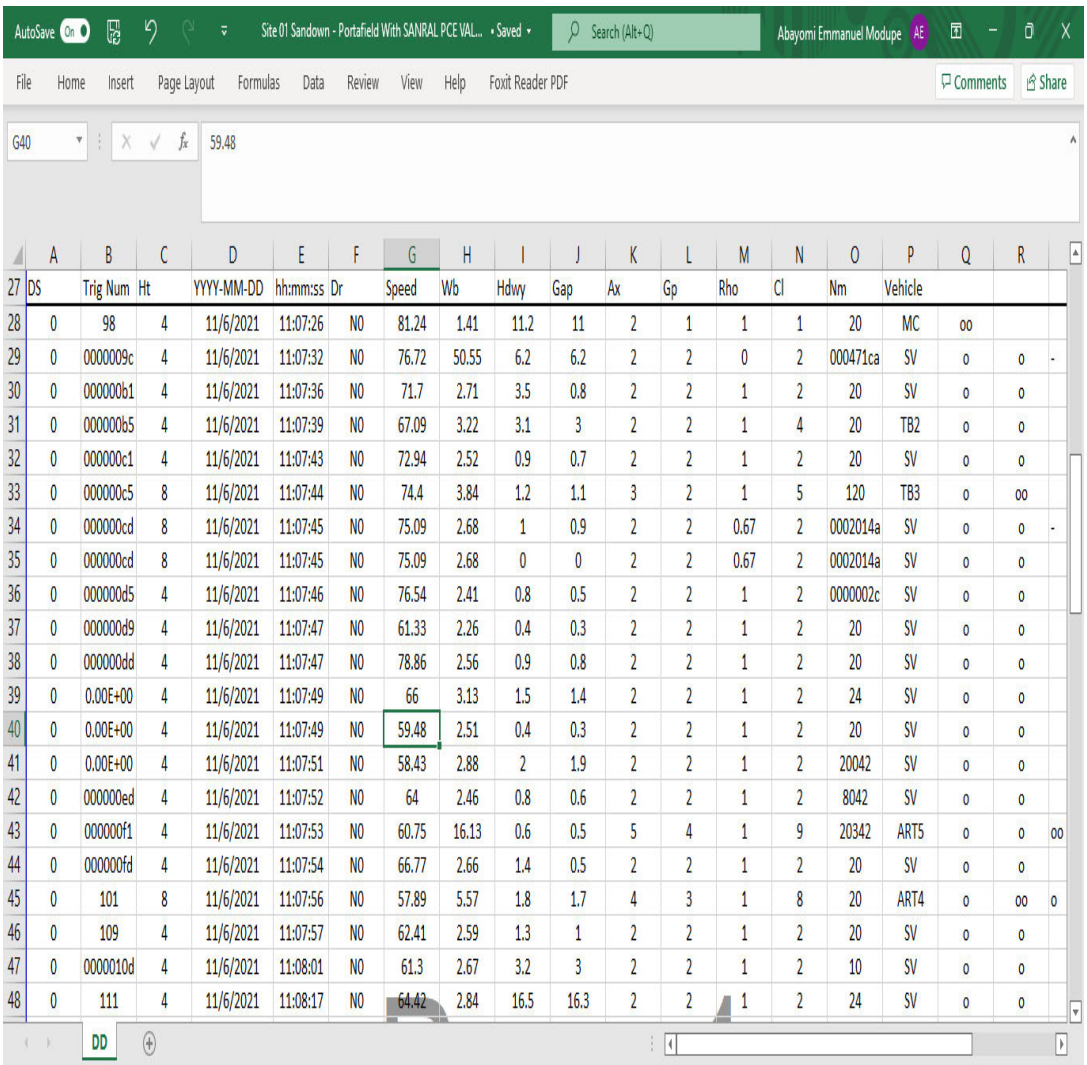

	A	B	C	D	E	F	G	H	I	J	K	L	M	N	O	P	Q	R	
27	DS	Trig Num	Ht	YYYY-MM-DD	hh:mm:ss	Dr	Speed	Wb	Hdwy	Gap	Ax	Gp	Rho	Cl	Nm	Vehicle			
28	0	98	4	11/6/2021	11:07:26	N0	81.24	1.41	11.2	11	2	1	1	1	20	MC	oo		
29	0	0000009c	4	11/6/2021	11:07:32	N0	76.72	50.55	6.2	6.2	2	2	0	2	000471ca	SV	o	o	-
30	0	000000b1	4	11/6/2021	11:07:36	N0	71.7	2.71	3.5	0.8	2	2	1	2	20	SV	o	o	
31	0	000000b5	4	11/6/2021	11:07:39	N0	67.09	3.22	3.1	3	2	2	1	4	20	TB2	o	o	
32	0	000000c1	4	11/6/2021	11:07:43	N0	72.94	2.52	0.9	0.7	2	2	1	2	20	SV	o	o	
33	0	000000c5	8	11/6/2021	11:07:44	N0	74.4	3.84	1.2	1.1	3	2	1	5	120	TB3	o	oo	
34	0	000000cd	8	11/6/2021	11:07:45	N0	75.09	2.68	1	0.9	2	2	0.67	2	0002014a	SV	o	o	-
35	0	000000cd	8	11/6/2021	11:07:45	N0	75.09	2.68	0	0	2	2	0.67	2	0002014a	SV	o	o	
36	0	000000d5	4	11/6/2021	11:07:46	N0	76.54	2.41	0.8	0.5	2	2	1	2	0000002c	SV	o	o	
37	0	000000d9	4	11/6/2021	11:07:47	N0	61.33	2.26	0.4	0.3	2	2	1	2	20	SV	o	o	
38	0	000000dd	4	11/6/2021	11:07:47	N0	78.86	2.56	0.9	0.8	2	2	1	2	20	SV	o	o	
39	0	0.00E+00	4	11/6/2021	11:07:49	N0	66	3.13	1.5	1.4	2	2	1	2	24	SV	o	o	
40	0	0.00E+00	4	11/6/2021	11:07:49	N0	59.48	2.51	0.4	0.3	2	2	1	2	20	SV	o	o	
41	0	0.00E+00	4	11/6/2021	11:07:51	N0	58.43	2.88	2	1.9	2	2	1	2	20042	SV	o	o	
42	0	000000ed	4	11/6/2021	11:07:52	N0	64	2.46	0.8	0.6	2	2	1	2	8042	SV	o	o	
43	0	000000f1	4	11/6/2021	11:07:53	N0	60.75	16.13	0.6	0.5	5	4	1	9	20342	ART5	o	o	oo
44	0	000000fd	4	11/6/2021	11:07:54	N0	66.77	2.66	1.4	0.5	2	2	1	2	20	SV	o	o	
45	0	101	8	11/6/2021	11:07:56	N0	57.89	5.57	1.8	1.7	4	3	1	8	20	ART4	o	oo	o
46	0	109	4	11/6/2021	11:07:57	N0	62.41	2.59	1.3	1	2	2	1	2	20	SV	o	o	
47	0	0000010d	4	11/6/2021	11:08:01	N0	61.3	2.67	3.2	3	2	2	1	2	10	SV	o	o	
48	0	111	4	11/6/2021	11:08:17	N0	64.42	2.84	16.5	16.3	2	2	1	2	24	SV	o	o	

Figure 3. 19: Typical Individual Vehicle Traffic Details (as captured by the ATC)

column J the headway, and column K the gap. The columns L, M, N, and O reflect the number

of axles and the number of axle groups, respectively, whereas columns P and Q denote the PCE values for each type of vehicle.

vii. Estimate flows for three observation periods viz (i) pre-BRT year 2009, (ii) pre-lockdown year (2019), and (iii) post-lockdown year (2021).

viii. By adopting and applying a compound traffic growth rate of 1.59% as established by (De Jongh & Bruwer, 2017) for the pre-BRT year 2009, and the national traffic growth rate of 3% (Marais, 2015) for the pre-lockdown year 2019, traffic volumes and densities were estimated by compounding the post-lockdown traffic data of 2021 backward to 2019 and 2009 respectively.

ix. To predict traffic flow, data for each roadway segment with respect to the with and without BRT survey periods, and for the mixed and non-mixed traffic conditions, the flow-density models were calibrated to calculate capacity, free-flow speed, the speed at capacity, density at capacity, time headway at capacity, travel time and their differentials, for the assessment of capacity evaluation effects.

x. The BRT traffic flow rates including the time headway were estimated using previously defined equation 3.4 – 3.11.

xi. BRT mixed traffic flow rates for the pilot site during the three survey periods were thereafter estimated using equation 3.7, which is the sum of BRT dedicated lane capacity and the 'without BRT' mixed traffic capacity on the adjoining lanes.

xii. The roadway capacity utilization criteria table was developed using peak traffic data.

xiii. Determination of the Level of Capacity Utilization (LCU) of the roadway was done using the developed criteria table.

xiv. The time headway distribution data for each site was analyzed using appropriate continuous probability distribution models, usually employed to fit headway data.

xv. The PDF (Probability Density Function), CDF (Cumulative Density Function), and P-P plots for the headway distributions were obtained with computer software and used to determine the model that had the best fit. The P-Values for each distribution were determined and the outcomes were evaluated with respect to the stated hypothesis.

3.5 Pilot Assessment of Capacity Utilization – '*Before and After BRT Approach*'

3.5.1 Organisation and Analysis of Extracted Data

Traffic data were organized appropriately and separated according to the traffic conditions considered in this study. Table 3.4 shows typical empirical data. Columns 1, 2, and 3 of this table, which represent passenger cars (PC), medium vehicles (MV), and heavy vehicles (HV), respectively, illustrate the traffic volume according to vehicle composition. Column 4 displays

the total number of vehicles by five-minute count. By multiplying columns 2 and 3 with the necessary values for passenger car equivalents, columns 5 and 6 represent the conversion of those columns to passenger cars. Sequel to that, the homogenous traffic volume in column 7, which is now in pce/5min was converted to flow in column 8 by multiplying it by 12, which is expressed in pce/hour.

Table 3. 4**:** Typical Empirical Peak - Traffic Volume Data

PC	MV	HV	Total Vol (/5mins)	MV (/pce)	HV (/pce)	Total Vol (pce/5mins)	Total Flow (pce/hr)
Col 1	Col 2	Col 3	Col 4	Col 5	Col 6	Col 7	Col 8
38	4	2	44	7	6	51	620
43	7	0	50	12	0	55	660
40	9	2	51	16	6	35	420
65	8	1	74	14	3	68	820
53	7	1	61	12	3	66	792
49	4	0	53	7	0	69	832
65	5	1	71	9	3	73	884
51	5	2	58	9	6	69	828
60	5	0	65	9	0	82	985
60	7	3	70	12	9	76	912
75	2	3	80	4	9	77	924
65	5	3	73	9	9	82	980
50	7	3	60	12	9	71	851
64	6	2	72	11	6	81	974
67	8	1	76	14	3	84	1008
72	4	0	76	7	0	79	952
67	1	0	68	2	0	69	827
58	4	1	63	7	3	68	816
56	4	1	61	7	3	66	792
59	9	0	68	16	0	75	897
58	6	0	64	11	0	69	822

*Note: col 4 = (col 1 + col 2 + col 3); col 5 = col 2 * 1,75*; *col 6 = col 3 * 3; col 7 = (col 1 +col 5 + col 6); col 8 = col 7 * 12*

Table 3.4 cont'd

Col 1	Col 2	Col 3	Col 4	Col 5	Col 6	Col 7	Col 8
70	8	0	78	14	0	84	1013
55	5	0	60	9	0	64	772
71	7	0	78	12	0	83	997
67	4	0	71	7	0	74	889
79	1	0	80	2	0	81	970
75	4	0	79	7	0	82	974
61	6	0	67	11	0	72	866
73	1	0	74	2	0	75	901
75	2	0	77	4	0	79	950
56	6	1	63	11	3	70	842
89	2	0	91	4	0	93	1120
59	8	1	68	14	3	76	920
60	4	0	64	7	0	67	804
77	4	1	82	7	3	87	1052
65	7	0	79	12	0	77	931
45	5	2	52	9	6	60	729
73	5	0	78	9	0	82	985
55	4	0	59	7	0	62	751
54	5	1	60	9	3	66	801
82	3	0	84	5	0	86	1032
61	3	0	64	5	0	66	795
76	5	1	82	9	3	88	1058
50	7	0	57	12	0	62	749
61	8	0	69	14	0	75	904
59	6	0	61	11	0	70	846
57	4	0	61	7	0	64	772
41	5	1	55	9	3	53	641

*Note: col 4 = (col 1 + col 2 + col 3); col 5 = col 2 * 1,75*; *col 6 = col 3 * 3; col 7 = (col 1 +col 5 + col 6); col 8 = col 7 * 12*

3.5.2 Modification of PCE Values

Initially, the PCE values employed in the analysis were those recommended by the SANRAL and computed during typical dry daylight conditions. The values must be changed to see if they

may be used in different circumstances, such as when a BRT bus is operating on the road and, for emergency reasons, may need to use the adjoining lanes. The headway method was used to modify the PCE values, as was indicated before under subsection 2.4.1, and it was tested. The headway equation as defined previously is again given by equation 3.11 as follows:

$$pce_i = \frac{H_i}{H_C} \qquad 3.11$$

where pce_i = passenger car equivalent of vehicle class i

H_i = average headway of vehicle class i (s) and

H_C = average headway of passenger car (s)

PCE values of the BRT buses were not modified because no vehicles were sharing the dedicated lane with them, hence the modification was carried out on vehicles moving on the adjoining lanes alone. Therefore, the PCE modification procedure for heterogeneous traffic on the adjoining lanes under non-mixed traffic conditions, including daylight and dry weather is outlined as follows:

$$Spacing = \frac{1}{Density} km/veh = \frac{1000}{Density} m/veh$$

Considering that density is the result of the model equation, spacing, therefore, is calculated as:

$$\frac{1000}{18} = 55.55 \approx 56 m/veh$$

Average speeds of identified vehicles class were considered.

Average speed of PC = 90.21km/hr = 25.06m/s (as obtained from ATC)
Average speed of MV = 91.13km/hr = 25.31m/s (as obtained from ATC)
Average speed of HV = 89.5km/hr = 24.86m/s (as obtained from ATC)

Thereafter, the average headway of each vehicle class was calculated using.

$$h_i = \frac{s}{u_i} \qquad 3.12$$

Where h_i = average headway of vehicle class i

s = spacing

u_i = speed of vehicle class i

Headway for PC = $56/25.06 = 2.23s$

Headway for MV = $56/25.31 = 2.21s$

Headway for HV = $56/24.86 = 2.25s$

The following modifications were made to PCEs using equation 3.5 and the headway values obtained:

PCE for PC = $2.23/2.23 = 1.00$

PCE for MV = $2.21/2.23 = 0.99$

PCE for HV = $2.25/2.23 = 1.001$

The summary is presented in Table 3.5 as follows:

Table 3. 5**:** Summary of modified PCE values

Vehicle Type	Standard PCE	Modified PCEs
Passenger Car	1.0	1.00
Medium Vehicle	1.75	0.99
Heavy Vehicle	3.00	1.001

The table clearly shows that the modified PCE values for medium and heavy vehicles in the heterogeneous traffic on the adjoining lanes do not match the typical PCE values recommended by SANRAL. Due to the presence of BRT dedicated lanes, capacity has been reduced, which may have has caused a shift in PCE values. The modified PCE and SANRAL values for medium and heavy vehicles were consequently subjected to a statistical test using the chi-square at a 95% level of confidence. The purpose of the test is to determine whether there exists a significant discrepancy between the updated PCE and SANRAL values. These two hypotheses were put forth:

- Null hypothesis (H_0): No distinction between SANRAL PCE values and the modified values
- Alternative hypothesis (H_1): There is a distinction between SANRAL PCE values and the modified values.

Equation 3.13 represents the chi-square test.

$$X^2 = \frac{(o-e)^2}{e} \qquad 3.13$$

where X^2 = chi-square

o = observed value

e = expected value

Based on a 95% confidence level and for one degree of freedom, the test was done taking $X^2 = 3.84$ from the chi-square distribution table (see appendix). However, if $X^2 > 3.84$, therefore the alternative (H_1) hypothesis is accepted, indicating that there is a significant difference between the standard PCE from SANRAL and the modified PCEs. On the other hand, if $X^2 < 3.84$, then, it means there is no significant difference between the standard PCE from SANRAL and the modified PCEs, and the null hypothesis (H_0) is accepted. Therefore, for medium vehicles (MV) with a modified PCE value of 0.99 under dry day-time conditions and SANRAL PCE value of 1.75:

$$X^2 = \frac{(0.99-1.75)^2}{1.75} = 0.33 < 3.84$$

and for heavy vehicles (HV) with a modified PCE value of 1.001 under dry day-time conditions and SANRAL PCE value of 3.0;

$$X^2 = \frac{(1.001-3)^2}{3} = 1.33 < 3.84$$

Thus, the null hypothesis (H_0) is accepted since $0.33 < 3.84$ and $1.33 < 3.84$ for the medium and heavy vehicles respectively and the alternate hypothesis (H_1) is rejected. At a 95 percent level of confidence for one degree of freedom, the results demonstrate no statistically significant difference between the adjusted PCE and SANRAL values. Because there is no discernible difference, either the SANRAL PCE or the modified PCE could be employed; hence, for this investigation, the SANRAL PCE values were used. Table 3.6 shows the empirical peak traffic volume and speed data and the estimated hourly flows and density for pilot sites SS001 to SS004. The hourly traffic flows and densities were calculated for all the sites using the SANRAL standard PCE values. The data obtained was with respect to the heterogeneous traffic on the adjoining lanes The PCE values were also applied to the BRT dedicated lane traffic flows, for the mixed traffic analysis 'with BRT' and is discussed later in this chapter.

Table 3. 6**:** Summary of volume, speed, density, and flow data with PCEs Applied – Peak

Vol (pce/5mins)	u (km/hr)	k (pce/km)	q (pce/hr)	Vol (pce/5mins)	u (km/hr)	k (pce/km)	q (pce/hr)

51	57	11	620	74	79	11	889
55	58	11	660	81	73	13	970
35	60	7	420	82	83	12	974
68	51	16	820	72	87	10	866
66	52	15	792	75	78	12	901
69	50	17	832	79	84	11	950
73	55	16	884	70	87	10	842
69	53	16	828	93	72	16	1120
82	55	18	985	76	80	12	920
76	51	18	912	67	82	10	804
77	49	19	924	87	86	12	1052
82	47	21	980	77	87	11	931
71	75	11	851	60	75	10	729
81	80	12	974	82	74	13	985
84	78	13	1008	62	85	9	751
79	71	13	952	66	79	10	801
69	79	10	827	86	73	14	1032
68	78	10	816	66	79	10	795
66	84	9	792	88	70	15	1058
75	73	12	897	62	77	10	749
69	78	11	822	75	79	11	904
84	72	14	1013	70	78	11	846
64	83	9	772	64	78	10	772
83	69	14	997	53	82	8	641

Note that, q denotes flow, u denotes speed and k denotes density where $q = uk$

Similarly, Table 3.7 shows the empirical off-peak traffic volume and speed data and the estimated hourly flows and density for pilot sites SS001 to SS004. Using the SANRAL standard PCE values. The data obtained was with respect to the heterogeneous traffic on the adjoining lanes.

Table 3. 7: Summary of volume, speed, density, and flow data with PCEs Applied – Off-Peak

Vol (pce/5mins)	u (km/hr)	k (pce/km)	q (pce/hr)	Vol (pce/5mins)	u (km/hr)	k (pce/km)	q (pce/hr)
24	67	4	288	43	80	6	468
30	68	5	360	42	98	5	504
30	72	5	360	37	82	5	444
55	71	9	612	45	88	6	552
37	72	6	444	36	92	5	432
25	71	4	300	36	85	5	432
45	75	7	540	44	88	6	528
34	73	6	408	51	95	6	612
37	75	6	444	50	96	6	600
54	72	9	600	32	93	4	384
58	77	9	696	46	97	6	552
51	73	8	612	35	92	5	420
43	84	6	516	51	78	8	612
28	89	4	336	39	77	6	468
42	85	6	504	38	89	5	456
35	92	5	420	36	82	5	384
45	82	7	492	30	85	4	360
32	87	4	384	33	82	5	396
30	88	4	360	44	73	7	480
38	87	5	456	39	80	6	420
34	87	5	408	35	82	5	372
39	90	5	468	36	81	5	432
36	90	5	432	23	81	3	276
50	92	6	600	31	85	4	324

Note that, q denotes flow, u denotes speed and k denotes density where $q = uk$

The data displayed in Tables 3.6 and 3.7 above from the field survey represent the peak and off-peak traffic situation during the post-lockdown survey period in 2021 after the pandemic and ease of lockdown, in terms of flow speed and density. Data collected on the adjoining lanes are hence referred to as non-mixed traffic, whilst those merged with BRT dedicated lane data are referred to as mixed traffic. The peak traffic data was used to develop the capacity utilization criteria table for each site later in this chapter, to benchmark off-peak traffic performance.

3.5.3 Non-Mixed Traffic Analytical Procedure

One other major reason besides the pandemic in 2020 for the consideration of data extrapolation to the pre-BRT 2009 and pre–lockdown period 2019, was due to the non-availability of pre-built design traffic volumes i.e., from periods before the advent of the BRT scheme, with attendant traffic growth rates to the pre-lockdown year 2019. Note that the MyCiTi BRT in Cape Town was opened in the year 2010 shortly before the World Cup, (Stone, 2009), hence the empirical traffic survey data collected for the post-lockdown year 2021 was back cast or extrapolated backward to the pre-BRT year 2009, and pre–lockdown 2019, using established traffic growth rates from literature. The following procedure was employed to estimate traffic volumes for the two survey periods and subsequently carry out an analysis of the influence of BRT on mixed traffic capacity utilization during these periods, using the 'before and after BRT' approach. The procedure is as follows:

i. Assume traffic survey data for the year 2021 is projected backward at a 3% national traffic growth rate according to the national department of Transport (NDOT), and from the study and findings of (Marais, 2015), for the pre-lockdown year 2019. Note that the pandemic lockdown affected the year 2020 traffic flow data. Keep the speed constant for all periods.

ii. Allow 3% traffic growth from the period 2016 to 2019 and a 1.59% ≈ 1.6% traffic growth rate adopted from the study and findings of (De Jongh & Bruwer, 2017) from period 2009 (pre-BRT) to the year 2015, therefore:

Contraction rate 3% compounded for 3 years (2016 to 2019) = 0.913, and
Contraction rate 1.6% compounded for 7 years (2009 to 2015) = 0.893

iii. Estimate traffic volumes using the contraction rates to compound the post-lockdown traffic data of 2021 backward to 2019 and 2009 respectively and calibrate the capacity models to obtain critical densities and capacities.

Consequently, the peak and off-peak traffic volumes were extrapolated for the pre-BRT year 2009 and the pre-lockdown year 2019, from the post-lockdown year 2021, when the actual survey was conducted. The compounded peak and off-peak traffic volumes are presented in Table 3.8 for the pilot site, with the contraction rates indicated.

STEP 1a: Backward Extrapolation of Pre-BRT 2009 and Pre-lockdown 2019 Peak Traffic Flow Rates.

Pilot Site (Peak)

Table 3. 8: Compounded Traffic Volumes, Speed and Flow for Pilot Site (Peak)

Pilot Site SS001 (Post-Lockdown 2021)			Pilot Site SS001 * 1.093 (Pre-Lockdown 2019)			Pilot Site SS001 * 0.893 (pre-BRT 2009)		
u	k	q	u	k	q	u	k	q
57	11	620	57	12	678	57	10	553
58	11	660	58	12	721	58	10	588
60	7	420	60	8	459	60	6	374
51	16	820	51	18	896	51	14	731
52	15	792	52	17	866	52	14	706
50	17	832	50	18	909	50	15	741
55	16	884	55	18	966	55	14	788
53	16	828	53	17	905	53	14	738
55	18	985	55	20	1077	55	16	878
51	18	912	51	20	997	51	16	813
49	19	914	49	20	999	49	17	814
47	21	980	47	23	1071	47	19	873

STEP 1b: Development of Non-Mixed Peak Traffic Capacity Models

According to Van Arem *et al*. (1994) and adopted by Minderhoud *et al*. (1996) and Ben-Edigbe (2005), flow-density equation has been shown to have a quadratic model, where flow is used as the objective function and density as the control parameter as shown in equation 3. Therefore, for roadway capacity estimations without BRT, the flow-density model is denoted as:

$$Q_{NM} = -ak_Q{}^2 + bk_Q - c \qquad 3.14$$

but $$\frac{\partial Q}{\partial k_Q} = 2(-ak_Q) + b = 0 \qquad 3.15$$

Therefore, Density at capacity, $k_Q = \frac{b}{2a}$ 3.16

where Q_{NM} – non-mixed traffic capacity k_Q = density at capacity, a and b are the model coefficients and c is a constant. Note that equation (3.14) must return a negative result or zero for coefficients c and a and a positive for b to satisfy the concavity requirement of the $q - k$ curve. The application of the quadratic equation for the computation of capacity is essential to be able to determine the point of curvature or 'maxima' that indicates the capacity, and this point corresponds to critical density or density at capacity. It is possible to achieve a maximum q – k function through mathematical extrapolations but the outcomes are often high and not a

good representation of real traffic situations, hence questionable (Ben-Edigbe & Ferguson, 2005). Using a multiplier (x12), 5mins volumes were converted to flow, and critical densities were calculated using equation 3.16. The traffic flow and density data generated above for the pilot site at peak traffic were used to calibrate the quadratic model equations 3.17 to 3.19 with coefficients, using Microsoft Excel software. The generated flow-density curves for the sites are shown in Figure 3.20.

Pilot Site (Peak)

$$q_{pre-BRT(2009)} = -1.3471k^2 + 74.948k - 42.261 \qquad R^2 = 0.96 \qquad (3.17)$$

$$q_{pre-lockdown(2019)} = -1.0983k^2 + 74.948k - 51.834 \qquad R^2 = 0.96 \qquad (3.18)$$

$$q_{post-lockdown(2021)} = -1.2005k^2 + 74.948k - 47.423 \qquad R^2 = 0.96 \qquad (3.19)$$

STEP 1c: Development of Non-Mixed Peak Traffic Flow-Density Curves

The capacity curves associated with the three survey periods explained above are displayed in Figure 3.20 for the pilot site. The model equations can also be seen on the capacity curves and the capacity values can be easily traced on them.

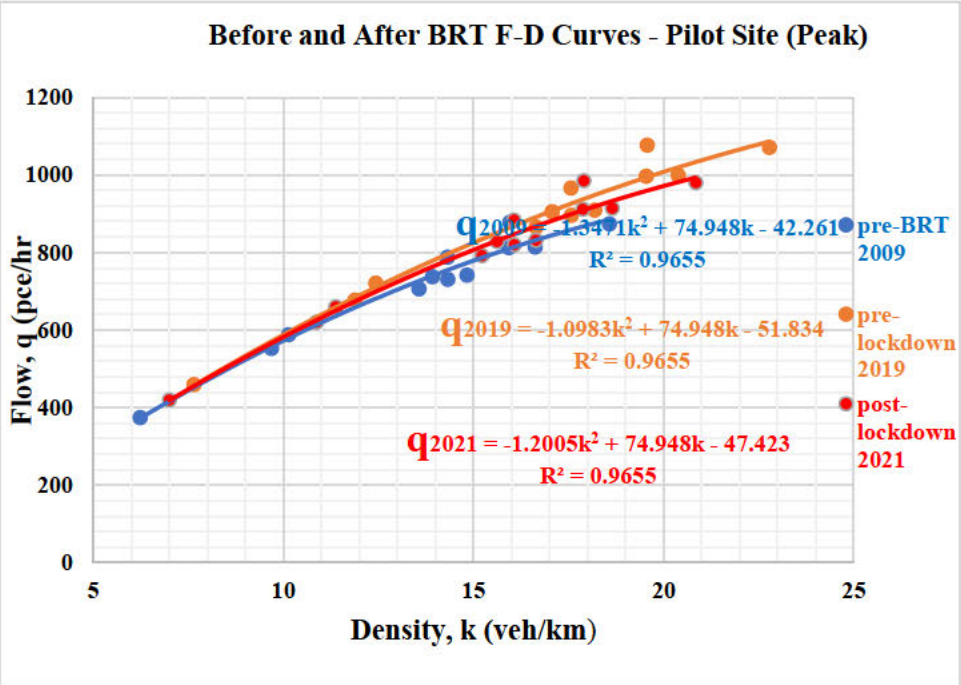

Figure 3. 20: Before and After BRT F-D Curves - Pilot Site (Peak)

STEP 1d: Estimation of Critical Density, Capacity, and Speed

Critical densities were determined by differentiating flow q, with respect to density k; for a maximum value of q in equations 3.17 to 3.19 above, $\partial q/\partial k = 0$, where ∂ is derivative. This resulted in densities at capacity for each model. The estimated densities were plugged back into each of the equations to determine the maximum flows for the pilot site, as well as the estimated speed at capacity. The travel speed of vehicles at capacity was estimated by just dividing the estimated capacity by the estimated critical density using the fundamental flow–density equation 2.17. The lines of calculation are shown below:

2021 flow-density model analysis at Peak:

$$q_{2021(peak)} = -1.2005k^2 + 74.948k - 47.423 \qquad R^2 = 0.96$$

By differentiating q with respect to k,

$$\frac{\partial q}{\partial k} = 2 * (-1.2005\text{k}) + 74.948 = 0$$

$$k_{crt} = k_Q = 31.13 pce/km \approx 31\, pce/km$$

By plugging the critical density k_Q into equation 3.19 the capacity is calculated and is given by:

$$Q = q_{2021(peak)} = -1.2005(31)^2 + 74.948(31) - 47.423$$

$$Q = q_{2021(peak)} = 1122.3 pce/hr \approx 1122 pce/hr$$

By substituting k_{crt} and the estimated Q into the fundamental diagram equation $q = uk$, the speed at capacity is therefore obtained as:

$$u_Q = \frac{q}{k} = \frac{1122}{31} = 36.19 \approx 36 km/hr$$

Step 2a: Backward Extrapolation of Pre-BRT 2009 and Pre-lockdown 2019 Off-Peak Traffic Flow Rates**.**

Off-peak traffic volumes were also extrapolated for the three observation periods viz (i) pre-BRT year 2009, and pre-lockdown year (2019) from the post-lockdown year 2021 data, when the actual survey was conducted. The compounded traffic volumes are presented in Table 3.9 for the investigated pilot site, with contraction rates indicated.

Pilot Site (Off-Peak)

Table 3. 9: Compounded Traffic Volumes, Speed and Flow for Pilot Site (Off-Peak)

Pilot Site SS001 (Post-lockdown 2021)			Pilot Site SS001 * 1.093 (Pre-lockdown 2019)			Pilot Site SS001 * 0.893 (pre-BRT 2009)		
u	k	q	u	k	q	u	k	q
67	4	282	67	5	308	67	4	251
68	5	357	68	6	390	68	5	318
72	5	363	72	6	397	72	4	323
71	9	654	71	10	715	71	8	583
72	6	441	72	7	482	72	5	393
71	4	294	71	5	321	71	4	262
75	7	543	75	8	593	75	6	484
73	6	411	73	6	449	73	5	366
75	6	447	75	7	489	75	5	398
72	9	645	72	10	705	72	8	575
77	9	693	77	10	757	77	8	618
73	8	615	73	9	672	73	8	548
		479			523			427

Step 2b: Development of Non-Mixed Off-Peak Traffic Capacity Models

Similarly, the off-peak traffic flow and density data generated above for the pilot site were used to calibrate the model equations 3.20 to 3.22 with coefficients, using Microsoft Excel software. The generated flow-density curves for the pilot site are shown in Figure 3.21.

Pilot Site (Off-Peak)

$$q_{pre-BRT(2009)} = -2.5647k^2 + 107.73k - 111.52 \qquad R^2 = 0.98 \qquad (3.20)$$

$$q_{pre-lockdown(2019)} = -2.091k^2 + 107.73k - 136.79 \qquad R^2 = 0.98 \qquad (3.21)$$

$$q_{post-lockdown(2021)} = -2.2855k^2 + 107.73k - 125.15 \qquad R^2 = 0.98 \qquad (3.22)$$

Step 2c: Development of Non-Mixed Peak Traffic Flow-Density Curves

The capacity curves associated with the three survey periods explained above at off-peak traffic flows are displayed in Figure 3.21 for the pilot site investigated. The model equations can also be seen on the capacity curves and the capacity values can also be easily traced on them.

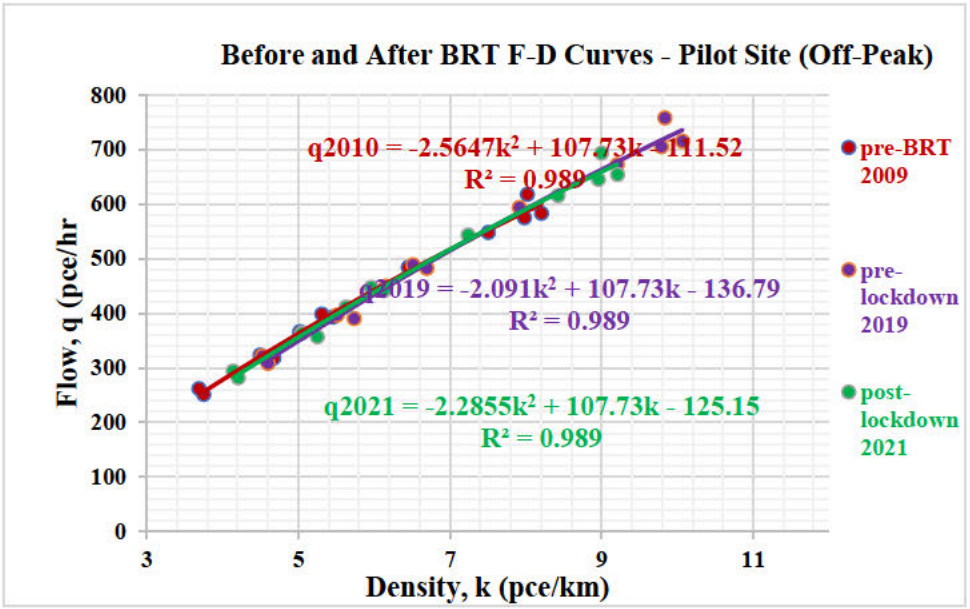

Figure 3. 21: Before and After BRT F-D Curves - Pilot Site (Off-Peak)

Step 2d: Estimation of Critical Density, Capacity, and Speed

Critical densities were also determined for the off-peak traffic flows by differentiating flow q, with respect to density k; for a maximum value of q in equations 3.20 to 3.22 above, $\partial q/\partial k = 0$, where ∂ is derivative. This resulted in densities at capacity for each model. The estimated densities were plugged back into each of the equations to determine the off-peak maximum flows or capacities for the pilot site, which are summarized in Table 3.10, as well as the estimated speed and headway at capacity. The travel speed of vehicles at capacity was estimated by simply dividing the estimated capacity by the estimated critical density using the fundamental flow-density equation 2.17. The lines of calculation are shown below:

2021 flow-density model analysis at Off-Peak:

$$q_{2021(off-peak)} = -2.2855k^2 + 107.73k - 125.15 \quad R^2 = 0.98$$

By differentiating q with respect to k,

$$\frac{\partial q}{\partial k} = 2 * -2.2855\text{k} + 107.73 = 0$$

$$k_{crt} = k_Q = 23.57 pce/km \approx 24\ pce/km$$

By plugging the critical density k_Q into equation 3.22 the capacity is calculated and is given by:

$$Q = q_{2021(off-peak)} = -2.2855(24)^2 + 107.73(24) - 125.15$$

$$Q = q_{2021(off-peak)} = 1143.92 pce/hr \approx 1144 pce/hr$$

By substituting k_{crt} and the estimated Q into the fundamental diagram equation $q = uk$, the speed at capacity is therefore obtained as:

$$u_Q = \frac{q}{k} = \frac{1144}{24} = 47.6 \approx 48km/hr$$

Table 3.10 shows the summary of the non-mixed peak and off-peak traffic flow rates for the pilot site.

Table 3. 10: Summary of Peak and Off-Peak Non-Mixed Traffic Flow Rates for Pilot Test (Before and After BRT)

SITE	Traffic Period	Survey Period	Q_{NM}	$k_{Q(NM)}$	$u_{Q(NM)}$	$u_{f(NM)}$
PILOT SITE	Peak	2009	1000	28	36	74.95
		2019	1227	34	36	74.95
		2021	1122	31	36	74.95
	Off-Peak	2009	1020	21	48	107.70
		2019	1251	26	48	107.70
		2021	1144	24	48	107.70

2009 ~ without BRT, 2019 ~ pre-lockdown, 2021 ~ post-lockdown, Q_{NM} ~ non-mixed traffic capacity, $k_{Q(NM}$ ~ mixed traffic critical density, $u_{Q(NM)}$ ~ mixed traffic speed at capacity, $u_{f(NM)}$ ~mixed traffic free flow speed.

3.5.4 BRT Traffic Flowrates Analytical Procedure for Pilot Test

Due to its homogeneous characteristics and fixed number of bus fleets the empirical BRT traffic flow data harvested from the 2021 survey were assumed constant for the pre-lockdown year 2019. Traffic flows for the pre-BRT year 2009 were considered because BRT was not in existence as of then, hence the 2021 data was processed for further analysis without extrapolation. It reflects the true characteristics of the current BRT traffic volumes, speeds, and densities. Tables 3.11 and 3.12 show the peak and off-peak BRT traffic flows, speeds, and densities harvested and processed with PCEs applied for further analysis.

BRT Traffic Flowrates - Pilot Site

Step 1: Estimation of Peak and Off-Peak BRT traffic volumes, densities, and speeds

Table 3. 11: Post Lock-down (2021) BRT Traffic Data for Pilot Site (Peak)

u (km/hr) ±15%	k (pce/km)	Total Flow (pce/hr)
Column 1	Column 2 (Col 3/Col 1)	Column 3
69	2	108
59	1	72
58	1	36
67	1	72
72	1	108
62	1	36
66	1	36
68	1	72
61	1	36
68	1	72
71	1	72
75	1	72

Table 3. 12: Post Lock-down (2021) BRT Traffic Data for Pilot Site (Off-Peak)

u (km/hr) ±15%	k (pce/km)	Total Flow (pce/hr)
Column 1	Column 2 (Col 3/Col 1)	Column 3
73	1	72
61	1	36
60	1	36
71	1	36
75	1	72
66	1	36
69	1	36
71	1	36
66	1	36
69	1	36
75	0	36
79	0	36

Step 2: Estimation of BRT Route Capacities for Pilot Test**.**

As aforementioned, the BRT headway was calculated using equation (3.4) previously defined as the tip-to-tip headway of vehicles on a dedicated route such as BRT. It became necessary at this point to estimate this parameter as it is very important for the estimation of the BRT route capacity. The outcome of the estimation is as outlined below: The BRT traffic flow rates were estimated by applying previously defined equations (3.4), (3.5), and (3.6). Recall that the length of an articulated BRT is 18m and the reaction time is taken as 2.5s, while the correction factor k is 1.5, hence BRT lane capacity without the application of PCEs is calculated as follows:

PILOT SITE (Peak)

The average speed of BRT Buses (at peak) $= 63.7km\ per\ hr = 18\,m/s$

BRT Vehicle Length $= 18m;\ assumed\ reaction\ time = 2.5s$ and correction factor $k = 1.5$

Using equation (3.4) the time headway was computed as:

$$T_h = \frac{18}{18} + 2.5 + \frac{1.5 \times 18}{2}\left(\frac{1}{2.5}\right) = 9s\ hence,$$

$$BRT\ Lane\ Capacity = {}^{3600}/_{9} = 400veh/hr$$

PILOT SITE (Off-Peak)

The average speed of BRT Buses (at off $-$ peak) $= 69.4km\ per\ hr = 19.3\,m/s$

BRT Vehicle Length $= 18m;\ reaction\ time = 2.5s$ and correction factor $k = 1.5$

Using equation (3.4) the time headway was computed as:

$$T_h = \frac{18}{19.3} + 2.5 + \frac{1.5 \times 19.3}{2}\left(\frac{1}{2.5}\right) = 9.2s\ hence,$$

$$BRT\ Lane\ Capacity = {}^{3600}/_{9.2} = 391veh/hr$$

From the results obtained, the peak and off-peak BRT traffic flowrates estimated for the pilot site have revealed the occurrence of capacity shifts or capacity differentials compared to the capacities of the adjoining lanes, and it will be recalled that this study investigates the influence of BRT on mixed traffic capacity utilization and its time headway implications therefore, to understand the attendant effects, the BRT mixed traffic capacities were estimated by summing up the non-mixed traffic capacities on the adjoining lanes and the BRT dedicated lane capacities. Capacity utilization rates were then determined for both the non-mixed and mixed traffic scenarios. It is worthy of note that the calculated BRT dedicated lanes capacities obtained were kept constant across the three survey periods. Having estimated the BRT mixed traffic capacities, it was also easy to estimate other traffic flow characteristics associated with

them such as, $k_{Q(M)}$ ~ mixed traffic density at capacity, $Q_{(M)}$ ~ mixed traffic capacity, and $u_{Q(M)}$ ~ mixed traffic speed at capacity. The summary of the before and after BRT mixed-traffic capacities and traffic flow rates for the pilot site at peak and off-peak periods is shown in Table 3.13.

Table 3. 13**:** Summary of Peak and Off-Peak Mixed Traffic Flow Rates for Pilot Test (Before and After BRT)

SITE	Traffic Period	Survey Period	Q_{BRT}	Q_M	$k_{Q(M)}$	$u_{Q(M)}$	$u_{f(M)}$
PILOT SITE	Peak	2009	400	1400	39	36	72
		2019	400	1627	45	36	72
		2021	400	1522	42	36	72
	Off-Peak	2009	391	1411	29	49	98
		2019	391	1642	34	48	96
		2021	391	1535	32	48	96

2009 ~ without BRT, 2019 ~ pre-lockdown, 2021 ~ post-lockdown, Q_{BRT} ~ BRT route capacity, Q_M ~ mixed traffic capacity, $k_{Q(M)}$ ~ mixed traffic critical density, $u_{Q(M)}$ ~ mixed traffic speed at capacity, $u_{f(M)}$ ~mixed traffic free flow speed

3.6 Determination of Roadway Capacity Utilization Criteria Table for Pilot Test

As previously defined, capacity utilization is *a measure of the extent to which the capacity of a roadway is being used*. In other words, roadway capacity utilization is a ratio of operational traffic flow and operational maximum roadway capacity, also referred to as volume-to-capacity ratio or degree of saturation. It is on this premise that the Level of Capacity Utilization (LCU) criteria table was developed. The operational flow or demand volume is the actual number of vehicles moving past a section or point on a roadway within a period (usually an hour). For simplicity, it is often referred to as the actual output volumes. Operating roadway capacity on the other hand is the maximum number of vehicles expected to move past a section or point within an hour. It is also referred to as the maximum possible vehicle output. This ratio gives the utilization rate of a typical road section under investigation. The objective function for quantitative assessment is traffic flow, while the independent parameter is density. The criteria table is underpinned by the fundamental relationship between flow, speed, and density, also known as the fundamental diagram, and the three variables are interconnected.

3.6.1 Determination of LCU Criteria Table – Pilot Site

3.6.1.1 Estimation of Operational Traffic Capacity

Recall that $q = uk$, and speed, $u = u_f - bk$, hence, capacity, $Q = u_f k - k^2 b$

$$\frac{\partial q}{\partial k} = u_f - 2bk = 0;\ k_Q = \frac{u_f}{2b}$$

Therefore, the speed at capacity, $u_Q = \frac{2b(u_f k - k^2 b)}{u_f}$

As stated in chapter two, the peak traffic data was used to develop the capacity utilization criteria table, while the LCU was determined using the off-peak traffic data. Recall the peak traffic flow-density model equation for the post-lock-down year 2021 is given previously by equation 3.19 as:

$$q_{2021(peak)pilotsite} = -1.2005k^2 + 74.948k - 47.423 \qquad R^2 = 0.96$$

Recall that from step 1d of subsection 3.5.3, the above model equation was used to estimate capacity, density at capacity, and speed at capacity as $1122veh/hr$, $31veh/km$, and $36km/hr$ respectively. The standard deviation of the 12-period flows was determined as 165, hence the operational capacity for the pilot site is $(1122 + 165) = 1287veh/hr$. The operational capacity $Q \approx 1287pce/hr$ can be approximated to $1300pce/hr$ and split into five capacity utilization levels for the LCU criteria table. As stated earlier, the capacity utilization levels are designated as (A to E), where LCU A is the best roadway capacity utilization and LCU E, is the worst. LCU A is the capacity level with a 100 percent volume-to-capacity ratio, which is the boundary between steady flow and forced flow sections of the flow-density curve, and the remaining percentages are distributed as 85 (LCU B), 75 (LCU C), 50 (LCU D) and 25 (LCU E) percent respectively.

3.6.1.2 Estimation of operational travel speed

The standard deviation of the 12-period speed was determined as 4, hence the operational travel speed at capacity for the pilot site is $(36 + 4) = 40km/hr$.

From the model equation above, speed is evenly distributed between the free-flow speed of 74.95km$/hr \approx 75km/hr$ for class E and the speed at capacity of $40km/hr$ for class A. The speed is used to compute the attendant densities and its time for 1km of roadway, and subsequently, the LCU criteria table was developed. Thus,

Level A (100%) = 1300 pce/hr

Level B (85%) = $0.85 * 1300 = 1105 pce/hr \approx 1200 pce/hr$

Level C (75%) = $0.75 * 1300 = 975 pce/hr \approx 1000 pce/hr$

Level D (50%) = $0.50 * 1300 = 650 pce/hr \approx 700 pce/hr$

Level E (25%) = $0.25 * 1300 = 325 pce/hr \approx 400 pce/hr$

By the estimated speeds, densities, and time for each capacity utilization level, the LCU criteria table is presented in Table 3.14.

Table 3. 14**:** LCU Criteria for Pilot Site

LCU	Qu %	Flow (Q) veh/h	Density (k) veh/km/lane	Speed(u) km/hr
A	86 - 100	1300	33	≤40
B	76 - 85	1200	27	45
C	51 - 75	1000	18	55
D	26 - 50	700	11	65
E	0 - 25	400	5	≥75

3.6.2 Determination of Capacity Utilisation Levels (Before and After BRT)

Having estimated the non-mixed and mixed traffic flow rates and capacities for the survey periods before and after BRT, the capacity utilization rates and levels for the pilot site at off-peak traffic periods were determined based on the fundamental flow-density relationship, as previously defined by equations 2.33, 2.34, and 2.35, as the ratio of actual traffic flow levels (5min) to the maximum possible flow or capacity and expressed as a percentage, as shown below:

$$Q_u = \frac{ku_f\left(1-\frac{k}{k_j}\right)^2}{\left(-\frac{u_f}{k_j}\left(\frac{u_f}{2\left(\frac{u_f}{k_j}\right)}\right)^2 + (u_f)\frac{u_f}{2\left(\frac{u_f}{k_j}\right)} - c\right)} \times 100\%$$

3.6.2.1 Determination of Non-Mixed Off-Peak Capacity Utilisation Levels

Based on the developed criteria table for LCU determination as shown in table 3.14 above, non-mixed off-peak capacity utilization rates and levels for the 5mins flow intervals within an hour were determined for the pilot site and across the three survey periods. Table 3.15 shows the summary of the 5mins non-mixed off-peak traffic capacity utilization rates and levels for

the pilot site during the post-lockdown year 2021, the pre-lockdown year 2019, and pre-BRT 2009 survey periods.

Table 3. 15**:** Summary of non-mixed off-Peak Capacity Utilization Rates and Levels

Pilot Site (off-Peak) – Non-mixed	Capacity Utilization								
Period(5mins)	Survey Periods			Qu Rates (%)			LCU		
	2009	2019	2021	2009	2019	2021	2009	2019	2021
1	251	308	282	22	22	22	E	E	E
2	318	390	357	28	28	28	D	D	D
3	323	397	363	28	28	28	D	D	D
4	583	715	654	51	51	51	D	D	D
5	393	482	441	34	34	34	D	D	D
6	262	321	294	23	23	23	E	E	E
7	484	593	543	42	42	42	D	D	D
8	366	449	411	32	32	32	D	D	D
9	398	489	447	35	35	35	D	D	D
10	575	705	645	50	50	50	D	D	D
11	618	757	693	54	54	54	C	C	C
12	548	672	615	48	48	48	D	D	D
Non-Mixed Operational Capacities	1150	1411	1290	37	37	37	D	D	D

3.6.2.2 Determination of Mixed Off-Peak Traffic Capacity Utilisation Rates and Levels

Based on the developed criteria table for LCU determination as shown in table 3.14 above, mixed off-peak capacity utilization rates and levels for the 5mins flow intervals within an hour were determined for the pilot site and across the three survey periods. Recall that the BRT dedicated lane traffic flows were added to the non-mixed traffic flows on the adjoining lanes to obtain the mixed-traffic flows. Table 3.16 shows the summary of the 5mins mixed off-peak traffic capacity utilization rates and levels for the pilot site during the post-lockdown year 2021, the pre-lockdown year 2019, and the pre-BRT year 2009 survey periods.

Table 3. 16: Summary of Mixed Off-Peak Capacity Utilization Levels

Pilot Site off-peak (mixed)				Capacity Utilization					
Period(5mins)	Survey Periods			Qu Rates (%)			LCU		
	2009	2019	2021	2009	2019	2021	2009	2019	2021
1	323	387	354	21	21	21	E	E	E
2	354	430	393	23	23	23	E	E	E
3	359	436	399	23	24	24	E	E	E
4	619	754	690	40	41	41	D	D	D
5	465	561	513	30	31	31	D	D	D
6	298	361	330	19	20	20	E	E	E
7	520	633	579	34	34	34	D	D	D
8	402	489	447	26	27	27	D	D	D
9	434	528	483	28	29	29	D	D	D
10	611	744	681	40	40	41	D	D	D
11	653	797	729	42	43	43	D	D	D
12	584	712	651	38	39	39	D	D	D
Mixed Operational Capacities	1540	1838	1681	30	31	31	D	D	D

3.6.5.6 Pilot Site Capacity Utilisation Rates by the Survey Periods

Figures 3.22 to 3.24 show the capacity utilization rates across the sites for the three survey periods:

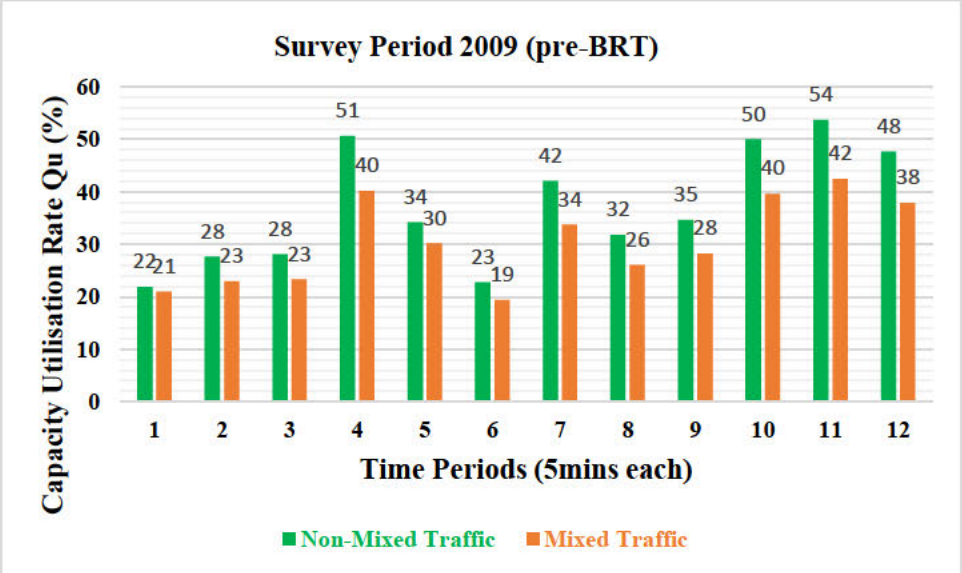

Figure 3. 22: Capacity Utilization Rates in 2009 (pre-BRT)

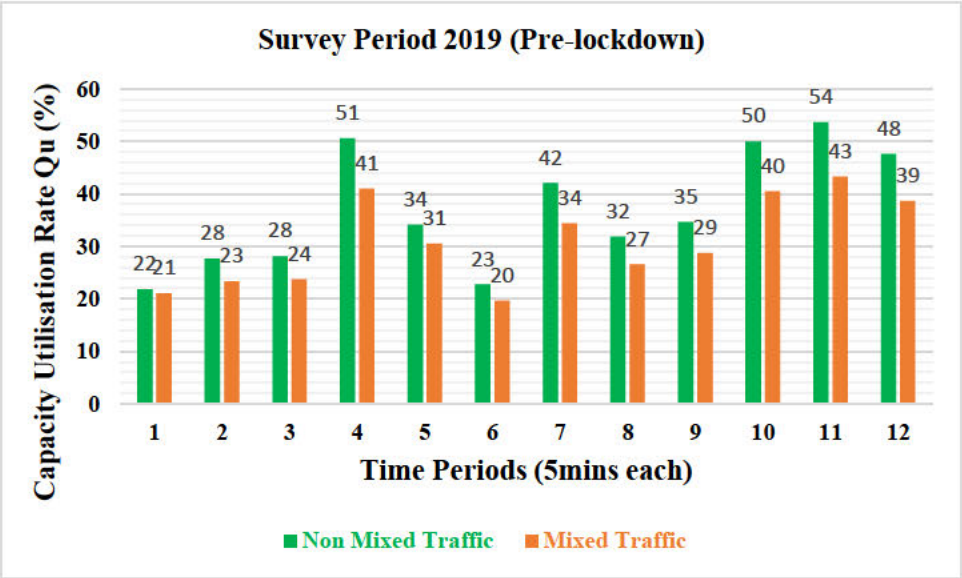

Figure 3. 23: Capacity Utilisation Rates in 2019 (Pre-Lockdown)

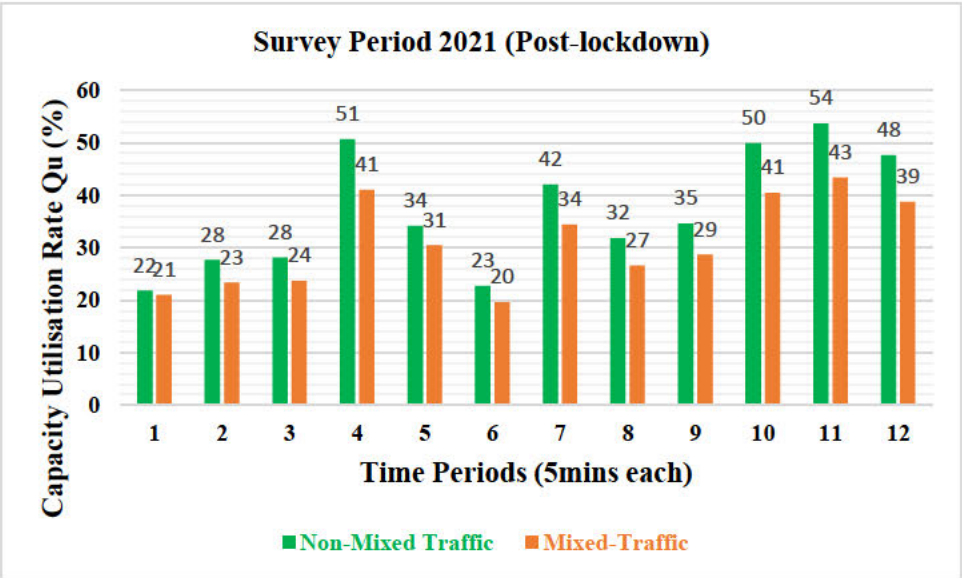

Figure 3. 24: Capacity Utilisation Rates in 2021 (Post-Lockdown)

3.6.6 Determination of Non-Mixed and Mixed Traffic Capacity Differentials

Non-mixed and mixed traffic capacity differentials were subsequently estimated as shown in Tables 3.17 and 3.18 to determine the extent of the differentials from the threshold of traffic flow 1700 veh/hr/lane. Recall that the threshold capacity is $0.85Q_D$, where Q_D is the design

capacity for multilane highways according to (HCM7, 2022; HCMTRB, 2012; Salisu et al., 2020a).

Table 3. 17**:** Summary of Non-Mixed Traffic Capacity Differentials for Pilot Test

SITE	Traffic Period	Survey Periods					
		2009 (pre-BRT)		2019 (Pre-lockdown)		2021 (Post-lockdown)	
		Q_{NM}	$\Delta Q/\ln$	Q_{NM}	$\Delta Q/\ln$	Q_{NM}	$\Delta Q/\ln$
PILOT SITE	Peak	1000	700	1227	473	1122	578
	Off Peak	1020	680	1251	450	1144	556

Note: Threshold of Traffic Flowrate; $0.85Q_D$ = 0.85 (2000 vehs/hr/lane) = 1700veh/hr/lane, $Q_{NM}/\ln$ ~ mixed traffic capacity per lane, Δ ~ Differential

Table 3. 18**:** Summary of Mixed Traffic Capacity Differentials for Pilot Test

SITE	Traffic Period	Survey Periods					
		2009 (pre-BRT)		2019 (Pre-lockdown)		2021 (Post-lockdown)	
		Q_M	$\Delta Q/\ln$	Q_M	$\Delta Q/\ln$	Q_M	$\Delta Q/\ln$
PILOT SITE	Peak	1400	300	1627	73	1522	178
	Off Peak	1411	289	1642	58	1535	165

Note: Threshold of Traffic Flowrate; $0.85Q_D$ = 0.85 (2000 vehs/hr/lane) = 1700veh/hr/lane, $Q_M/\ln$ ~ mixed traffic capacity per lane, Δ ~ Differential

3.6.7 Summary of Findings Based on the 'Before and After BRT' Approach

The Pilot study, through the application of the 'Before and After BRT' methodology which involved the extrapolation of post-lockdown data backward to the pre-BRT year 2009 and the pre-lockdown year 2019, has shown logical results with respect to the estimated capacity utilization rates and determined levels of capacity utilization of the R27 BRT corridor. Even though the results showed fair capacity utilization rates and levels, and the selection of the approach was engendered by some research limitations during the preliminary survey, the extrapolated data for the pre-BRT year 2009 and the pre-lockdown year 2019 were not a true representation of the traffic situation for the periods, and for the pilot site investigated.

Whilst the 'before and after BRT' approach is theoretical and predictive due to the backward extrapolation of data using traffic growth rates from literature, it is only applicable to the period

before the advent of BRT (the pre-BRT year 2009) and the periods (the pre-lockdown year 2019, and post-lockdown 2021) after its construction hitherto. It is however not 100% reliable and applicable for an empirical approach which is a 'with and without BRT' scenario.

Recall that as stated earlier, the methodology employed for this study would be empirical, based on survey data obtained directly from the various sites. The data were collected through ATC loggers connected to pneumatic tubes lying in parallel and spaced 1m apart. The empirical method involves the application of a 'with and without BRT' scenario, where the traffic flow on the adjoining lanes is referred to as the 'without BRT' scenario and described as a 'with BRT' scenario when traffic flow on the BRT dedicated lanes, i.e., the BRT buses are mixed with the adjoining lanes' traffic. This implies that with the empirical approach, the mixed traffic scenario 'with BRT', was created by the fusion of mixed traffic 'without BRT' on adjoining lanes with BRT dedicated lane traffic flows. This is considered with the assumption that the physical barrier between the dedicated lanes and the adjoining lanes is taken off. Therefore, to obtain the traffic characteristics of the 'with BRT' traffic scenario, there is the need to isolate for analysis and determine the BRT dedicated lane traffic flow rates as shown later in this chapter.

Consequently, the empirical method considered the three scenarios illustrated in Figure 2.8 of Chapter 2 for this analysis viz: Scenario (1) roadway without the influence of BRT (without BRT), scenario (2) roadway with the influence of BRT (with BRT), and scenario (3) roadway with dedicated carriageway lane to BRT service only (BRT dedicated lane). The empirical method (with and without BRT) is better than the 'before and after BRT approach as it allows the direct measurement or collection of real-time traffic data, and the data so collected gives a true representation of the traffic situation during the collection period. In view of the foregoing discussion, the 'before and after BRT' is discontinued as it cannot hold for an empirical study, hence the 'with and without BRT' approach was applied for further analysis.

3.7 Pilot Assessment of Capacity Utilization – 'With and Without BRT' Approach

The empirical method, which involves three traffic scenarios as stated in the previous section follows most of the procedural steps employed for the 'before and after BRT approach, but in this case, the data extracted were analyzed directly and not extrapolated. The empirical data extracted for the 'before and after BRT' approach was analyzed using the 'with and without BRT' approach.

3.7.1 Capacity Utilization Criteria Table for Pilot Site

To develop the capacity utilization criteria table, it will be recalled that the peak traffic data was used for this purpose. Therefore, recalling the empirical data reported in Table 3.6, the following stepwise procedure was employed for the development of the capacity utilization criteria table.

Step 1. Using the peak traffic flow data, the five-minute traffic volumes are converted first into PCEs using SANRAL's standard PCE values given as PC = 1, MV = 1.75, and HV = 3.0. Using a multiplier (x12), the 5mins volumes were converted to flow rates in pce per hour, and with the speed known, densities were calculated using equation 2.17, $q = uk$. Table 3.19 shows the estimated flow, speed, and density at peak hour.

Table 3. 19: Level of Capacity Utilization (LCU) Parameters for the Pilot Site

	PC	MV	HV	Vol	MV	HV	q	u	k	q
Period	*1*	*2*	*3*	*4*	*5*	*6*	*7*	*8*	*9*	*10*
					*2*1.75*	*3*3*	*1 + 5 + 6*		*10/8*	*7*12*
1	38	4	2	44	7	6	51	57	11	620
2	43	7	0	50	12	0	55	58	11	660
3	40	9	2	51	16	6	35	60	7	420
4	65	8	1	74	14	3	68	51	16	820
5	53	7	1	61	12	3	66	52	15	792
6	49	4	0	53	7	0	69	50	17	832
7	65	5	1	71	9	3	73	55	16	884
8	51	5	2	58	9	6	69	53	16	828
9	60	5	0	65	9	0	82	55	18	985
10	60	7	3	70	12	9	76	51	18	912
11	75	2	3	80	4	9	77	49	19	924
12	65	5	3	73	9	9	82	47	21	980
1hr	1102	66	24	1192				83±1		804±47

1, 2, 3…10 ~ column numbers, column 1 - 4 ~ volume by 5mins, columns 5 - 7 ~ flow (pce/5mins), q ~ total flow(pce/hr), u ~ speed (km/hr), k ~ density (pce/km), PC ~ passenger car, MV ~ medium vehicle, HV ~ heavy vehicle

Step 2. The density and flow parameters in Table 3.40 were used to calibrate a flow-density model using Microsoft Excel, which has been shown by (Ben-Edigbe & Ferguson, 2005; Minderhoud *et al*., 1996; van Arem *et al*., 1994), to have a quadratic function given by equation 3.23. Figure 3.25 shows the graphical representation of the flow-density relationship.

$$q = -ak^2 + bk - c \qquad 3.23$$

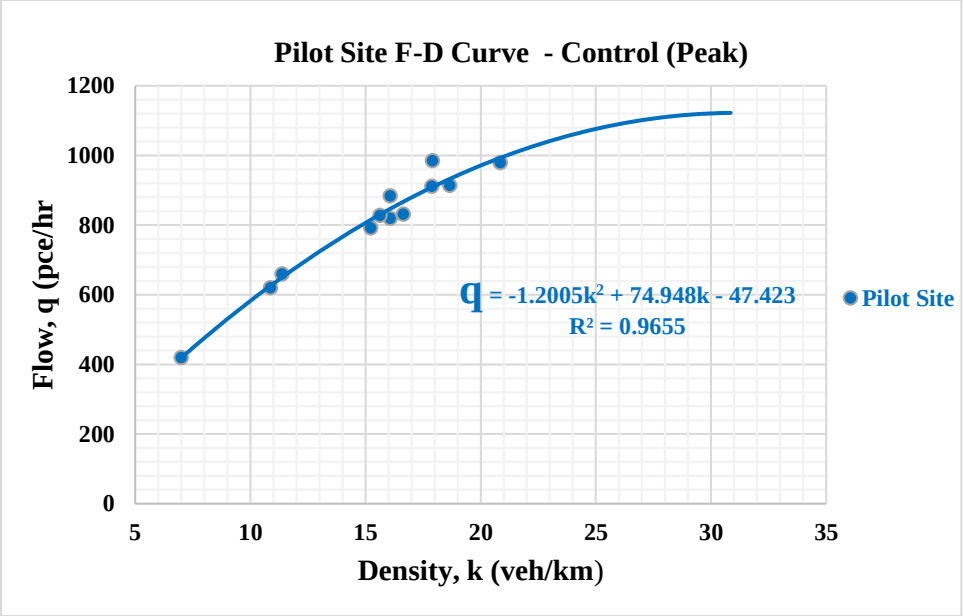

Figure 3. 25: Traffic Flow-Density (F-D) Curve for Pilot Site (Peak)

The calibrated model equation is given as equation 3.24:

$$q_{PilotSite(Control)} = -1.2005k^2 + 74.948k - 47.423 \quad R^2 = 0.96 \qquad 3.24$$

Step 3: Statistical testing of the calibrated model for validity. Table 3.20 below shows the results of the validity test carried out on the model for the pilot site 'without BRT' influence. As shown, the coefficients of the derived model have the anticipated sign conventions for concavity, while the coefficient of determination $R^2 = 0.9655$ is greater than 0.5, which indicates the existence of a strong relationship between density and flow, and the capability of predicting capacity.

Table 3. 20**:** Level of Capacity Utilization Model Validity Tests for Pilot Site

Parameters	*q*	*k*	Constant
t' values	16.9	2.2	
Coefficients	-1.2005	74.95	-47.423
Std. Error	47	1	
R^2	0.96		
F	1755	2.81	
df	11		
Residuals	-9.619	-1.245	

The F-observed statistics at ten degrees of freedom is bigger than the F-critical value of 2.81, suggesting that the model equation 3.24 did not occur by chance. Additionally, the value of the

t-observed statistic at the 5% level of significance is higher than 2.2, indicating that the variables used are useful, and density is a crucial factor in flow estimation. The statistics data sequel to the analysis, was directly pulled from a Microsoft Excel file. It is important to note that the coefficient of "k" denotes the free-flow speed, roughly 75 km/hr. The study hypothesizes that the extent of road capacity utilization level resulting from BRT is significant. The aggregated model was subsequently used to predict capacity, estimate density at capacity, and speed at capacity in step 4 by differentiating *q* with respect to *k* and feeding back necessary values.

Step 4: The density at capacity, capacity or maximum flow, and the speed at maximum flow were determined using equation 3.24 as follows:

$$q_{Pilotsite(control)peak} = 1.2005k^2 + 74.948k - 47.423 \qquad R^2 = 0.96$$

By differentiating q with respect to k,

$$\frac{\partial q}{\partial k} = 2 * (-1.2005\text{k}) + 74.948 = 0$$

$$k_{crt} = k_Q = 31.13 pce/km \approx 31\, pce/km$$

By plugging the critical density k_Q into equation 3.24, the capacity is calculated and is given as:

$$Q = q_{Pilotsite(control)peak} = -1.2005(31)^2 + 74.948(31) - 47.423$$

$$Q = q_{Pilotsite(control)peak} = 1122.3 pce/hr \approx 1122 pce/hr$$

By substituting k_Q and the estimated Q into the fundamental diagram equation $q = uk$, the speed at capacity is therefore obtained as:

$$u_Q = \frac{Q}{k} = \frac{1122}{31} = 36.19 \approx 36 km/hr$$

Hence the capacity or maximum flow is $1122 pce/hr$, with a corresponding speed at capacity $u_Q = 36 km/hr$.

Step 5: The estimated capacity $Q \approx 1122 pce/hr$ can be approximated to $1200 pce/hr$ and split into five capacity utilization levels for the LCU criteria table. As stated earlier, the capacity utilization levels are designated as (A to E), where LCU A is the best roadway capacity utilization and LCU E, is the worst. LCU A is the capacity level with a 100 percent volume-to-capacity ratio, which is the boundary between steady flow and forced flow sections of the flow-density curve, and the remaining percentages are distributed as 85% (LCU B), 75% (LCU C), 50% (LCU D) and 25% (LCU E) percent respectively, therefore,

Level A (100%) = 1200 pce/hr

Level B (85%) = $0.85 * 1200 = 1020 pce/hr \approx 1100 pce/hr$

Level C (75%) = $0.75 * 1200 = 900pce/hr \approx 900pce/hr$

Level D (50%) = $0.50 * 1200 = 600pce/hr \approx 600pce/hr$

Level E (25%) = $0.25 * 1200 = 400pce/hr \approx 300pce/hr$

Step 6: From the model equation above, speed is evenly distributed between its free-flow speed of 74.95km$/hr \approx 75km/hr$ for class E and speed at capacity of $36km/hr \approx 40km/hr$ for class A. The speed is used to compute the attendant densities and its corresponding time for 1km of roadway, and subsequently, the LCU criteria table is developed. Thus, the LCU criteria table for the pilot site is presented in Table 3.21.

Table 3. 21**:** LCU Criteria for Pilot Site

LCU	Qu %	Flow (Q) veh/h	Density (k) veh/km/lane	Speed(u) km/hr
A	86 – 100	1200	30	≤40
B	76 – 85	1100	24	45
C	51 – 75	900	16	55
D	26 – 50	600	9	65
E	0 – 25	300	4	≥75

3.7.2 BRT Dedicated Lane Capacity Utilization for Pilot Site

Step 1. Estimation of five-minute BRT traffic volume using SANRAL's standard PCE values for heavy vehicle class as shown in table 3.22 below.

Table 3. 22**:** BRT Dedicated Lane Level of Capacity Utilization Parameters

Period	BRT 1	BRT 2	u 3	k 4	k 5	q 6	q 7
		1*3		*6/3*	*7/3*	1*12	2*12
1	3	9	69	0	2	36	108
2	2	6	59	0	1	24	72
3	1	3	58	0	1	12	36
4	2	6	67	0	1	24	72
5	3	9	72	0	1	36	108
6	1	3	62	0	1	12	36
7	1	3	66	0	1	12	36
8	2	6	68	0	1	24	72
9	1	3	61	0	1	12	36
10	2	6	68	0	1	24	72
11	2	6	71	0	1	24	72
12	2	6	75	0	1	24	72
1hr	22		66±2			22	66

1, 2, ...8 ~ column numbers, column 1 ~ volume by 5mins, column 2 ~ BRT flow (pce/5mins), u ~ speed (km/hr), k5 ~ density (veh/km), k6 ~ density (pce/km) q7 ~ total flow(veh/hr), q8 ~ total flow(pce/hr) BRT ~ Bus Rapid Transit.

Step 2: Determination of BRT dedicated lane capacity: The BRT time headway, defined by braking performance and measured tip-to-tail, is given by equation 3.25:

$$T_h = \frac{L}{V} + t_r + \frac{kV}{2}\left(\frac{1}{a_f} - \frac{1}{a_l}\right) \quad 3.25$$

Where T_h – time headway (s); V – vehicle speed; L – Length of vehicle.

t_r – Reaction time; $k -$ arbitrary safety factor (usually greater than or equal to 1)

$a_f -$ Minimum braking deceleration of the following vehicle

$a_l -$ Maximum braking deceleration of the lead vehicle

Note that for brick wall considerations, a_l is infinite and is usually eliminated.

The capacity of vehicles on a single roadway lane is the inverse of the tip-to-tip headway.

Hence the BRT lane capacity in vehicles per hour can be expressed as:

$$Q_{BRT} = \frac{3600}{\frac{L}{V} + t_r + \frac{kV}{2}\left(\frac{1}{a_f} - \frac{1}{a_l}\right)} \quad 3.26$$

The BRT traffic flow rates were estimated by applying equations (3.25) and (3.26), with the following standard and measured parameters:

The average speed of BRT Buses (at off $-$ peak) $= 63.7 km\ per\ hr = 18\ m/s$

BRT Vehicle Length $= 18m;\ reaction\ time = 2.5s$ and correction factor $k = 1.5$

Using equation (3.4) the time headway was computed as:

$$T_h = \frac{18}{18} + 2.5 + \frac{1.5 \times 18}{2}\left(\frac{1}{2.5}\right) = 9s\ hence,$$

$$BRT\ Lane\ Capacity = {}^{3600}/_{9} = 400 veh/hr$$

Step 3: Estimation of capacity utilization rate for BRT:

Recall that capacity utilization rate had been defined as the ratio of actual traffic flow levels (5min) to the maximum possible flow or capacity and expressed as a percentage, as shown below:

$$Q_u = \frac{k u_f \left(1 - \frac{k}{k_j}\right)}{\left(-\frac{u_f}{k_j}\left(\frac{u_f}{2\left(\frac{u_f}{k_j}\right)}\right)^2 + (u_f)\frac{u_f}{2\left(\frac{u_f}{k_j}\right)} - c\right)} \times 100\% \quad 3.27$$

Therefore $Q_u = {}^{66}/_{400} \times 100\% = 16.8 \approx 17\%$. Therefore, the level of capacity utilization from the criteria table for the pilot site's BRT dedicated lane is E**.** With the LCU at E, the other associated performance parameters are a density of 4veh/km and a speed of 75km/hr. This implies that the LCU of the BRT dedicated lane at E is characterized by or associated with a low volume of vehicles, high speed, and reduced travel time to destinations for vehicles moving on it. Perhaps the design of a mixed traffic scenario may be a solution to this capacity utilization loss, however, one is not completely sure whether it would be feasible until further analyses in that regard are completed in the remaining sections of this chapter. As earlier mentioned, the peak traffic data for the pilot site was used to set up the LCU criteria table and was used as a control for the subsequent traffic performance evaluations at the pilot site. Consequently, these analyses continue in the next section with the determination of the LCU 'without BRT' influence at the pilot site, using the off-peak traffic data.

3.7.3 Without BRT Influence Capacity Utilization for the Pilot Site

Step 1: Estimation of off-peak 5mins and hourly flows, speeds, and densities for the pilot site using the empirical data from Table 3.7, as shown in Table 3.23 below.

Table 3. 23**:** Without BRT LCU Parameters for Pilot Site (off-peak)

Period	PC	MV	HV	Vol	MV	HV	q	u	k	q
	1	*2*	*3*	*4*	*5*	*6*	*7*	*8*	*9*	*10*
					*2*1.75*	*3*3*	*1 + 5 + 6*		10/8	7*12
1	14	2	2	18	4	6	24	67	4	282
2	21	5	0	26	9	0	30	68	5	357
3	12	7	2	21	12	6	30	72	5	363
4	41	6	1	48	11	3	55	71	9	654
5	25	5	1	31	9	3	37	72	6	441
6	21	2	0	23	4	0	25	71	4	294
7	37	3	1	41	5	3	45	75	7	543
8	23	3	2	28	5	6	34	73	6	411
9	32	3	0	35	5	0	37	75	6	447
10	36	5	3	44	9	9	54	72	9	645
11	47	1	3	51	2	9	58	77	9	693
12	37	3	3	43	5	9	51	73	8	615
1hr	346	45	18	409			479	(72±1)		479

1, 2, 3…10 ~ column numbers, column 1 - 4 ~ volume by 5mins, columns 5 - 7 ~ flow (pce/5mins), column 10 ~ total flow(pce/h), u ~ speed (km/hr), k ~ density (pce/km), PC ~ passenger car, MV ~ medium vehicle, HV ~ heavy vehicle

Step 2. Calibration of flow-density models using the density and flow parameters in Table 3.23 with PCEs applied. Figure 3.26 shows the graphical representation of the flow-density relationship:

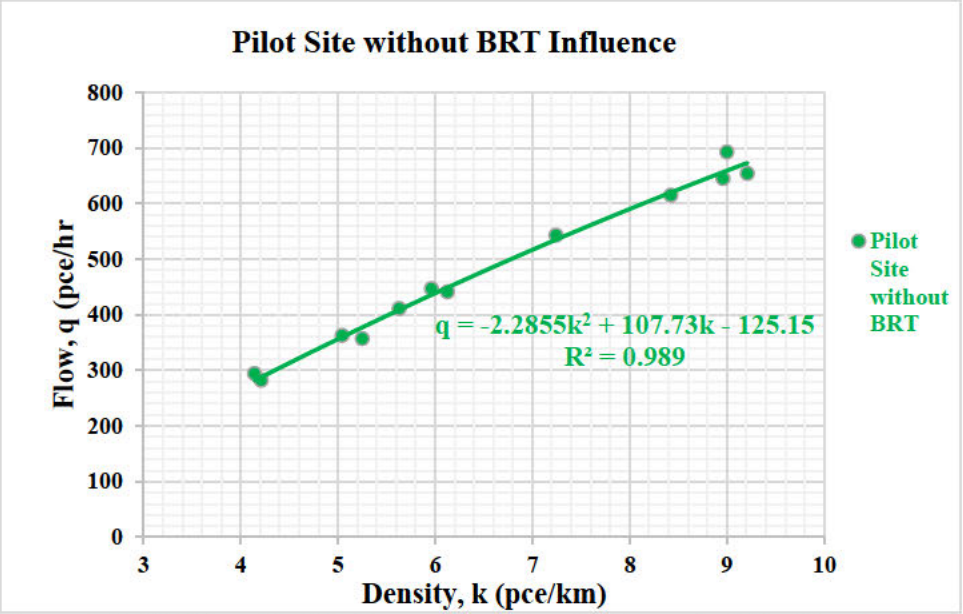

Figure 3. 26: Without BRT Influence Flow-Density Curve for Pilot Site (Off-Peak)

The calibrated flow-density model is given as equation 3.26:

$$q_{withoutBRT(Pilot)off-peak} = -2.2855k^2 + 107.73k - 125.15 \quad R^2 = 0.98 \qquad 3.28$$

Step 3: Statistical testing of the calibrated model for validity. Table 3.24 below shows the results of the validity test carried out on the off-peak flow-density models for the pilot site 'without BRT' influence. As shown, the coefficients of the derived model have the anticipated sign conventions for concavity, while the coefficient of determination $R^2 = 0.989$ is greater than 0.5, which indicates the existence of a strong relationship between density and flow, and the capability of predicting capacity.

Table 3. 24 Level of Capacity Utilization Model Validity Tests

	q	*k*	Constant
t' values	11.3	2.2	
Coefficients	**-2.2855**	**107.73**	**-125.15**
Std. Error	42	1	
R^2	0.98		
F	6026	2.81	
df	11		
Residuals	-11.574	-1.576	

The F-observed statistics at eleven degrees of freedom is bigger than the F-critical value of 2.81, suggesting that the model equation did not occur by chance. Additionally, the value of the t-observed statistic at the 5% level of significance is higher than 2.2, indicating that the variables used are useful, and density is a crucial factor in flow estimation. The statistics data sequel to its analysis, was directly pulled from a Microsoft Excel file. It is important to note

that the coefficient of "k" denote the free-flow speed of roughly 108 km/hr. The aggregated model was subsequently used to predict capacity, estimate density at capacity, and speed at capacity in step 4 by differentiating q with respect to k in each model equation and feeding back necessary values.

Step 4: The density at capacity, capacity or maximum flow, and the speed at maximum flow were determined using equation 3.28 as follows:

$$q_{withoutBRT(off-Peak)pilotsite} = -2.2855k^2 + 107.73k - 125.15 \quad R^2 = 0.98$$

By differentiating q with respect to k,

$$\frac{\partial q}{\partial k} = 2 * -2.2855\text{k} + 107.73 = 0$$

$$k_{crt} = k_Q = 23.57 pce/km \approx 24\, pce/km$$

By plugging the critical density k_Q into equation 3.28 the capacity is calculated and is given by:

$$Q = q_{withoutBRT(off-Peak)pilotsite} = -2.2855(24)^2 + 107.73(24) - 125.15$$

$$Q = q_{withoutBRT(off-Peak)pilotsite} = 1143.92 pce/hr \approx 1144 pce/hr$$

By substituting k_Q and the estimated Q into the fundamental diagram equation $q = uk$, the speed at capacity is therefore obtained as:

$$u_Q = \frac{Q}{k} = \frac{1144}{24} = 47.6 \approx 48 km/hr$$

Hence the capacity or maximum flow at off-peak traffic period is $1144 pce/hr$, with a corresponding speed at capacity $u_Q = 48 km/hr$.

As shown in Table 3.23 above, the mean flow per hour which represents the 12-period flows for the pilot site is 479 veh/hr, therefore the capacity utilization rate Q_u for the pilot site is ${}^{479}/_{1144} \times 100\% = 41.8 \approx 42\%$. Hence based on the criteria table 3.21, the LCU for the pilot site 'without BRT' influence is D. Where the LCU is at D, the other attendant performance parameters from the criteria table are a density of 9veh/km, and a speed of 65km/hr.

3.7.4 'With BRT' Influence Capacity Utilization for Pilot Site

Step 1: Estimation of 'with BRT' off-peak 5mins and hourly flows, speeds, and densities for the pilot site is shown in table 3.25. Note that the BRT dedicated lane traffic flows in table 3.23 with applied PCEs were added to the 'without BRT' traffic flows in table 3.24.

Table 3. 25**: 'With BRT'** level of Capacity Utilization Parameters for Pilot Site (off-peak)

Period	PC	MV	HV	*BRT*	Vol	MV	HV	*BRT*	q	μ	k	q
	1	*2*	*3*	*4*	*5*	*6*	*7*	*8*	*8*	*10*	*11*	*12*
						*2*1.75*	*3*3*	*4*3*	*1 + 6 + 7+8*		12/10	7*12
1	14	2	2	3	21	4	6	9	33	67	6	390
2	21	5	0	2	28	9	0	6	36	68	6	429
3	12	7	2	1	22	12	6	3	33	72	6	399
4	41	6	1	2	50	11	3	6	61	71	10	726
5	25	5	1	3	34	9	3	9	46	72	8	549
6	21	2	0	1	24	4	0	3	28	71	5	330
7	37	3	1	1	42	5	3	3	48	75	8	579
8	23	3	2	2	30	5	6	6	40	73	7	483
9	32	3	0	1	36	5	0	3	40	75	6	483
10	36	5	3	2	46	9	9	6	60	72	10	717
11	47	1	3	2	53	2	9	6	64	77	10	765
12	37	3	3	2	45	5	9	6	57	73	9	687
1hr	246	45	18	22	431				545	72±1		545

1, 2, 3…10 ~ column numbers, column 1 - 4 ~ volume by 5mins, columns 5 -7 ~ flow (pce/5mins), column 10 ~ total flow(pce/h), u ~ speed (km/hr), k ~ density (pce/km), PC ~ passenger car, MV ~ medium vehicle, HV ~ heavy vehicle

Step 2. Calibration of the 'with BRT' flow-density model using the density and flow parameters in Table 3.25 with PCEs applied. Figure 3.27 shows the graphical representation of the models:

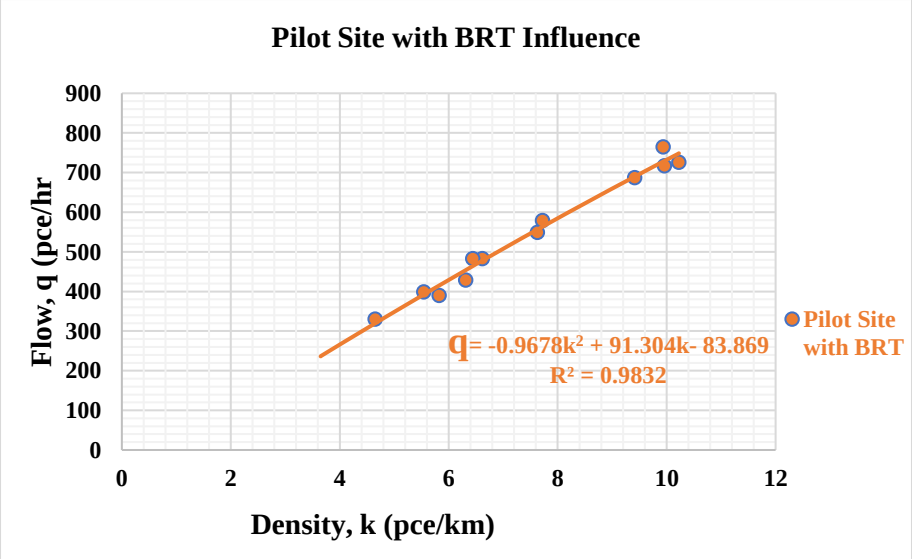

Figure 3. 27: With BRT Influence Flow-Density Curve for Pilot site (Off-Peak)

The calibrated flow-density model is given as equation 3.47:

$$q_{withBRT(off-peak)pilot} = -0.9678k^2 + 91.304k - 83.869 \quad R^2 = 0.98 \qquad 3.29$$

Step 3: Statistical testing of the calibrated model for validity. Table 3.26 below shows the results of the validity test carried out on the off-peak flow-density model for the pilot site 'with BRT' influence. As shown, the coefficients of the derived model have the anticipated sign conventions for concavity, while the coefficient of determination $R^2 = 0.9832$ is greater than 0.5, which indicates the existence of a strong relationship between density and flow, and the capability of predicting capacity.

Table 3. 26**:** Level of Capacity Utilization Model Validity Tests

	q	*k*	Constant
t' values	12.6	2.2	
Coefficients	**-0.9678**	**91.304**	**-83.869**
Std. Error	43	1	
R^2	0.98		
F	6630	2.81	
df	11		
Residuals	-7.046	-1.917	

The F-observed statistics at eleven degrees of freedom is bigger than the F-critical value of 2.81, suggesting that the model equation did not occur by chance. Additionally, the value of the t-observed statistic at the 5% level of significance is higher than 2.2, indicating that the variables used are useful, and density is a crucial factor in flow estimation. The statistics data sequel to its analysis, was directly pulled from a Microsoft Excel file. It is important to note that the coefficient of "*k*" denotes the free-flow speed of roughly 91 km/hr. The aggregated model was subsequently used to predict capacity, estimate density at capacity, and speed at capacity in step 4 by differentiating *q* with respect to *k* and feeding back necessary values.

Step 4: The density at capacity, capacity or maximum flow, and the speed at maximum flow were determined using equation 3.29 as follows:

$$q_{withBRT(off-Peak)pilotsite} = -0.9678k^2 + 91.304k - 83.869 \quad R^2 = 0.98$$

By differentiating q with respect to k,

$$\frac{\partial q}{\partial k} = 2 * -0.9678\text{k} + 91.304 = 0$$

$$k_{crt} = k_Q = 47.2pce/km \approx 47\ pce/km$$

By plugging the critical density k_Q into equation 3.29 the capacity is calculated and is given by:

$$Q = q_{withBRT(off-Peak)pilotsite} = -0.9678(47)^2 + 91.304(47) - 83.869$$

$$Q = q_{withBRT(off-Peak)pilotsite} = 2069.5pce/hr \approx 2070pce/hr$$

By substituting k_{crt} and the estimated Q into the fundamental diagram equation $q = uk$, the speed at capacity is therefore obtained as:

$$u_Q = \frac{Q}{k} = \frac{2070}{47} = 44.04 \approx 44km/hr$$

Hence, the capacity or maximum flow 'with BRT' influence at off-peak traffic period is $2070pce/hr$, with a corresponding speed at capacity $u_Q = 44km/hr$. As shown in Table 3.25 above, the mean 'with BRT' flow per hour which represents the 12-period flows is 545 veh/hr, therefore the capacity utilization rate Q_u 'with BRT' = $^{545}/_{2070} \times 100\% = 26.3 \approx 26\%$. Based on the criteria table 3.21, the LCU for the pilot site 'with BRT' influence is D. With the LCU at D, the other attendant performance parameters from the criteria table are a density of 9veh/km and, a speed of 65km/hr.

3.7.5 Comparative Assessment of Capacity Utilization for Pilot Site Summary

Based on the findings from the analysis of empirical data at the pilot site, a comparative assessment and synthesis of evidence among the three roadway and flow scenarios discussed in Chapter 2 which include (1) roadway with dedicated carriageway lane to BRT service only; (2) roadway without the influence of BRT, and (3) roadway with the influence of BRT, are discussed. Having developed a criteria table, it is necessary to evaluate and compare traffic performance at the pilot site during each 5mins flow interval or period in terms of capacity utilization rates and hence determine the level of capacity utilization, (LCU) using the criteria table. Recall that analysis is based on the fundamental flow-density relationship, and capacity utilization rate had been defined as the ratio of actual traffic flow levels (5min) to the maximum possible flow or capacity and expressed as a percentage. Table 3.27 shows the summary of capacity utilization levels for the pilot site. The table depicts BRT dedicated lane as having the worst average level capacity utilization (LCU E) of the three scenarios. Mixed traffic with BRT influence has an average LCU D same as without BRT. It suggests that during the off-peak period, the influence of BRT on capacity utilization is not significant.

Table 3. 27**:** Summary of Off-Peak Capacity Utilization Rates and Levels for Pilot Site

Period	q BRT (pce/hr)	q without BRT (pce/hr)	q with BRT (pce/hr)	Q_u BRT (%)	Q_u without BRT (%)	Q_u with BRT (%)	LCU BRT	LCU without BRT	LCU With BRT
1	108	282	390	28	25	19	D	E	E
2	72	357	429	18	31	21	E	D	E
3	36	363	399	9	32	19	E	D	E
4	72	654	726	18	57	35	E	C	D
5	108	441	549	28	39	27	D	D	D
6	36	294	330	9	26	16	E	E	E
7	36	543	579	9	47	28	E	D	D
8	72	411	483	18	36	23	E	D	E
9	36	447	483	9	39	23	E	D	E
10	72	645	717	18	56	35	E	C	D
11	72	693	765	18	61	37	E	C	D
12	72	615	687	18	54	33	E	C	D
1hr				17	42	26	E	D	D

3.7.5.1 Based on BRT Dedicated Lane Performance

The LCU E of the BRT dedicated lane shows that the Bus route is substantially underutilized, hence, the level of capacity utilization is poor. This is caused by the designation of the lane solely for BRT buses with no competition from other vehicle classes moving on the adjoining lanes. From this finding, and with respect to the geometric characteristics of the BRT dedicated lane, coupled with vehicle characteristics, the LCU of the BRT lane may not improve from E. This is due to the observed width of the BRT dedicated lane of 4.3m. Besides, with a BRT vehicle width of 3.1m, only one bus can move on the dedicated lane at once, making it impossible for two buses to move side by side.

3.7.5.2 Based on Traffic Flowrate 'without BRT' Influence

In comparison with the LCU of the BRT dedicated lane at E, it can be observed that at level D, there is an associated reduction in speed, as well as an increase in density but increased travel time. Besides, the LCU of the adjoining lanes at D shows that the capacity utilization improved due to the traffic mix on those lanes which comprise of passenger cars, medium vehicles, and a few heavy vehicles in different proportions; whereas the BRT dedicated lane is used by only one vehicle class which are the BRT buses.

3.7.5.3 Based on Traffic Flowrate 'with BRT' Influence

In comparison with the LCU 'without BRT' influence, it can be observed that both LCUs are the same, as well as all parameters associated with them. Although as expected, the maximum

flow was higher, while the speed dropped. However, it may be expected that the level of capacity utilization would improve to level C. This outcome may be caused by the poor utilization of the BRT dedicated lanes. In other words, this may imply that there is an insufficient number of BRT buses in the BRT transit scheme, even though the 'with BRT' traffic flow scenario was characterized by 5mins (pce/5mins) flow lane and one hour (pce/hr) capacity differentials, increase in density, speed reduction, and increase in travel time. In summary, the overall LCU D, with BRT influence at the pilot site shows that capacity utilization can be significantly enhanced by mixed traffic scenarios as against having a BRT dedicated lane, especially one with a median configuration design.

3.7.6 Summary of Capacity Differentials at the Pilot Site

In summary, a criteria table has been developed for the assessment of traffic flow performance under different flow scenarios such as roadway 'with BRT', roadway 'without BRT', and BRT dedicated lane only. Sequel to the comparisons and synthesis of evidence that have emerged from the pilot analysis, the different levels of capacity utilization for the various scenarios considered are caused by differentials in germane traffic flow parameters such as capacity, speed, density, and travel time. Figure 3.34 below gives a pictorial description of the capacity and other traffic characteristics differentials that are responsible for the traffic flow performance and levels of capacity utilization observed at the pilot site.

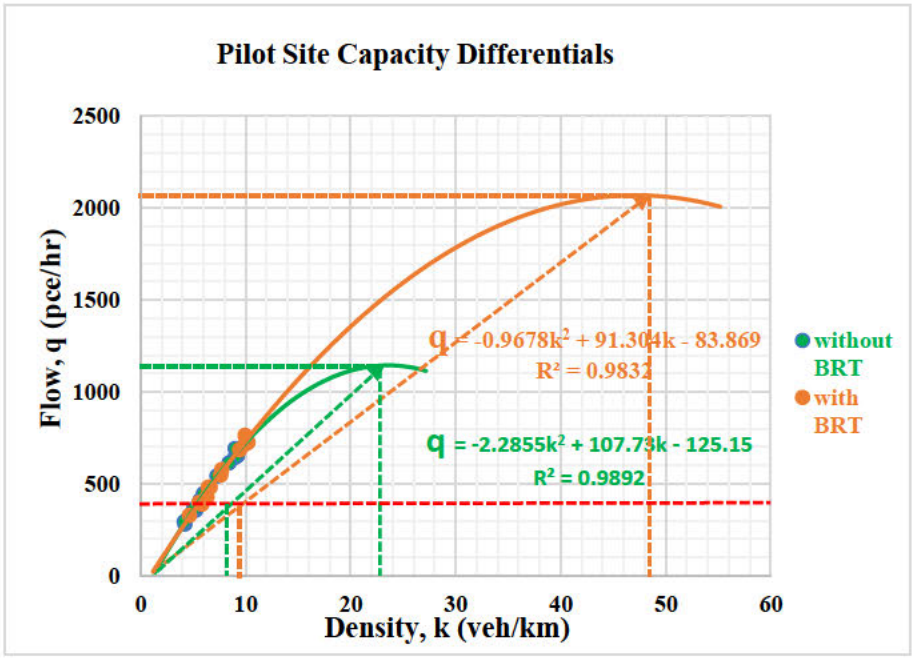

Figure 3. 28: Capacity Differentials at Pilot site

With respect to capacity differentials shown in Figure 3.28, the capacity Q_1 of roadway 'with BRT', indicated by the yellow line is $2070pce/hr$, capacity Q_2 of roadway without BRT, indicated by the green line is $1144pce/hr$, and BRT dedicated lane capacity Q_3, indicated by the red line is 391pce/hr. The corresponding speed at capacity of roadway 'with BRT' is $44km/hr$, the speed at capacity of roadway 'without BRT' is $48km/hr$. Similarly, the corresponding density at capacity k_1 of roadway with BRT is $47pce/km$, density at capacity k_2 of roadway without BRT is $24pce/km$. Likewise, the BRT dedicated lane density k_{31} based on travel speed 'with BRT' influence is approximately $9veh/km$, while the BRT dedicated lane density k_{32} based on travel speed 'without BRT' influence is approximately $8veh/km$. Table 3.28 shows the summary of capacity utilization rates and levels, as well as the associated traffic characteristics differentials for the pilot site.

Table 3. 28**:**Summary of capacity utilization differentials for Pilot Test

Site/ Survey Period	Roadway Condition	u_f	Q			U		K				Q_u (%)	LCU
			Q_1	Q_2	Q_3	u_1	u_2	k_1	k_2	k_{31}	k_{32}		
Pilot Site	with BRT	91	2070	1144	400	44	48	47	24	10	8	26	D
	without BRT	108										42	D
	BRT Dedicated Lane	60										17	E

u_f ~ free-flow speed (km/hr),Q_1 ~ capacity with BRT(pce/hr), Q_2 ~ capacity without BRT(pce/hr), Q_3 ~ BRT capacity(veh/hr), u_1 ~ speed at capacity with BRT(km/hr), u_2 ~ speed at capacity without BRT(km/hr), k_1 ~ density at capacity with BRT (pce/km), k_2 ~ density at capacity without BRT (pce/km), ~ k_{31} ~ dedicated lane density with BRT (pce/km), k_{32} ~ dedicated lane density without BRT (pce/km), Q_u ~ capacity utilization rate (%), LCU ~ level of capacity utilization

3.12 Pilot Assessment of Time Headway Implications – Deterministic Approach

Recall that as opined by (Ben-Edigbe *et al*., 2013; J. Ben-Edigbe *et al*., 2014). the capacity of a roadway is very sensitive to the distribution of headways, and sequel to estimating the time headways for the mixed traffic 'with and without BRT' scenarios, and on the BRT dedicated lanes at off-peak periods, the attendant time headway differentials between the 'with and without BRT' were also estimated using equation (3.30) which is the difference between them and is given as:

$$\Delta T_h = T_{h(without\ BRT)} - T_{h(with\ BRT)} \quad 3.30$$

With respect to the without BRT situation, and with the applied traffic growth rates compounded backward, the results displayed in the tables above show that between the pre-BRT year 2009 and the pre-lockdown year 2019, the roadway capacity cumulatively increased by 22% in all the sites. In 2021 post lockdown, when the actual time empirical data was taken, there was a 9% decline in capacity from pre-lockdown year 2019, in all the sites investigated. Note that the pandemic lockdown in 2020 had an impact on traffic flow data from the pre-lockdown year 2019, resulting in the capacity decline. Critical densities also increased on average by 29 percent and decreased by 9 percent. However, the increase in capacity resulted in a decrease in time headway between the pre-BRT year 2009 and the pre-lockdown year 2019, while the opposite occurred between the pre-lockdown year 2019 and the post-lockdown year 2021 due to the capacity decline. For the BRT mixed traffic condition, the same increment and decline in capacity and critical densities were observed as shown except for the time headways whose values were different due to the increase in capacity. With respect to the 'without BRT' scenario between each survey period, and as traffic grew from the pre-BRT year 2009, time headways on average declined accordingly by 18% in the pre-lockdown year 2019 and increased by 9% in the post-lockdown year 2021 due to capacity reduction. Similarly, for mixed traffic 'with BRT' situations, headways declined from the pre-BRT year 2009 by 14 percent in the pre-lockdown year 2019 and increased by 6% in the post-lockdown year 2021. In summary, the results have revealed significant declines and increments in time headway values. For instance, the BRT mixed traffic scenario resulted in 21%, 18%, and 19% average time headway reductions in the pre-BRT year 2009, the pre-lockdown year 2019, and the post-lockdown year 2021 survey periods respectively. The summary of the time headways for the 'with and without BRT', and BRT dedicated lane scenarios estimated via the deterministic approach with attendant differentials is shown in Table 3.29.

Table 3. 29**:** Summary of Time Headway Differentials for Pilot Test

SITE	Traffic Period	Survey Period	$T_{h(BRT)}$	T_h Without BRT	T_h With BRT	ΔT_h
PILOT SITE	Peak	2009	9.0	2.8	2.1	0.7
		2019	9.0	2.3	1.8	0.5
		2021	9.0	2.5	1.9	0.6
	Off-Peak	2009	9.2	3.5	2.6	0.9
		2019	9.2	2.9	2.2	0.7
		2021	9.2	3.2	2.3	0.9

$T_{h(BRT)}$~ BRT time headway; $T_{h(without\ BRT)}$ ~ time headway without BRT; $T_{h(with\ BRT)}$ ~ time headway with BRT; ΔT_h ~ time headway differential

The result shown are indications that mixed traffic flow 'with BRT' influence, is indeed characterized by changes in both macroscopic and microscopic traffic characteristics as observed generally in all the investigated sites. In order words, there are differentials in macroscopic and microscopic traffic characteristics such as speed, density, capacity, and time headways which indicate the possibility of anomalous capacity utilization effects on the roadway. This confirms the assertion by (J. Ben-Edigbe *et al*., 2014) that in a mixed traffic stream, the capacity of a roadway has a significant impact on time headway distribution, which needs to be studied properly via a stochastic approach due to its variabilities, nature of occurrence and the stochastic study is discussed in the next section.

3.12.1 Pilot Assessment of Time Headway Implications – Stochastic Approach

ModelRisk software, a Monte Carlo simulation software from Vose software was used to fit the distributions to data with attendant PDF, CDF, and P-P plots, and carry out hypothesis testing. The ModelRisk software is employed due to it is an open-source software, it is easy to use and is user friendly. It is capable of fitting data to various probability distributions at the same time, with visualizations of the PDF, CDF, P-P plots, and the probability, P-values can be taken from the results interface of the Software. Furthermore, ModelRisk also has the ability to carry out hypothesis testing of any fitted distribution or goodness of fit tests on the models and displays all the result values of the AIC, SIC, and HQIC testing criteria for easy interpretation. The following procedural analytical steps were employed for the fitting of the probability distributions to the time headway data without BRT. Peak and off-peak traffic headway data of the pilot site were used for this pilot assessment. The stepwise procedure employed for the pilot test was replicated in this analysis is as follows:

Step 1: Recall empirical traffic volume data from Tables 3.4 to 3.6, extracted from the ATC, and determine the descriptive statistics of its headway.

Step 2: Fit continuous probability distributions to the headway distribution data and plot the joint PDF, CDF, and P-P plots of each fitted probability distribution model examined for each site and evaluate the statistical results of the model fitting.

Step 3: Carry out the hypothesis testing of the fitted distribution or goodness of fit tests on the models using the Akaike Information Criterion (AIC), Schwarz Information Criterion (SIC), and Hannan Quinn Information Criterion (HQIC) as described in the methodology.

Step 4: Calculate the P-value for each distribution at 95% confidence and 5% significance levels respectively. The higher the P-value and the more it exceeds 0.05 in all three tests at a 5 percent level of significance, the more compatible the model.

Step 5: Select the model that best fits the data based on the smallest AIC value and the largest Loglikelihood (LLH) value. Use the P-value obtained in step 4 and according to the criterion, accept or reject the stated hypothesis.

Step 6: Compare the model parameters as well as the mean time headway of the fitted empirical data with the mixed traffic time headway data and evaluate the outcomes with respect to capacity utilization of the study site.

The descriptive statistics of the headway data for the pilot site are shown in Table 3.31:

Table 3. 30: Summary Statistical Characteristics of the Headways

Descriptive Statistics of Headways	PILOT SITE
Mean	3.67
Standard Error	0.14
Median	2.1
Mode	1
Standard Deviation	4.55
Coefficient of Variation	1.23
Sample Variance	20.69
Kurtosis	13.00
Skewness	3.21
Coefficient of Variance	1.23
Range	37
Minimum	0
Maximum	37
Sum	3711
Sample Size	1010

The PDF, CDF, and P-P plots of the fitted probability distributions for the pilot site are shown in Figures 3.29, 3.30, and 3.31. The P-value of the best-fitted distribution was included in

Figure 3.32. A summary of the probability distribution parameters and how the distributions performed are presented in tables 3.31 and 3.32.

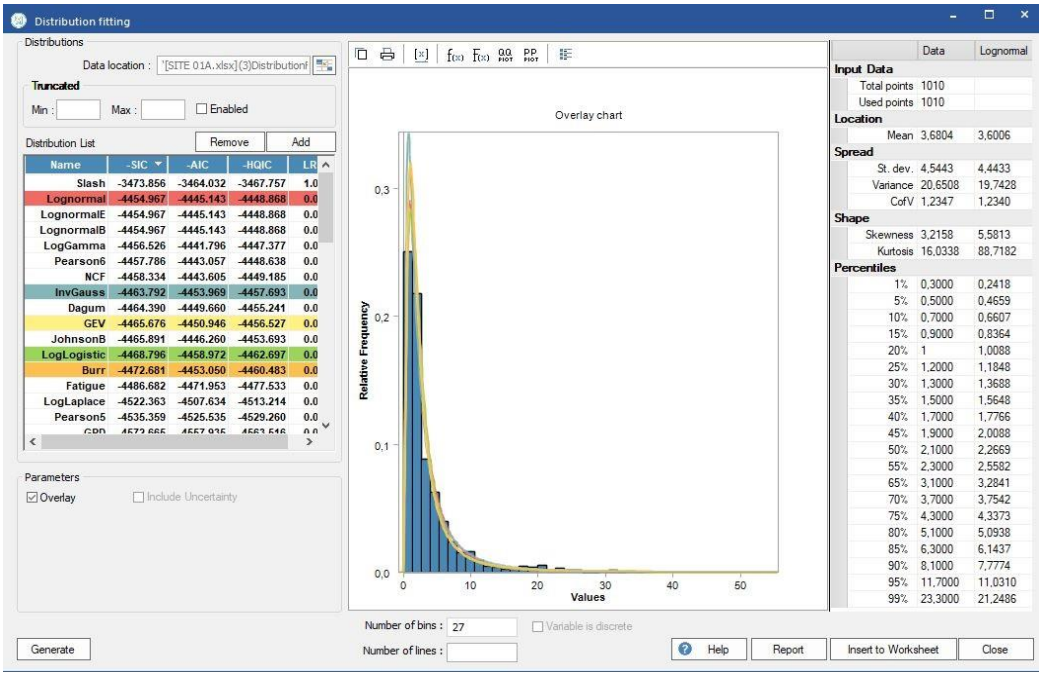

Figure 3. 29: PDF Plot for Pilot Site

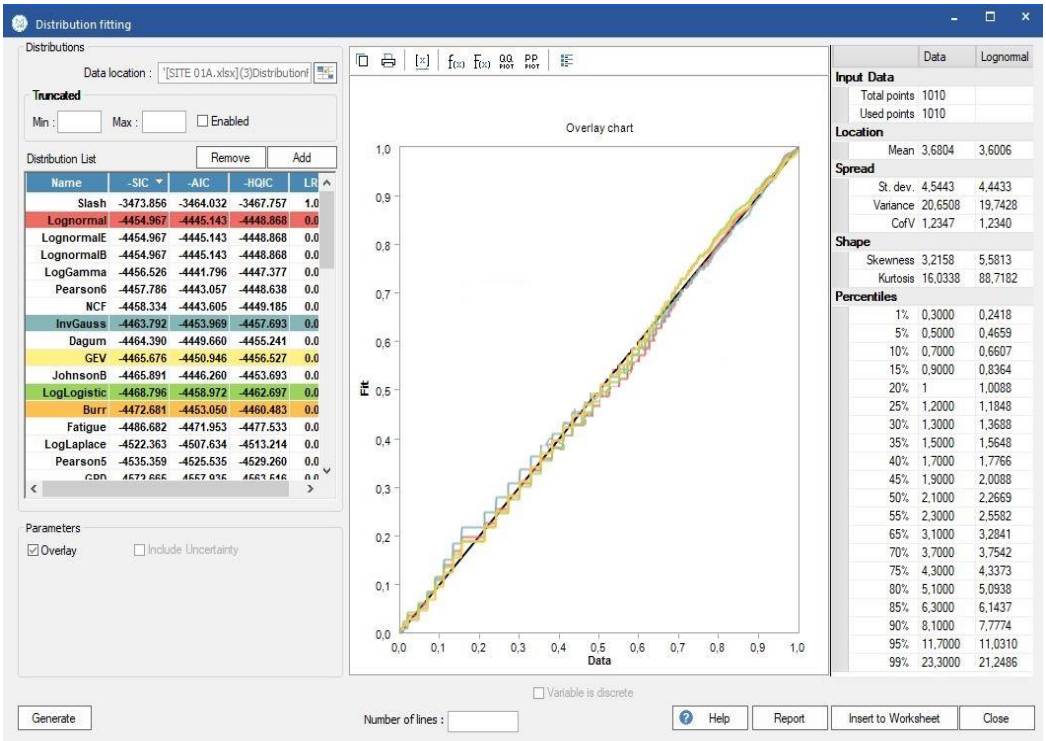

Figure 3. 30: P-P Plot for Pilot Site

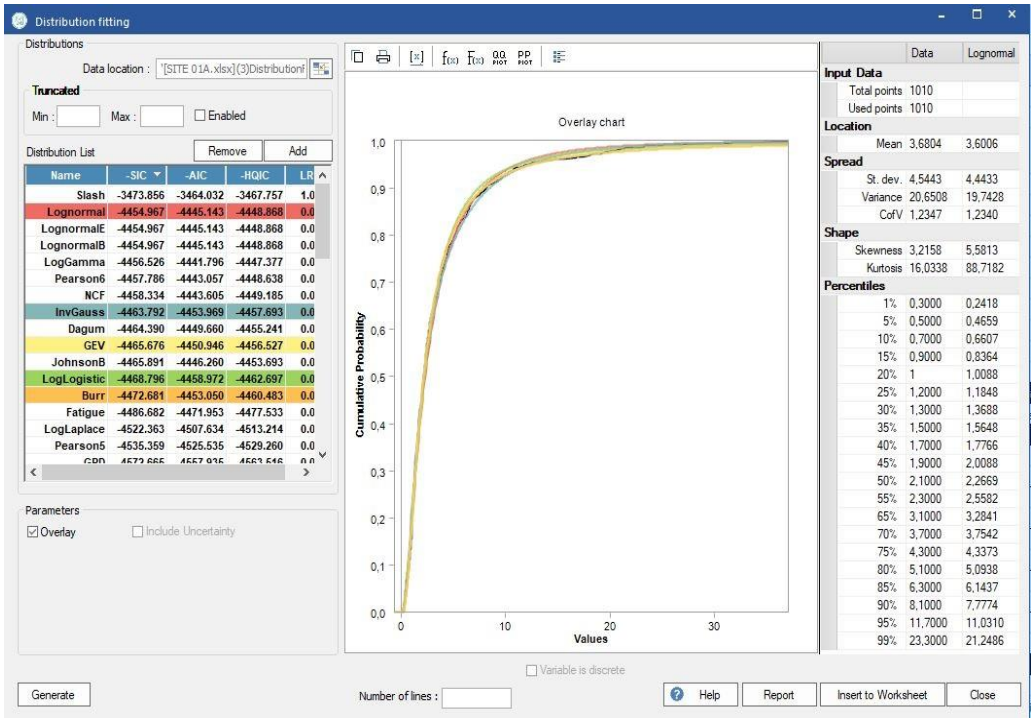

Figure 3. 31: CDF Plot for Pilot Site

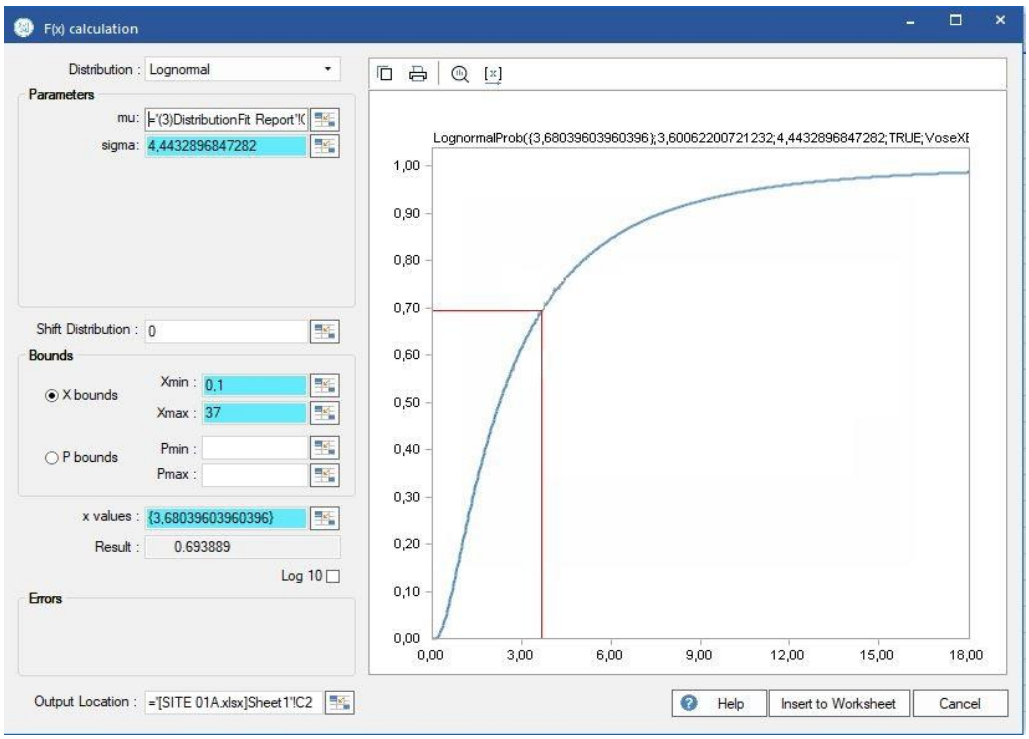

Figure 3. 32: Estimated P-Value and Plot for Pilot Site

Table 3. 31: Summary of Goodness of Fit Tests and Performance of the Probability Models for Pilot Study

Location	Rank	Probability Model	SIC	AIC	HQIC	LLH	P Value	Sig. Level	Hypo. Test	Best Fit
PILOT SITE	2ND	GEV	4042.28	4027.29	4032.96	-2010.64	0.7832	0.5	Accept	Burr
	1ST	Burr	4045.97	**4025.99**	4033.52	**-2008.98**	0.7872	0.5	Accept	
	3RD	Loglogistic	4086.84	4076.84	4080.62	-2036.42	0.7962	0.5	Accept	
	4TH	Lognormal	4150.91	4140.91	4144.69	-2068.45	0.7461	0.5	Accept	
	5TH	InvGauss	4162.53	4152.53	4156.30	-2074.26	0.7055	0.5	Accept	

The summary of the model parameters is shown in Table 3.32:

Table 3. 32: Summary of Parameters of the Probability Distributions for Pilot Study

Location	Probability Distribution	Shape Parameter		Scale Parameter	Location Parameter
PILOT SITE	GEV	0.627169	-	0.887089	1.12756
	Burr	2.80529	0.462925	0.937949	-
	LogLogistic	0.517502	-	0.429871	-
	Lognormal	0.962479	-	0.498461	-
	InvGauss	1.75999	-	3.11653	-

3.13 Inferences from Pilot Study Findings

The pilot study has assessed the influence of BRT on mixed traffic capacity utilization and its time headway implications on regional road R27, along major BRT trunk route T03, in Cape Town South Africa, and arrived at concrete findings that have established the postulated hypotheses and achieved the stated objectives through the application of the aforementioned analytical methods. Firstly, using the 'before and after BRT' approach, coupled with the data obtained from the surveyed sites, flow-density models were calibrated for the prediction of capacity and other germane traffic parameters. A capacity utilization criteria table was developed for the evaluation of traffic flow performance before and after BRT. To determine the level of capacity utilization (LCU) from the criteria table, capacity utilization rates were estimated as the ratio of actual flow to the maximum possible flow (or capacity) for the three survey periods viz pre-BRT year 2009, the pre–lockdown year 2019, and the post-lockdown year 2021. Capacity differentials were evaluated for the survey periods as well. The results from the pilot study showed the existence of anomalous capacity utilization. In other words,

the roadway was underutilized with regard to capacity as seen from the estimated capacity utilization rates. Even though the observed capacity underutilization is caused by the provision of additional lanes during the construction of the BRT corridor, which is justified by this finding and serves as an advantage and solution to the incessant traffic congestion usually experienced on the roadway before the advent of BRT, capacity, therefore, is not maximized. Secondly, similar outcomes were also obtained using the empirical 'with and without BRT' approach, however, due to the shortcomings of the 'before and after BRT' approach, further analysis of the main study is based on the 'with and without BRT' methodology.

Secondly, from the deterministic approach, the pilot analysis has also revealed the existence of stochastic time headway distribution variabilities in the non-mixed traffic flow, with anomalous consequences on the estimated capacities, and speed. With respect to travel time for the proposed mixed traffic design, which was observed to increase and decrease at some point across the sites, these anomalous changes were caused by the stochastic nature of the time headways and speed, hence the time headways were subjected to further analysis to understand how its distribution affected both the estimated mixed and non- traffic characteristics and ultimately capacity utilization. Consequently, using the stochastic approach, the time headway distributions were modelled using continuous probability distributions to see which ones effectively fitted the vehicle time headways of non-mixed traffic on adjoining lanes. Five models were fitted to the time headway distribution data extracted from the ATC, using the ModelRisk software, and the attendant PDF, CDF, and P-P plots were extracted from the software. The goodness of fit of the probability models was assessed by the Akaike Information Criterion (AIC), the Schwartz or Bayesian Information Criterion (SIC or BIC), and the Hannan Quinn Information Criterion (HQIC) model performance criteria respectively. The criterion with the lowest value describes the model that best fits the headways. The Burr distribution provided the best fit based on the AIC and LLH values at 95% level of confidence, and 0.05 level of significance. It had the lowest values of AIC and the largest Log likelihood values at the pilot site. The P-Values, which ranged between 0.70 and 0.79, showed the likelihood of the occurrence of the data sets under the null hypothesis, hence the null hypothesis was accepted. The headway characteristics results which were found to be continuously distributed, showed significant head decrement with the considered mixed traffic scenario.

3.14 Summary

This chapter described has described the two analytical methods employed in this study which are the 'before and after BRT' approach and the empirical 'with and without BRT' approach.

It also described the procedure for collecting the necessary traffic data for both methods. The chapter also emphasized the geometric characteristics of the chosen road segments and the factors for choosing the study site. The technique for gathering traffic statistics, the survey crew, and the site coding for identification were all clearly specified. The best equipment for collecting traffic data was determined to be the automatic traffic counter. Furthermore, the chapter described the stepwise method of analyzing data for model formulation. The pilot study presented in this chapter was used to confirm and ascertain the suitability of the two proposed analytical methods. Therefore, based on the findings, the empirical 'with and without BRT' methodology, which has been tested through the pilot assessment was replicated for the main study. Analysis from the preliminary investigation suggests a distinctive pattern of the determinant of capacity utilization – high speed, and low flow rate. One is not completely sure of such a pattern till the isolated empirical result is compared against findings from unrelated sample survey data. By virtue of the isolated nature of the data on which the preliminary investigation was based, the results of the roadway capacity utilization analysis conducted at best could be described as broadly suggestive. Consequently, the data in this chapter begs a number of questions about the influence of BRT on roadway capacity utilization. For this purpose, the next three chapters (4, 5, and 6) will address issues on the determination of roadway capacity utilization resulting from BRT, their effects on time headway, and their relationship with roadway capacity utilization. Conclusions and recommendations are drawn in Chapter 7.

CHAPTER 4

EMPIRICAL SAMPLE SURVEYS

4.1 Overview

In attempting to explain road traffic reality, the choice of variables that describe a phenomenon is often an issue. One such choice is a selection of variables regarded as the main determinants of the traffic process. In light of the objectives set out in the introduction of this study, empirical results of the interrelationships between the main variables (traffic volume, speed, and BRT) which simultaneously influence roadway capacity utilization at the surveyed sites are presented in this chapter. On the evidence of the preliminary capacity utilization analysis in the last chapter, it can be suggested that there is a distinctive pattern of high speed (without BRT) and low speed (with BRT) resulting from Bus Rapid Transit (BRT). One is not completely sure of such a speed pattern till the isolated empirical result is compared against findings from unrelated survey data. In any case, this chapter will present the results from survey data that would be analyzed in the subsequent chapters.

The tabulated results in this chapter will show the following: site code, total surveyed road length, capacity utilization variability, and site features. Since the study is empirically based, the attendant traffic data is essential to achieving the stated study objectives. The essential traffic data, as well as the appropriate methods employed for its collection, were discussed in the preceding chapter. The traffic data includes details like speed, volume, headway, vehicle type, and time of vehicle movement as recorded by the ATC under the current circumstances. Other traffic characteristics, such as density and capacity, and time headways, were estimated from the empirically surveyed data while the traffic composition is examined utilizing the fundamental relationship of flow. In any case, the remainder of the chapter is divided into three sections, with section 4.4 concluding the chapter. In section 4.2, a summary of the geometric data for the four sites is presented. Along with the geometric data, section 4.3 also includes individual site reports for each study site that were harvested from the automatic traffic counters (ATC). The following is the order of presentation of each site report: the flow-time profile, volume-density graph, speed-density graph, traffic composition, hourly traffic volume, and speed for each prevailing condition. The chapter is summarized in section 4.4.

4.2 Empirical Results from Sites

The study site is R27, situated along the major trunk route T02 (Atlantis – Table View – Civic Centre), as shown in Figure 2.1 is not an exception to this design. It is a provincial route in South Africa that belongs to the second category of roads in the South African route-numbering

scheme and is referred to as a major regional route. It can be recalled that R27 already satisfied the criteria for site selection, as outlined in section 3.3, subsection 3.3.1, the data collected on it are reliable and appropriate for the investigation. Based on these criteria, four sites or roadway segments were selected on R27. For easy identification, they were assigned codes, which are a combination of alphabets and numbers. The study sites are SS001 (Sandown Station – Porterfield Station), SS002 (Porterfield Station – Sandown Station), SS003 (Table View Station – Sunset City Junction), and SS004 (Sunset City Junction – Table View Station). Table 4.1 summarises the physical or geometric features of the four selected sites.

Table 4. 1**:** Summary of Geometric Features of Selected Study Sites

Site Features	SS001	SS002	SS003	SS004
Name of Road	SS to PS	PS to SS	TVS to SCJ	SCJ to TVS
Type of road	R27	R27	R27	R27
Terrain Type	Level Terrain	Level Terrain	Level Terrain	Level Terrain
Annual Daily Traffic (ADT)	12355 veh/day	12069 veh/day	14887 veh/day	14140 veh/day
BRT Lane	Yes	Yes	Yes	Yes
Number of Adjoining Lanes	2	2	2	2
Width of Adjoining Lanes	3.7m/ln	3.7m/ln	3.7m/ln	3.7m/ln
Pavement Surfacing	Asphalt	Asphalt	Asphalt	Asphalt
Length of Road Segment	1250	1250	1200	1200
Presence of Shoulder	Yes	Yes	Yes	Yes
Width of Shoulder	2.5m	2.4m	2.1m	0.98m
Width of BRT Lane	4.3m	4.3m	4.3m	4.3m
Posted Speed	70km/hr	70km/hr	70km/hr	70km/hr

SS ~ Sandown Station, PS ~ Porterfield Station, TVS ~ Table View Station, SCJ ~ Sunset City Junction

Traffic data were collected both on the BRT dedicated lane and adjoining lanes in each site. The ATC was used to collect the data, sequel to being installed on both lanes. The target data, through its analysis, was intended to show differentials in traffic characteristics such as speed, volume, density, headway, and capacity. Manual data collection had initially been carried out for the pilot test, and data collected was compared with automatic data for quality checks. The

four sites were characterized by straight segments with a BRT dedicated and two adjoining lanes located in parallel with it.

4.2.1 Individual Site Data

4.2.1.1 Sandown Station to Porterfield Station SS001

The Sandown Station – Porterfield Station roadway is a three-lane segment with one BRT dedicated lane running parallel to the median and two adjoining lanes also running parallel to it. It is a typical provincial road with an average daily traffic count of 12355 veh/day and a design speed of 80km/h. A speed limit of 70 km/h is posted on the asphalt-paved road, which has a 20-year pavement design life. The roadway is flat with minimal horizontal curves where it is situated. Vehicle traffic on this road is directed from Sandown Station – Porterfield Station. The two adjoining lanes are both 3.7 m wide and with a shoulder 2.5 m in width. The length of the road segment is 2120 m long and runs along the Atlantis axis to Sunset City route, precisely between Sandown Station – Porterfield Station. The length of the road exceeds the permitted stopping sight distances from Sandown Station and Porterfield Station, which are 210m and 550m, respectively. Figure 4.1 shows the setup at site SS001 with installed ATCs and pneumatic tubes ready for data logging. For twelve weeks, the road section's traffic data were continually recorded. There are a variety of vehicle types on this road, including motorcycles, lightweight, medium-weight, and heavy-weight automobiles, however, the proportions of each type of vehicle vary. Figure 4.2 shows the flow versus time profile as obtained from the ATC.

Figure 4. 1**:** Set-Up at Site SS001 with Installed Pneumatic Tubes and ATCs

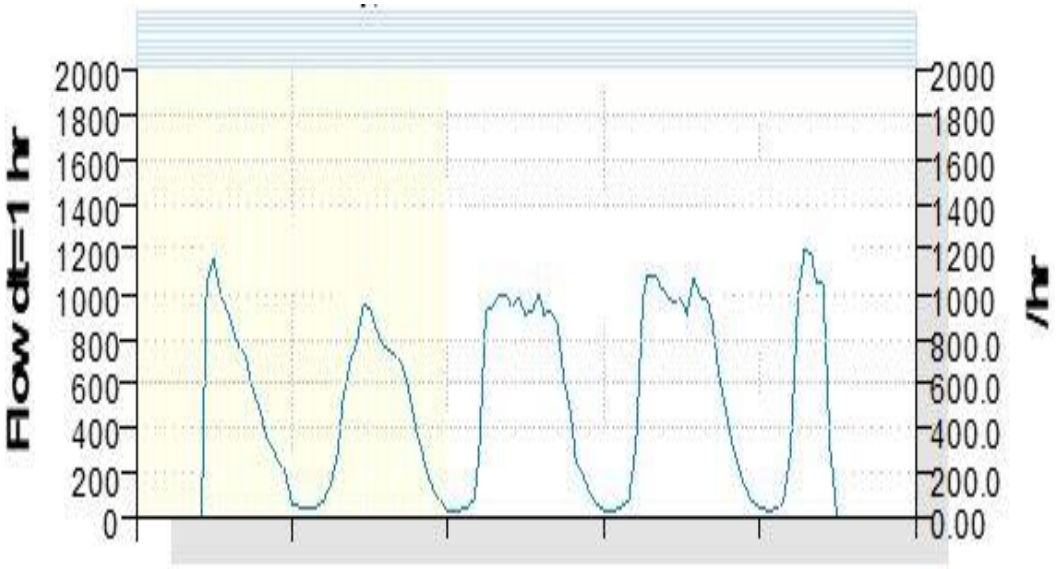

Figure 4. 2: Flow versus Time Profile of SS001

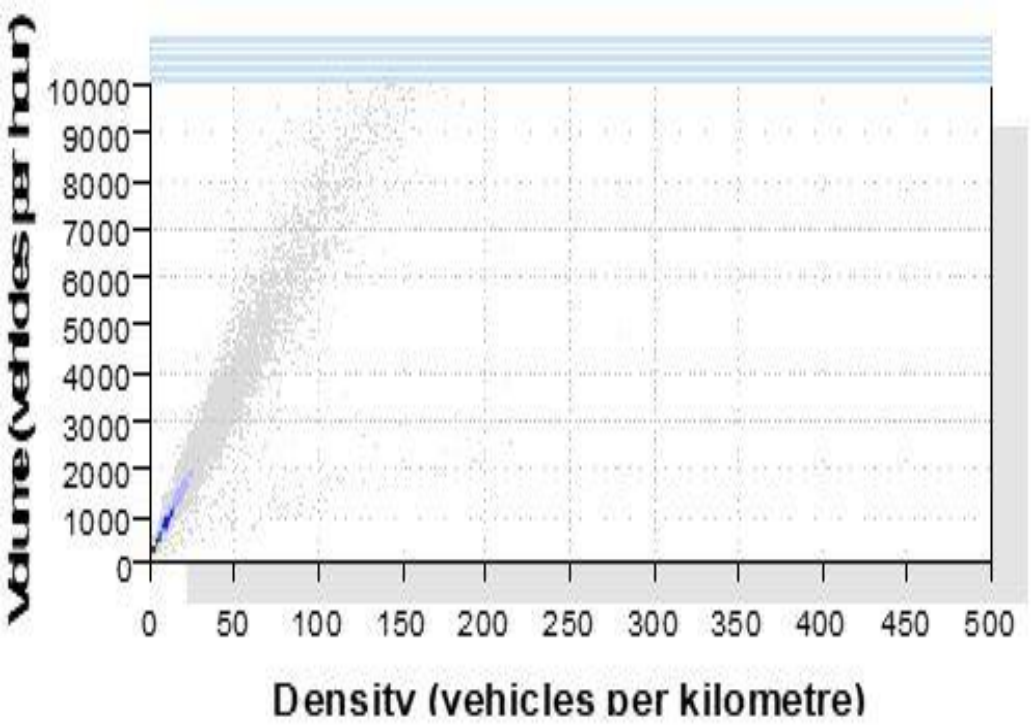

Figure 4. 3: Volume vs Density Plot of SS001

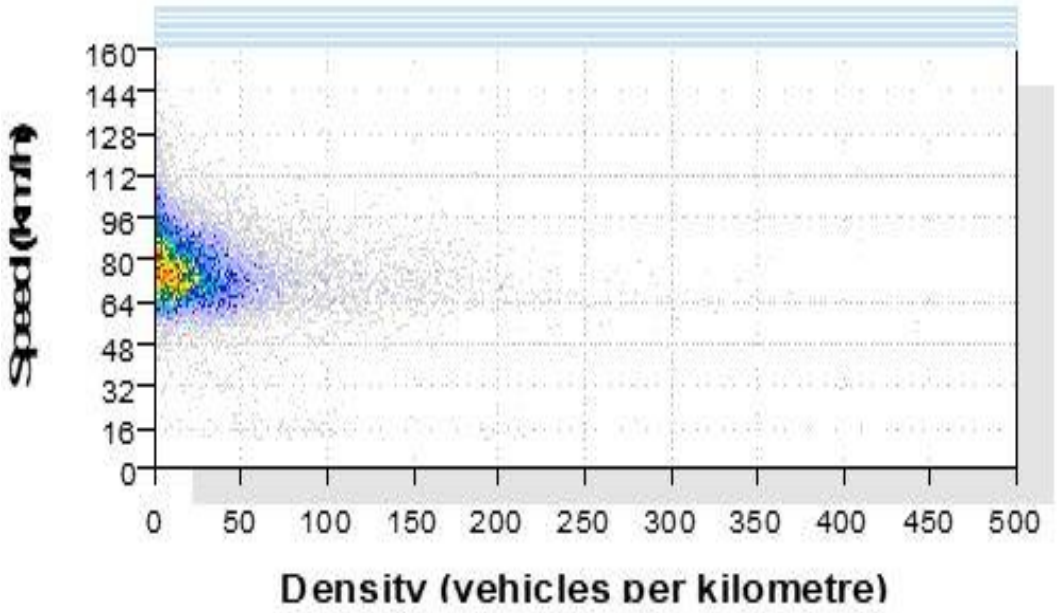

Figure 4. 4: Speed vs Density Plot of SS001

4.2.1.1.1 Empirical Hourly Traffic Volumes at SS001

Traffic data was logged, as shown in the flow vs time profile for site SS001. The period referred to as peak traffic is between 6:30am to 7:30am, while off peak traffic is between 11:00 am and 12:00 pm. Vehicle flow rate and data collection date are connected. The traffic flow/time profile shows that time was the primary factor in the daily variance in traffic flow. Additionally, it's unclear how traffic moves during the week; for instance, Sundays witnessed less movement than other days. Likewise, Figures 4.3 and 4.4, respectively, depict the volume-density and speed-density plots. According to the nature of the relationship between flow and density, in the fundamental diagram. The dispersion plot in Figure 4.3 follows a parabolic curve pattern. Furthermore, it agrees with the fundamental diagram's unrestricted region. Similarly, Figure 4.3 depicts the speed-density plot of the data collected and it is in alignment with the speed-density relationship plot of the fundamental diagram. However, it is necessary to keep in mind that the graph's scope is about a variety of moving vehicles in a traffic stream.

At SS001, four vehicle classes were recognized for the dry condition considered. They are passenger cars (PC), motorcyclists (MC), light vehicles (LV), medium vehicles (MV), and heavy vehicles (HV). However, as was already said, motorbikes especially power bikes, which were scarcely found on the road due to private use and not commercial, were not considered when analyzing the data, The reason motorcycles weren't considered is that there is no car following influence on motorcyclists in the flow of traffic. Tables 4.2 and 4.3 also present the typical hourly composition of traffic volume and speed of the vehicle classes at SS001 during peak and off-peak hour flows, while Table 4.4 presents hourly traffic volume and speed for BRT.

Table 4. 2**:** Typical Volume and Speed for SS001 (Peak Period)

Period	PC per 5mins	MV per 5mins	HV per 5mins	Total per 5mins	μ (Km/hr)
1	95	2	0	97	85
2	92	4	4	100	83
3	97	3	1	101	84
4	101	5	3	109	76
5	86	4	1	91	89
6	95	7	1	103	88
7	98	6	0	104	79
8	95	9	0	104	83
9	85	6	4	95	86
10	89	9	2	100	78
11	80	8	5	93	79
12	89	3	3	95	82
1hr	1102	66	24	1192	83

PC - passenger, MV - medium vehicle, HV - heavy vehicle, u - speed

Table 4. 3**:** Typical Volume and Speed for SS001 (Off-Peak Period)

Period	PC per 5mins	MV per 5mins	HV per 5mins	Total per 5mins	μ (Km/hr)
1	66	12	2	80	88
2	80	9	1	90	84
3	77	6	1	84	82
4	77	9	2	88	85
5	75	6	2	83	82
6	79	6	3	88	83
7	70	8	2	80	85
8	56	5	1	62	88
9	63	8	1	72	83
10	55	8	2	65	85
11	72	3	1	76	81
12	40	1	0	41	77
1hr	810	81	18	909	84

PC - passenger, MV - medium vehicle, HV - heavy vehicle, u - speed

Table 4. 4: Typical BRT Volume and Speed for SS001

Period	BRT (per 5mins)	Total (per 5mins)	u (km/hr)
1	3	3	69
2	2	2	59
3	1	1	58
4	2	2	67
5	3	3	72
6	1	1	62
7	1	1	66
8	2	2	68
9	1	1	61
10	2	2	68
11	2	2	71
12	2	2	75
1hr	22	22	66

BRT – Bus Rapid Transit, u – speed

4.2.1.2 Porterfield Station to Sandown Station SS002

The Porterfield Station – Sandown Station roadway is located on the opposite side of the Sandown Station – Porterfield Station roadway. It has the same features as that of the Sandown Station – Porterfield Station roadway. Vehicle traffic on this segment is directed from Porterfield Station – Sandown Station. The two adjoining lanes are both 3.7 m wide and with a shoulder width of 2.4m. The average daily traffic is about 12069 vehs/day with a design speed of 80km/hr, but the posted speed is 70km/hr. Figure 4.5 shows the setup at site SS002 with

installed ATCs and pneumatic tubes ready for data logging. Due to a shift in the direction of vehicle travel as recorded by the ATC, the traffic statistics changed. Different vehicle types are present in different quantities in the traffic mix. Figure 4.6 shows the flow versus time profile as obtained from the ATC. Traffic data was collected from November 10 to November 16, 2021, as seen by the flow vs time profile for SS002. Vehicle flow rate and data collection date are connected. The traffic flow/time profile shows that time was the primary factor in the daily variance in traffic flow. Additionally, it's unclear how traffic moves during the week; for instance, Sundays witnessed less movement than other days. Likewise, Figures 4.7 and 4.8, respectively, depict the volume-density and speed-density plots. According to the nature of the relationship between flow and density, in the fundamental diagram, the dispersion plot in Figure 4.7 follows a parabolic curve pattern. Furthermore, it is a replica of the fundamental diagram's unrestricted region. Similarly, Figure 4.8 depicts the speed-density plot of the data collected and it is in alignment with the speed-density relationship plot of the fundamental diagram.

Figure 4. 5: Set-Up at Site SS002 with Installed Pneumatic Tubes and ATCs

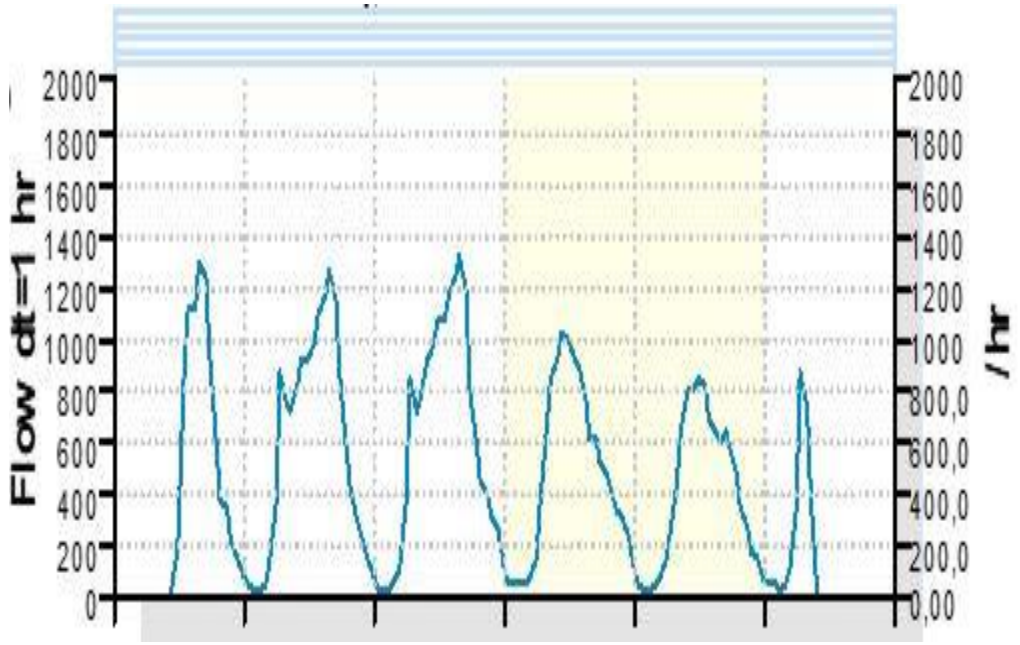

Figure 4. 6: Flow vs Time Profile of SS002

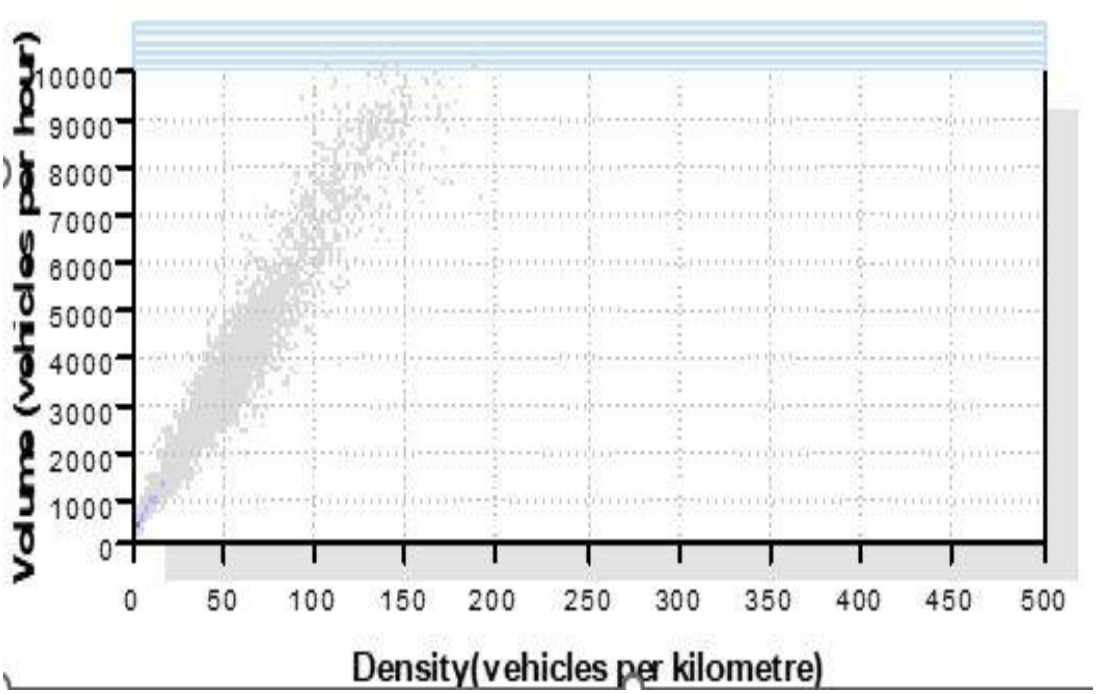

Figure 4. 7: Volume vs Density Plot of SS002

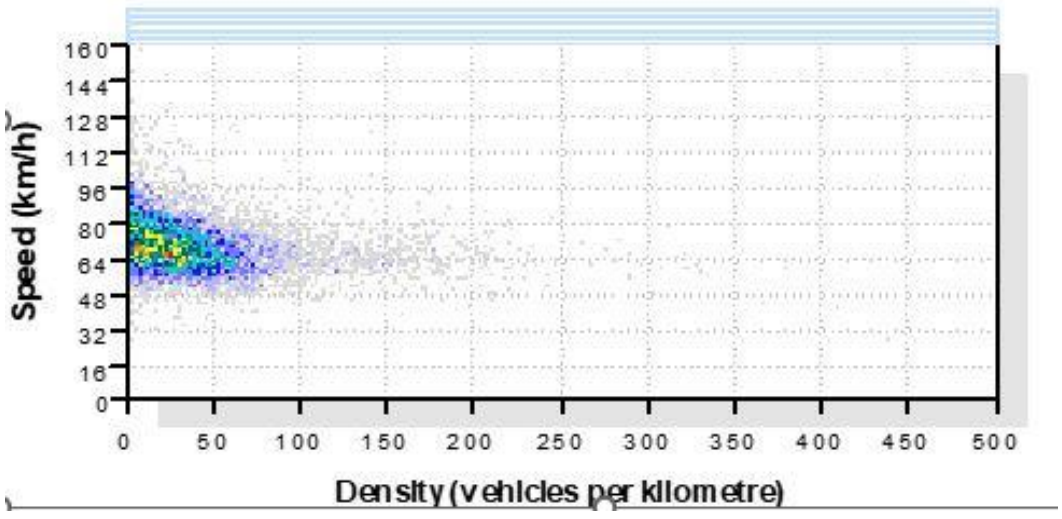

Figure 4. 8: Speed vs Density Plot of SS002

4.2.1.2.1 Empirical Hourly Traffic Volumes at SS002

At SS002, four vehicle classes were also recognized for the prevailing conditions considered. They are passenger cars (PC), motorcyclists (MC), light vehicles (LV), medium vehicles (MV), and heavy vehicles (HV). However, as was already said, motorbikes especially power bikes, which were scarcely found on the road due to private use and not commercial, were not considered when analyzing the data, The reason motorcycles weren't considered is that there is no car following influence on motorcyclists in the flow of traffic. Tables 4.5 and 4.6 likewise show the typical hourly composition of traffic volume and speed of the vehicle classes at SS002 during peak and off-peak hour flows, while Table 4.7 presents hourly traffic volume and speed for BRT.

Table 4. 5**:** Typical Volume and Speed for SS002 (Peak Period)

Period	PC per 5mins	MV per 5mins	HV per 5mins	Total per 5mins	μ (Km/hr)
1	121	4	5	130	70
2	110	7	4	121	73
3	98	1	4	103	75
4	104	5	4	113	74
5	82	1	3	86	79
6	111	0	5	116	81
7	92	3	1	96	76
8	98	2	8	108	70
9	106	3	4	113	71
10	96	3	5	104	71
11	114	1	2	117	78
12	94	2	3	99	72
1hr	1226	32	48	1306	74

PC - passenger, MV - medium vehicle, HV - heavy vehicle, u - speed

Table 4. 6**:** Typical Volume and Speed for SS002 (Off-Peak Period)

Period	PC per 5mins	MV per 5mins	HV per 5mins	Total per 5mins	μ (Km/hr)
1	90	4	5	99	75
2	65	7	4	76	77
3	73	1	4	78	75
4	74	5	4	83	76
5	80	1	3	84	74
6	72	0	5	77	74
7	82	3	1	86	72
8	80	2	8	90	68
9	85	3	4	92	70
10	79	3	5	87	72
11	80	1	2	83	71
12	79	2	3	84	75
1hr	939	32	48	1019	73

PC - passenger, MV - medium vehicle, HV - heavy vehicle, u - speed

Table 4. 7: Typical BRT Volume and Speed for SS002

Period	BRT (per 5mins)	Total (per 5mins)	u (Km/hr)
1	3	3	71
2	3	3	64
3	2	2	60
4	3	3	80
5	2	2	59
6	3	3	76
7	2	2	69
8	1	1	66
9	1	1	66
10	2	2	74
11	1	1	77
12	3	3	72
1hr	26	26	69

BRT – Bus Rapid Transit, u – speed

4.2.1.3 Table View Station to Sunset City Junction SS003

The Table View Station – Sunset City Junction roadway is also a three-lane segment with one BRT dedicated lane running parallel to the median and two adjoining lanes also running parallel to it. It is also a typical provincial road with an average daily traffic count of 14888veh/day and a design speed of 80km/h. A speed limit of 70 km/h is posted on the asphalt-paved road, which has a 20-year pavement design life. The roadway is flat with minimal horizontal curves where it is situated. Vehicle traffic on this road is directed from the Table View Station towards Sunset City Junction. Figure 4.9 shows the setup at site SS003 with

installed ATCs and pneumatic tubes ready for data logging. The two adjoining lanes are both 3.7 m wide and with a shoulder width of 2.1 m. The length of the road segment is 2120 m long and runs along the Atlantis axis to the Sunset City route, precisely between Table View Station – Sunset City Junction. The length of the road exceeds the permitted stopping sight distances from Sandown Station and Porterfield Station, which are 210m and 550m, respectively. Figure 4.10 shows the flow versus time profile as obtained from the ATC.

Figure 4. 9: Set-Up at Site SS003 with Installed Pneumatic Tubes and ATCs

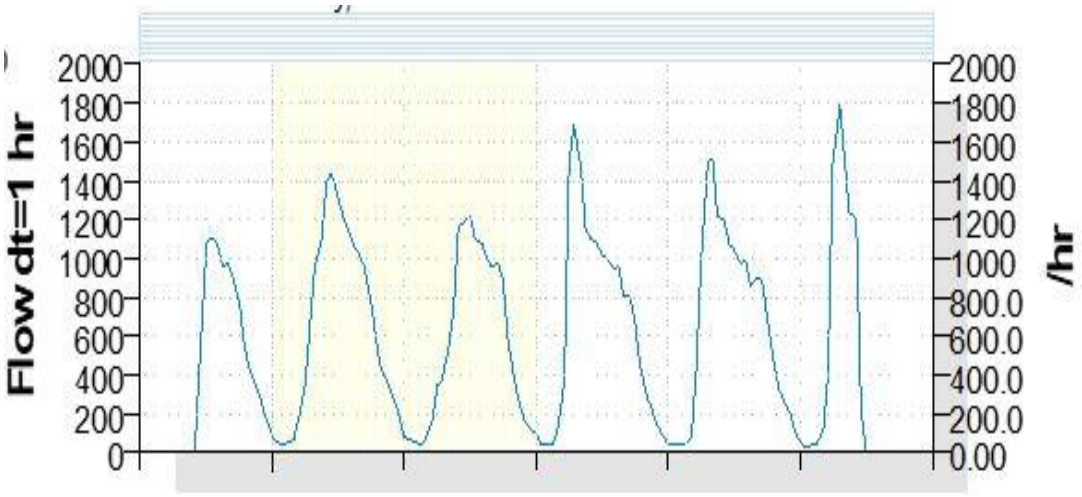

Figure 4. 10: Flow vs Time Profile of SS003

Traffic data was logged, as shown by the flow vs time profile for SS003. Vehicle flow rate and data collection date are connected. The traffic flow/time profile shows that time was the

primary factor in the daily variance in traffic flow. Additionally, it's unclear how traffic moves during the week; for instance, here, Friday and Sunday witnessed less movement than other days. Likewise, Figures 4.11 and 4.12 respectively, depict the volume-density and speed-density plots. According to the nature of the relationship between flow and density, in the fundamental diagram, the dispersion plot in Figure 4.11 follows a parabolic curve pattern. Furthermore, it follows the pattern of the fundamental diagram's unrestricted region. Similarly, Figure 4.12 shows the speed-density plot of the data collected and it is in alignment with the speed-density relationship plot of the fundamental diagram. However, it is important to keep in mind that the graph’s scope is about a variety of moving vehicles in a traffic stream.

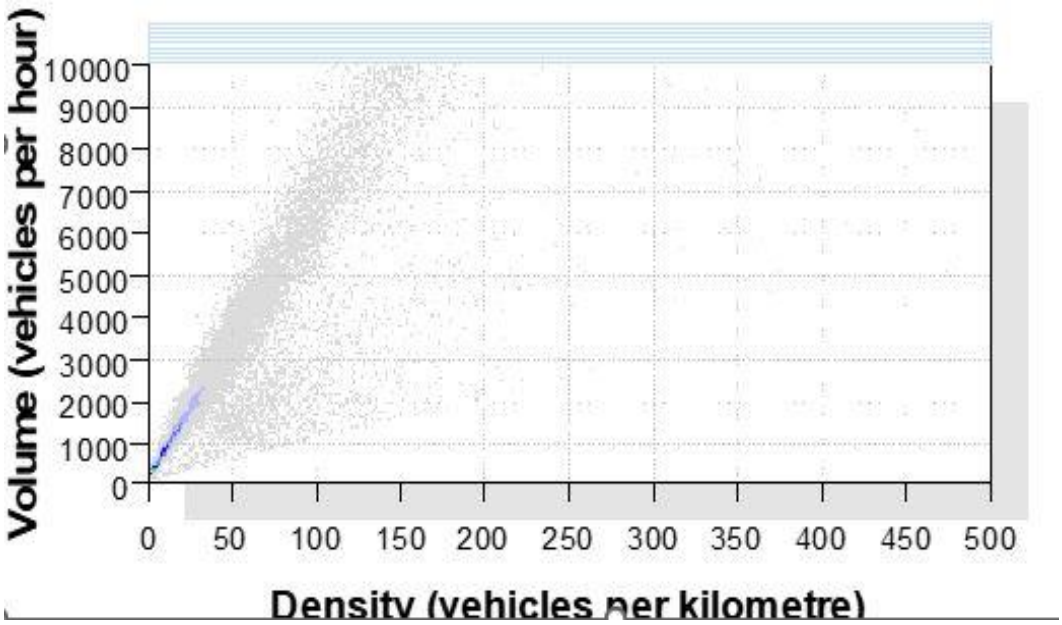

Figure 4. 11: Volume vs Density Plot of SS003

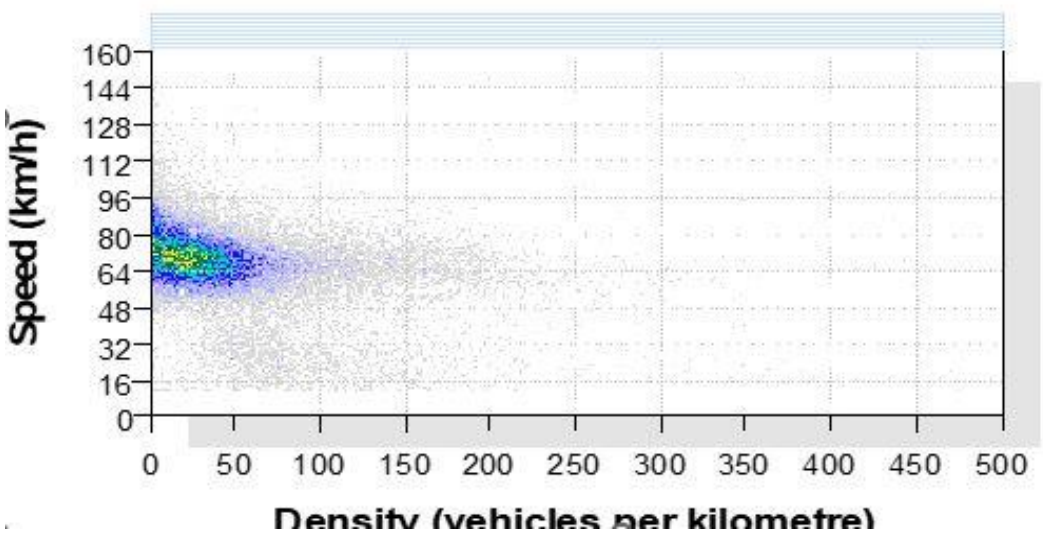

Figure 4. 12: Speed vs Density Plot of SS003

4.2.1.3.1 Empirical Hourly Traffic Volumes at SS003

At SS003, four vehicle classes were also recognized for the prevailing conditions considered. They are passenger cars (PC), motorcyclists (MC), light vehicles (LV), medium vehicles (MV), and heavy vehicles (HV). However, as was already said, motorbikes especially power bikes, which were scarcely found on the road due to private use and not commercial, were not considered when analyzing the data, The reason motorcycles weren't considered is that there is no car following influence on motorcyclists in the flow of traffic. Tables 4.8 and 4.9 also show the typical hourly composition of traffic volume and speed of the vehicle classes at SS003 during peak and off-peak hour flows, while Table 4.10 presents hourly traffic volume and speed for BRT.

Table 4. 8**:** Typical Volume and Speed for SS003 (Peak Period)

Period	PC per 5mins	MV per 5mins	HV per 5mins	Total per 5mins	μ (Km/hr)
1	110	3	5	118	74
2	101	4	2	107	75
3	130	11	6	147	70
4	122	8	5	135	68
5	158	8	8	174	68
6	128	3	10	141	68
7	137	10	13	160	66
8	156	14	5	175	67
9	155	6	17	178	62
10	159	10	7	176	61
11	144	4	10	158	34
12	156	7	4	167	26
1hr	1656	88	92	1836	62

PC – passenger, MV – medium vehicle, HV – heavy vehicle, u – speed

Table 4. 9**:** Typical Volume and Speed for SS003 (Off-Peak Period)

Period	PC per 5mins	MV per 5mins	HV per 5mins	Total per 5mins	μ (Km/hr)
1	72	8	2	82	80
2	68	7	2	77	73
3	72	4	4	80	73
4	65	5	2	72	74
5	62	9	3	74	75
6	65	8	3	76	78
7	63	5	2	70	74
8	70	4	4	78	73
9	67	4	3	74	78
10	69	6	4	79	74
11	73	11	3	87	75
12	67	4	10	81	73
1hr	813	75	42	930	75

PC – passenger, MV – medium vehicle, HV – heavy vehicle, u – speed

Table 4. 10: Typical BRT Volume and Speed for SS003

Period	BRT (per 5mins)	Total (per 5mins)	u (Km/hr)
1	4	4	64
2	2	2	63
3	3	3	66
4	2	2	70
5	3	3	64
6	1	1	61
7	3	3	70
8	2	2	63
9	4	4	63
10	3	3	69
11	2	2	65
12	4	4	61
1hr	33	33	65

BRT – Bus Rapid Transit, u – speed

4.2.1.4 Sunset City Junction to Table View Station SS004

The Sunset City Junction – Table View Station roadway is located in the opposite direction of the Table View Station – Sunset City Junction roadway. It has the same features as that of the Table View Station – Sunset City Junction roadway. Vehicle traffic on this road is directed from the Sunset City Junction – Table View Station. Figure 4.13 shows the setup at site SS004 with installed ATCs and pneumatic tubes ready for data logging. The two adjoining lanes are both 3.7 m wide and with a shoulder width of 0.98m. The average daily traffic is about 14140 veh/day with a design speed of 70km/hr. Due to a shift in the direction of vehicle travel as recorded by the ATC, the traffic statistics changed. Different vehicle types are present in

different quantities in the traffic mix. Figure 4.14 shows the flow versus time profile as obtained from the ATC.

Figure 4. 13: Set-Up at Site SS004 with Installed Pneumatic Tubes and ATCs

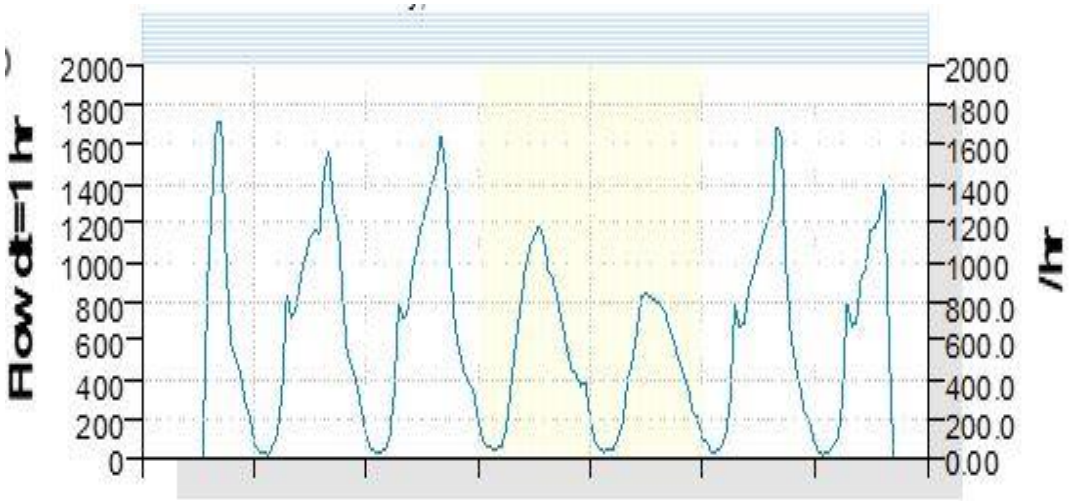

Figure 4. 14: Flow vs Time Profile of SS004

Traffic data at SS004 was collected from November 24 to December 1, 2021, as seen by the flow vs time profile. Vehicle flow rate and data collection date are connected. The traffic flow/time profile shows that time was the primary factor in the daily variance in traffic flow. Additionally, it's unclear how traffic moves during the week; for instance, here, Saturday and

Sunday witnessed less movement than other days. Likewise, Figures 4.15 and 4.16 respectively depict the volume-density and speed-density plots. According to the nature of the relationship between flow and density, in the fundamental diagram, the dispersion plot in Figure 4.15 follows a parabolic curve pattern. Furthermore, it follows the pattern of the fundamental diagram's unrestricted region. Similarly, Figure 4.16 shows the speed-density plot of the data collected and it is in alignment with the speed-density relationship plot of the fundamental diagram. However, it is important to keep in mind that the graph's scope is about a variety of moving vehicles in a traffic stream.

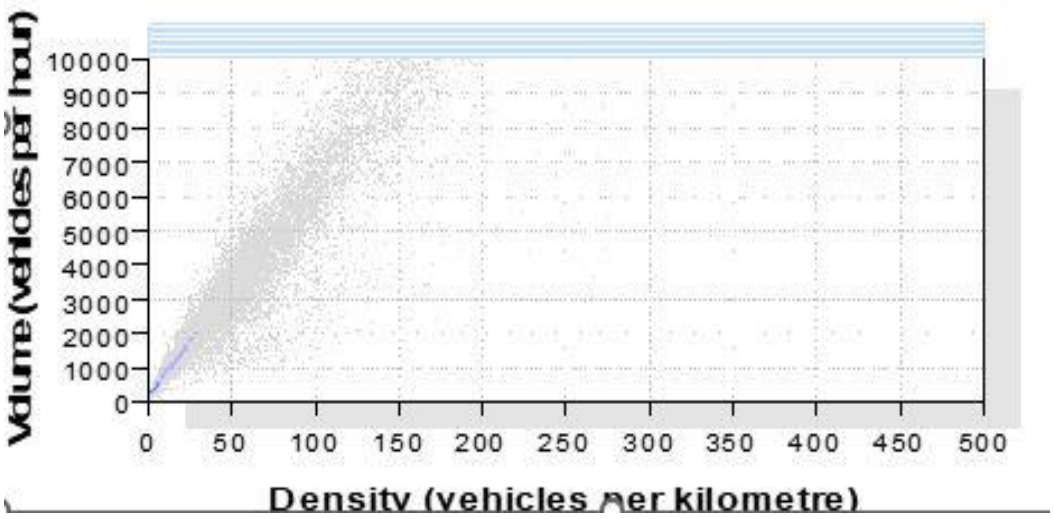

Figure 4. 15: Volume vs Density Plot of SS004

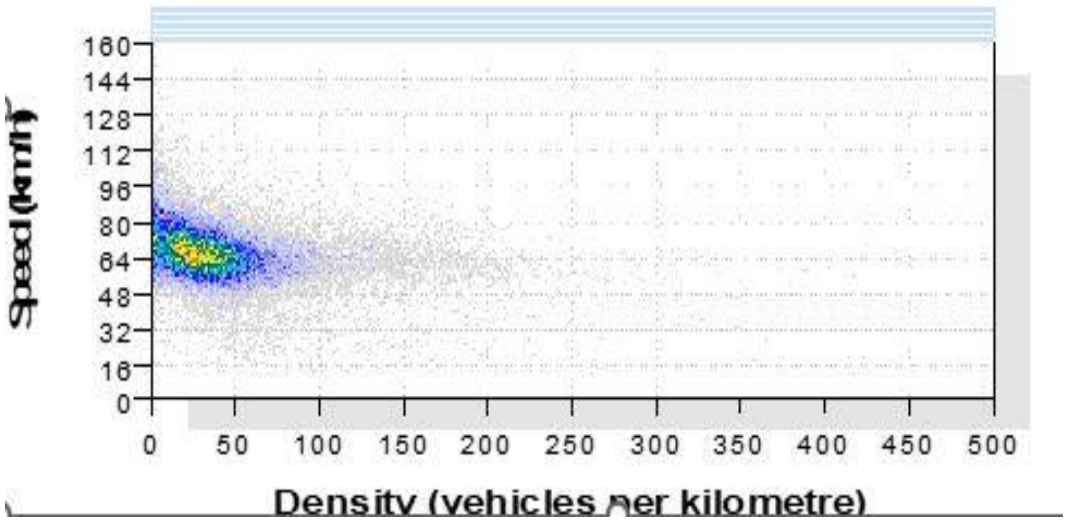

Figure 4. 16: Speed vs Density Plot of SS004

4.2.1.4.1 Empirical Hourly Traffic Volumes at SS004

At SS004, four vehicle classes were also recognized for the prevailing conditions considered. They are passenger cars (PC), motorcyclists (MC), light vehicles (LV), medium vehicles (MV), and heavy vehicles (HV). However, as was already said, motorbikes especially power bikes, which were scarcely found on the road due to private use and not commercial, were not considered when analyzing the data. Tables 4.11 and 4.12 also show the typical hourly composition of traffic volume and speed of the vehicle classes at SS004 during peak and off-peak hour flows, while Table 4.13 presents hourly traffic volume and speed for BRT.

Table 4. 11**:** Typical Volume and Speed for SS004 (Peak Period)

Period	PC per 5mins	MV per 5mins	HV per 5mins	Total per 5mins	μ (Km/hr)
1	142	5	7	154	72
2	122	9	2	133	74
3	108	7	5	120	75
4	138	7	4	149	73
5	107	8	3	118	78
6	141	4	5	150	74
7	120	5	2	127	69
8	132	6	2	140	67
9	135	7	2	144	68
10	127	7	5	139	69
11	139	4	4	147	65
12	146	5	3	154	65
1hr	1557	74	44	1675	71

PC - passenger, MV - medium vehicle, HV - heavy vehicle, u - speed

Table 4. 12**:** Typical Volume and Speed for SS004 (Off-Peak Period)

Period	PC per 5mins	MV per 5mins	HV per 5mins	Total per 5mins	μ (Km/hr)
1	60	3	0	63	89
2	65	1	0	66	86
3	67	2	1	70	82
4	55	0	2	57	84
5	45	1	0	46	81
6	43	2	1	46	80
7	80	2	2	84	79
8	76	3	3	82	78
9	53	2	2	57	77
10	75	2	3	80	75
11	79	1	4	84	80
12	67	3	1	71	80
1hr	765	22	19	806	81

PC - passenger, MV - medium vehicle, HV - heavy vehicle, u - speed

Table 4. 13: Typical BRT Volume and Speed for SS004

Period	BRT (per 5mins)	Total (per 5mins)	u (Km/hr)
1	3	3	52
2	4	4	81
3	4	4	65
4	4	4	72
5	4	4	70
6	2	2	61
7	4	4	73
8	4	4	70
9	2	2	61
10	4	4	73
11	2	2	73
12	1	1	68
1hr	38	38	68

BRT – Bus Rapid Transit, u - speed

Table 4.14 gives the summary of vehicle volumes recorded in one-hour across the four sites.

Table 4. 14**:** Traffic volume Summary

Traffic Period	SS001	SS002	SS003	SS004
Peak	1184	1306	1836	1675
Off-Peak	909	1019	930	806

According to the table, SS003 recorded the maximum volume of vehicles throughout the one-hour peak daytime count with a total of 1836 vehicles, while SS001 recorded the lowest with 1184 vehicles. The largest recorded number of vehicles during the one-hour off-peak daytime count was accounted for by SS002, with a total of 1019 vehicles, and the lowest by SS004, with 806 vehicles. Similarly, for BRT traffic volumes, a total of 38 vehicles were observed in SS004, followed by SS003 (33), SS002 (26), and finally SS001 (22), which is the lowest as shown in Table 4.15

Table 4. 15**:** BRT Traffic volume Summary

Site	SS001	SS002	SS003	SS004
Peak	22	26	33	38
Off-Peak	14	17	17	27

4.3 Summary

The empirical results from surveyed sites have now been presented showing volume, speed, and the extent of prevailing road traffic volume. The tables presented in this section are classified into four distinct divisions (with and without BRT; peak and off-peak periods).

Traffic volume fluctuates widely with time and the nature of variation depends on the type of the highway. Four different categories of traffic vehicles for each location, viz motorcycles, light vehicles (passenger cars), moderate vehicles, and heavy vehicles. Nevertheless, the mix of different vehicle types in the traffic varied from site to site. Motorcycles were omitted particularly because they have little influence on the traffic stream vehicle following order and also because of their near absence or insignificant volume. Despite the COVID-19 pandemic and other unanticipated mobility inhibitors, passenger cars, dominated traffic flow, accounting for an average of 91% of all vehicle movements during off-peak hours across the four sites. Medium vehicles made up 6% of this total, and heavy trucks made up 4%. In terms of percentages during peak traffic flows, passenger cars also made up the largest amount (92%) across the four sites, followed by medium vehicles and heavy vehicles with 4% and 3.6% respectively.

Overall, a total of 9, 665 vehicles were surveyed in one hour during both peak and off-peak periods. The highest recorded traffic volume of vehicles at peak was at site SS003 with 1816 vehicles during the one-hour duration count and site SS001 with the lowest traffic volume of 1184 per hour. The highest recorded traffic volume of vehicles at off-peak was at site SS002 with 1019 vehicles during the one-hour duration count and site SS004 with the lowest traffic volume of 866 per hour. The highest recorded percentage of passenger cars at peak was 93.9% at site SS002, and the lowest was 91.2% at site SS003. The highest recorded percentage of passenger cars at off-peak was 92.1% at site SS002 and the lowest was 87.4 % at site SS003. Site SS003 has the highest recorded percentage of commercial vehicles at 5.1% at peak, with Site SS004 having the lowest at 2.6% at peak. By contrast, Site SS002 with 4.2% has the highest percentage of commercial vehicles during off-peak periods with site SS001, 2%. In all cases, empirical evidence shows a drop in vehicle speeds induced by BRT, especially regarding passenger cars.

CHAPTER 5

EFFECT OF BRT ON MIXED-TRAFFIC CAPACITY UTILIZATION

5.1 Overview

This chapter analyzes the empirical data from chapter four to evaluate how Bus Rapid Transit (BRT) dedicated lane affects the capacity utilization of mixed traffic flows on the adjoining lanes of a multilane roadway. Mixed traffic conditions refer to both the macro and micro characteristics of the traffic stream and the stream elements that use the facility, such as traffic composition, directional distribution, the proportion of various vehicle types, and their performance capability relative to the prevailing geometric conditions, which include the road surface and geometric parameters like lane widths, number of intersections, horizontal and vertical alignments. The measure of capacity utilization relies on two germane parameters which are the operational traffic flows/5mins period (actual output) and the operational traffic capacity (maximum possible output). These parameters, as well as speed, are used to develop the capacity utilization criteria table, under daylight and dry weather conditions. The table is then used to evaluate the capacity utilization levels.

In the process, the fundamental diagram's flow and density relationship was used to model and estimate capacity, which is an important parameter in the determination of capacity utilization rates on the roadway, while the relationship between speed and density was used to estimate the optimum flow and speed required for unrestricted traffic movement under steady flow conditions. In the relationship between flow and density, density functions as the control parameter and flow as the objective function. In the speed/density relationship, density is used as the control parameter and speed is the objective function. The coefficient of determination serves as the foundation for the model equations' validity. The estimated and actual flow values are related by the coefficient of determination, which has values between 0 and 1. If it is 1, then the sample has a perfect correlation, meaning that the estimated and real flow values are identical. The quadratic equation, however, cannot be used to make predictions if the coefficient of determination is 0. This is because it cannot be used to forecast flow. However, before estimating roadway capacity utilization, it is crucial to model traffic flow to determine the maximum flow or capacity before assessing the usage or Utilization of the roadway. To do this, estimated volumes were converted into passenger car equivalent (PCE) values. The stepwise estimation of parameters for the determination of the effect of BRT on capacity

utilization follows the procedure outlined for the pilot test in chapter three. Consequently, the remainder of this chapter is such that section 5.2 discusses the estimation of PCE values, section 5.3, the non-mixed traffic capacity, and section 5.4 explains the estimation of mixed traffic capacity. In section 5.5, the determination of capacity utilization is given. Optimum flows and speeds are presented in section 5.6, while the determination of traffic capacity differentials was discussed in section 5.7. Section 5.8 gives a summary of the chapter.

5.2 Passenger Car Equivalent Values

Even though the standard PCE values obtained from SANRAL for South African roads had been investigated in the pilot test in chapter three and considered applicable due to the results of the hypothesis as there was no significant difference between the expected and the calculated PCE, the PCE values for the other sites are additionally estimated to confirm compliance or compatibility of the study site with it. According to The HCM (2010, p. 9–13), it will be recalled that a passenger car equivalent refers to '*the number of passenger cars that will result in the same operational conditions as a single heavy vehicle of a particular type under specified roadway, traffic, and control conditions*' (HCM, 2010). As previously mentioned, the passenger car equivalent values listed in table 2.3 are with respect to favourable weather, daylight, and level roadway conditions, and are based on data from the South African National Roads Agency Limited (SANRAL). However, due to the introduction of the BRT infrastructure with median dedicated lanes configuration and the conditions under which this study was conducted, including the presence and operation of BRT buses, assessing if the PCE values are suitable is therefore necessary. Due to variations in estimation techniques, the calculation of passenger car equivalent values continues to be a contentious issue. It's easy to use the headway method. It is calculated as the difference between the target vehicle's average headway and the car's average headway. It is mathematically expressed as:

$$PCE_{ij} = \frac{H_{ij}}{H_{pcj}} \qquad 5.1$$

where PCE_{ij} = passenger car equivalent of vehicle type i under conditions j, and H_{ij}, H_{pcj} is the average headway for vehicle type i and passenger car (PC) conditions j. According to the (HCM, 2010), $headway = Spacing\,(m/veh)/Speed\,(m/s)$ and $Spacing = 1000/Density\,(m/veh)$. The estimated densities for each section of roadway and their corresponding relative average speeds were imputed into the above equations for the different vehicle types (PCs, MVs, and HVs). For instance,

At site **SS001** (at peak traffic flow): where spacing = $1000/45 = 22.22m/veh$, the individual headways for each vehicle class are calculated thus:

Headway (PC) $= 22.22/22.86 = 0.97$sec/veh

Headway (MV) $= 22.22/23.04 = 0.96$sec/veh

Headway (HV) $= 22.22/21.52 = 1.03$sec/veh

Therefore, the passenger car equivalent values for each class of vehicle are thus estimated as follows:

PCE (PC) $= 0.97/0.97 = 1.0$ unit

PCE (MV) $= 0.96/0.97 = 0.98$ unit

PCE (HV) $= 1.03/0.97 = 1.06$ unit

At site **SS002** (at peak traffic flow): where spacing = $1000/46 = 21.74m/veh$, the individual headways for each vehicle class are calculated thus:

Headway (PC) $= 21.74/21.83 = 0.99$sec/veh

Headway (MV) $= 21.74/19.55 = 1.11$sec/veh

Headway (HV) $= 21.74/19.31 = 1.13$sec/veh

Therefore, the passenger car equivalent values for each class of vehicle are thus estimated as follows:

PCE (PC) $= 0.99/0.99 = 1.0$ unit

PCE (MV) $= 1.11/0.99 = 1.12$ unit

PCE (HV) $= 1.13/0.99 = 1.14$ unit

At site **SS003** (at peak traffic flow): where spacing = $1000/55 = 18.18m/veh$, the individual headways for each vehicle class are calculated thus:

Headway (PC) $= 18.18/20.58 = 0.88$sec/veh

Headway (MV) $= 18.18/18.92 = 0.96$sec/veh

Headway (HV) $= 18.18/18.31 = 0.99$sec/veh

Therefore, the passenger car equivalent values for each class of vehicle are thus estimated as follows:

PCE (PC) $= 0.88/0.88 = 1.0$ unit

PCE (MV) $= 0.96/0.88 = 1.09$ unit

PCE (HV) $= 0.99/0.88 = 1.13$ unit

At site **SS004** (at peak traffic flow): where spacing = $1000/47 = 21.28m/veh$, the individual headways for each vehicle class are calculated thus:

$$\text{Headway (PC)} = 21.28/20.42 = 1.04\text{sec/veh}$$

$$\text{Headway (MV)} = 21.28/19.17 = 1.11\text{sec/veh}$$

$$\text{Headway (HV)} = 21.28/18.33 = 1.16\text{sec/veh}$$

Therefore, the passenger car equivalent values for each class of vehicle are thus estimated as follows:

$$\text{PCE (PC)} = 1.04/1.04 = 1.0 \text{ unit}$$

$$\text{PCE (MV)} = 1.11/1.04 = 1.07 \text{ unit}$$

$$\text{PCE (HV)} = 1.16/1.04 = 1.12 \text{ unit}$$

The headway method has the merit of being simple to use and the ease with which empirical headway data can be calculated. The headway method could also be used to distinguish between the effects of congested and free-flowing traffic. Table 5.1 gives the summary of the modified PCE values.

Table 5. 1**:** Modified PCEs

Site	VC	k	s	u	h	PCE
SS001	PC	45	22.22	22.86	0.97	1.00
	MV			23.04	0.96	0.98
	HV			21.52	1.03	1.06
SS002	PC	46	21.74	21.83	0.99	1.00
	MV			19.55	1.11	1.12
	HV			19.31	1.13	1.14
SS003	PC	55	18.18	20.58	0.88	1.00
	MV			18.92	0.96	1.09
	HV			18.31	0.99	1.13
SS004	PC	47	21.28	20.42	1.04	1.00
	MV			19.17	1.11	1.07
	HV			18.33	1.16	1.12

VC ~ vehicle class, PC ~ passenger car, MV ~ medium vehicle, HV ~ heavy vehicle, k ~ density, s ~ spacing, u ~ speed, h ~ headway

5.2.1 Comments on Modified PCE Values and Statistical Tests

From the summary of the modified PCE values shown in table 5.1 above, and as observed in the pilot test, the modified PCE values for medium and heavy vehicles in the non-mixed traffic on the adjoining lanes do not match the PCE values recommended by SANRAL. Due to the presence of BRT dedicated lanes, capacity has been underutilized, which has caused a shift in PCE values. The modified PCE and SANRAL values for medium and heavy vehicles were consequently subjected to a statistical test using the chi-square at a 95% level of confidence. The purpose of the test is to determine whether there exists a significant discrepancy between the adjusted PCE values and SANRAL's. These two hypotheses were put forth:

- Null hypothesis (H_0): No distinction between SANRAL PCE values and the modified values
- Alternative hypothesis (H_1): There is a distinction between SANRAL PCE values and the modified values.

Equation 3.14, the chi-square test from chapter 3 is recalled here and is given as:

$$X^2 = \frac{(o-e)^2}{e}$$

where X^2 = chi-square, o = observed value, e = expected value

Based on a 95% confidence level and for one degree of freedom, the test was done taking $X^2 = 3.84$ from the chi-square distribution table (see appendix). However, if $X^2 > 3.84$, therefore the alternative (H_1) hypothesis is accepted, indicating that there is a significant difference between the standard PCE from SANRAL and the modified PCEs. On the other hand, if $X^2 < 3.84$, then, it means there is no significant difference between the standard PCE from SANRAL and the modified PCEs, hence the null hypothesis (H_0) is accepted. Therefore, for medium vehicles (MV) with a modified PCE value of 0.98 under dry day-time conditions and SANRAL PCE value of 1.75:

$$X^2 = \frac{(0.98-1.75)^2}{1.75} = 0.34 < 3.84$$

and for heavy vehicles (HV) with a modified PCE value of 1.06 under dry day-time conditions and SANRAL PCE value of 3.0;

$$X^2 = \frac{(1.06-3)^2}{3} = 1.25 < 3.84$$

Thus, the null hypothesis (H_0) is accepted since $0.33 < 3.84$ and $1.33 < 3.84$ for the medium and heavy vehicles respectively and the alternate hypothesis (H_1) is rejected. Therefore, at 95 percent level of confidence for one degree of freedom, the results demonstrate no statistically significant difference between the adjusted PCE and SANRAL values. Hence, because there is no discernible difference, either the SANRAL PCE or the modified PCEs could be employed; hence, it was deemed safe and fit to use the SANRAL PCE values for this study. It is important to keep in mind that the PCE value depends on three key factors: the roadway, the weather, and the composition of traffic. It is not a fixed value associated with any one vehicle type. The sections that follow deal with the estimation of non-mixed and subsequently mixed traffic capacity utilization for the main study and show how the SANRAL PCE values were applied.

5.3 Site SS001 Capacity Utilization

Recall that roadway capacity utilization had been described as a ratio of operational traffic flow/5mins period and operational roadway capacity, also referred to as volume-to-capacity ratio or degree of saturation. It is on this premise that the Level of Capacity Utilization (LCU) criteria table is developed. The operational flow or demand volume is the actual number of vehicles moving past a section or point on a roadway within a period of time (usually an hour). For simplicity, it is often referred to as the actual output volumes. Operating roadway capacity on the other hand is the maximum number of vehicles expected to move past a section or point within an hour. It is also referred to as the maximum possible vehicle output. This ratio, sequel to it computation gives the utilization rate of a typical road section under investigation. The objective function for quantitative assessment is traffic flow, while the independent parameter is density.

These parameters were employed in developing the criteria table for the evaluation of the level of capacity utilization of the roadway in the presence of BRT dedicated lanes. In this investigation, the empirical data at peak traffic under daylight and dry weather conditions at the study sites were used to set up the criteria table. This is important to allow for the consideration of the worst-case scenario on the roadway to be utilized, given that the road reaches its maximum capacity during peak traffic periods with comparable traffic performance. The stepwise procedure employed for the pilot assessment was replicated for the main study and presented in the sections that follow. Figure 5.1 shows a schematic framework of the analytical steps employed for the development of the criteria table for each site. The analytical step is adopted due to its simplicity and clarity.

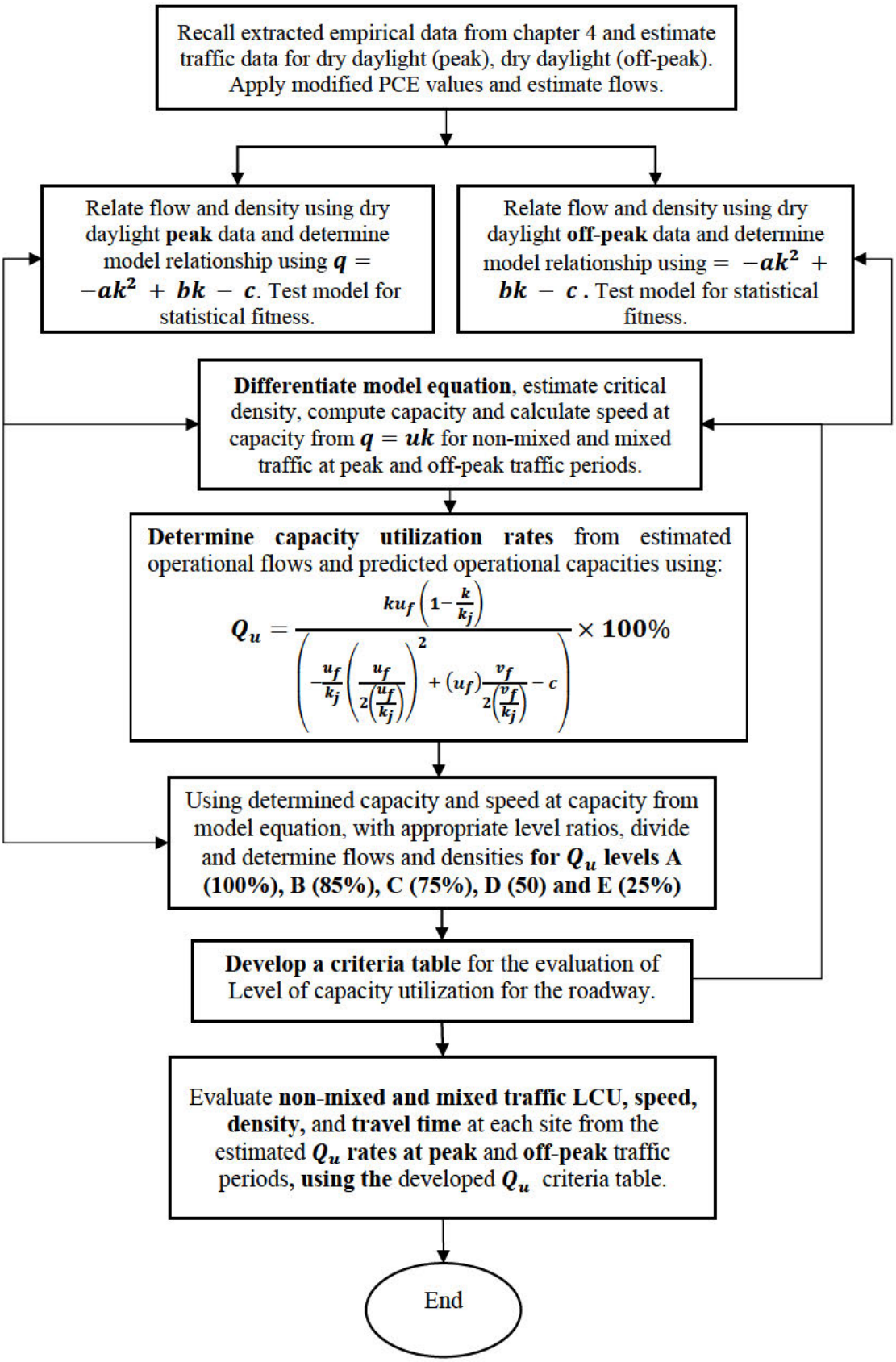

Figure 5. 1: Schematic Framework for Level of Capacity Utilization (LCU) Analysis

5.3.1 Capacity Utilization Criteria Table for SS001

The following stepwise procedure was employed for the development of the capacity utilization criteria table for site SS001 (without BRT influence).

Step 1. Using the peak traffic flow data from the empirical results reported in chapter four, the five-minute traffic volumes are converted first into PCEs using SANRAL's standard PCE values given as PC = 1, MV = 1.75, and HV = 3.0. Using a multiplier (x12), the 5mins volumes were converted to flow rates in pce per hour, and with the speed known, densities were calculated using equation 2.17, $q = uk$. Table 5.2 shows the estimated flow, speed, and density at peak hours for SS001.

Table 5. 2**:** Level of Capacity Utilization (LCU) Parameters

	PC	MV	HV	Vol	MV	HV	q	u	k	q
Period	*1*	*2*	*3*	*4*	*5*	*6*	*7*	*8*	*9*	*10*
					*2*1.75*	*3*3*	*1 + 5 + 6*		*10/8*	*7*12*
1	95	2	0	97	4	0	99	85	14	1188
2	92	4	4	100	7	12	111	83	16	1332
3	97	3	1	101	5	3	105	84	15	1260
4	101	5	3	109	9	9	119	76	19	1428
5	86	4	1	91	7	3	96	89	13	1152
6	95	7	1	103	12	3	110	88	15	1320
7	98	6	0	104	11	0	109	79	17	1308
8	95	9	0	104	16	0	111	83	16	1332
9	85	6	4	95	11	12	108	86	15	1296
10	89	9	2	100	16	6	111	78	17	1332
11	80	8	5	93	14	15	109	79	17	1308
12	89	3	3	95	5	9	103	82	15	1236
1hr	1102	66	24	1192				83±1		1296

1, 2, 3…10 ~ column numbers, column 1 - 4 ~ volume by 5mins, columns 5 - 7 ~ flow (pce/5mins), q ~ total flow(pce/hr), u ~ speed (km/hr), k ~ density (pce/km), PC ~ passenger car, MV ~ medium vehicle, HV ~ heavy vehicle

Step 2. The density and flow parameters in table 5.2 were used to calibrate a relationship between flow and density using Microsoft Excel, which has been shown by (Ben-Edigbe & Ferguson, 2005; Minderhoud *et al*., 1996; van Arem *et al*., 1994), to have a quadratic function given by equation 5.2. Figure 5.2 shows the graphical representation of the flow-density relationship, and in-set is the calibrated model equation, presented in equation 5.3.

$$q = -ak^2 + bk - c \qquad 5.2$$

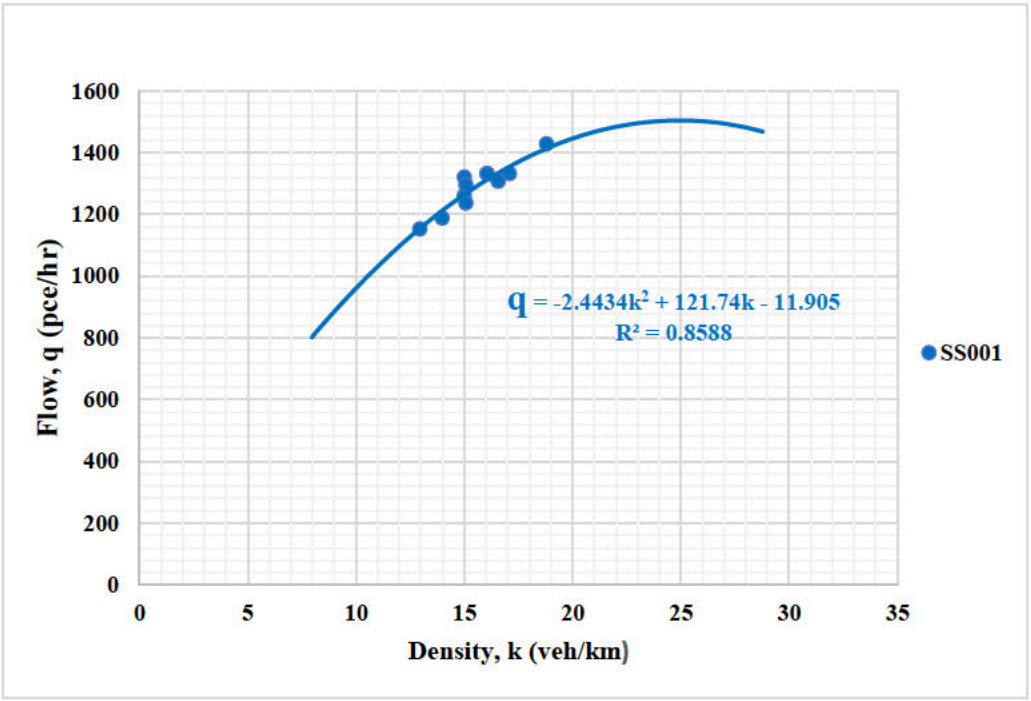

Figure 5. 2: Traffic Flow-Density (F-D) Curve for SS001(Peak) - Control

The calibrated model equation is given as equation 5.3:

$$q_{SS001(Control)} = -2.4434k^2 + 121.74k - 11.905 \qquad R^2 = 0.86 \qquad 5.3$$

Step 3: Statistical testing of the calibrated model for validity. Table 5.3 below shows the results of the validity test carried out on the model for site SS001 without BRT influence. As shown, the coefficients of the derived model have the anticipated sign conventions for concavity, while the coefficient of determination $R^2 = 0.8588$ is greater than 0.5, which indicates the existence of a strong relationship between density and flow, and the capability of predicting capacity.

Table 5. 3: Level of Capacity Utilization Model Validity Tests

	q	*k*	Constant
t' values	61.4	2.2	
Coefficients	**-2.4434**	**121.74**	**11.905**
Std. Error	21	1	
R^2	0.86		
F	2094	2.81	
df	11		
Residuals	-10.619	-0.137	

The F-observed statistics at ten degrees of freedom is bigger than the F-critical value of 2.81, suggesting that the model equation 5.3 did not occur by chance. Additionally, the value of the

t-observed statistic at the 5% level of significance is higher than 2.2, indicating that the variables used are useful, and density is a crucial factor in flow estimation. The statistics data sequel its analysis, was directly pulled from a Microsoft Excel file. It is important to note that the coefficient of "k" denotes the free-flow speed, roughly 122 km/hr. The study hypothesizes that the extent of road capacity utilization level resulting from BRT is significant. The aggregated model was subsequently used to predict capacity, estimate density at capacity, and speed at capacity in step 4 by differentiating q with respect to k and feeding back necessary values.

Step 4: The density at capacity, capacity or maximum flow, and the speed at maximum flow were determined using equation 5.3 as follows:

$$q_{control(Peak)} = -2.4434k^2 + 121.74k - 11.905 \qquad R^2 = 0.86$$

By differentiating q with respect to k,

$$\frac{\partial q}{\partial k} = 2 * 2.4434k + 121.74 = 0$$

$$k_{crt} = k_Q = 24.9pce/km \approx 25\, pce/km$$

By plugging the critical density k_Q into equation 5.3, capacity is calculated and is given by:

$$Q = q_{withoutBRT(Peak)} = -2.4434(25)^2 + 121.74(25) - 11.905$$

$$Q = q_{withoutBRT(Peak)} \approx 1504pce/hr$$

By substituting k_Q and the estimated q into the fundamental diagram equation $q = uk$, the speed at capacity is therefore obtained as:

$$u_Q = \frac{q}{k} = \frac{1492}{25} = 59.6 \approx 60km/hr$$

Hence the capacity or maximum flow is $1504pce/hr$, with a corresponding speed at capacity $u_Q = 60km/hr$.

Step 5: The estimated capacity $Q \approx 1504pce/hr$ can be approximated to $1600pce/hr$ and split into five capacity utilization levels for the LCU criteria table. As stated earlier, the capacity utilization levels are designated as (A to E), where LCU A is the best roadway capacity

utilization and LCU E, is the worst. LCU A is the capacity level with a 100 percent volume-to-capacity ratio, which is the boundary between steady flow and forced flow sections of the flow-density curve, and the remaining percentages are distributed as 85% (LCU B), 75% (LCU C), 50% (LCU D) and 25% (LCU E) percent respectively, therefore,

Level A (100%) = 1600 pce/hr

Level B (85%) = $0.85 * 1600 = 1360 pce/hr \approx 1400 pce/hr$

Level C (75%) = $0.75 * 1600 = 1200 pce/hr \approx 1200 pce/hr$

Level D (50%) = $0.50 * 1600 = 800 pce/hr \approx 800 pce/hr$

Level E (25%) = $0.25 * 1600 = 400 pce/hr \approx 400 pce/hr$

Step 6: From the model equation above, speed is evenly distributed between its free-flow speed of 121.74km$/hr \approx 125 km/hr$ for class E and the speed at capacity of $60 km/hr$ for class A. The speed is used to compute the attendant densities and its corresponding time for 1km of roadway, and subsequently, the LCU criteria table is developed. Thus, the LCU criteria table for SS001 is presented in table 5.4.

Table 5. 4**:** LCU Criteria Table for SS001

LCU	Qu %	Flow (Q) veh/h	Density (k) veh/km/lane	Speed(u) km/hr
A	86 - 100	1600	27	60
B	76 - 85	1400	18	80
C	51 - 75	1200	13	95
D	26 - 50	800	7	110
E	0 - 25	400	3	125

5.3.2 BRT Dedicated Lane Capacity Utilization for Site SS001

Step 1. Estimation of five-minute BRT traffic volume using SANRAL's standard PCE values for heavy vehicle class as shown in table 5.5 below.

Table 5. 5**:** BRT Dedicated Lane Level of Capacity Utilization Parameters

Period	BRT 1	BRT 2	u 3	k 4	k 5	q 6	q 7
		1*3		6/3	7/3	1*12	2*12
1	3	9	69	0	2	36	108
2	2	6	59	0	1	24	72
3	1	3	58	0	1	12	36
4	2	6	67	0	1	24	72
5	3	9	72	0	1	36	108
6	1	3	62	0	1	12	36
7	1	3	66	0	1	12	36
8	2	6	68	0	1	24	72
9	1	3	61	0	1	12	36
10	2	6	68	0	1	24	72
11	2	6	71	0	1	24	72
12	2	6	75	0	1	24	72
1hr	22		66±2			22	66

1, 2, …8 ~ column numbers, column 1 ~ volume by 5mins, column 2 ~ BRT flow (pce/5mins), u ~ speed (km/hr), k5 ~ density (veh/km), k6 ~ density (pce/km) q7 ~ total flow(veh/hr), q8 ~ total flow(pce/hr) BRT ~ Bus Rapid Transit.

Step 2: Determination of BRT dedicated lane capacity:

The BRT time headway, defined by braking performance and measured tip-to-tail, is given by equation 5.4:

$$T_h = \frac{L}{V} + t_r + \frac{kV}{2}\left(\frac{1}{a_f} - \frac{1}{a_l}\right) \quad (5.4)$$

Where T_h – time headway (s); V – vehicle speed; L – Length of vehicle.

t_r – Reaction time; $k -$ arbitrary safety factor (usually greater than or equal to 1)

$a_f -$ Minimum braking deceleration of the following vehicle

$a_l -$ Maximum braking deceleration of the lead vehicle

Note that for brick wall considerations, a_l is infinite and is usually eliminated.

The capacity of vehicles on a single roadway lane is the inverse of the tip-to-tip headway.

Hence the BRT lane capacity in vehicles-per-hour can be expressed as:

$$Q_{BRT} = \frac{3600}{T_h} \quad (5.5)$$

The BRT traffic flow rates were estimated by applying equations (5.4) and (5.5) as with the following standard and measured parameters:

Average speed of BRT Buses (at peak) $= 66.3km/hr = 18.4\,m/s$

BRT Vehicle Length $= 18m;\ reaction\ time = 2.5s$: Adjustment factor $k = 1.5$

Using equation (5.4) the tip-to-tip time headway was computed as:

$$T_h = \frac{18}{18.4} + 2.5 + \frac{1.5 \times 18.4}{2}\left(\frac{1}{2.5}\right) = 8.9s \approx 9s\ hence,$$

$$BRT\ Lane\ Capacity = {}^{3600}/_{9} = 400veh/hr$$

Step 3: Estimation of capacity utilization rate for BRT:
Recall that capacity utilization rate had been defined as the ratio of actual traffic flow levels (5min) to the maximum possible flow or capacity and expressed as a percentage, as shown below:

$$Q_u = \frac{k u_f \left(1 - \frac{k}{k_j}\right)^2}{\left(-\frac{u_f}{k_j}\left(\frac{u_f}{2\left(\frac{u_f}{k_j}\right)}\right) + (u_f)\frac{v_f}{2\left(\frac{v_f}{k_j}\right)} - c\right)} \times 100\% \qquad (5.6)$$

Therefore $Q_u = {}^{66}/_{400} \times 100\% \approx 17\%$. Therefore, the level of capacity utilization from the criteria table for SS001 BRT dedicated lane is **E.** With the LCU at E, the other associated performance parameters are a density of 3veh/km and a speed of 125km/hr. This implies that the LCU of the BRT dedicated lane at E is characterized by or associated with a low volume of vehicles, high speed, and reduced travel time to destinations for vehicles moving on it.

Perhaps the design of a mixed traffic scenario may be a solution to this underutilization, however, one is not completely sure whether it would be feasible until further analyses in that regard are completed in the remaining sections of this chapter. As earlier mentioned, the peak traffic data for SS001 was used to set up the LCU criteria table and was used as the control for the subsequent traffic performance evaluations at SS001. Consequently, these analyses continue in the next section with the determination of the LCU without BRT influence at site SS001, using the off-peak traffic data.

5.3.3 Without BRT Influence Capacity Utilization for Site SS001

Step 1: Estimation of off-peak 5mins and hourly flows, speeds, and densities for site SS001 from the empirical data in chapter 4, as shown in table 5.6 below.

Table 5. 6: Without BRT level of Capacity Utilization Parameters for SS001 (off – peak)

Period	PC	MV	HV	Vol	MV	HV	*q*	*u*	*k*	*q*
	1	*2*	*3*	*4*	*5*	*6*	*7*	*8*	*9*	*10*
					*2*1.75*	*3*3*	*1 + 5 + 6*		10/8	7*12
1	58	12	2	72	21	6	85	78	13	1020
2	73	9	1	83	16	3	92	84	13	1104
3	69	6	1	76	11	3	83	82	12	996
4	69	9	2	80	16	6	91	85	13	1092
5	67	6	2	75	11	6	84	82	12	1008
6	71	6	3	80	11	9	91	83	13	1092
7	62	8	2	72	14	6	82	85	12	984
8	56	5	1	62	9	3	68	88	9	816
9	63	8	1	72	14	3	80	83	12	960
10	55	8	2	65	14	6	75	85	11	900
11	72	3	1	76	5	3	80	81	12	960
12	57	1	0	58	2	0	59	80	9	708
1hr	772						970	(83±1)		(970±34)

1, 2, 3…10 ~ column numbers, column 1 - 4 ~ volume by 5mins, columns 5 - 7 ~ flow (pce/5mins), column 10 ~ total flow(pce/h), u ~ speed (km/hr), k ~ density (pce/km), PC ~ passenger car, MV ~ medium vehicle, HV ~ heavy vehicle

Step 2. Calibration of flow-density model using the density and flow parameters in Table 5.6. with PCEs applied. Figure 5.3 shows the graphical representation of the flow-density relationship:

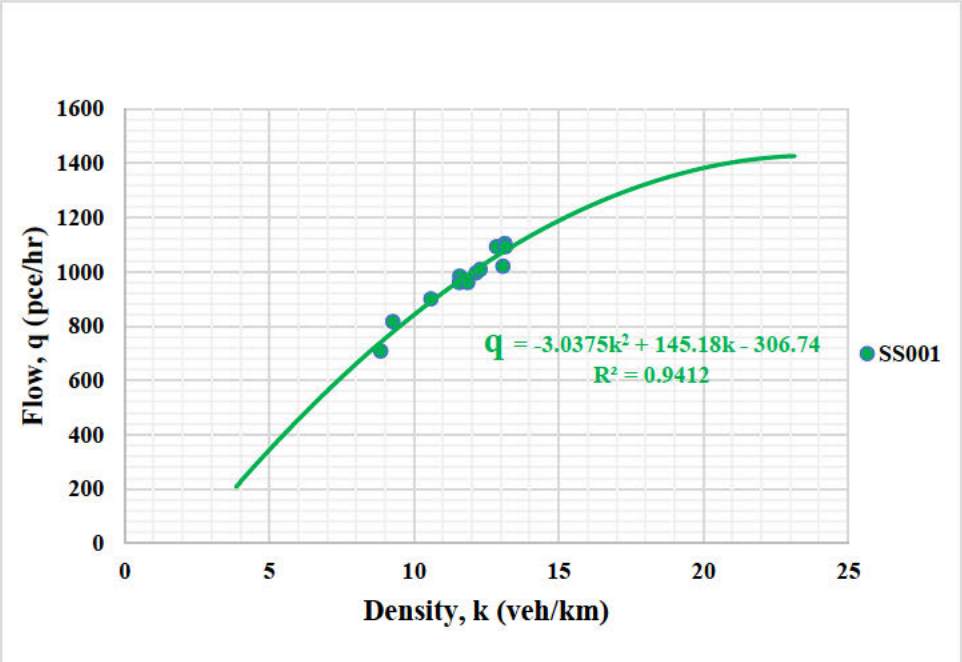

Figure 5. 3: Without BRT Influence Flow-Density Curve for site SS001 (Off-Peak)

The calibrated flow-density model is given as equation 5.7:

$$q_{withoutBRT(off-peak)} = -3.0375k^2 + 145.18k - 306.74 \quad R^2 = 0.94 \quad 5.7$$

Step 3: Statistical testing of the calibrated model for validity. Table 5.7 below shows the results of the validity test carried out on the off-peak flow-density model for site SS001 without BRT influence. As shown, the coefficients of the derived model have the anticipated sign conventions for concavity, while the coefficient of determination $R^2 = 0.9412$ is greater than 0.5, which indicates the existence of a strong relationship between density and flow, and the capability of predicting capacity.

Table 5. 7**:** Level of Capacity Utilization Model Validity Tests

	q	*k*	Constant
t' values	28.8	2.2	
Coefficients	-3.0375	145.18	306.74
Std. Error	34	1	
R^2	0.94		
F	6741	2.81	
df	11		
Residuals	-9.672	-2.412	

The F-observed statistics at ten degrees of freedom is bigger than the F-critical value of 2.81, suggesting that the model equation 5.7 did not occur by chance. Additionally, the value of the t-observed statistic at the 5% level of significance is higher than 2.2, indicating that the variables used are useful, and density is a crucial factor in flow estimation. The statistics data sequel to its analysis, was directly pulled from a Microsoft Excel file. It is important to note that the coefficient of "k" denotes the free-flow speed of roughly 145 km/hr. The aggregated model was subsequently used to predict capacity, estimate density at capacity, and speed at capacity in step 4 by differentiating *q* with respect to *k* and feeding back necessary values.

Step 4: The density at capacity, capacity or maximum flow, and the speed at maximum flow were determined using equation 5.7 as follows:

$$q_{withoutBRT(off-Peak)} = -3.0375k^2 + 145.18k - 306.74 \quad R^2 = 0.94$$

By differentiating q with respect to k,

$$\frac{\partial q}{\partial k} = 2 * -3.0375\text{k} + 145.18 = 0$$

$$k_{crt} = k_Q = 23.8pce/km \approx 24\, pce/km$$

By plugging the critical density k_Q into equation 5.7 the capacity is calculated and is given by:

$$Q = q_{withoutBRT(off-peak)} = -3.0375(24)^2 + 145.18(24) - 306.74$$

$$Q = q_{withoutBRT(off-peak)} = 1427.9pce/hr \approx 1428pce/hr$$

By substituting k_{crt} and the estimated Q into the fundamental diagram equation $q = uk$, the speed at capacity is therefore obtained as:

$$u_Q = \frac{q}{k} = \frac{1428}{24} \approx 60km/hr$$

Hence the capacity or maximum flow at off-peak traffic period is $1428pce/hr$, with a corresponding speed at capacity $u_Q = 60km/hr$. As shown in table 5.6 above, the mean flow per hour which represents the 12 period flows for site SS001 is 970 veh/hr, therefore the capacity utilization rate Q_u for site SS001 is $^{970}/_{1428} \times 100\% = 67.8 \approx 68\%$. Hence based on the criteria table 5.4, the LCU for site SS001 without BRT influence is C. This is concerning the traffic flowing on the adjoining lanes to BRT. Where the LCU is at C, the other attendant performance parameters from the table are a density of 13veh/km and a speed of 95km/hr.

5.3.4 With BRT Influence Capacity Utilization for Site SS001

Step 1: Estimation of 'with BRT' off-peak 5mins and hourly flows, speeds, and densities for site SS001 is shown in Table 5.8. Note that the BRT flows with applied PCEs were added to the without BRT traffic flows from table 5.6.

Table 5. 8**:** With BRT level of Capacity Utilization Parameters for SS001 (off – peak)

Period	PC	MV	HV	*BRT*	Vol	MV	HV	*BRT*	q	µ	k	q
	1	*2*	*3*	*4*	*5*	*6*	*7*	*8*	*8*	*10*	*11*	*12*
						*2*1.75*	*3*3*	*4*3*	*1 + 6 + 7+8*		12/10	7*12
1	58	12	2	*3*	72	21	6	*9*	94	80	14	1128
2	73	9	1	*2*	83	16	3	*6*	98	84	14	1176
3	69	6	1	*1*	76	11	3	*3*	86	82	13	1032
4	69	9	2	*2*	80	16	6	*6*	97	85	14	1164
5	67	6	2	*3*	75	11	6	*9*	93	82	14	1116
6	71	6	3	*1*	80	11	9	*3*	94	83	14	1128
7	62	8	2	*1*	72	14	6	*3*	85	85	12	1020
8	56	5	1	*2*	62	9	3	*6*	74	88	10	888
9	63	8	1	*1*	72	14	3	*3*	83	83	12	996
10	55	8	2	*2*	65	14	6	*6*	81	85	11	972
11	72	3	1	*2*	76	5	3	*6*	86	81	13	1032
12	57	1	0	*2*	58	2	0	*6*	65	80	10	780
1hr	772								1034	83±1		1034

1, 2, 3…10 ~ column numbers, column 1 - 4 ~ volume by 5mins, columns 5 -7 ~ flow (pce/5mins), column 10 ~ total flow(pce/h), u ~ speed (km/hr), k ~ density (pce/km), PC ~ passenger car, MV ~ medium vehicle, HV ~ heavy vehicle

Step 2. Calibration of with BRT flow-density model using the density and flow parameters in Table 5.8. with PCEs applied. Figure 5.4 shows the graphical representation of the flow-density relationship:

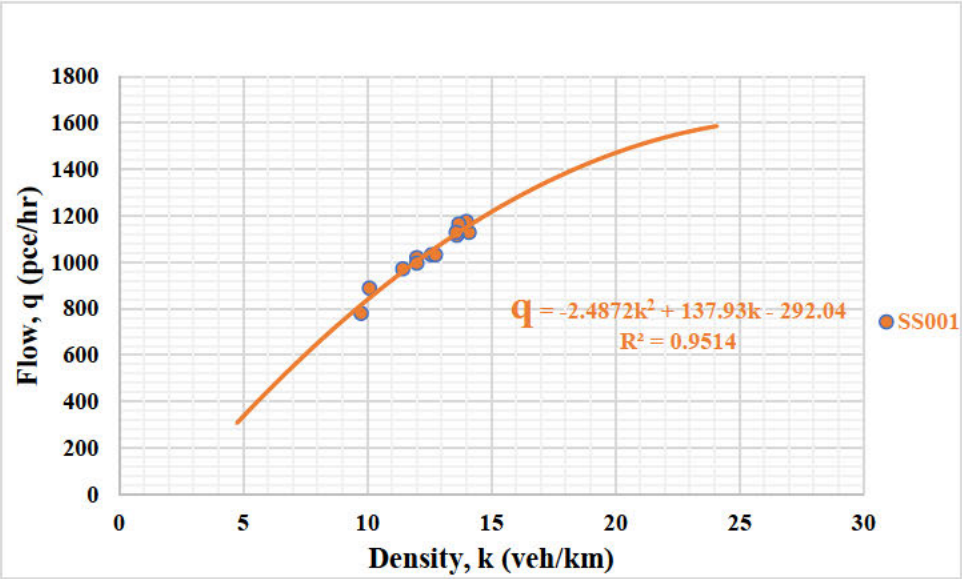

Figure 5. 4: With BRT Influence Flow-Density Curve for site SS001 (Off-Peak)

The calibrated flow-density model is given as equation 5.8:

$$q_{withBRT(off-peak)} = -2.4872k^2 + 137.93k - 292.04 \quad R^2 = 0.95 \qquad 5.8$$

Step 3: Statistical testing of the calibrated model for validity. Table 5.9 below shows the results of the validity test carried out on the off-peak flow-density model for site SS001 without BRT influence. As shown, the coefficients of the derived model have the anticipated sign conventions for concavity, while the coefficient of determination $R^2 = 0.9514$ is greater than 0.5, which indicates the existence of a strong relationship between density and flow, and the capability of predicting capacity.

Table 5. 9: Level of Capacity Utilization Model Validity Tests

	q	*k*	Constant
t' values	30.5	2.2	
Coefficients	-2.4872	137.93	292.04
Std. Error	34	1	
R^2	0.95		
F	5674	2.81	
df	11		
Residuals	-9.09	-2.91	

The F-observed statistics at ten degrees of freedom is bigger than the F-critical value of 4, suggesting that the model equation 5.8 did not occur by chance. Additionally, the value of the t-observed statistic at the 5% level of significance is higher than 2.5, indicating that the variables used are useful, and density is a crucial factor in flow estimation. The statistics data sequel to its analysis, was directly pulled from a Microsoft Excel file. It is important to note that the coefficient of "k" denotes the free-flow speed of roughly 137 km/hr. The aggregated

model was subsequently used to predict capacity, estimate density at capacity, and speed at capacity in step 4 by differentiating q with respect to k and feeding back necessary values.

Step 4: The density at capacity, capacity or maximum flow, and the speed at maximum flow were determined using equation 5.7 as follows:

$$q_{withBRT(off-Peak)} = -2.4872k^2 + 137.93k - 292.04 \quad R^2 = 0.95$$

By differentiating q with respect to k,

$$\frac{\partial q}{\partial k} = 2 * -2.4872\text{k} + 137.93 = 0$$

$$k_{crt} = k_Q = 27.7 pce/km \approx 28\, pce/km$$

By plugging the critical density k_Q into equation 5.8 the capacity is calculated and is given by:

$$Q = q_{withBRT(off-peak)} = -2.4872(28)^2 + 137.93(28) - 292.04$$

$$Q = q_{withBRT(off-peak)} = 1620.04 pce/hr \approx 1620 pce/hr$$

By substituting k_{crt} and the estimated Q into the fundamental diagram equation $q = uk$, the speed at capacity is therefore obtained as:

$$u_Q = \frac{q}{k} = \frac{1620}{28} \approx 58 km/hr$$

Hence, the capacity or maximum flow at off-peak traffic period is $1620 pce/hr$, with a corresponding speed at capacity $u_Q = 58 km/hr$. As shown in table 5.8 above, the mean 'with BRT' flow per hour which represents the 12 period flows for site SS001 is 1034 veh/hr, therefore the capacity utilization rate with BRT Q_u for site SS001 is $^{1034}/_{1620} \times 100\% = 63.8 \approx 64\%$. Based on the criteria table 5.4, the LCU for site SS001 'with BRT' influence is **C**. Where the LCU is at **C**, the other attendant performance parameters from the table are density of 13veh/km, and speed of 95km/hr.

5.3.5 Comparative Assessment of Capacity Utilization for Site SS001 Summary

Based on the findings from the analysis of empirical data at site SS001, a comparative assessment and synthesis of evidence among the three roadway and flow scenarios discussed in chapter 2 which include: scenario one, a roadway with dedicated carriageway lane to BRT service only; scenario two, a roadway without the influence of BRT; and scenario three, a

roadway with the influence of BRT, are discussed. Having developed criteria tables for each site in the previous section, it is necessary to evaluate and compare traffic performance at site SS001 during each 5mins flow interval or period in terms of capacity utilization rates and hence determine the LCU using the criteria table. Recall that analysis is based on the fundamental flow-density relationship, and capacity utilization rate had been defined as the ratio of actual traffic flow levels (5min) to the maximum possible flow or capacity and expressed as a percentage, given by equation 5.6.

Table 5.10 shows the 5mins off-peak capacity utilization rates and levels at site SS001 for the three scenarios.

Table 5. 10**:** Summary of Off-Peak Capacity Utilization Rates and Levels for SS001

Period	q BRT (pce/hr)	q without BRT (pce/hr)	q with BRT (pce/hr)	Q_u BRT (%)	Q_u without BRT (%)	Q_u with BRT (%)	LCU BRT	LCU without BRT	LCU With BRT
1	108	1020	1128	27	71	70	D	C	C
2	72	1104	1176	18	77	73	E	B	C
3	36	996	1032	9	70	64	E	C	C
4	72	1092	1164	18	76	72	E	B	C
5	108	1008	1116	27	71	69	D	C	C
6	36	1092	1128	9	76	70	E	B	C
7	36	984	1020	9	69	63	E	C	C
8	72	816	888	18	57	55	E	C	C
9	36	960	996	9	67	61	E	C	C
10	72	900	972	18	63	60	E	C	C
11	72	960	1032	18	67	64	E	C	C
12	72	708	780	18	50	48	E	D	D
1hr	66	970	1036	17	68	64	E	C	C
	400	1428	1620						

5.3.5.1 Based on BRT Dedicated Lane Performance

The LCU E of the BRT dedicated lane shows that the Bus route is substantially underutilized, hence, the level of capacity utilization is poor. This is caused by the designation of the lane solely for BRT buses with no competition from other vehicle classes moving on the adjoining lanes. From this finding, and concerning the geometric characteristics of the BRT dedicated lane, coupled with vehicle characteristics, the LCU of the BRT lane may not improve from E. This is due to the observed width of the BRT dedicated lane of 4.3m. Besides, with a BRT vehicle width of 3.1m, only one bus can move on the dedicated lane at once, making it impossible for two buses to move side by side.

5.3.5.2 Based on Traffic Flowrate 'without BRT' Influence

In comparison with the LCU of the BRT dedicated lane at E, it can be observed that at level C, there is an associated reduction in speed, as well as an increase in density but increased travel time. Besides, the LCU of the adjoining lanes at C shows that the capacity utilization improves due to the traffic mix on those lanes which comprise passenger cars, medium vehicles, and a few heavy vehicles in different proportions; whereas the BRT dedicated lane is used by only one vehicle class which are the BRT buses.

5.3.5.3 Based on Traffic Flowrate 'with BRT' Influence

In comparison with the LCU without BRT influence, it can be observed that both are the same, as well as all parameters associated with that level. Although as expected, the maximum flow was higher, while the speed dropped. However, it may be expected that the level of capacity utilization would improve to level B. This outcome could have resulted from the poor Utilization of the BRT dedicated lanes. In other words, this simply means that there is an insufficient number of BRT buses in the BRT transit scheme, as the mixed traffic scenario tested with BRT did not have a significant effect on traffic flow and capacity Utilization. Nevertheless, in comparison with the LCU on the BRT dedicated lane, there was a speed reduction, as well as an increase in density and travel time. Overall, the LCU C with BRT influence at site SS001 shows that the capacity utilization can be significantly enhanced by mixed traffic scenarios as against having a BRT dedicated lane, especially one with a median configuration design.

5.3.4 Summary of Capacity Differentials – SS001

In summary, a criteria table has been developed for the assessment of traffic flow performance under different flow scenarios such as roadway with BRT, roadway without BRT, and BRT dedicated lane only. Sequel to the comparisons and synthesis of evidence that have emerged from the analysis, the different levels of capacity utilization for the various scenarios considered are caused by differentials in germane traffic flow parameters such as capacity, speed, density, and travel time. Figure 5.5 below gives a pictorial description of the traffic characteristics differentials that are responsible for the traffic flow performance and Levels of capacity Utilization observed at site SS001.

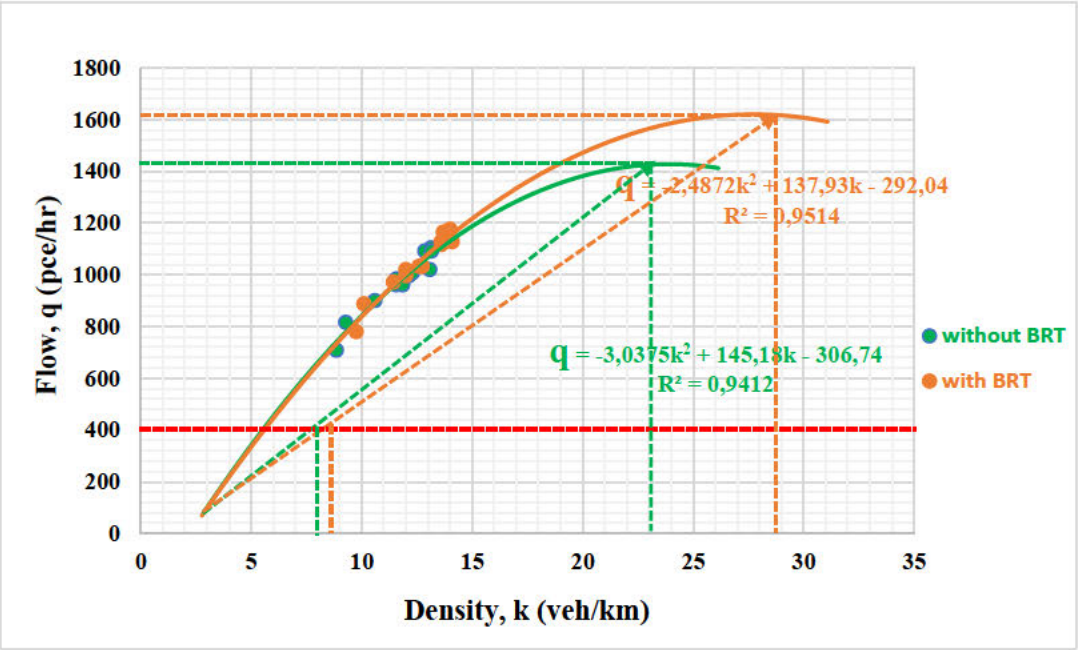

Figure 5. 5: Capacity Differentials at site SS001

From the arguments raised in chapter two and the hypothesis put forward in this regard, it can be observed from Figure 5.5 under steady flow conditions that the capacity Q_1 of roadway with BRT, indicated by the yellow line is $1620pce/hr$, capacity Q_2 of roadway without BRT, indicted by the green line is $1428pce/hr$, and BRT dedicated lane capacity Q_3, indicated by the red line is 400pce/hr. The corresponding speed at capacity of the roadway with BRT is $58km/hr$, the speed at capacity of the roadway without BRT is $60km/hr$. Similarly, the corresponding density at capacity k_1 of roadway with BRT is $28pce/km$, density at capacity k_2 of roadway without BRT is $24pce/km$. Likewise, the BRT dedicated lane density k_{31} based on travel speed with the influence of BRT is approximately $9veh/km$, while the BRT dedicated lane density k_{32} based on travel speed without the influence of BRT is approximately $8veh/km$. Table 5.11 shows the summary of capacity Utilization rates and levels, as well as the associated traffic characteristics differentials for site SS001.

Table 5. 11: Summary of capacity Utilization and traffic characteristics differentials for SS001

S/N	Roadway Condition	u_f	Q			U		K				Q_u (%)	LCU
			Q_1	Q_2	Q_3	u_1	u_2	k_1	k_2	k_{31}	k_{32}		
SS001	with BRT	145	1620	1428	400	58	60	28	24	9	8	64	C
	without BRT	137										68	C
	BRT Dedicated Lane	60										17	E

u_f ~ free-flow speed (km/hr),Q_1 ~ capacity with BRT(pce/hr), Q_2 ~ capacity without BRT(pce/hr), Q_3 ~ BRT capacity(veh/hr), u_1 ~ speed at capacity with BRT(km/hr), u_2 ~ speed at capacity without BRT(km/hr), k_1 ~ density at capacity with BRT (pce/km), k_2 ~ density at capacity without BRT (pce/km), ~ k_{31} ~ dedicated lane density with BRT (pce/km), k_{32} ~ dedicated lane density without BRT (pce/km), Q_u ~ capacity Utilization rate (%), LCU ~ level of capacity Utilization

To avoid repetitions from the previous section he criteria table, the LCU criteria table determination for the other three sites is abridged by using the stepwise analytical procedure.

5.4 Site SS002 Capacity Utilization

5.4.1 Capacity Utilization Criteria Table for SS002

Step 1. Analysis of empirical data in Table 5.12.

Table 5. 12: Level of Capacity Utilization (LCU) Parameters – SS002(Peak)

	PC	MV	HV	Vol	MV	HV	*q*	*u*	*k*	*q*
Period	*1*	*2*	*3*	*4*	*5*	*6*	*7*	*8*	*9*	*10*
					*2*1.75*	*3*3*	*1 + 5 + 6*		*10/8*	*7*12*
1	116	4	5	125	7	15	138	70	24	1661
2	110	7	4	121	12	12	134	73	22	1611
3	98	1	4	103	2	12	112	76	18	1341
4	104	5	4	113	9	12	125	74	20	1497
5	82	1	3	86	2	9	93	79	14	1113
6	111	0	5	116	0	15	126	75	20	1512
7	92	3	1	96	5	3	100	76	16	1203
8	98	2	8	108	4	24	126	72	21	1506
9	106	3	4	113	5	12	123	71	21	1479
10	96	3	5	104	5	15	116	73	19	1395
11	114	1	2	117	2	6	122	75	19	1461
12	94	2	3	99	4	9	107	74	17	1278
1hr	1102	66	24	1192			1421	83±1		1421

1, 2, 3…10 ~ column numbers, column 1 - 4 ~ volume by 5mins, columns 5 - 7 ~ flow (pce/5mins), q ~ total flow(pce/hr), u ~ speed (km/hr), k ~ density (pce/km), PC ~ passenger car, MV ~ medium vehicle, HV ~ heavy vehicle

Step 2. Calibration of flow-density model using the LCU parameters in table 5.12. Figure 5.6 shows the graphical representation of the flow-density relationship.

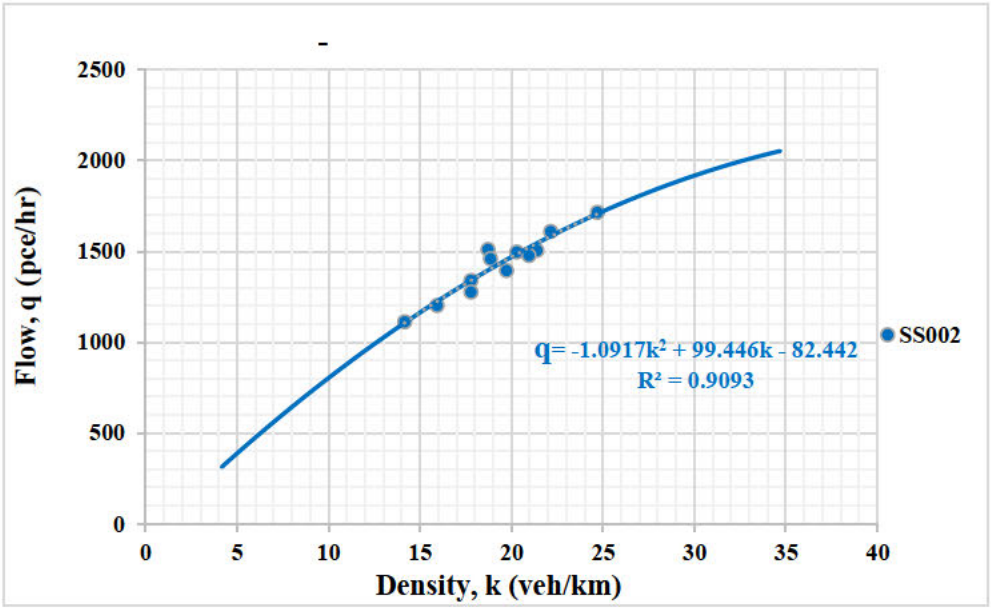

Figure 5. 6: Traffic Flow-Density (F-D) Curve for SS002(Peak) – Control

The calibrated model equation is given as equation 5.9:

$$q_{SS002(Control)} = -1.0917k^2 + 99.446k - 82.442 \qquad R^2 = 0.91 \qquad 5.9$$

Step 3: Statistical testing of the calibrated model for validity. Table 5.13 below shows the results of the validity test carried out on the model for site SS002 without BRT influence.

Table 5. 13**:** Level of Capacity Utilization Model Validity Tests

	q	*k*	Constant
t' values	30.4	2.2	
Coefficients	-1.0917	99.446	82.442
Std. Error	47	1	
R^2	0.91		
F	10768	2.82	
df	11		
Residuals	-9.14	-2.84	

Step 4: Determination **of** density at capacity, capacity or maximum flow, and the speed at maximum equation 5.9 as follows:

$$q = -1.0917k^2 + 99.446k - 82.442 \qquad R^2 = 0.91$$

By differentiating q with respect to k,

$$\frac{\partial q}{\partial k} = 2 * -1.0917\text{k} + 99.446 = 0$$

$$k_{crt} = k_Q = 45.5 pce/km \approx 46\, pce/km$$

By plugging the critical density k_Q into equation 5.11 the capacity is calculated and is given by:

$$Q = q_{2021(peak)} = -1.0917(46)^2 + 99.446(46) - 82.442$$

$$Q = q_{2021(peak)} = 2182.03 pce/hr \approx 2182 pce/hr$$

By substituting k_{crt} and the estimated Q into the fundamental diagram equation $q = uk$, the speed at capacity is therefore obtained as:

$$u_Q = \frac{q}{k} = \frac{2182}{46} = 47.4 \approx 47 km/hr$$

Hence the capacity or maximum flow is $2182 pce/hr$, with a corresponding speed at capacity $u_Q = 47 km/hr$.

Step 5: The estimated capacity $Q \approx 2182 pce/hr$ can be approximated to $2200 pce/hr$ and split into five capacity Utilization levels for the LCU criteria table. therefore,

Level A (100%) = 2200 pce/hr

Level B (85%) = $0.85 * 2200 = 1870 pce/hr \approx 1900 pce/hr$

Level C (75%) = $0.75 * 2200 = 1650pce/hr \approx 1700pce/hr$

Level D (50%) = $0.50 * 2200 = 1100pce/hr \approx 1100pce/hr$

Level E (25%) = $0.25 * 2200 = 550pce/hr \approx 600pce/hr$

Step 6: From the model equation above, speed is evenly distributed between its free-flow speed of 99.446km$/hr \approx 100km/hr$ for class E and speed at the capacity of $47km/hr \approx 50km/hr$ for class A. The speed is used to compute the attendant densities and its corresponding time for 1km of roadway, and subsequently, the LCU criteria table is developed. Thus, the LCU criteria table for SS002 is presented in table 5.14.

Table 5. 14**:** LCU Criteria Table for SS002

LCU	Qu %	Flow (Q) veh/h	Density (k) veh/km/lane	Speed(u) km/hr
A	86 - 100	2200	44	50
B	76 - 85	1900	27	70
C	51 - 75	1700	21	80
D	26 - 50	1100	12	90
E	0 - 25	600	6	100

5.4.2 BRT Dedicated Lane Capacity Utilization for Site SS002

Step 1. Estimation of five-minute BRT traffic volume using SANRAL's standard PCE values for heavy vehicle class as shown in table 5.15 below.

Table 5. 15**:** BRT Dedicated Lane Level of Capacity Utilization Parameters

Period	BRT	BRT	u	k	k	q	q
	1	2	3	4	5	6	7
		1*3		*6/3*	*7/3*	1*12	2*12
1	3	9	71	0	2	36	108
2	3	9	64	0	1	36	108
3	2	6	60	0	1	24	72
4	3	9	80	0	1	36	108
5	2	6	59	0	1	24	72
6	3	9	76	0	1	36	108
7	2	6	69	0	1	24	72
8	1	3	66	0	1	12	36
9	1	3	66	0	1	12	36
10	2	6	74	0	1	24	72
11	1	3	77	0	1	12	36
12	3	9	72	0	1	36	108
1hr	26		69±2			26±2	78±9

1, 2, …8 ~ column numbers, column 1 ~ volume by 5mins, column 2 ~ BRT flow (pce/5mins), u ~ speed (km/hr), k4 ~ density (veh/km), k5 ~ density (pce/km) q6 ~ total flow(veh/hr), q7 ~ total flow(pce/hr) BRT ~ Bus Rapid Transit.

Step 2: Determination of BRT dedicated lane capacity:

The average speed of BRT Buses (at peak) $= 69.5km\ per\ hr = 19.30\ m/s$

BRT Vehicle Length $= 18m;\ reaction\ time = 2.5s$ and correction factor $k = 1.5$

Using equation (3.4) the time headway was computed as:

$$T_h = \frac{18}{19.3} + 2.5 + \frac{1.5 \times 19.3}{2}\left(\frac{1}{2.5}\right) = 9.2s\ hence,$$

$$BRT\ Lane\ Capacity = {}^{3600}/_{9.2} = 391veh/hr$$

Step 3: Estimation of capacity utilization rate for BRT:

Recall that capacity Utilization rate had been defined as the ratio of actual traffic flow levels (5min) to the maximum possible flow or capacity and expressed as a percentage, therefore $Q_u = {}^{78}/_{391} \times 100\% = 19.9 \approx 20\%$. Therefore, the level of capacity Utilization based on the criteria table for SS002 BRT dedicated lane is E**.** With the LCU at E, the other associated performance parameters are a density of 6veh/km and a speed of 100km/hr. This implies that when there are fewer vehicles on a road, as is the case of BRT buses, the free-flow speed is high, and travel time decreases. The LCU E of the BRT dedicated lane shows that the Bus route is substantially underutilized, hence, the level of capacity utilization is poor.

5.4.3 'Without BRT' Influence Capacity Utilization for Site SS002

Step 1: Estimation of off-peak 5mins and hourly flows, speeds, and densities for site SS002 using the empirical data in chapter 4, shown in Table 5.16 below:

Table 5. 16**:** Without BRT level of Capacity Utilization Parameters for SS002 (off – peak)

	PC	MV	HV	Vol	MV	HV	*q*	*u*	*k*	*q*
Period	*1*	*2*	*3*	*4*	*5*	*6*	*7*	*8*	*9*	*10*
					*2*1.75*	*3*3*	*1 + 5 + 6*		10/8	7*12
1	90	4	5	99	7	15	112	75	18	1344
2	65	7	4	76	12	12	89	77	14	1068
3	73	1	4	78	2	12	87	75	14	1044
4	74	5	4	83	9	12	95	76	15	1140
5	80	1	3	84	2	9	91	74	15	1092
6	72	0	5	77	0	15	87	74	14	1044
7	82	3	1	86	5	3	90	72	15	1080
8	80	2	8	90	4	24	108	68	19	1296
9	85	3	4	92	5	12	102	70	17	1224
10	79	3	5	87	5	15	99	72	17	1188
11	80	1	2	83	2	6	88	71	15	1056
12	79	2	3	84	4	9	92	75	15	1104
1hr	939						1140	73±1		1140

1, 2, 3…10 ~ column numbers, column 1 - 4 ~ volume by 5mins, columns 5 - 7 ~ flow (pce/5mins), column 10 ~ total flow(pce/h), u ~ speed (km/hr), k ~ density (pce/km), PC ~ passenger car, MV ~ medium vehicle, HV ~ heavy vehicle

Step 2. Calibration of flow-density model using the density and flow parameters in Table 5.15. with PCEs applied. Figure 5.7 shows the graphical representation of the flow-density relationship:

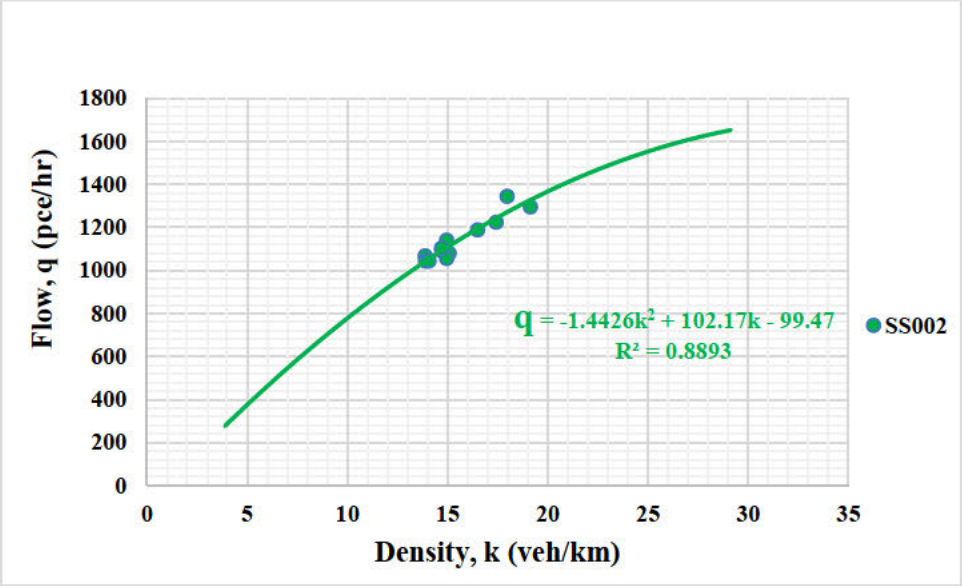

Figure 5. 7: Without BRT Influence Flow-Density Curve for site SS002 (Off-Peak)

The calibrated flow-density model is given as equation 5.10:

$$q_{withoutBRT(off-peak)} = -1.4426k^2 + 102.17k - 99.47 \quad R^2 = 0.89 \quad 5.10$$

Step 3: Statistical testing of the calibrated model for validity. Table 5.17 below shows the results of the validity test carried out on the off-peak flow-density model for site SS002 without BRT influence.

Table 5. 17: Level of Capacity Utilization Model Validity Tests

	q	*k*	Constant
t' values	39	2.2	
Coefficients	-1.4426	102.17	99.47
Std. Error	29	1	
R^2	0.89		
F	3690	2.82	
df	11		
Residuals	-21.72	-2.203	

Step 4: The density at capacity, capacity or maximum flow, and the speed at maximum flow were determined using equation 5.10 as follows:

$$q_{withoutBRT(off-Peak)} = -1.4426k^2 + 102.17k - 99.47 \quad R^2 = 0.89$$

By differentiating q with respect to k,

$$\frac{\partial q}{\partial k} = 2 * -1.4426\text{k} + 102.17 = 0$$

$$k_{crt} = k_Q = 35.4 pce/km \approx 35\, pce/km$$

By plugging the critical density k_Q into equation 5.14 the capacity is calculated and is given by:

$$Q = q_{withoutBRT(off-Peak)} = -1.4426(35)^2 + 102.17(35) - 99.479$$

$$Q = q_{withoutBRT(off-Peak)} = 1709.28 pce/hr \approx 1709 pce/hr$$

By substituting k_{crt} and the estimated Q into the fundamental diagram equation $q = uk$, the speed at capacity is therefore obtained as:

$$u_Q = \frac{q}{k} = \frac{1709}{35} \approx 49 km/hr$$

Hence the capacity or maximum flow at off-peak traffic period is $1709 pce/hr$, with a corresponding speed at capacity $u_Q = 49 km/hr$. As shown in table 5.12 above, the mean flow per hour which represents the 12 period flows for site SS002 is 1140 veh/hr, therefore the capacity utilization rate Q_u for site SS002 is ${}^{1140}/_{1709} \times 100\% = 66.7 \approx 67\%$. Hence based on the criteria table 5.13, the LCU for site SS002 without BRT influence is C. Where the LCU is at C, the other attendant performance parameters from the table are a density of 21veh/km and a speed of 80km/hr. In comparison with the LCU of the BRT dedicated lane at E, it can be observed that at level C, there is an associated reduction in speed, as well as an increase in density and travel time. Besides, the LCU of the adjoining lanes at C shows that the capacity utilization is better due to the traffic mix on those lanes which comprise passenger cars, medium vehicles, and a few heavy vehicles in different proportions; whereas the BRT dedicated lane is used by only one vehicle class which are the BRT buses.

5.4.4 'With BRT' Influence Capacity Utilization for Site SS002

Step 1: Estimation of 'with BRT' off-peak 5mins and hourly flows, speeds, and densities for site SS002 is shown in table 5.17. Note that the BRT flows with applied PCEs were added to the without BRT traffic flows from table 5.15.

Table 5. 18: With BRT level of Capacity Utilization Parameters for SS002 (off – peak)

Period	PC	MV	HV	*BRT*	Vol	MV	HV	*BRT*	q	μ	k	q
	1	*2*	*3*	*4*	*5*	*6*	*7*	*8*	*8*	*10*	*11*	*12*
						*2*1.75*	*3*3*	*4*3*	*1 + 6 + 7+8*		12/10	7*12
1	90	4	5	3	102	7	15	9	121	75	19	1452
2	65	7	4	3	79	12	12	9	98	76	15	1179
3	73	1	4	2	80	2	12	6	93	75	15	1113
4	74	5	4	3	86	9	12	9	104	76	16	1245
5	80	1	3	2	86	2	9	6	97	74	16	1161
6	72	0	5	3	80	0	15	9	96	74	16	1152
7	82	3	1	2	88	5	3	6	96	72	16	1155
8	80	2	8	1	91	4	24	3	111	68	20	1326
9	85	3	4	1	93	5	12	3	105	70	18	1263
10	79	3	5	2	89	5	15	6	105	72	18	1263
11	80	1	2	1	84	2	6	3	91	71	15	1089
12	79	2	3	3	87	4	9	9	101	75	16	1206
1hr	939								1217	73±1		1217

1, 2, 3…10 ~ column numbers, column 1 - 4 ~ volume by 5mins, columns 5 -7 ~ flow (pce/5mins), column 10 ~ total flow(pce/h), u ~ speed (km/hr), k ~ density (pce/km), PC ~ passenger car, MV ~ medium vehicle, HV ~ heavy vehicle

Step 2. Calibration of with BRT flow-density model using the density and flow parameters in Table 5.17. with PCEs applied. Figure 5.8 shows the graphical representation of the flow-density relationship:

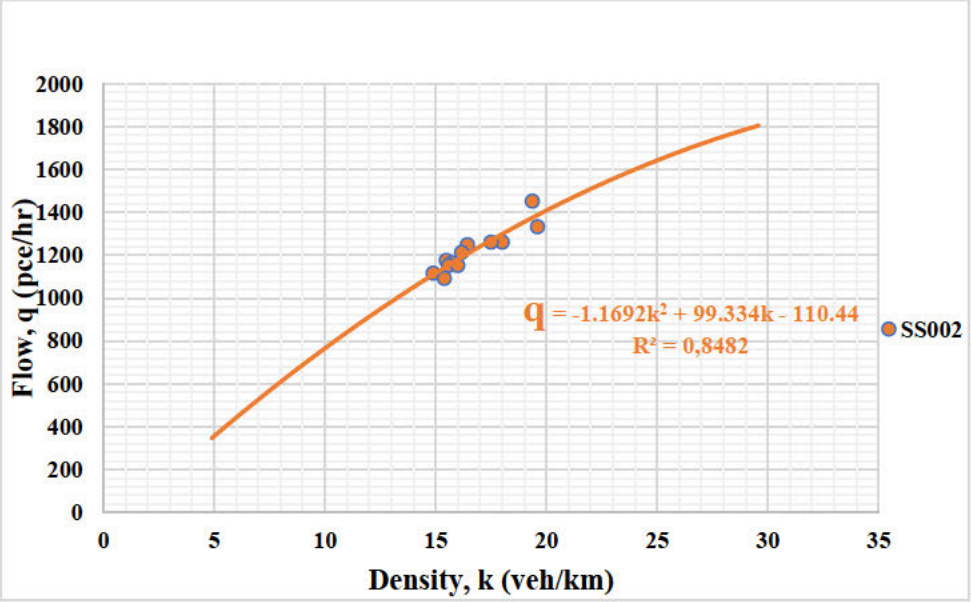

Figure 5. 8: With BRT Influence Flow-Density Curve for site SS002 (Off-Peak)

The calibrated flow-density model is given as equation 5.8:

$$q_{withBRT(off-peak)} = -1.1692k^2 + 99.334k - 110.44 \quad R^2 = 0.85 \quad 5.11$$

Step 3: Statistical testing of the calibrated model for validity. Table 5.19 below shows the results of the validity test carried out on the off-peak flow-density model for site SS002 with BRT influence.

Table 5. 19**:** Level of Capacity Utilization Model Validity Tests

	q	*k*	Constant
t' values	41.7	2.2	
Coefficients	-1.1692	99.334	110.44
Std. Error	29	1	
R^2	0.85		
F	3655	2.82	
df	11		
Residuals	-1.692	-2.265	

Step 4: The density at capacity, capacity or maximum flow, and the speed at maximum flow were determined using equation 5.11 as follows:

$$q_{withBRT(off-Peak)} = -1.1692k^2 + 99.334k - 110.44 \quad R^2 = 0.85$$

By differentiating q with respect to k,

$$\frac{\partial q}{\partial k} = 2 * -1.1692\text{k} + 99.334 = 0$$

$$k_{crt} = k_Q = 42.5pce/km \approx 43\, pce/km$$

By plugging the critical density k_Q into equation 5.8 the capacity is calculated and is given by:

$$Q = q_{withBRT(off-peak)} = -1.1692(43)^2 + 99.334(43) - 110.44$$

$$Q = q_{withBRT(off-peak)} = 1999.07pce/hr \approx 1999pce/hr$$

By substituting k_{crt} and the estimated Q into the fundamental diagram equation $q = uk$, the speed at capacity is therefore obtained as:

$$u_Q = \frac{q}{k} = \frac{1999}{43} \approx 46km/hr$$

Hence, as expected, the capacity or maximum flow at off-peak traffic period is $1999pce/hr$, with a corresponding speed at capacity $u_Q = 46km/hr$. As shown in table 5.18 above, the mean 'with BRT' flow per hour which represents the 12 period flows for site SS002 is 1217 veh/hr, therefore the capacity utilization rate 'with BRT' influence Q_u for site SS002 is $^{1217}/_{1999} \times 100\% = 60.8 \approx 61\%$. Hence based on the criteria table 5.10, the LCU for site SS002 'with BRT' influence is C. Where the LCU is at C, the other attendant performance parameters from the table are a density of 21veh/km and a speed of 80km/hr.

5.4.5 Comparative Assessment of Capacity Utilization for Site SS002 Summary

Table 5.20 shows the 5mins off-peak capacity Utilization rates and levels at site SS002 for the three scenarios.

Table 5. 20**:** Summary of Off-Peak Capacity Utilization Rates and Levels for SS002

Period	q BRT	q without BRT	q with BRT	Qu BRT (%)	Qu without BRT (%)	Qu with BRT (%)	LCU BRT	LCU without BRT	LCU With BRT
1	108	1344	1452	28	79	73	D	B	C
2	108	1068	1179	28	62	59	D	C	C
3	72	1044	1113	18	61	56	E	C	C
4	108	1140	1245	28	67	62	D	C	C
5	72	1092	1161	18	64	58	E	C	C
6	108	1044	1152	28	61	58	D	C	C
7	72	1080	1155	18	63	58	E	C	C
8	36	1296	1326	9	76	66	E	C	C
9	36	1224	1263	9	72	63	E	C	C
10	72	1188	1263	18	70	63	E	C	C
11	36	1056	1089	9	62	54	E	C	C
12	108	1104	1206	28	65	60	D	C	C
1hr	78	1140	1217	20	67	61	E	C	C
	391	1709	1999						

5.4.5.1 Based on BRT Dedicated Lane Performance

The LCU E of the BRT dedicated lane shows that the Bus route is substantially underutilized, hence, the level of capacity utilization is poor. This is caused by the designation of the lane solely for BRT buses with no competition from other vehicle classes moving on the adjoining lanes. From this finding, and concerning the geometric characteristics of the BRT dedicated lane, coupled with vehicle characteristics, the LCU of the BRT lane may not improve from E. This is due to the observed width of the BRT dedicated lane of 4.3m. Besides, with a BRT vehicle width of 3.1m, only one bus can move on the dedicated lane at once, making it impossible for two buses to move side by side.

5.4.5.2 Based on Traffic Flowrate 'without BRT' Influence

In comparison with the LCU of the BRT dedicated lane at **E**, it can be observed that at level **C**, there is an associated reduction in speed, as well as an increase in density but increased travel time. Besides, the LCU of the adjoining lanes at **C** shows that the capacity utilization improves due to the traffic mix on those lanes which comprise passenger cars, medium vehicles, and a few heavy vehicles in different proportions; whereas the BRT dedicated lane is used by only one vehicle class which are the BRT buses.

5.4.5.3 Based on Traffic Flowrate 'with BRT' Influence

In comparison with the LCU without BRT influence, it can be observed that both are the same, as well as all parameters associated with that level. Although as expected, the maximum flow was higher, while the speed dropped. However, it may be expected that the level of capacity utilization would improve to level B. This outcome could have resulted from the poor Utilization of the BRT dedicated lanes. In other words, this simply means that there is an insufficient number of BRT buses in the BRT transit scheme, as the mixed traffic scenario tested with BRT did not have a significant effect on traffic flow and capacity Utilization. Nevertheless, in comparison with the LCU on the BRT dedicated lane, there was a speed reduction, as well as an increase in density and travel time. Overall, the LCU C with BRT influence at site SS002 shows that the capacity utilization can be significantly enhanced by mixed traffic scenarios as against having a BRT dedicated lane, especially one with a median configuration design.

5.4.6 Summary of Capacity Differentials – SS002

In summary, a criteria table has been developed for the assessment of traffic flow performance under different flow scenarios such as roadway with BRT, roadway without BRT, and BRT dedicated lane only. Sequel to the comparisons and synthesis of evidence that have emerged from the analysis, the different levels of capacity Utilization for the various scenarios considered are caused by differentials in germane traffic flow parameters such as capacity, speed, density, and travel time. Figure 5.9 below gives a pictorial description of the traffic characteristics differentials that are responsible for the traffic flow performance and Levels of capacity utilization observed at site SS002.

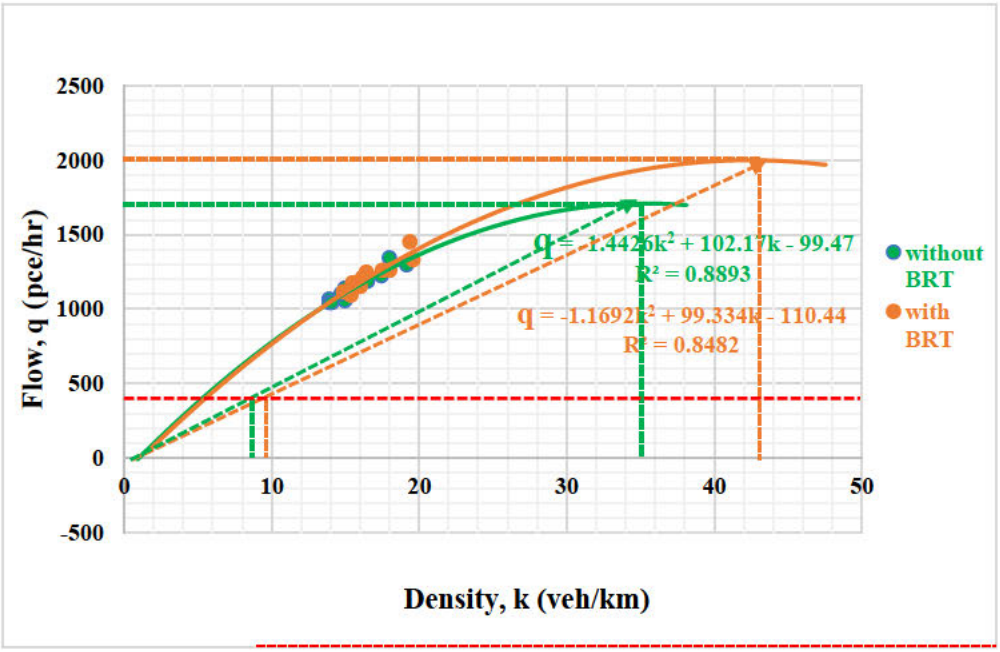

Figure 5. 9: Capacity Differentials at site SS002

From the arguments raised in chapter two and the hypothesis put forward in this regard, it can be observed from Figure 5.9 under steady flow conditions that the capacity Q_1 of roadway with BRT, indicated by the yellow line is $1999pce/hr$, capacity Q_2 of roadway without BRT, indicted by the green line is $1709pce/hr$, and BRT dedicated lane capacity Q_3, indicated by the red line is 391pce/hr. The corresponding speed at capacity of the roadway with BRT is $46km/hr$, and the speed at capacity of the roadway without BRT is $49km/hr$. Similarly, the corresponding density at capacity k_1 of roadway with BRT is $43pce/km$, density at capacity k_2 of roadway without BRT is $35pce/km$. Likewise, the BRT dedicated lane density k_{31} based on travel speed with the influence of BRT is approximately $10veh/km$, while the BRT dedicated lane density k_{32} based on travel speed without the influence of BRT is approximately $8veh/km$. Table 5.21 shows the summary of capacity Utilization rates and levels, as well as the associated traffic characteristics differentials for site SS002.

Table 5. 21: Summary of capacity utilization and traffic characteristics differentials for SS002

S/N	Roadway Condition	u_f	Q			U		K				Q_u (%)	LCU
			Q_1	Q_2	Q_3	u_1	u_2	k_1	k_2	k_{31}	k_{32}		
SS002	with BRT	99	1999	1709	391	43	49	43	35	10	8	61	C
	without BRT	102										67	C
	BRT Dedicated Lane	60										20	E

u_f ~ free-flow speed (km/hr),Q_1 ~ capacity with BRT(pce/hr), Q_2 ~ capacity without BRT(pce/hr), Q_3 ~ BRT capacity(veh/hr), u_1 ~ speed at capacity with BRT(km/hr), u_2 ~ speed at capacity without BRT(km/hr), k_1 ~ density at capacity with BRT (pce/km), k_2 ~ density at capacity without BRT (pce/km), ~ k_{31} ~ dedicated lane density with BRT (pce/km), k_{32} ~ dedicated lane density without BRT (pce/km), Q_u ~ capacity Utilization rate (%), LCU ~ level of capacity Utilization

5.5 Site SS003 Capacity Utilization

5.5.1 Capacity Utilization Criteria Table for SS003

Step 1. Analysis of empirical data in Table 5.22.

Table 5. 22: Level of Capacity Utilization (LCU) Parameters – SS003(Peak)

	PC	MV	HV	Vol	MV	HV	*q*	*u*	*k*	*q*
Period	*1*	*2*	*3*	*4*	*5*	*6*	*7*	*8*	*9*	*10*
					*2*1.75*	*3*3*	*1 + 5 + 6*		*10/8*	*7*12*
1	110	3	5	118	5	15	130	74	21	1560
2	101	4	2	107	7	6	114	75	18	1368
3	130	11	6	147	19	18	167	70	29	2004
4	122	8	5	135	14	15	151	68	27	1812
5	158	8	8	174	14	24	196	68	35	2352
6	128	3	10	141	5	30	163	68	29	1956
7	137	10	13	160	18	39	194	66	35	2328
8	156	14	5	175	25	15	196	67	35	2352
9	155	6	17	178	11	51	217	62	42	2604
10	159	10	7	176	18	21	198	61	39	2376
11	144	4	10	158	7	30	181	34	65	2172
12	156	7	4	167	12	12	180	26	82	2160
1hr	1656						2087	62±4		2087

1, 2, 3…10 ~ column numbers, column 1 - 4 ~ volume by 5mins, columns 5 - 7 ~ flow (pce/5mins), q ~ total flow(pce/hr), u ~ speed (km/hr), k ~ density (pce/km), PC ~ passenger car, MV ~ medium vehicle, HV ~ heavy vehicle

Step 2. Calibration of flow-density model using the LCU parameters in table 5.16. Figure 5.10 shows the graphical representation of the flow-density relationship.

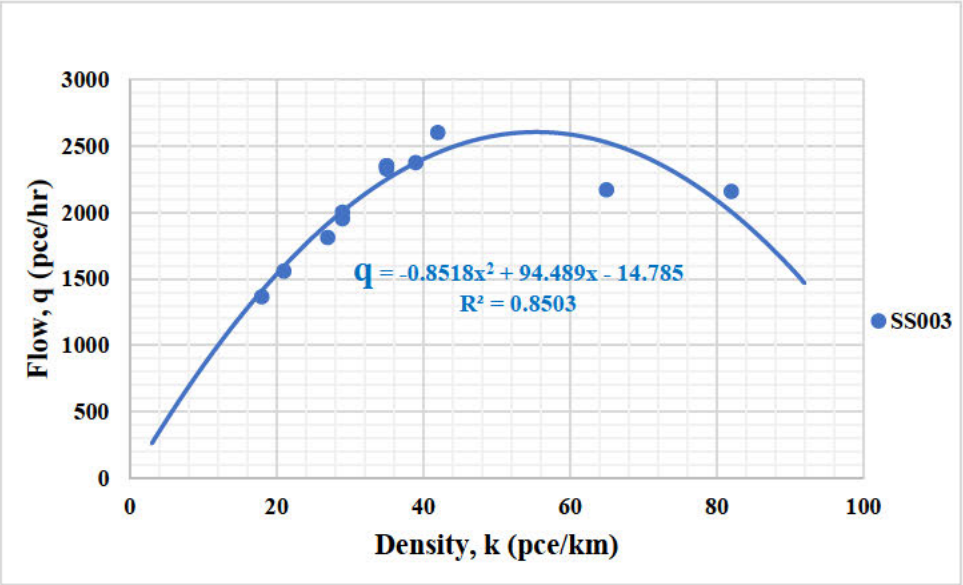

Figure 5. 10: Traffic Flow-Density (F-D) Curve for SS003(Peak) - Control

The model equation is given s equation 5.12.

$$q_{SS003(Control)} = -0.8518k^2 + 94.489k - 14.785 \qquad R^2 = 0.85 \quad 5.12$$

Step 3: Statistical testing of the calibrated model for validity. Table 5.23 below shows the results of the validity test carried out on the model for site SS003 without BRT influence.

Table 5. 23**:** Level of Capacity Utilization Model Validity Tests

	q	*k*	Constant
t' values	19.95	2.2	
Coefficients	-0.8518	94.489	14.785
Std. Error	104	4	
R^2	0.85		
F	395.6243	2.82	
df	11		
Residuals	-9.692	-2.265	

Step 4: Determination of density at capacity, capacity or maximum flow, and the speed at maximum using equation 5.12 as follows:

$$q = -0.8518k^2 + 94.489k - 14.785 \qquad R^2 = 0.85$$

By differentiating q with respect to k,

$$\frac{\partial q}{\partial k} = 2 * -0.8518\text{k} + 94.489 = 0$$

$$k_{crt} = k_Q = 55.4pce/km \approx 55\, pce/km$$

By plugging the critical density k_Q into equation 5.12 the capacity is calculated and is given by:

$$Q = q_{SS001(peak)} = -0.8518(55)^2 + 94.489(55) - 14.785$$

$$Q = q_{SS001(peak)} = 2605.4pce/hr \approx 2605pce/hr$$

By substituting k_{crt} and the estimated Q into the fundamental diagram equation $q = uk$, the speed at capacity is therefore obtained as:

$$u_Q = \frac{q}{k} = \frac{2605}{55} \approx 47km/hr$$

Hence the capacity or maximum flow is $2605pce/hr$, with a corresponding speed at capacity $u_Q = 47km/hr$.

Step 5: The estimated capacity $Q \approx 2605pce/hr$ can be approximated to $2700pce/hr$ and

split into five capacity Utilization levels for the LCU criteria table. As stated earlier, the capacity Utilization levels are designated as (A to E), where LCU A is the best roadway capacity Utilization and LCU E, is the worst. therefore,

Level A (100%) = 2700 pce/hr

Level B (85%) = $0.85 * 2700 = 2295 pce/hr \approx 2400 pce/hr$

Level C (75%) = $0.75 * 2700 = 2025 pce/hr \approx 2100 pce/hr$

Level D (50%) = $0.50 * 2700 = 1350 pce/hr \approx 1400 pce/hr$

Level E (25%) = $0.25 * 2700 = 675 pce/hr \approx 700 pce/hr$

Step 6: From the model equation above, speed is evenly distributed between its free-flow speed of 94.489km$/hr \approx 95 km/hr$ for class E and speed at capacity of $47 km/hr \approx 50 km/hr$ for class A. The speed is used to compute the attendant densities and their corresponding time for 1km of roadway, and subsequently, the LCU criteria table is developed. Thus, the LCU criteria table for SS003 is presented in table 5.24.

Table 5. 24**:** LCU Criteria Table for SS003

LCU	Qu %	Flow (Q) veh/h	Density (k) veh/km/lane	Speed(u) km/hr
A	86 - 100	2700	54	50
B	76 - 85	2400	37	65
C	51 - 75	2100	28	75
D	26 - 50	1400	16	85
E	0 - 25	700	7	95

5.5.2 BRT Dedicated Lane Capacity Utilization for Site SS003

Step 1. Estimation of five-minute BRT traffic volume using SANRAL's standard PCE values for heavy vehicle class as shown in table 5.25 below.

Table 5. 25**:** BRT Dedicated Lane Level of Capacity Utilization Parameters

Period	BRT 1	BRT 2	u 3	k 4	k 5	q 6	q 7
		1*3		6/3	7/3	1*12	2*12
1	4	12	64	1	2	48	144
2	2	6	63	0	1	24	72
3	3	9	66	1	2	36	108
4	2	6	70	0	1	24	72
5	3	9	64	1	2	36	108
6	1	3	61	0	1	12	36
7	3	9	70	1	2	36	108
8	2	6	63	0	1	24	72
9	4	12	63	1	2	48	144
10	3	9	69	1	2	36	108
11	2	6	65	0	1	24	72
12	4	12	61	1	2	48	144
1hr	33		65±1			33	99

1, 2, ...8 ~ column numbers, column 1 ~ volume by 5mins, column 2 ~ BRT flow (pce/5mins), u ~ speed (km/hr), k4 ~ density (veh/km), k5 ~ density (pce/km) q6 ~ total flow(veh/hr), q7 ~ total flow(pce/hr) BRT ~ Bus Rapid Transit.

Step 2: Determination of BRT dedicated lane capacity:

The average speed of BRT Buses (at peak) $= 64.8 km\ per\ hr = 18\, m/s$

BRT Vehicle Length $= 18m;\ reaction\ time = 2.5s$ and correction factor $k = 1.5$

Using equation (3.4) the time headway was computed as:

$$T_h = \frac{18}{18} + 2.5 + \frac{1.5 \times 18}{2}\left(\frac{1}{2.5}\right) = 8.87s\ hence,$$

$$BRT\ Lane\ Capacity = {}^{3600}/_{8.87} = 406 veh/hr$$

Step 3: Estimation of capacity utilization rate for BRT:

Recall that capacity Utilization rate had been defined as the ratio of actual traffic flow levels (5min) to the maximum possible flow or capacity and expressed as a percentage, therefore $Q_u = {}^{99}/_{406} \times 100\% = 24.4 \approx 24\%$. Therefore, the level of capacity utilization based on the criteria table for SS003 BRT dedicated lane is **E.** With the LCU at E, the other associated performance parameters are a density of 7veh/km and a speed of 95km/hr. This implies that when there are fewer vehicles on a road, as is the case of BRT buses, the free-flow speed is high, and travel time decreases. The LCU **E** of the BRT dedicated lane shows that the Bus route is substantially underutilized, hence, the level of capacity utilization is poor.

5.5.3 'Without BRT' Influence Capacity Utilization for Site SS003

Step 1: Estimation of off-peak 5mins and hourly flows, speeds, and densities for site SS003 using the empirical data in chapter 4, shown in Table 5.26 below:

Table 5. 26: Without BRT level of Capacity Utilization Parameters for SS003 (off – peak)

Period	PC	MV	HV	Vol	MV	HV	*q*	*u*	*k*	*q*
	1	*2*	*3*	*4*	*5*	*6*	*7*	*8*	*9*	*10*
					*2*1.75*	*3*3*	*1 + 5 + 6*		10/8	7*12
1	72	8	2	82	14	6	92	80	14	1104
2	68	7	2	77	12	6	86	73	14	1032
3	72	4	4	80	7	12	91	75	15	1092
4	65	5	2	72	9	6	80	74	13	960
5	62	9	3	74	16	9	87	75	14	1044
6	65	8	3	76	14	9	88	78	14	1056
7	63	5	2	70	9	6	78	74	13	936
8	70	4	4	78	7	12	89	73	15	1068
9	67	4	3	74	7	9	83	78	13	996
10	69	6	4	79	11	12	92	74	15	1104
11	73	11	3	87	19	9	101	75	16	1212
12	67	4	10	81	7	30	104	73	17	1248
1hr	813						1071	75±1		1071

1, 2, 3…10 ~ column numbers, column 1 - 4 ~ volume by 5mins, columns 5 - 7 ~ flow (pce/5mins), column 10 ~ total flow(pce/h), u ~ speed (km/hr), k ~ density (pce/km), PC ~ passenger car, MV ~ medium vehicle, HV ~ heavy vehicle

Step 2. Calibration of flow-density model using the density and flow parameters in Table 5.20. with PCEs applied. Figure 5.11 shows the graphical representation of the flow-density relationship:

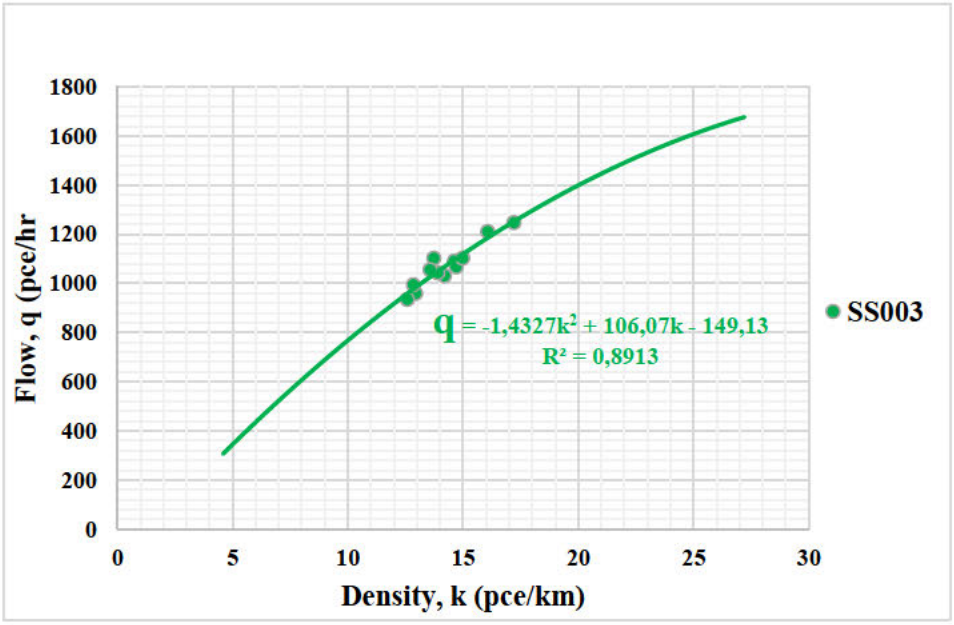

Figure 5. 11: Without BRT Influence Flow-Density Curve for site SS003 (Off-Peak)

The calibrated flow-density model is given as equation 5.10:

$$q_{withoutBRT(off-peak)} = -1.4327k^2 + 106.07k - 149.13 \quad R^2 = 0.89 \; 5.13$$

Step 3: Statistical testing of the calibrated model for validity. Table 5.27 below shows the results of the validity test carried out on the off-peak flow-density model for site SS003 without BRT influence. As shown, the coefficients of the derived model have the anticipated sign conventions for concavity, while the coefficient of determination $R^2 = 0.8913$ is greater than 0.5, which indicates the existence of a strong relationship between density and flow, and the capability of predicting capacity. It is important to note that the coefficient of "k" denotes the free-flow speed of roughly 106 km/hr. The aggregated model was subsequently used to predict capacity, estimate density at capacity, and speed at capacity in step 4 by differentiating *q* with respect to *k* and feeding back necessary values.

Table 5. 27**:** Level of Capacity Utilization Model Validity Tests

	q	*k*	Constant
t' values	40.4	2.2	
Coefficients	-1.4327	106.07	149.13
Std. Error	26	1	
R^2	0.89		
F	5467.03	2.82	
df	11		
Residuals	-9.397	-2.603	

Step 4: The density at capacity, capacity or maximum flow, and the speed at maximum flow were determined using equation 5.13 as follows:

$$q_{withoutBRT(off-Peak)} = -1.4327k^2 + 106.07k - 149.13 \quad R^2 = 0.89$$

By differentiating q with respect to k,

$$\frac{\partial q}{\partial k} = 2 * 1{,}4327\text{k} + 106{,}07 = 0$$

$$k_{crt} = k_Q = 37.02pce/km \approx 37\, pce/km$$

By plugging the critical density k_Q into equation 5.20 the capacity is calculated and is given by:

$$Q = q_{2021(peak)} = -1{,}4327(37)^2 + 106{,}07(37) - 149{,}13$$

$$Q = q_{2021(off-peak)} = 1814.09pce/hr \approx 1814pce/hr$$

By substituting k_{crt} and the estimated Q into the fundamental diagram equation $q = uk$, the speed at capacity is therefore obtained as:

$$u_Q = \frac{q}{k} = \frac{1814}{37} = 49.03 \approx 49km/hr$$

Hence the capacity or maximum flow at off-peak traffic period is $1814pce/hr$, with a corresponding speed at capacity $u_Q = 49km/hr$. As shown in table 5.12 above, the mean flow per hour which represents the 12 period flows for site SS002 is 1071 pce/hr, therefore the capacity utilization rate Q_u for site SS002 is ${}^{1071}/_{1814} \times 100\% \approx 59\%$. Therefore, based on the criteria table 5.18, the LCU for site SS002 without BRT influence is C. Where the LCU is at C, the other attendant performance parameters from the table are a density of 28veh/km and a speed of 75km/hr. In comparison with the LCU of the BRT dedicated lane at E, it can be observed that at level C, there is an associated reduction in speed, as well as an increase in density. Besides, the LCU of the adjoining lanes at C shows that the capacity utilization is better due to the traffic mix on those lanes which comprise passenger cars, medium vehicles, and a few heavy vehicles in different proportions; whereas the BRT dedicated lane is used by only one vehicle class which are the BRT buses.

5.5.4 With BRT Influence Capacity Utilization for Site SS003

Step 1: Estimation of 'with BRT' off-peak 5mins and hourly flows, speeds, and densities for site SS003 is shown in table 5.28. Note that the BRT flows with applied PCEs were added to the without BRT traffic flows from table 5.24.

Table 5. 28**:** With BRT level of Capacity Utilization Parameters for SS003 (off – peak)

Period	PC	MV	HV	*BRT*	Vol	MV	HV	*BRT*	q	μ	k	q
	1	*2*	*3*	*4*	*5*	*6*	*7*	*8*	*8*	*10*	*11*	*12*
						*2*1.75*	*3*3*	*4*3*	*1 + 6 + 7+8*		12/10	7*12
1	72	8	2	4	86	14	6	12	104	82	15	1248
2	68	7	2	2	79	12	6	6	92	73	15	1104
3	72	4	4	3	83	7	12	9	100	73	16	1200
4	65	5	2	2	74	9	6	6	86	74	14	1032
5	62	9	3	3	77	16	9	9	96	75	15	1152
6	65	8	3	1	77	14	9	3	91	78	14	1092
7	63	5	2	3	73	9	6	9	87	75	14	1044
8	70	4	4	2	80	7	12	6	95	73	16	1140
9	67	4	3	4	78	7	9	12	95	77	15	1140
10	69	6	4	3	82	11	12	9	101	74	16	1212
11	73	11	3	2	89	19	9	6	107	75	17	1284
12	67	4	10	4	85	7	30	12	116	73	19	1392
1hr	813			33					1169	75±1		1169

1, 2, 3…10 ~ column numbers, column 1 - 4 ~ volume by 5mins, columns 5 -7 ~ flow (pce/5mins), column 10 ~ total flow(pce/h), u ~ speed (km/hr), k ~ density (pce/km), PC ~ passenger car, MV ~ medium vehicle, HV ~ heavy vehicle

Step 2. Calibration of the 'with BRT' flow-density model using the density and flow parameters in Table 5.22. with PCEs applied. Figure 5.12 shows the graphical representation of the flow-density relationship:

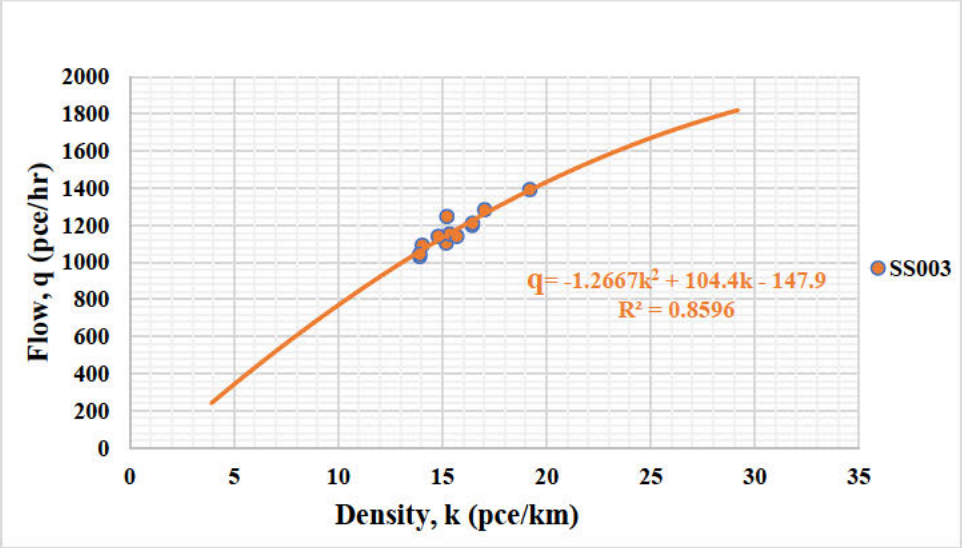

Figure 5. 12: With BRT Influence Flow-Density Curve for site SS002 (Off-Peak)

The calibrated flow-density model is given as equation 5.14:

$$q_{withBRT(off-peak)} = -1.2667k^2 + 104.4k - 147.49 \quad R^2 = 0.86 \quad 5.14$$

Step 3: Statistical testing of the calibrated model for validity. Table 5.29 below shows the results of the validity test carried out on the off-peak flow-density model for site SS003 with BRT influence. As shown, the coefficients of the derived model have the anticipated sign conventions for concavity, while the coefficient of determination $R^2 = 0.8596$ is greater than 0.5, which indicates the existence of a strong relationship between density and flow, and the capability of predicting capacity. It is important to note that the coefficient of "k" denotes the free-flow speed of roughly 104 km/hr. The aggregated model was subsequently used to predict capacity, estimate density at capacity, and speed at capacity in step 4 by differentiating q with respect to k and feeding back necessary values.

Table 5. 29: Level of Capacity Utilization Model Validity Tests

	q	k	Constant
t' values	39	2.2	
Coefficients	-1.2667	104.4	-147.49
Std. Error	30	1	
R^2	0.86		
F	5152.7	2.82	
df	11		
Residuals	-11.769	-1.2308	

Step 4: The density at capacity, capacity or maximum flow, and the speed at maximum flow were determined using equation 5.11 as follows:

$$q_{withBRT(off-Peak)} = -1.2667k^2 + 104.4k - 147.49 \quad R^2 = 0.85$$

By differentiating q with respect to k,

$$\frac{\partial q}{\partial k} = 2 * -1.2667k + 104.4 = 0$$

$$k_{crt} = k_Q = 41.2pce/km \approx 41\, pce/km$$

By plugging the critical density k_Q into equation 5.8 the capacity is calculated and is given by:

$$Q = q_{withBRT(off-peak)} = -1.2667(41)^2 + 104.4(41) - 147.49$$

$$Q = q_{withBRT(off-peak)} = 2003.18pce/hr \approx 2003pce/hr$$

By substituting k_{crt} and the estimated Q into the fundamental diagram equation $q = uk$, the speed at capacity is therefore obtained as:

$$u_Q = \frac{q}{k} = \frac{2003}{41} \approx 48km/hr$$

Hence, as expected, the capacity or maximum flow at off-peak traffic period is $2003pce/hr$, with a corresponding speed at capacity $u_Q = 48km/hr$. As shown in table 5.22 above, the mean 'with BRT' flow per hour which represents the 12 period flows for site SS003 is 1169 pce/hr, therefore the capacity utilization rate 'with BRT' influence Q_u for site SS003 is $^{1169}/_{2003} \times 100\% \approx 58\%$. Hence based on the criteria table 5.4, the LCU for site SS003 'with BRT' influence is C. Where the LCU is at C, the other attendant performance parameters from the table are a density of 21veh/km and a speed of 80km/hr.

5.5.5 Comparative Assessment of Capacity Utilization for Site SS003 Summary

Table 5.30 shows the 5mins off-peak capacity utilization rates and levels at site SS003 for the three scenarios.

Table 5. 30**:** Summary of Off-Peak Capacity Utilization Rates and Levels for SS003

Period	q BRT	q without BRT	q with BRT	Qu BRT (%)	Qu without BRT (%)	Qu with BRT (%)	LCU BRT	LCU without BRT	LCU With BRT
1	144	1104	1248	35	61	62	D	C	C
2	72	1032	1104	18	57	55	E	C	C
3	108	1092	1200	27	60	60	D	C	C
4	72	960	1032	18	53	52	E	C	C
5	108	1044	1152	27	58	58	D	C	C
6	36	1056	1092	9	58	55	E	C	C
7	108	936	1044	27	52	52	D	C	C
8	72	1068	1140	18	59	57	E	C	C
9	144	996	1140	35	55	57	D	C	C
10	108	1104	1212	27	61	61	D	C	C
11	72	1212	1284	18	67	64	E	C	C
12	144	1248	1392	35	69	69	D	C	C
1hr	99	1071	1170	24	59	58	E	C	C
	406	1814	2003						

5.5.5.1 Based on BRT Dedicated Lane Performance

The LCU E of the BRT dedicated lane shows that the Bus route is substantially underutilized, hence, the level of capacity utilization is poor. This is caused by the designation of the lane solely for BRT buses with no competition from other vehicle classes moving on the adjoining lanes. From this finding, and concerning the geometric characteristics of the BRT dedicated lane, coupled with vehicle characteristics, the LCU of the BRT lane may not improve from E. This is due to the observed width of the BRT dedicated lane of 4.3m. Besides, with a BRT vehicle width of 3.1m, only one bus can move on the dedicated lane at once, making it impossible for two buses to move side by side.

5.5.5.2 Based on Traffic Flowrate 'without BRT' Influence

In comparison with the LCU of the BRT dedicated lane at **E**, it can be observed that at level **C**, there is an associated reduction in speed, as well as an increase in density but increased travel time. Besides, the LCU of the adjoining lanes at **C** shows that the capacity utilization improves due to the traffic mix on those lanes which comprise passenger cars, medium vehicles, and a few heavy vehicles in different proportions; whereas the BRT dedicated lane is used by only one vehicle class which are the BRT buses.

5.5.5.3 Based on Traffic Flowrate 'with BRT' Influence

In comparison with the LCU without BRT influence, it can be observed that both are the same, as well as all parameters associated with that level. Although as expected, the maximum flow was higher, while the speed dropped. However, it may be expected that the level of capacity utilization would improve to level B. This outcome could have resulted from the poor utilization of the BRT dedicated lanes. In other words, this simply means that there is an insufficient number of BRT buses in the BRT transit scheme, as the mixed traffic scenario tested with BRT did not have a significant effect on traffic flow and capacity Utilization, every though there were observed increments in capacity utilization rates at first and ninth 5mins period flows. Nevertheless, in comparison with the LCU on the BRT dedicated lane, there was a speed reduction, as well as an increase in density and travel time. Overall, the LCU C with BRT influence at site SS003 shows that the capacity utilization can be significantly enhanced by mixed traffic scenarios as against having a BRT dedicated lane, especially one with a median configuration design.

5.5.6 Summary of Capacity Differentials – SS003

In summary, a criteria table has been developed for the assessment of traffic flow performance under different flow scenarios such as roadway with BRT, roadway without BRT, and BRT dedicated lane only. Sequel to the comparisons and synthesis of evidence that have emerged from the analysis, the different levels of capacity Utilization for the various scenarios considered are caused by differentials in germane traffic flow parameters such as capacity, speed, density, and travel time. Figure 5.13 below gives a pictorial description of the traffic characteristics differentials that are responsible for the traffic flow performance and Levels of capacity Utilization observed at site SS003.

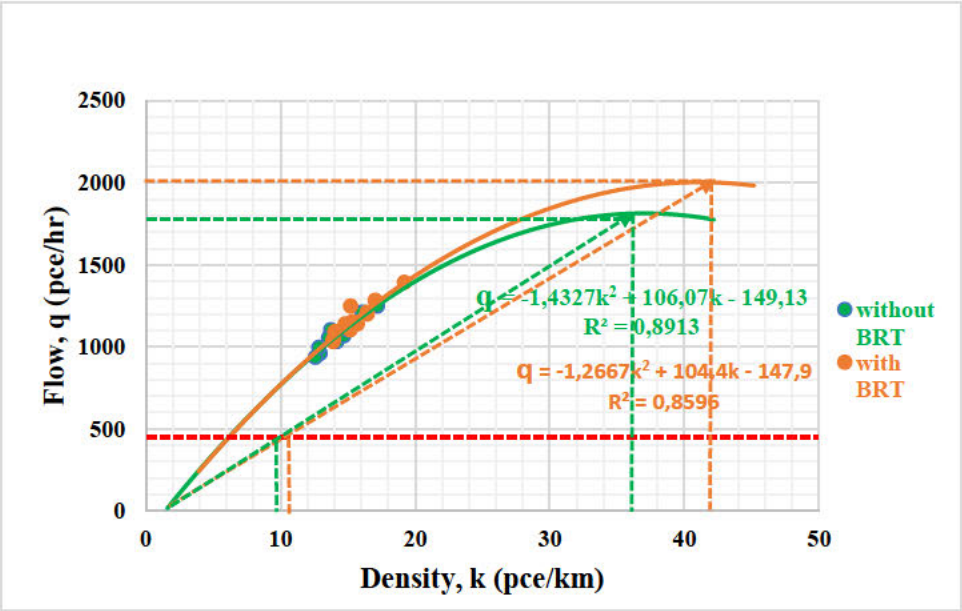

Figure 5. 13: Capacity Differentials at site SS003

From the arguments raised in chapter two and the hypothesis put forward in this regard, it can be observed from Figure 5.9 under steady flow conditions that the capacity Q_1 of roadway with BRT, indicated by the yellow line is $2003pce/hr$, capacity Q_2 of roadway without BRT, indicted by the green line is $1814pce/hr$, and BRT dedicated lane capacity Q_3, indicated by the red line is 391pce/hr. The corresponding speed at capacity of the roadway with BRT is $48km/hr$, the speed at capacity of the roadway without BRT is $49km/hr$. Similarly, the corresponding density at capacity k_1 of roadway with BRT is $41pce/km$, density at capacity k_2 of roadway without BRT is $37pce/km$. Likewise, the BRT dedicated lane density k_{31} based on travel speed with the influence of BRT is approximately $10veh/km$, while the BRT dedicated lane density k_{32} based on travel speed without the influence of BRT is approximately $8veh/km$. Table 5.31 shows the summary of capacity Utilization rates and levels, as well as the associated traffic characteristics differentials for site SS003.

Table 5. 31**:** Summary of capacity Utilization and traffic characteristics differentials for SS003

S/N	Roadway Condition	u_f	Q			U		K				Q_u (%)	LCU
			Q_1	Q_2	Q_3	u_1	u_2	k_1	k_2	k_{31}	k_{32}		
SS003	with BRT	104	2003	1814	406	48	49	41	35	10	8	58	C
	without BRT	106										59	C
	BRT Dedicated Lane	60										24	E

u_f ~ free-flow speed (km/hr),Q_1 ~ capacity with BRT(pce/hr), Q_2 ~ capacity without BRT(pce/hr), Q_3 ~ BRT capacity(veh/hr), u_1 ~ speed at capacity with BRT(km/hr), u_2 ~ speed at capacity without BRT(km/hr), k_1 ~ density at capacity with BRT (pce/km), k_2 ~ density at capacity without BRT (pce/km), ~ k_{31} ~ dedicated lane density with BRT (pce/km), k_{32} ~ dedicated lane density without BRT (pce/km), Q_u ~ capacity Utilization rate (%), LCU ~ level of capacity Utilization

5.6 Site SS004 Capacity Utilization

5.6.1 Capacity Utilization Criteria Table for SS004

Step 1. Analysis of empirical data in Table 5.32.

Table 5. 32: Level of Capacity Utilization (LCU) Parameters – SS004(Peak)

	PC	MV	HV	Vol	MV	HV	*q*	*u*	*k*	*q*
Period	*1*	*2*	*3*	*4*	*5*	*6*	*7*	*8*	*9*	*10*
					*2*1.75*	*3*3*	*1 + 5 + 6*		*10/8*	*7*12*
1	142	5	7	154	9	21	172	72	29	2061
2	122	9	2	133	16	6	144	74	23	1725
3	108	7	5	120	12	15	135	75	22	1623
4	138	7	4	149	12	12	162	73	27	1947
5	107	8	3	118	14	9	130	78	20	1560
6	141	4	5	150	7	15	163	74	26	1956
7	120	5	2	127	9	6	135	69	23	1617
8	132	6	2	140	11	6	149	67	27	1782
9	135	7	2	144	12	6	153	68	27	1839
10	127	7	5	139	12	15	154	69	27	1851
11	139	4	4	147	7	12	158	65	29	1896
12	146	5	3	154	9	9	164	65	30	1965
1hr	1557						1819	71±1		1819

1, 2, 3…10 ~ column numbers, column 1 - 4 ~ volume by 5mins, columns 5 - 7 ~ flow (pce/5mins), q ~ total flow(pce/hr), u ~ speed (km/hr), k ~ density (pce/km), PC ~ passenger car, MV ~ medium vehicle, HV ~ heavy vehicle

Step 2. Calibration of flow-density model using the LCU parameters in table 5.24. Figure 5.14 shows the graphical representation of the flow-density relationship.

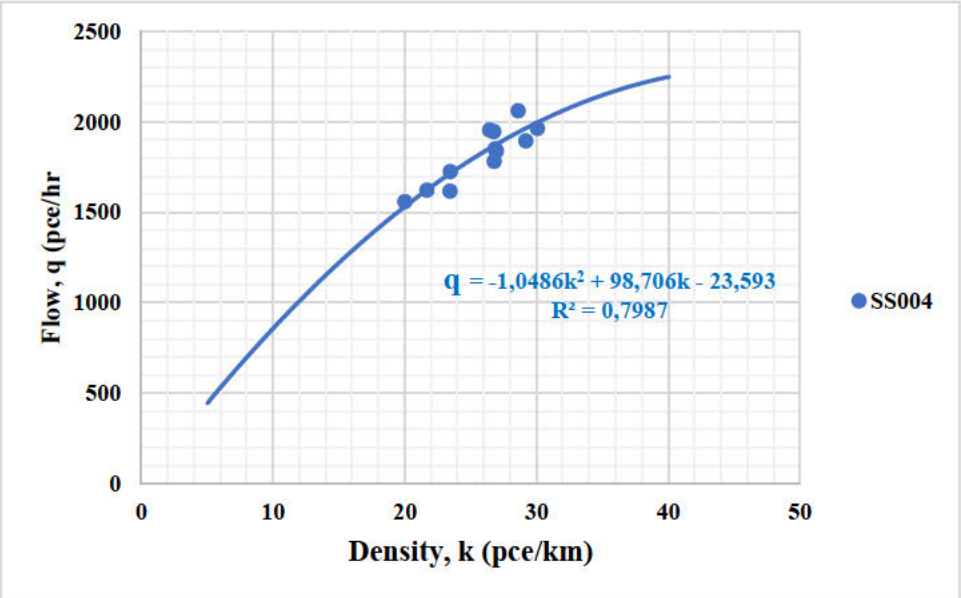

Figure 5. 14: Traffic Flow-Density (F-D) Curve for SS004(Peak) - Control

The model equation is given as equation 5.15.

$$q_{SS004(Control)} = -1.0486k^2 + 98.706k - 23.593 \quad R^2 = 0.79 \qquad 5.15$$

Step 3: Statistical testing of the calibrated model for validity. Table 5.33 below shows the results of the validity test carried out on the model for site SS004 without BRT influence.

Table 5. 33: Level of Capacity Utilization Model Validity Tests

	q	*k*	Constant
t' values	39.7	2.2	
Coefficients	-1.0486	98.706	-25.593
Std. Error	46	1	
R^2	0.79		
F	2590.3	2.82	
df	11		
Residuals	-9.743	-2.276	

Step 4: Determination of density at capacity, capacity or maximum flow, and the speed at maximum using equation 5.15 as follows:

$$q_{SS004(Control)} = -1.0486k^2 + 98.706k - 23.593 \quad R^2 = 0.79$$

By differentiating q with respect to k,

$$\frac{\partial q}{\partial k} = 2 * -1{,}0486\text{k} + 98{,}706 = 0$$

$$k_{crt} = k_Q = 47.07 pce/km \approx 47\ pce/km$$

By plugging the critical density k_Q into equation 5.23 the capacity is calculated and is given by:

$$Q = q_{SS004(Control)} = -1.0486(47)^2 + 98.706(47) - 23.593$$

$$Q = q_{SS004(Control)} = 2299.23 pce/hr \approx 2299 pce/hr$$

By substituting k_{crt} and the estimated Q into the fundamental diagram equation $q = uk$, the speed at capacity is therefore obtained as:

$$u_Q = \frac{q}{k} = \frac{2299}{47} \approx 49 km/hr$$

Hence the capacity or maximum flow is $2299 pce/hr$, with a corresponding speed at capacity $u_Q = 49 km/hr$.

Step 5: The estimated capacity $Q \approx 2299 pce/hr$ can be approximated to $2300 pce/hr$ and split into five capacity Utilization levels for the LCU criteria table. As stated earlier, the

capacity Utilization levels are designated as (A to E), where LCU A is the best roadway capacity Utilization and LCU E, is the worst. therefore,

Level A (100%) = 2300 pce/hr

Level B (85%) = $0.85 * 2300 = 1955 pce/hr \approx 2000 pce/hr$

Level C (75%) = $0.75 * 2300 = 1725 pce/hr \approx 1800 pce/hr$

Level D (50%) = $0.50 * 2300 = 1150 pce/hr \approx 1200 pce/hr$

Level E (25%) = $0.25 * 2300 = 575 pce/hr \approx 600 pce/hr$

Step 6: From the model equation above, speed is evenly distributed between its free-flow speed of 98.706km$/hr \approx 100 km/hr$ for class E and speed at capacity of $49 km/hr \approx 50 km/hr$ for class A. The speed is used to compute the attendant densities and their corresponding time for 1km of roadway, and subsequently, the LCU criteria table is developed. Thus, the LCU criteria table for SS004 is presented in table 5.34.

Table 5. 34**:** LCU Criteria Table for SS004

LCU	Qu %	Flow (Q) veh/h	Density (k) veh/km/lane	Speed(u) km/hr
A	86 - 100	2300	46	50
B	76 - 85	2000	29	70
C	51 - 75	1800	23	80
D	26 - 50	1200	13	90
E	0 - 25	600	6	100

5.6.2 BRT Dedicated Lane Capacity Utilization for Site SS004

Step 1. Estimation of five-minute BRT traffic volume using SANRAL's standard PCE values for heavy vehicle class as shown in table 5.35 below.

Table 5. 35**:** BRT Dedicated Lane Level of Capacity Utilization Parameters

Period	BRT 1	BRT 2	u 3	k 4	k 5	q 6	q 7
		1*3		6/3	7/3	1*12	2*12
1	3	9	52	1	2	36	108
2	4	12	81	0	1	48	144
3	4	12	65	1	2	48	144
4	4	12	72	0	1	48	144
5	4	12	70	1	2	48	144
6	2	6	61	0	1	24	72
7	4	12	73	0	2	48	144
8	4	12	70	0	1	48	144
9	2	6	61	1	2	24	72
10	4	12	73	0	2	48	144
11	2	6	73	0	1	24	72
12	1	3	68	1	2	12	36
1hr	38		68±2			38	114

1, 2, …8 ~ column numbers, column 1 ~ volume by 5mins, column 2 ~ BRT flow (pce/5mins), u ~ speed (km/hr), k4 ~ density (veh/km), k5 ~ density (pce/km) q6 ~ total flow(veh/hr), q7 ~ total flow(pce/hr) BRT ~ Bus Rapid Transit.

Step 2: Determination of BRT dedicated lane capacity:

The average speed of BRT Buses (at peak) $= 68.2km\ per\ hr = 18.94\,m/s$

BRT Vehicle Length $= 18m;\ reaction\ time = 2.5s$ and correction factor $k = 1.5$

Using equation (3.4) the time headway was computed as:

$$T_h = \frac{18}{18.94} + 2.5 + \frac{1.5 \times 18.94}{2}\left(\frac{1}{2.5}\right) = 9.12s\ hence,$$

$$BRT\ Lane\ Capacity = {}^{3600}/_{9.12} = 395veh/hr$$

Step 3: Estimation of capacity utilization rate for BRT:

Recall that capacity Utilization rate had been defined as the ratio of actual traffic flow levels (5min) to the maximum possible flow or capacity and expressed as a percentage, therefore $Q_u = {}^{114}/_{395} \times 100\% = 28.8 \approx 29\%$. Therefore, the level of capacity Utilization based on the criteria table for SS004 BRT dedicated lane is D. With the LCU at D, the other associated performance parameters are a density of 13veh/km and a speed of 90km/hr. This implies that when there are fewer vehicles on a road, as is the case of BRT buses, the free-flow speed is high, and travel time decreases. The LCU D of the BRT dedicated lane shows that the Bus route is substantially underutilized, hence, the level of capacity utilization is poor. However, it is better utilized than the other three sites.

5.6.3 'Without BRT' Influence Capacity Utilization for Site SS004

Step 1: Estimation of off-peak 5mins and hourly flows, speeds, and densities for site SS004 using the empirical data in chapter 4, shown in Table 5.36 below:

Table 5. 36: Without BRT level of Capacity Utilization Parameters for SS004 (off-peak)

Period	PC	MV	HV	Vol	MV	HV	*q*	*u*	*k*	*q*
	1	*2*	*3*	*4*	*5*	*6*	*7*	*8*	*9*	*10*
					*2*1.75*	*3*3*	*1 + 5 + 6*		10/8	7*12
1	76	6	4	86	11	12	99	76	16	1182
2	66	5	5	76	9	15	90	73	15	1077
3	52	0	2	54	0	6	58	77	9	696
4	83	5	5	93	9	15	107	78	16	1281
5	97	5	5	107	9	15	121	67	22	1449
6	68	7	3	78	12	9	89	73	15	1071
7	56	6	2	64	11	6	73	75	12	870
8	82	7	6	95	12	18	112	73	18	1347
9	71	9	0	80	16	0	87	76	14	1041
10	75	9	3	87	16	9	100	71	17	1197
11	99	3	6	108	5	18	122	75	19	1467
12	71	4	1	76	7	3	81	72	14	972
1hr	896			1004			1138	74±1		1138

1, 2, 3...10 ~ column numbers, column 1 - 4 ~ volume by 5mins, columns 5 - 7 ~ flow (pce/5mins), column 10 ~ total flow(pce/h), u ~ speed (km/hr), k ~ density (pce/km), PC ~ passenger car, MV ~ medium vehicle, HV ~ heavy vehicle

Step 2. Calibration of flow-density model using the density and flow parameters in Table 5.28. with PCEs applied. Figure 5.12 shows the graphical representation of the flow-density relationship:

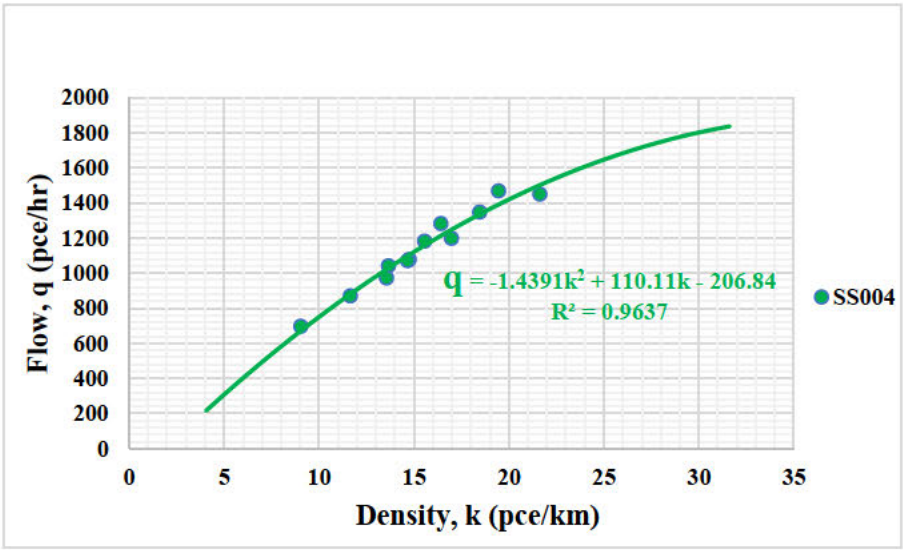

Figure 5. 15: Without BRT Influence Flow-Density Curve for site SS004 (Off-Peak)

The calibrated flow-density model is given as equation 5.16:

$$q_{withoutBRT(off-peak)} = -1.4391k^2 + 110.11k - 206.84 \quad R^2 = 0.96 \quad 5.16$$

Step 3: Statistical testing of the calibrated model for validity. Table 5.37 below shows the results of the validity test carried out on the off-peak flow-density model for site SS004 without BRT influence.

Table 5. 37**:** Level of Capacity Utilization Model Validity Tests

	q	*k*	Constant
t' values	17.1	2.2	
Coefficients	-1.4391	110.11	-206.84
Std. Error	67	1	
R^2	0.96		
F	4774.5	2.82	
df	11		
Residuals	-10.693	-3.247	

Step 4: The density at capacity, capacity or maximum flow, and the speed at maximum flow were determined using equation 5.16 as follows:

$$q_{withoutBRT(off-Peak)} = -1.4391k^2 + 110.11k - 206.84 \quad R^2 = 0.96$$

By differentiating q with respect to k,

$$\frac{\partial q}{\partial k} = 2 * -1.4391\text{k} + 110.11 = 0$$

$$k_{crt} = k_Q = 38.3pce/km \approx 38\, pce/km$$

By plugging the critical density k_Q into equation 5.16 the capacity is calculated and is given by:

$$Q = q_{withoutBRT(off-Peak)} = -1.4391(38)^2 + 110.11(38) - 206.84$$

$$Q = q_{withoutBRT(off-Peak)} = 1899.28pce/hr \approx 1899pce/hr$$

By substituting k_{crt} and the estimated Q into the fundamental diagram equation $q = uk$, the speed at capacity is therefore obtained as:

$$u_Q = \frac{q}{k} = \frac{1899}{38} = 49.9 \approx 50km/hr$$

Hence the capacity or maximum flow at off-peak traffic period is $1899pce/hr$, with a corresponding speed at capacity $u_Q = 50km/hr$. As shown in Table 5.28 above, the mean flow per hour which represents the 12 period flows for site SS004 is 863 pce/hr, therefore the

capacity utilization rate Q_u for site SS004 is $^{1138}/_{1899} \times 100\% = 59.9 \approx 60\%$. Therefore, based on the criteria table 5.34, the LCU for site SS004 without BRT influence is C. Where the LCU is at C, the other attendant performance parameters from the table are a density of 23veh/km, and a speed of 80km/hr.

5.6.4 'With BRT' Influence Capacity Utilization for Site SS004

Step 1: Estimation of 'with BRT' off-peak 5mins and hourly flows, speeds, and densities for site SS004 is shown in table 5.38. Note that the BRT flows with applied PCEs were added to the without BRT traffic flows from table 5.36.

Table 5. 38: With BRT level of Capacity Utilization Parameters for SS004 (off-peak)

Period	PC	MV	HV	*BRT*	Vol	MV	HV	*BRT*	q	μ	k	q
	1	*2*	*3*	*4*	*5*	*6*	*7*	*8*	*8*	*10*	*11*	*12*
						*2*1.75*	*3*3*	*4*3*	*1 + 6 + 7+8*		12/10	7*12
1	76	6	4	3	89	11	12	9	108	75	17	1296
2	66	5	5	4	80	9	15	12	102	73	17	1224
3	52	0	2	4	58	0	6	12	70	78	11	840
4	83	5	5	4	97	9	15	12	119	77	19	1428
5	97	5	5	4	111	9	15	12	133	67	24	1596
6	68	7	3	2	80	12	9	6	95	73	16	1140
7	56	6	2	4	68	11	6	12	85	75	14	1020
8	82	7	6	4	99	12	18	12	124	73	20	1488
9	71	9	0	2	82	16	0	6	93	71	16	1116
10	75	9	3	4	91	16	9	12	112	70	19	1344
11	99	3	6	2	110	5	18	6	128	75	20	1536
12	71	4	1	1	77	7	3	3	84	71	14	1008
1hr	896			38	1042				1252	73±1		1253

1, 2, 3…10 ~ column numbers, column 1 - 4 ~ volume by 5mins, columns 5 -7 ~ flow (pce/5mins), column 10 ~ total flow(pce/h), u ~ speed (km/hr), k ~ density (pce/km), PC ~ passenger car, MV ~ medium vehicle, HV ~ heavy vehicle

Step 2. Calibration of 'with BRT' flow-density model using the density and flow parameters in Table 5.38. with PCEs applied. Figure 5.16 shows the graphical representation of the flow-density relationship:

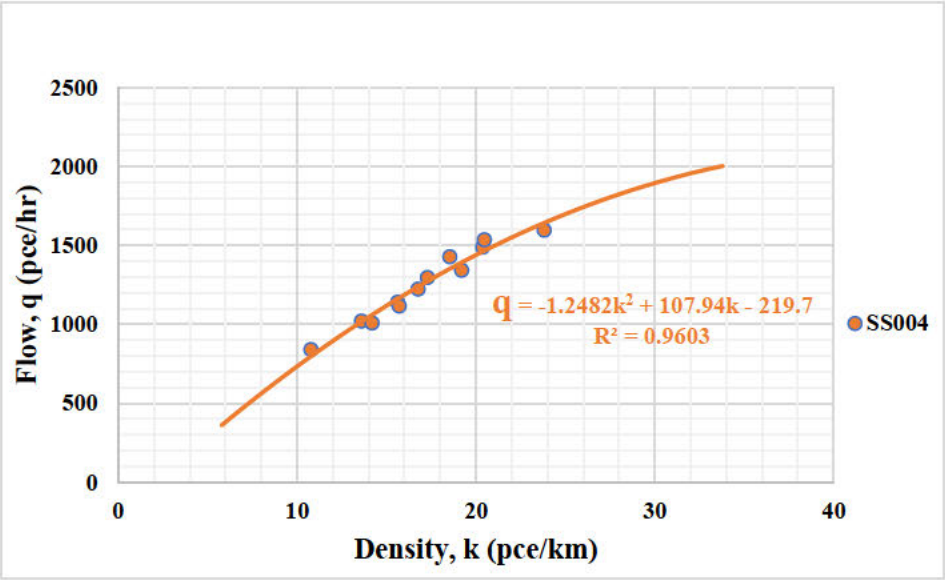

Figure 5. 16: With BRT Influence Flow-Density Curve for site SS004 (Off-Peak)

The calibrated flow-density model is given as equation 5.17:

$$q_{withBRT(off-peak)} = -1.2482k^2 + 107.94k - 219.7 \quad R^2 = 0.96 \qquad 5.17$$

Step 3: Statistical testing of the calibrated model for validity. Table 5.39 below shows the results of the validity test carried out on the off-peak flow-density model for site SS004 'with BRT' influence.

Table 5. 39: Level of Capacity Utilization Model Validity Tests

	q	*k*	Constant
t' values	18.4	2.2	
Coefficients	-1.2482	107.94	-219.7
Std. Error	71	1	
R^2	0.96		
F	4690.8	2.82	
df	11		
Residuals	-8.263	-2.699	

Step 4: The density at capacity, capacity or maximum flow, and the speed at maximum flow were determined using equation 5.17 as follows:

$$q_{withBRT(off-Peak)} = -1.2482k^2 + 107.94k - 219.7 \quad R^2 = 0.96$$

By differentiating q with respect to k,

$$\frac{\partial q}{\partial k} = 2 * -1.2482k + 107.94 = 0$$

$$k_{crt} = k_Q = 43.2pce/km \approx 43\, pce/km$$

By plugging the critical density k_Q into equation 5.17 the capacity is calculated and is given by:

$$Q = q_{withBRT(off-peak)} = -1.2482(43)^2 + 107.94(43) - 219.7$$

$$Q = q_{withBRT(off-peak)} = 2113.8pce/hr \approx 2114pce/hr$$

By substituting k_{crt} and the estimated Q into the fundamental diagram equation $q = uk$, the speed at capacity is therefore obtained as:

$$u_Q = \frac{q}{k} = \frac{2114}{43} = 49km/hr$$

Hence, as expected, the capacity or maximum flow at off-peak traffic period is $2114pce/hr$, with a corresponding speed at capacity $u_Q = 49km/hr$. As shown in table 5.22 above, the mean 'with BRT' flow per hour which represents the 12 period flows for site SS004 is 1253 pce/hr, therefore the capacity utilization rate 'with BRT' influence Q_u for site SS004 is ${}^{1253}/_{2113} \times 100\% = 59.2 \approx 59\%$. Hence based on the criteria table 5.4, the LCU for site SS003 'with BRT' influence is C. Where the LCU is at C, the other attendant performance parameters from the table are a density of 23veh/km and a speed of 80km/hr.

5.6.5 Comparative Assessment of Capacity Utilization for Site SS004 Summary

Table 5.40 shows the 5mins off-peak capacity Utilization rates and levels at site SS004 for the three scenarios.

Table 5. 40**:** Summary of Off-Peak Capacity Utilization Rates and Levels for SS004

Period	q BRT	q without BRT	q with BRT	Qu BRT (%)	Qu without BRT (%)	Qu with BRT (%)	LCU BRT	LCU without BRT	LCU With BRT
1	108	1182	1296	27	62	61	D	C	C
2	144	1077	1224	36	57	58	D	C	C
3	144	696	840	36	37	40	D	D	D
4	144	1281	1428	36	67	68	D	C	C
5	144	1449	1596	36	76	75	D	B	C
6	72	1071	1140	18	56	54	E	C	C
7	144	870	1020	36	46	48	D	D	D
8	144	1347	1488	36	71	70	D	C	C
9	72	1041	1116	18	55	53	E	C	C
10	144	1197	1344	36	63	64	D	C	C
11	72	1467	1536	18	77	73	E	B	C
12	36	972	1008	9	51	48	E	C	D
1hr	114	1138	1253	29	60	59	D	C	C
	395	1899	2114						

5.6.5.1 Based on BRT Dedicated Lane Performance

The LCU D of the BRT dedicated lane shows that the Bus route is substantially underutilized, hence, the level of capacity utilization is poor. This is caused by the designation of the lane solely for BRT buses with no competition from other vehicle classes moving on the adjoining lanes. From this finding, and concerning the geometric characteristics of the BRT dedicated lane, coupled with vehicle characteristics, the LCU of the BRT lane may not improve from D. This is due to the observed width of the BRT dedicated lane of 4.3m. Besides, with a BRT vehicle width of 3.1m, only one bus can move on the dedicated lane at once, making it impossible for two buses to move side by side.

5.6.5.2 Based on Traffic Flowrate 'without BRT' Influence

In comparison with the LCU of the BRT dedicated lane at D, it can be observed that at level C, there is an associated reduction in speed, as well as an increase in density but increased travel time. Besides, the LCU of the adjoining lanes at C shows that the capacity utilization improves due to the traffic mix on those lanes which comprise passenger cars, medium vehicles, and a few heavy vehicles in different proportions; whereas the BRT dedicated lane is used by only one vehicle class which are the BRT buses.

5.6.5.3 Based on Traffic Flowrate 'with BRT' Influence

In comparison with the LCU without BRT influence, it can be observed that both are the same, as well as all parameters associated with that level. Although as expected, the maximum flow was higher, while the speed dropped. However, it may be expected that the level of capacity utilization would improve to level B. This outcome could have resulted from the poor utilization of the BRT dedicated lanes. In other words, this simply means that there is an insufficient number of BRT buses in the BRT transit scheme, as the mixed traffic scenario tested with BRT did not have a significant effect on traffic flow and capacity utilization. Nevertheless, in comparison with the LCU on the BRT dedicated lane, there was a speed reduction, as well as an increase in density and travel time. Overall, the LCU C with BRT influence at site SS004 shows that the capacity utilization can be significantly enhanced by mixed traffic scenarios as against having a BRT dedicated lane, especially one with a median configuration design.

5.6.6 Summary of Capacity Differentials – SS004

In summary, a criteria table has been developed for the assessment of traffic flow performance under different flow scenarios such as roadway with BRT, roadway without BRT, and BRT dedicated lane only. Sequel to the comparisons and synthesis of evidence that have emerged from the analysis, the different levels of capacity utilization for the various scenarios considered are caused by differentials in germane traffic flow parameters such as capacity, speed, density, and travel time. Figure 5.17 below gives a pictorial description of the traffic characteristics differentials that are responsible for the traffic flow performance and Levels of capacity utilization observed at site SS004.

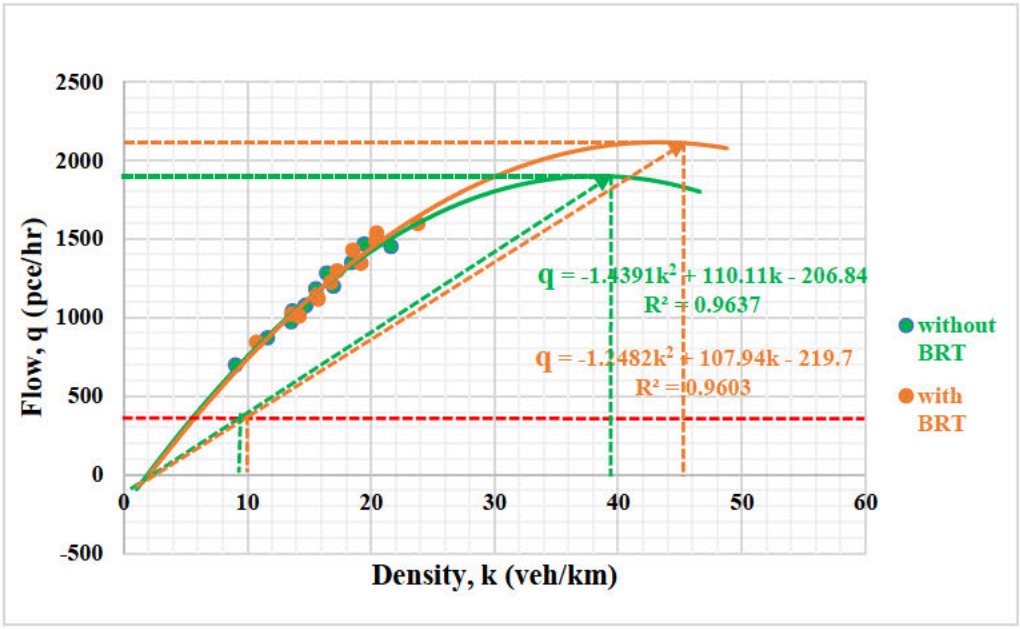

Figure 5. 17: Capacity Differentials at site SS004

From the arguments raised in chapter two and the hypothesis put forward in this regard, it can be observed from Figure 5.14 under steady flow conditions that the capacity Q_1 of roadway with BRT, indicated by the yellow line is $2114pce/hr$, capacity Q_2 of roadway without BRT, indicted by the green line is $1899pce/hr$, and BRT dedicated lane capacity Q_3, indicated by the red line is 395pce/hr. The corresponding speed at capacity of the roadway with BRT is $49km/hr$, the speed at capacity of the roadway without BRT is $50km/hr$. Similarly, the corresponding density at capacity k_1 of roadway with BRT is $43pce/km$, density at capacity k_2 of roadway without BRT is $38pce/km$. Likewise, the BRT dedicated lane density k_{31} based on travel speed with the influence of BRT is approximately $10veh/km$, while the BRT dedicated lane density k_{32} based on travel speed without the influence of BRT is approximately $9veh/km$. Table 5.41 shows the summary of capacity Utilization rates and levels, as well as the associated traffic characteristics differentials for site SS004.

Table 5. 41**:** Summary of capacity Utilization and traffic characteristics differentials for SS004

S/N	Roadway Condition	u_f	Q			U		K				Q_u (%)	LCU
			Q_1	Q_2	Q_3	u_1	u_2	k_1	k_2	k_{31}	k_{32}		
SS004	with BRT	108	2114	1899	395	49	50	43	38	10	9	59	C
	without BRT	110										60	C
	BRT Dedicated Lane	60										29	D

u_f ~ free-flow speed (km/hr),Q_1 ~ capacity with BRT(pce/hr), Q_2 ~ capacity without BRT(pce/hr), Q_3 ~ BRT capacity(veh/hr), u_1 ~ speed at capacity with BRT(km/hr), u_2 ~ speed at capacity without BRT(km/hr), k_1 ~ density at capacity with BRT (pce/km), k_2 ~ density at capacity without BRT (pce/km), ~ k_{31} ~ dedicated lane density with BRT (pce/km), k_{32} ~ dedicated lane density without BRT (pce/km), Q_u ~ capacity Utilization rate (%), LCU ~ level of capacity Utilization

5.7 Summary

This chapter has analyzed and presented the Level of Capacity Utilization (LCU) of the roadway segments investigated in this study. To achieve this, a LCU criteria table that considers traffic flow and density as major determining factors of the traffic performance on a roadway was developed using the peak traffic data, and used to determine the LCU for each site, with and without BRT. Other associated traffic performance characteristics were speed and travel time, which were observed to change with respect to the traffic conditions considered. Prior to the determination of LCU at each site and other associated analyses, empirical traffic data from the survey was extracted and the standard PCE values were modified and from the results, the use of the standard PCE values from SANRAL was sustained due to the insignificant difference between the SANRAL values and the modified PCEs. Besides, Empirical data with PCEs applied were used to calibrate flow-density models for the prediction of capacity and determination of other capacity Utilization parameters.

Using the off-peak traffic data, the with and without BRT maximum flows were predicted using the quadratic capacity model equation that relates flow with density from the fundamental diagram approach. Furthermore, BRT flow rates were determined, which subsequently engendered the estimation of the 'with and without BRT' traffic scenarios. It can be observed from the tables that capacity utilization or the pattern of traffic flow in the vicinity of BRT is indeed characterized by high speed with a corresponding low flow rate and low speed with a corresponding high flowrate. In other words, as speed increases, capacity utilization decreases, and as speed decreases, the level of capacity utilization increases. It is noteworthy that density is directly proportional to flow under steady flow conditions, hence the more vehicles in the stream, the better the level of capacity utilization. It can also be observed from the tables that speed is inversely proportional to travel time, hence as speed increases, travel time decreases, and vice versa. The criteria tables were employed to evaluate the LCU of each site at peak traffic sequel to the determination of their capacity utilization rates at steady flow conditions, hence, the LCU results of the off-peak traffic scenario analyzed have clearly shown that the BRT corridor has substantially been underutilized in the vicinity of BRT dedicated lanes. The extent of observed capacity underutilization was shown by the with and without BRT situation considered, which revealed the capacity differentials, as well as differentials in other traffic characteristics with respect to capacity utilization.

It can be observed from the summary of the capacity and other capacity utilization parameters' differentials at each site, that the 'with BRT' scenario triggered an increase in capacity and density, and capacity utilization with a contrary decrease in speed. Although the differentials in the LCU between the 'without' and 'with' BRT traffic scenarios were not as significant as the LCU differential between the BRT dedicated lanes and the 'with and without' BRT scenario, the increase in capacity and attendant capacity differentials show that there may be implications on the time headway distribution on the adjoining lanes caused by the presence of BRT under the steady flow condition considered. It simply implies that there would be influx of more vehicles, especially the BRT buses into the mixed traffic 'without BRT' traffic stream. Therefore, by way of hypothesizing, will the merger of BRT buses on the dedicated lanes with vehicles on the adjoining lanes have any effect on the time headways of the mixed 'with BRT' stream? If yes, will the time headways increase or decrease in magnitude? The next chapter which discusses the time headway implications of the with and without BRT scenarios and provides answers to these queries through the stochastic modelling of the attendant time headway distributions.

CHAPTER 6

TIME HEADWAY IMPLICATIONS

6.1 Overview

In the previous chapter, the findings of the influence of BRT scenarios on levels of capacity utilization and their attendant implications on density, speed, and travel time differentials were presented. These differentials, estimated through the deterministic approach are caused by the presence of BRT dedicated lanes. As observed from the estimated capacity and other traffic characteristics differentials, the mixed traffic or 'with BRT traffic scenario which resulted in an increase in capacity, coupled with a corresponding increase in density (due to the influx of more vehicles into the stream), and a decrease in speed and travel time, will cause a reduction in time headways under the mixed traffic consideration.

Note that according to the Highway Capacity Manual (HCM) 2010, time headway had been referred to as "*the time between two successive vehicles as they pass a point on a lane or roadway, measured in seconds from the same point on each vehicle*" (HCM, 2010). Time headway in traffic flow modelling and planning is considered a relevant control parameter that affects the behaviour of drivers, and it particularly plays a major role in the estimation of roadway capacity (Moridpour, 2014). Time headway is a microscopic characteristic of flow that has also found useful application in the estimation of Passenger Car Units (PCUs), Level of Service (LOS) evaluations, analysis of safety, gap acceptance studies, and delay studies (Aderinlewo *et al*., 2020; J. Ben-Edigbe *et al*., 2014) It is a fundamental characteristic of the quality and quantity of traffic flow (Alhassan & Ben-Edigbe, 2012a), that describes the order in which a leading car and the one that follows it arrive at selected points on a roadway (Das & Maurya, 2017). Its analysis is one of the most important methods in traffic engineering, employed to understand the position of one vehicle relative to the other in a mixed traffic flow (Das & Maurya, 2017).

The empirical time headway distribution 'without BRT' captured by the ATCs was observed to follow certain probability distributions, hence the application of stochastic methodology. Consequently, the remainder of this chapter which presents the results and discussion on the stochastic approach employed is organized as follows: section 6.2 presents the fitting of probability distributions to the observed time headway data; section 6.3, discusses the hypothesis Testing and Performance of the Probability Distribution Models, and section 6.4

introduces the stepwise analytical framework for the statistical modelling of the time headways. In section 6.5, comments on the descriptive statistics of the time headway data are presented, while section 6.6 gives comments on the fitted probability distribution models. Section 6.7 presents comments on the hypothesis and performance of the probability distribution models, while section 6.8 gives comments on the model parameters. The summary of the chapter is presented in section 6.9.

6.2 Fitting of Probability Distribution Models to Observed Time Headway Data

As earlier stated, statistical models should be applied to fit time headway data to identify a suitable model for headway distribution. ModelRisk software, a Monte Carlo Simulation tool was employed to fit selected probability distributions to data, generate the attendant Probability Density Function (PDF), Cumulative Density Function (CDF), and Probability Plots (P-P), as well as carry out the hypothesis testing or goodness of fit tests. In this investigation, five distributions were fitted to the observed time headway data and were rated in the order in which they best fit the data. Recall that similarly, this approach had been tested in the pilot study using both peak and off-peak traffic flow scenarios. The subsequent analysis discussed in this section is with respect to the headway data of the BRT flow scenarios of the main study across the four sites.

6.3 Hypothesis Testing and Performance of the Probability Distribution Models

Sequel to the fitting of continuous probability distribution models to the observed time headway data, the fitted models should be tested to determine their performance and ultimately the distribution that provides the best fit. This section presents the hypothesis testing, also referred to as 'Goodness of Fit' tests of a continuous time series distribution, and used to confirm and determine whether a probability distribution is suitable for simulating a specific phenomenon. It will be recalled that the hypothesis to be tested was stated earlier which postulates that "*The compatibility of observed time headway distribution with fitted probability distribution model is rejected if* $(P-value < \alpha)$ *or accepted if* $(P-value > \alpha)$. Consequently, this test was carried out using the already defined Akaike Information Criterion (AIC), Schwarz Information Criterion (SIC), also known as Bayesian Information Criterion (BIC) and Hannan Quinn Information Criterion (HQIC), and the distribution which gives the smallest values of AIC, SIC, and HQIC is considered the best-fitted model. The test statistics of each of the performance indicators were computed at α = 5% (0.05) significance level and 95% level of confidence. The performance values of the AIC, SIC, and HQIC, as well as the

log-likelihood and P-values, are obtained from the report of the model fitting and directly from the plots respectively.

6.4 Analytical Framework for Statistical Modelling of Time Headway

The schematic flowchart of time headway analysis is illustrated in figure 6.1 below and the stepwise procedure employed for the pilot test was replicated in this analysis as follows:

Step 1: Recall empirical traffic volume data from chapter four, extracted from the ATC, and determine the descriptive statistics of its headway.

Step 2: Fit continuous probability distributions to the headway distribution data and plot the joint PDF, CDF, and P-P plots of each fitted probability distribution model examined for each site and evaluate the statistical results of the model fitting.

Step 3: Carry out the hypothesis testing of the fitted distribution or goodness of fit tests on the models using the Akaike Information Criterion (AIC), Schwarz Information Criterion (SIC), and Hannan Quinn Information Criterion (HQIC) as described in the methodology.

Step 4: Calculate the P-value for each distribution at 95% confidence and 5% significance levels respectively. The higher the P-value and the more it exceeds 0.05 in all three tests at a 5 percent level of significance, the more compatible the model.

Step 5: Select the model that best fits the data based on the smallest AIC value and the largest Loglikelihood (LLH) value. Use the P-value obtained in step 4 and according to the criterion, accept or reject the stated hypothesis.

Step 6: Compare the model parameters as well as the mean time headway of the fitted empirical data with the mixed traffic time headway data and evaluate the outcomes with respect to capacity utilization of the study site.

Figure 6.1 shows the schematic flowchart of the time headways implications analysis.

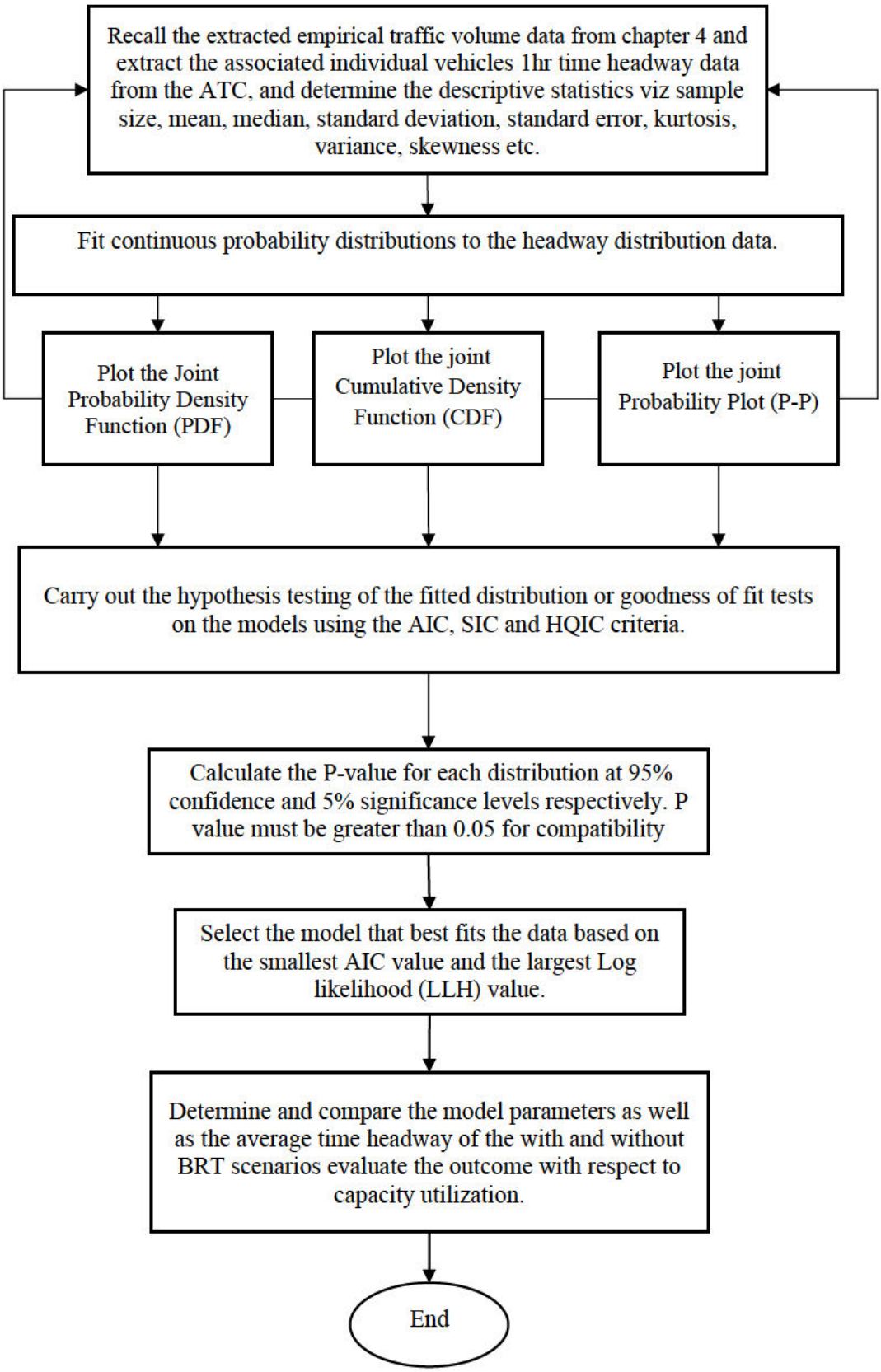

Figure 6. 1: Schematic Flowchart of Time Headway Analysis

6.4.1 Statistical Modelling of Time Headway Data for Site SS001

Step 1: Determination of Descriptive Statistics of Peak Traffic Headway Distribution Data

Recall the extracted empirical hourly traffic volume data shown in Table 4.2, chapter 4 and extract the associated individual vehicles' 1hr time headway distribution data from the ATC. Hence determine the descriptive statistics viz sample size, mean, median, standard deviation, standard error, kurtosis, variance, and skewness. Table 6.1 shows the descriptive statistics of the observed time headways for site SS001 at peak.

Table 6. 1: Descriptive Statistics of the Time Headways – SS001 (Peak)

Descriptive Statistics	SS001
Mean	2.930313901
Standard Error	0.111690434
Median	1.8
Mode	1
Standard Deviation	3.729524037
Coefficient of Variation	1.29
Sample Variance	13.90934954
Kurtosis	21.98952129
Skewness	3.969629326
Range	39.8
Minimum	0.2
Maximum	40
Sum	3267.3
Sample Size	1115

Step 2: Fitting of continuous probability distribution models to headway data

Using the Model Risk software, probability models were fitted to the headway data, and the PDF, CDF, P-P plots and the P-value with its plot of the best-fitted distribution were generated from the software. Figures 6.2, 6.3, 6.4, and 6.5 show the PDF, P-P, CDF, and P-Value plots respectively.

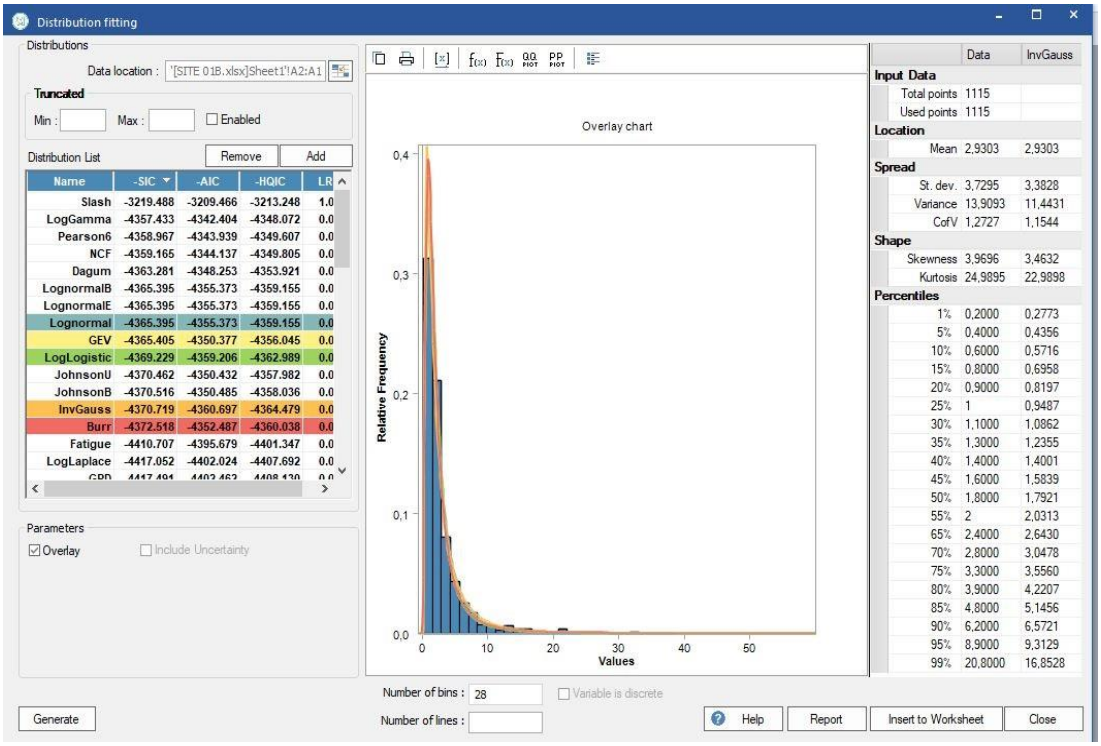

Figure 6. 2: PDF Plot for SS001 (Peak)

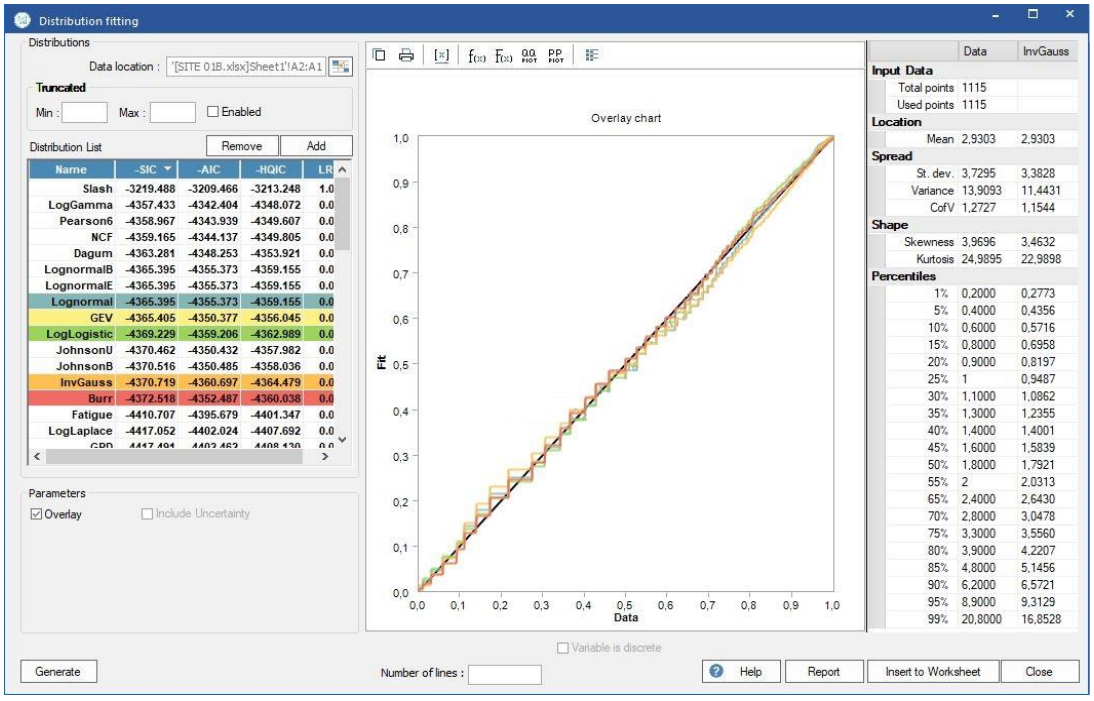

Figure 6. 3: P-P Plot for SS001 (Peak)

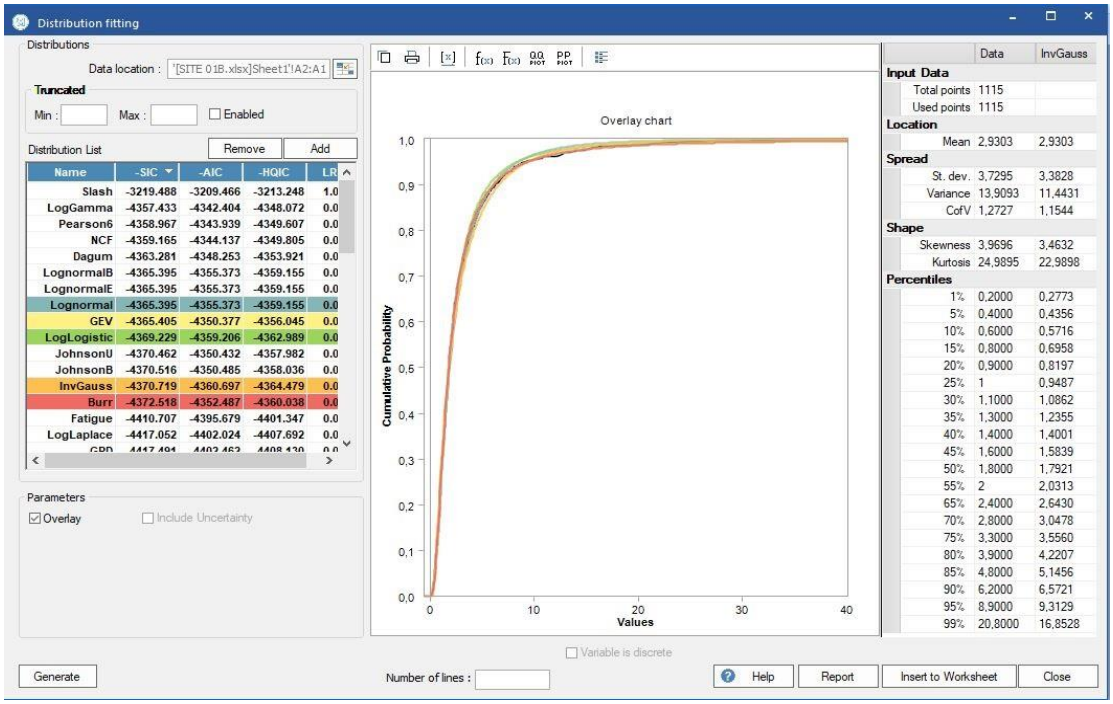

Figure 6. 4: CDF Plot for SS001 (Peak)

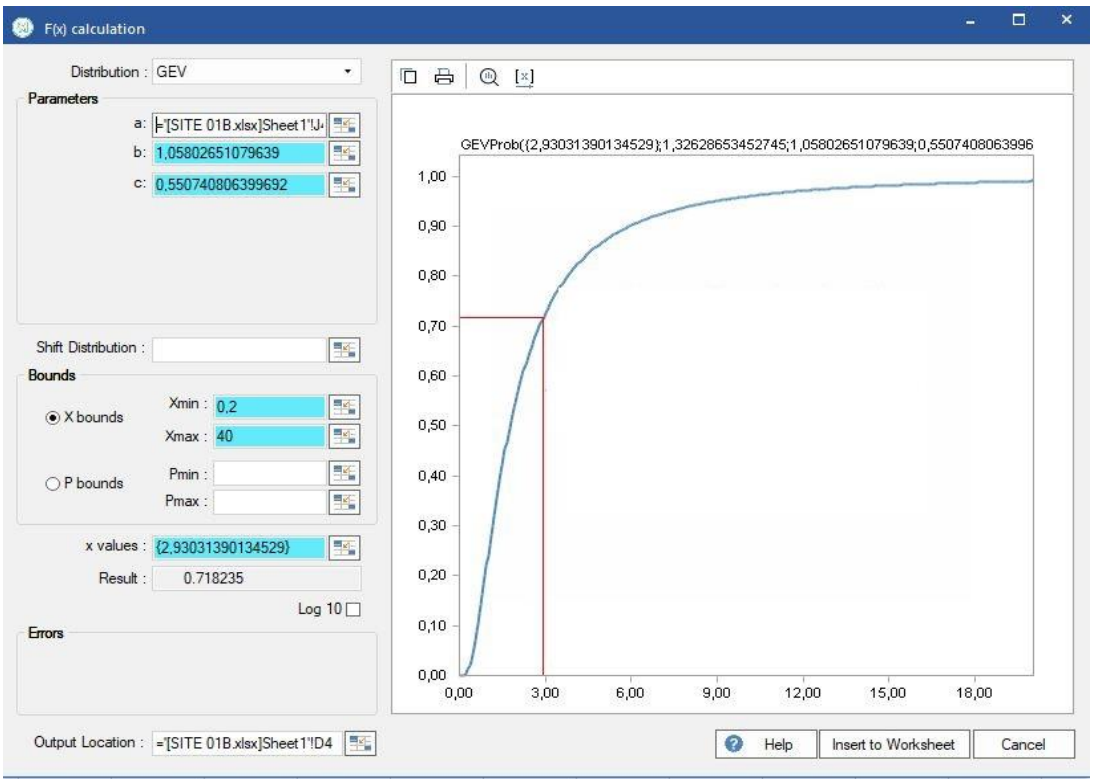

Figure 6. 5: P-Value Plot for SS001 (Peak)

Step 3: Analysis of **Off- Peak** Traffic Headway Distribution Data

Recall the extracted empirical hourly traffic volume data shown in Table 4.3, chapter 4, and extract the associated individual vehicles' 1hr time headway distribution data from the ATC. Hence determine the descriptive statistics viz sample size, mean, median, standard deviation, standard error, kurtosis, variance, and skewness. Table 6.2 shows the descriptive statistics of the observed time headways for site SS001 at off-peak.

Table 6. 2: Descriptive Statistics of the Time Headways – SS001 (Off-Peak)

Descriptive Statistics	SS001
Mean	3.61577381
Standard Error	0.164384644
Median	1.9
Mode	1
Standard Deviation	5.219050658
Coefficient of Variation	1.47
Sample Variance	27.23848977
Kurtosis	23.87798607
Skewness	4.199696492
Range	53.2
Minimum	0.2
Maximum	53.4
Sum	3644.7
Sample Size	1008

Step 4: Fitting of continuous probability distribution models to headway data

Using the Model Risk software, probability models were fitted to the headway data, and the PDF, CDF, P-P plots and the P-value with its plot of the best-fitted distribution were generated from the software. Figures 6.6, 6.7, 6.8, and 6.9 show the PDF, P-P, CDF, and P-Value plots respectively.

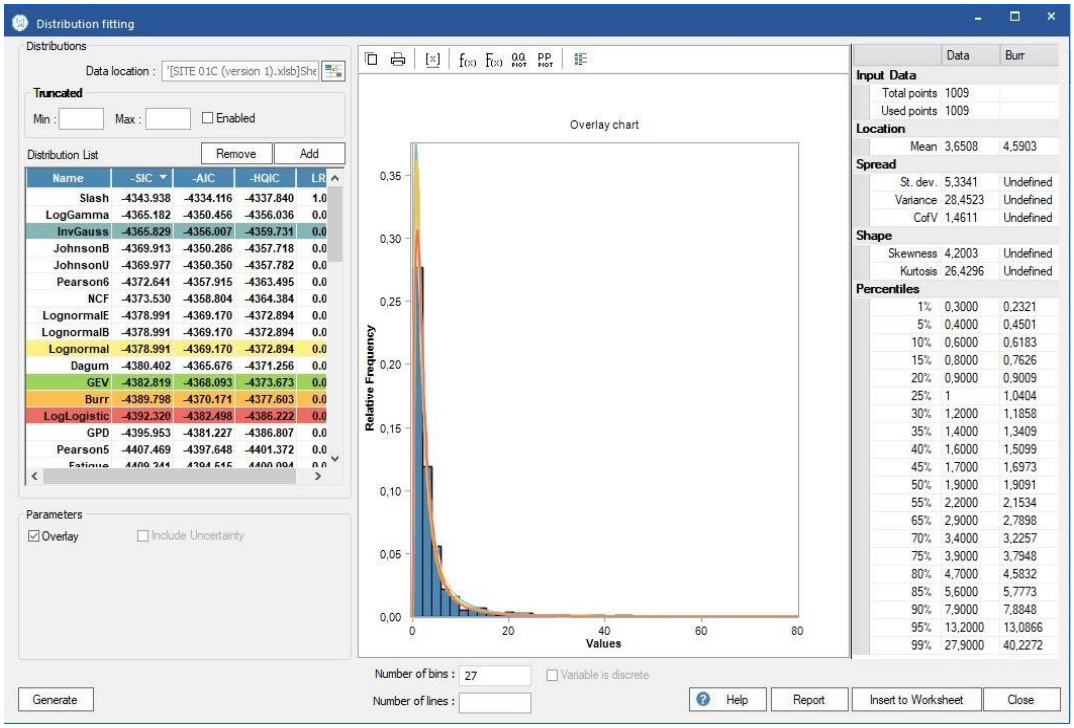

Figure 6. 6: PDF Plot for SS001 (Off-Peak)

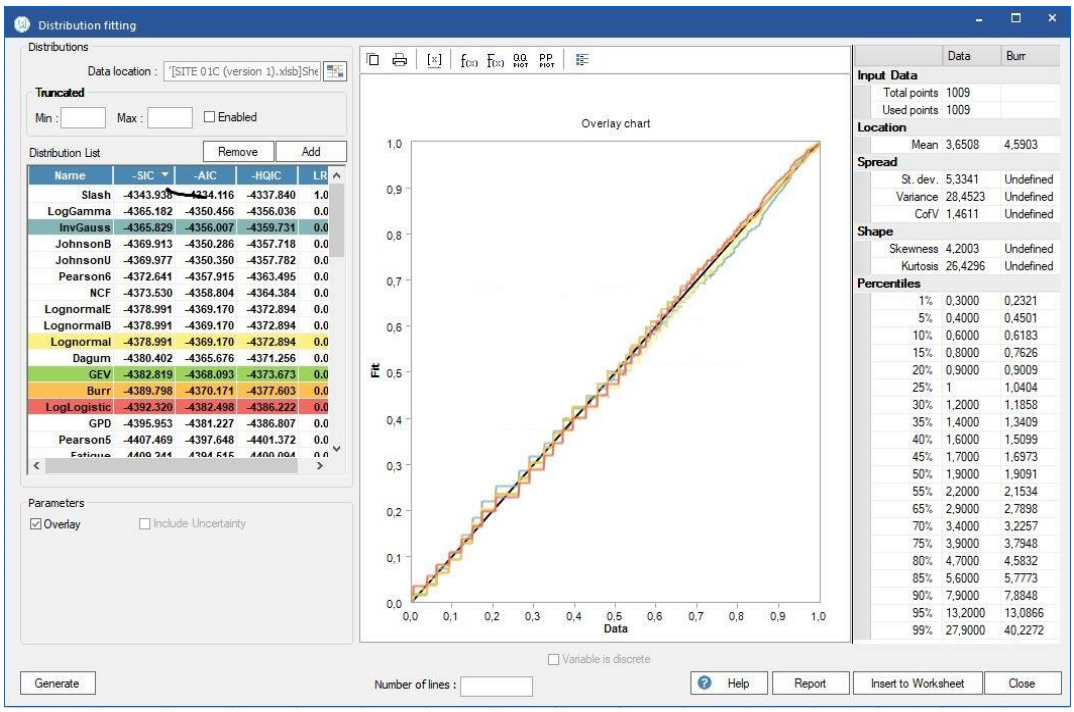

Figure 6. 7: P-P Plot for SS001 (Off-Peak)

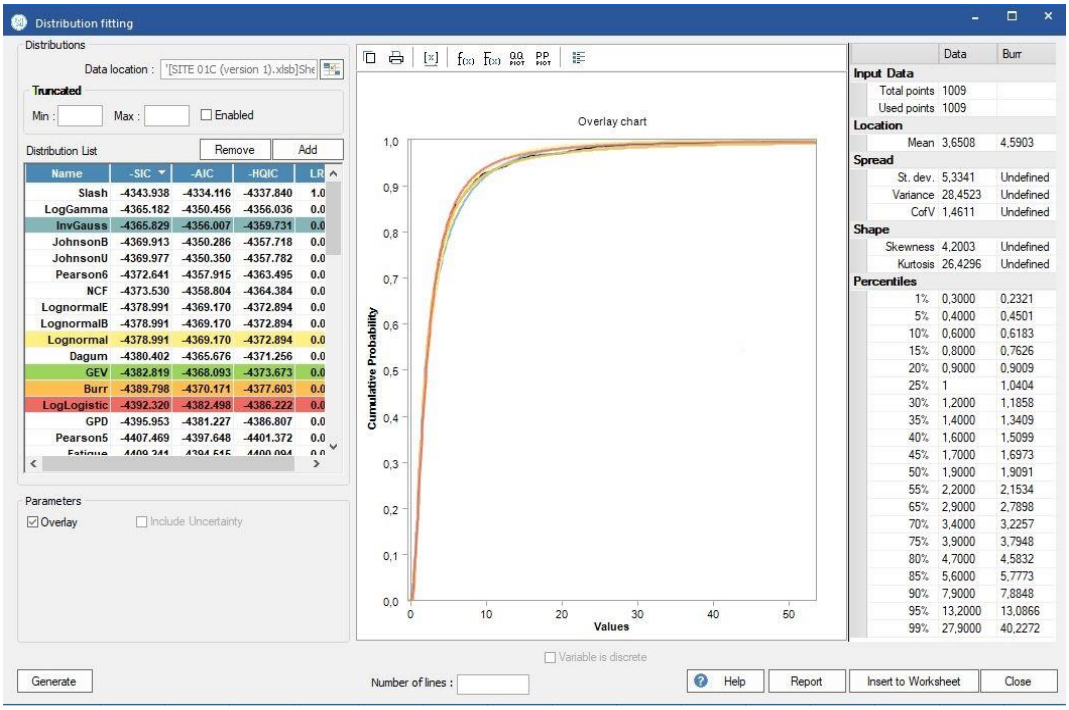

Figure 6. 8: CDF Plot for SS001 (Off-Peak)

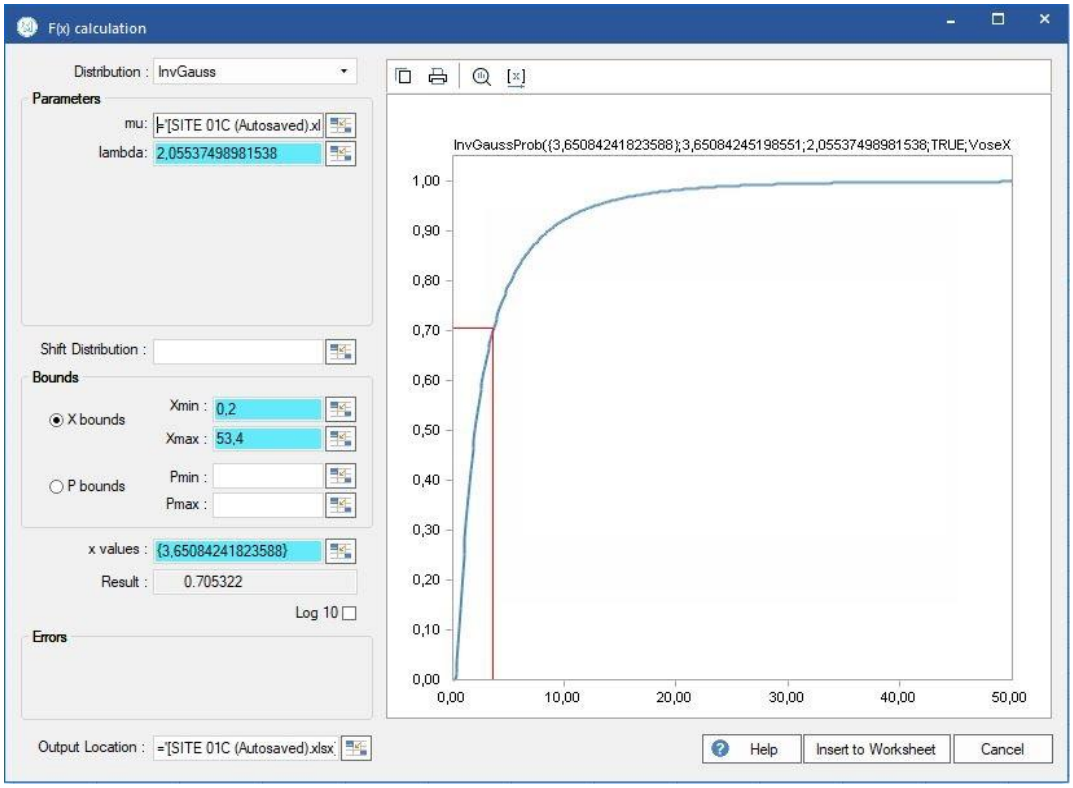

Figure 6. 9: P-Value Plot for SS001 (Off-Peak)

Step 5: Hypothesis testing of the fitted distribution models using the Akaike Information Criterion (AIC), Schwarz Information Criterion (SIC), and Hannan Quinn Information Criterion (HQIC), including the determination of the Log likelihood value (LLH). A summary of how the fitted distribution models performed is presented in Table 6.3.

Table 6. 3: Goodness of Fit and Model Performance Summary – SS001

Location	Rank	Prob. Model	SIC	AIC	HQIC	LLH	Sig. Level	P Value	Hyp. Test	Best Fit
SS001 (Peak)	3RD	Lognormal	4365.40	4355.37	4359.16	-2175.68	0.05	0.69	Accept	GEV
	1ST	GEV	4365.41	**4350.38**	4356.05	**-2175.18**	0.05	0.72	Accept	
	4TH	Log Logistic	4369.23	4359.21	4362.99	-2177.60	0.05	0.72	Accept	
	5TH	InvGauss	4370.72	4360.70	4364.48	-2178.34	0.05	0.69	Accept	
	2ND	Burr	4372.52	4352.49	4360.04	-2172.23	0.05	0.72	Accept	
SS001 (Off-Peak)	1ST	InvGauss	4365.83	**4356.01**	4357.73	**-2176.00**	0.05	0.71	Accept	Inverse Gaussian
	3RD	Lognormal	4378.99	4369.17	4372.89	-2182.58	0.05	0.71	Accept	
	2ND	GEV	4382.82	4368.09	4373.67	-2181.03	0.05	0.74	Accept	
	4TH	Burr	4389.80	4370.17	4377.60	-2181.07	0.05	0.74	Accept	
	5TH	Log Logistic	4392.32	4382.50	4386.22	-2189.24	0.05	0.74	Accept	

*SIC ~ Schwarz Information Criterion; AIC ~ Akaike Information Criterion; HQIC ~ Hannan Quinn Information Criterion; LLH ~ Log likelihood; P ~ Probability *IC used for Ranking - AIC*

As shown in Table 6.3, it can be observed that five continuous probability distribution models were fitted to the empirical time headway data viz: Lognormal, Inverse Gaussian, Generalized Extreme Value (GEV), Log-logistic, and Burr. The models were ranked according to performance using the AIC, SIC, and HQIC criteria as mentioned earlier. Sequel to ranking and comparison with the SIC and HQIC, the smallest AIC value determines the overall best-performed model. Although at peak traffic period, the GEV distribution was the best-performed model, with the lowest AIC value of 4350.38, and the largest Log-likelihood (LLH) value of -2175.18. However, the off-peak traffic is the concern of this analysis under the steady flow condition considered. The inverse Gaussian distribution performed the best with the lowest AIC value of 4356.01 and the largest LLH value of -2176.00. The P-values were acceptable and within the range of 0.69 and 0.74.

Step 6: Determination of, and comparison of the model parameters.

Each continuous distribution model has two or three scale, shape, and location parameters respectively. These parameters were extracted from the report generation by the ModelRisk software that was used for the modelling. A summary of the probability distribution model parameters is shown in Table 6.4.

Table 6. 4: Summary of Probability Distribution Parameters – SS001

Location	Probability Distribution	Shape Parameters		Scale Parameter	Location Parameter
SS001 (Peak)	Lognormal	2.8277	-	3.2462	-
	GEV	1.3263	-	1.0580	0.5507
	Log Logistic	1.9353	-	1.8108	-
	InvGauss	2.9303	-	2.1989	-
	Burr	-0.5855	0.1049	1.8123	193.2064
SS001 (Off-Peak)	InvGauss	3.6500	-	2.0554	-
	Lognormal	3.4706	-	4.6389	-
	GEV	1.4001	-	1.2257	0.6759
	Burr	-0.4097	0.0357	-	333.1296
	Log Logistic	1.7378	-	2.0149	-

As shown in Table 6.4, the distributions fitted to the time headways revealed varied estimated parameters. Amongst these distributions, only the Lognormal, Inverse Gaussian, and Log logistic have two parameters (shape and scale). The Burr distribution has all four parameters (two shape parameters, 1 scale, and 1 location), while the GEV distribution has three which are the shape, scale, and location parameters. Each of the parameters of the distributions varied in different proportions and they revealed the expected outcomes. Their magnitudes and differentials are significant.

Step 7: Comparison of the average time headways of the without (empirical data) and with BRT scenarios vis a vis level of capacity Utilization. Table 6.5 shows the summary of the average time headway of the BRT scenarios.

Table 6. 5: Summary of Probability Distribution Parameters – SS001

Location	Mean Time Headway T_h (Without BRT)	Mean Time Headway T_h (With BRT)	LCU
SS001 (Off-Peak)	3.6	2.2	C

To avoid repetition, statistical modelling for the other sites followed the stepwise procedure.

6.4.2 Statistical Modelling of Time Headway Data for Site SS002

Step 1: Determination of Descriptive Statistics of Peak Traffic Headway Distribution Data

Recall the extracted empirical hourly traffic volume data shown in Table 4.5, chapter 4. Table 6.6 shows the descriptive statistics of the observed time headways for site SS002 at peak.

Table 6. 6: Descriptive Statistics of the Time Headways – SS002 (Peak)

Descriptive Statistics	SS002
Mean	2.70149
Standard Error	0.169099
Median	1.4
Mode	1
Standard Deviation	5.877246
Coefficient of Variation	2.19
Sample Variance	34.54202
Kurtosis	49.4649
Skewness	6.708744
Range	56.9
Minimum	0.1
Maximum	57
Sum	3263.4
Sample Size	1208

Step 2: Fitting of continuous probability distribution models to headway data. Figures 6.10, 6.11, 6.12, and 6.13 show the PDF, P-P, CDF, and P-value plots respectively.

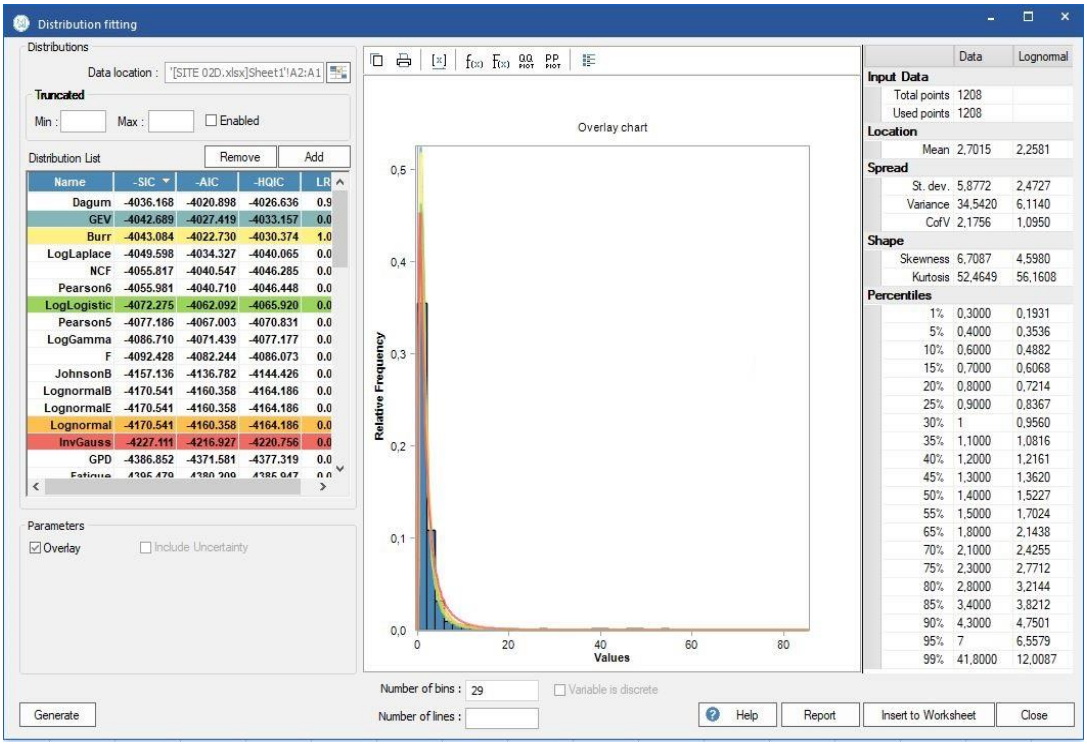

Figure 6. 10: PDF Plot for SS002 (Peak)

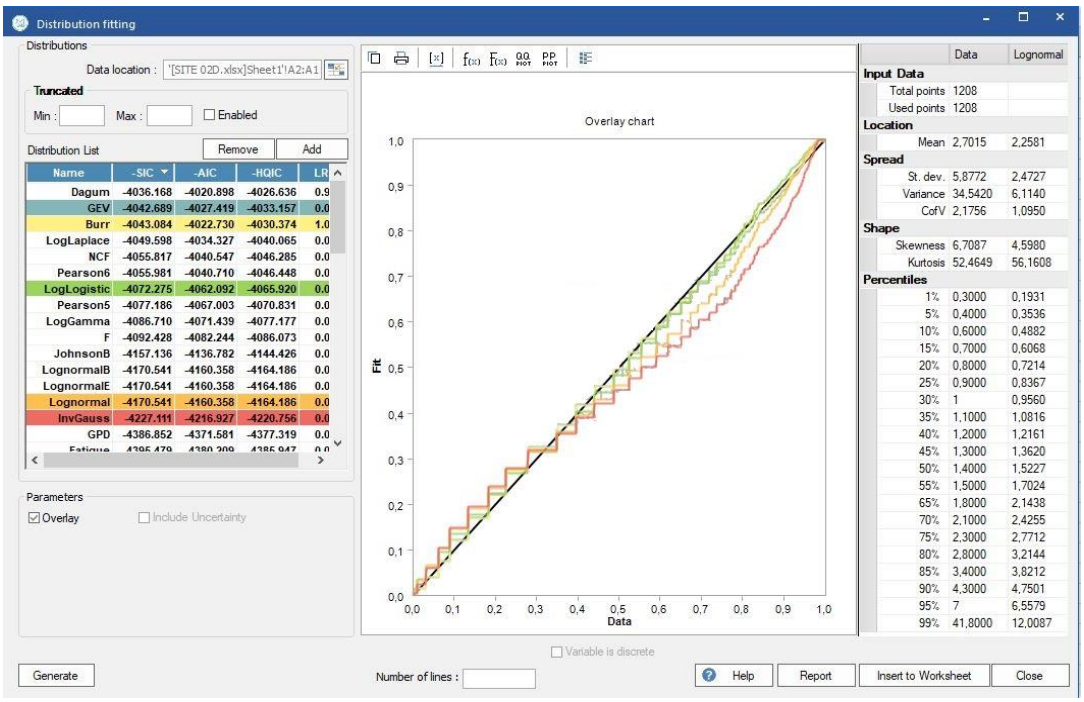

Figure 6. 11: P-P Plot for SS002 (Peak)

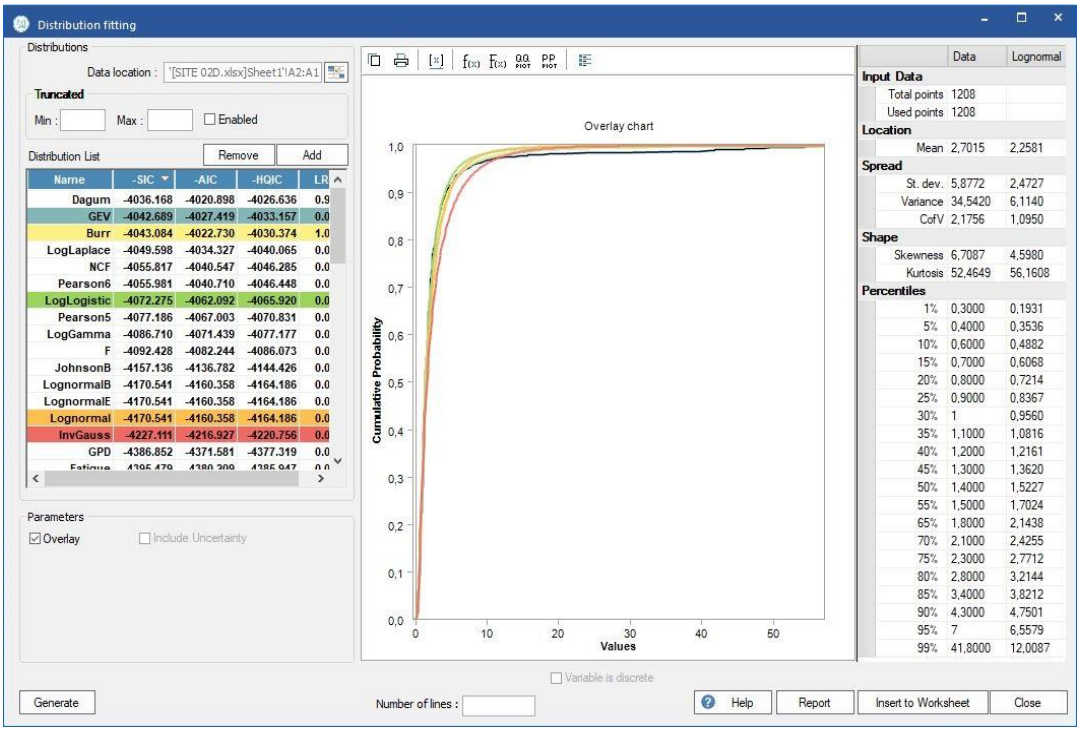

Figure 6. 12: CDF Plot for SS002 (Peak)

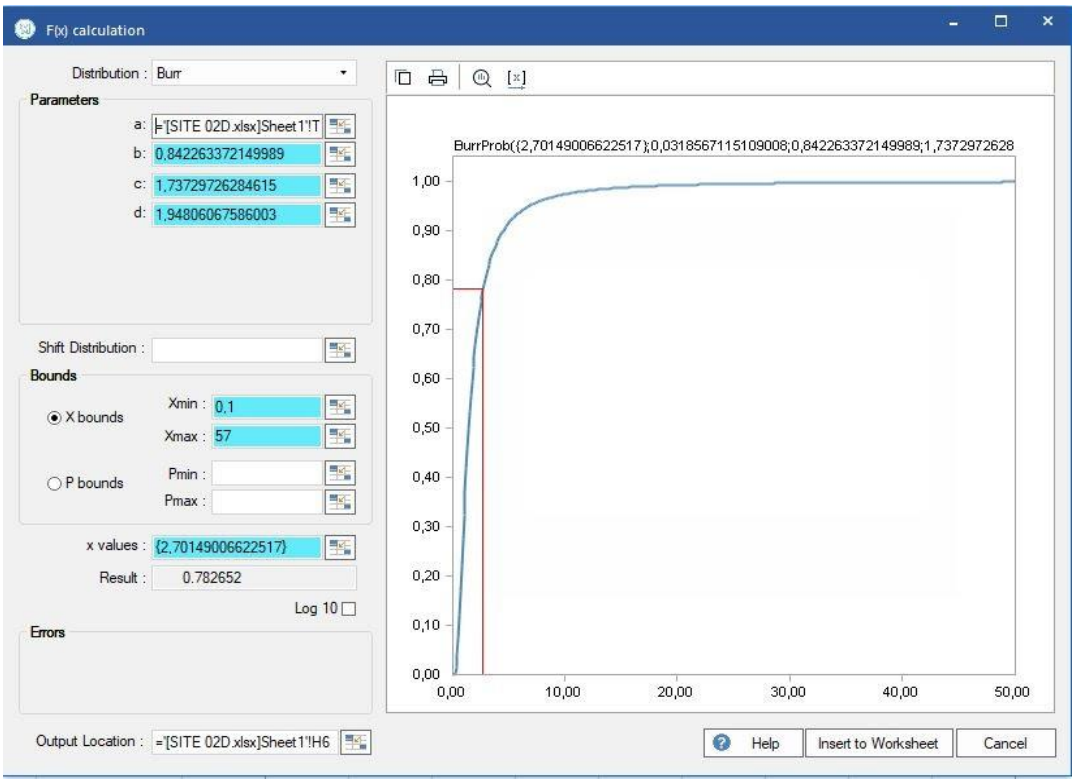

Figure 6. 13: P-Value Plot for SS002 (Peak)

Step 3: Analysis of **Off- Peak** Traffic Headway Distribution Data

Recall the extracted empirical hourly traffic volume data shown in Table 4.6, chapter 4. Table 6.7 shows the descriptive statistics of the observed time headways for site SS002 at off-peak.

Table 6. 7: Descriptive Statistics of the Time Headways – SS002 (Off-Peak)

Descriptive Statistics	SS002
Mean	3.623555
Standard Error	0.244865
Median	1.55
Mode	1
Standard Deviation	7.483434
Coefficient of Variation	2.08
Sample Variance	56.00178
Kurtosis	24.48827
Skewness	4.794042
Range	54.9
Minimum	0.2
Maximum	55.1
Sum	3384.4
Sample Size	934

Step 4: Fitting of continuous probability distribution models to headway data

Using the Model Risk software, probability models were fitted to the headway data, and the PDF, CDF, P-P plots and the P-value with its plot of the best-fitted distribution were generated from the software. Figures 6.14, 6.15, 6.16, and 6.17 show the PDF, P-P, CDF, and P-Value plots respectively.

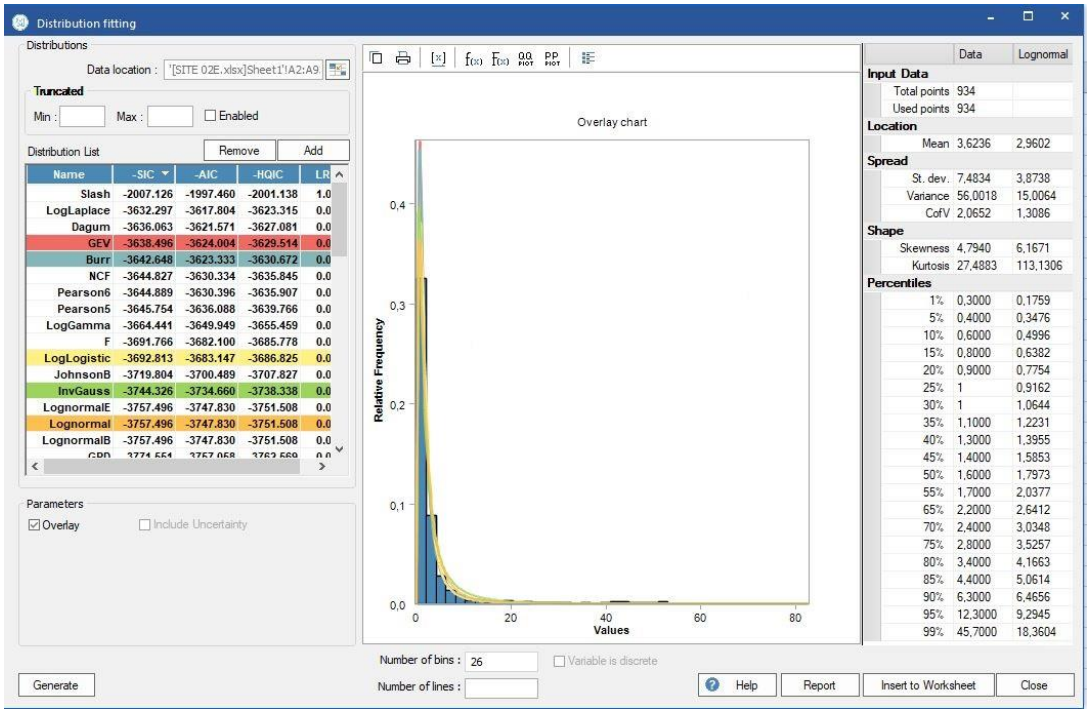

Figure 6. 14: PDF Plot for SS002 (Off-Peak)

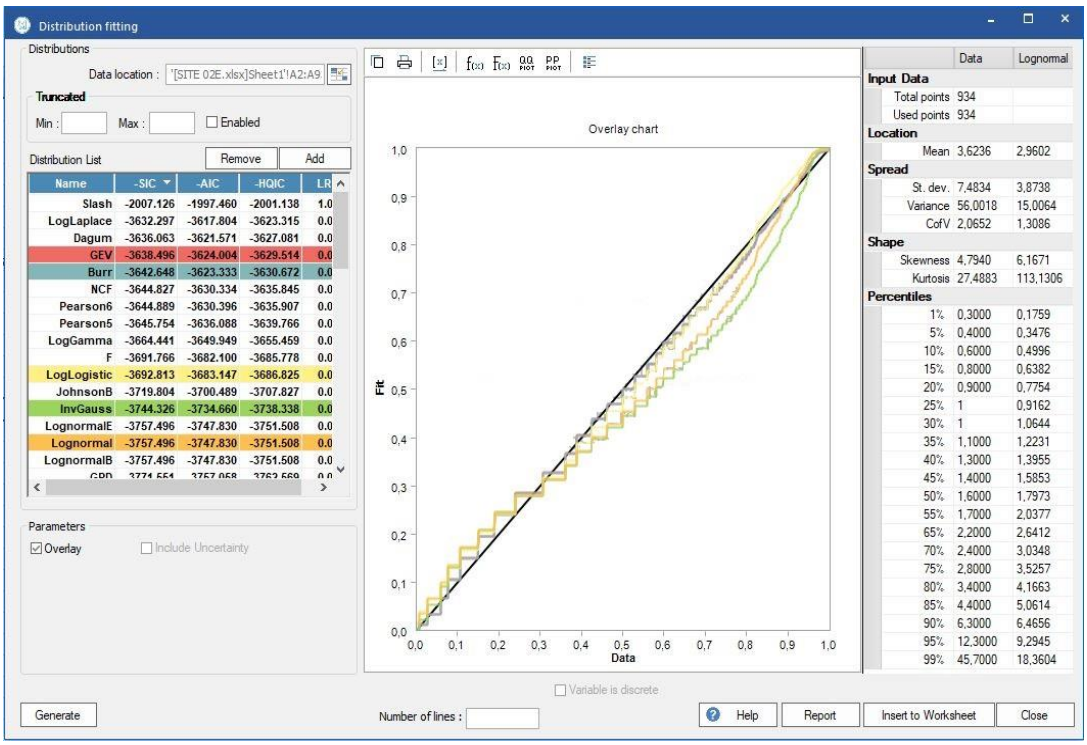

Figure 6. 15: P-P Plot for SS002 (Off-Peak)

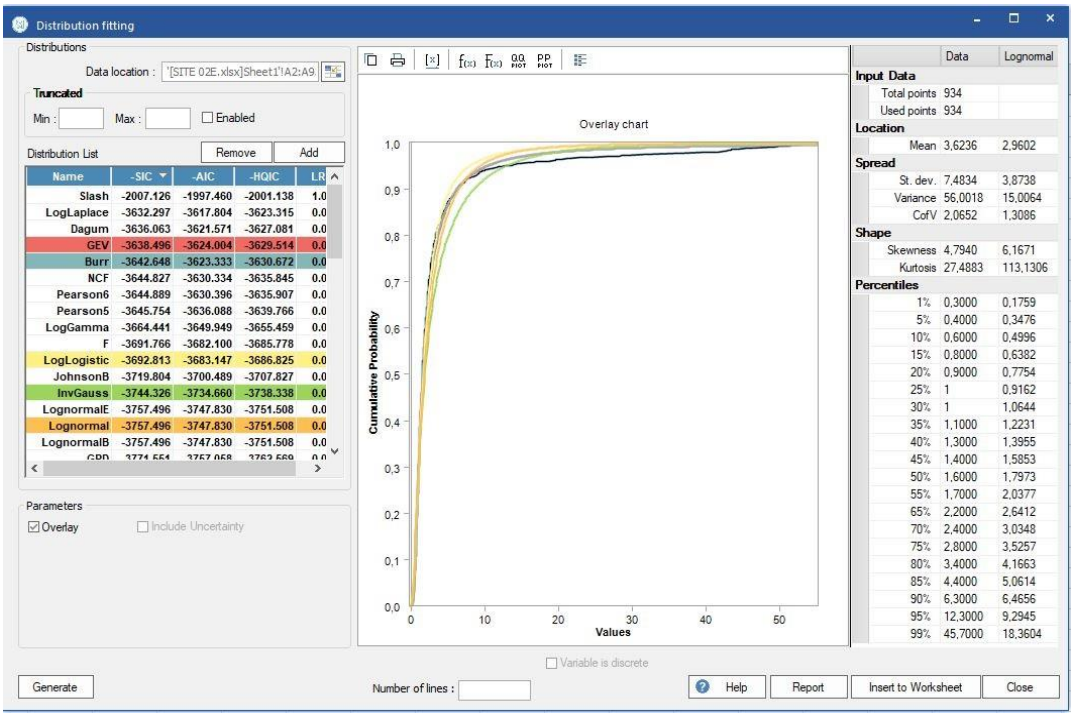

Figure 6. 16: CDF Plot for SS002 (Off-Peak)

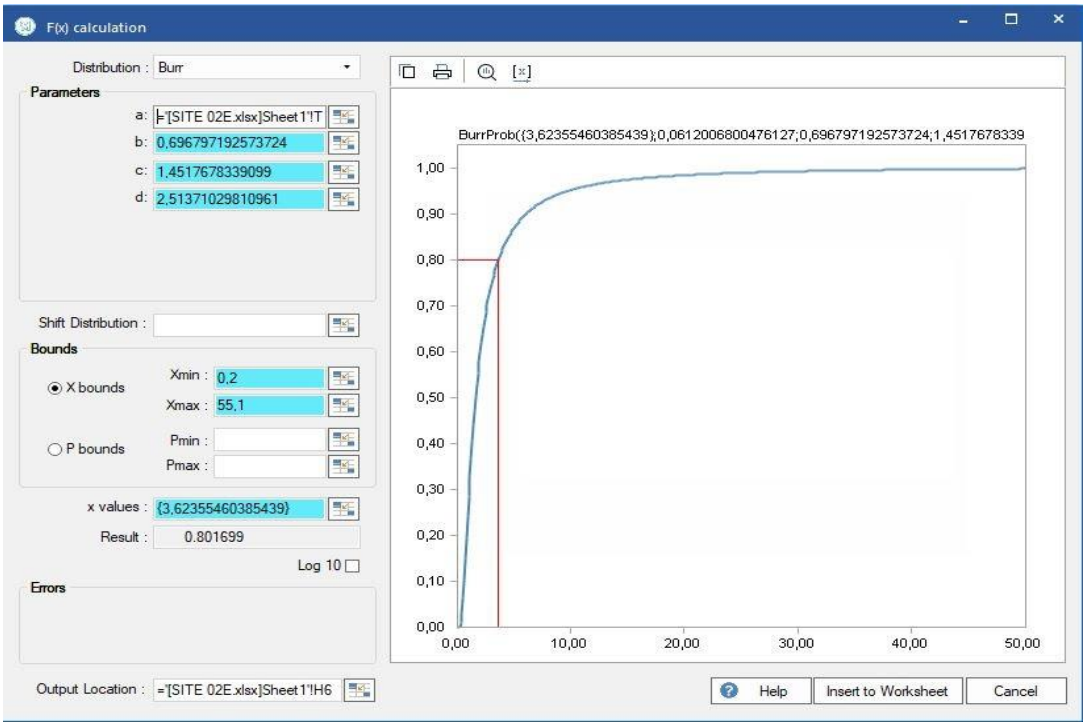

Figure 6. 17: P-Value Plot for SS002 (Off-Peak)

Step 5: Hypothesis testing of the fitted distribution models using the AIC, SIC, and HQIC. A summary of how the fitted distribution models performed is presented in Table 6.8.

Table 6. 8: Goodness of Fit and Model Performance Summary – SS002

Location	Rank	Prob. Model	SIC	AIC	HQIC	LLH	Sig. Level	P Value	Hyp. Test	Best Fit
SS002 (Peak)	2ND	GEV	4042.69	4027.42	4033.16	-2010.70	0.05	0.78	Accept	Burr
	1ST	Burr	4043.08	**4022.73**	4030.37	**-2007.35**	0.05	0.78	Accept	
	3RD	Log Logistic	4072.28	4062.09	4065.92	-2029.04	0.05	0.79	Accept	
	4TH	Lognormal	4170.54	4160.36	4164.19	-2078.17	0.05	0.74	Accept	
	5TH	InvGauss	4227.11	4216.93	4220.76	-2106.46	0.05	0.69	Accept	
SS002 (Off-Peak)	2ND	GEV	3638.50	3624.00	3629.51	-1808.99	0.05	0.80	Accept	Burr
	1ST	Burr	3642.65	**3623.33**	3630.67	**-1807.64**	0.05	0.80	Accept	
	3RD	Log Logistic	3692.81	3683.15	3686.83	-1839.57	0.05	0.81	Accept	
	4TH	InvGauss	3744.33	3734.66	3738.34	-1865.32	0.05	0.71	Accept	
	5TH	Lognormal	3757.50	3747.83	3751.51	-1871.91	0.05	0.76	Accept	

*SIC ~ Schwarz Information Criterion; AIC ~ Akaike Information Criterion; HQIC ~ Hannan Quinn Information Criterion; LLH ~ Log likelihood; P ~ Probability *IC used for Ranking - AIC*

As shown in table 6.8, it can be observed that five continuous probability distribution models were fitted to the empirical time headway data viz: Lognormal, Inverse Gaussian, Generalized Extreme Value (GEV), Log-logistic, and Burr. The models were ranked according to performance using the AIC, SIC, and HQIC criteria as mentioned earlier. Sequel to ranking and comparison with the SIC and HQIC, the smallest AIC value determines the overall best-performed model. Although at peak traffic period, the Burr distribution was the best-performed model, with the lowest AIC value of 4022.73, and the largest Log-likelihood (LLH) value of -2007.35. However, the off-peak traffic is the concern of this analysis under the steady flow condition considered. The Burr distribution performed the best with the lowest AIC value of 3623.33 and the largest LLH value of -1807.64. The P-values were acceptable and within the range of 0.71 and 0.81.

Step 6: Determination of, and comparison of the model parameters.

A summary of the probability distribution model parameters is shown in Table 6.9.

Table 6. 9: Summary of Probability Distribution Parameters – SS002

Location	Probability Distribution	Shape Parameters		Scale Parameter	Location Parameter
SS002 (Peak)	GEV	1.0859	-	0.7914	0.5461
	Burr	0.0319	0.8423	1.7373	1.9481
	Log Logistic	2.1235	-	1.4417	-
	Lognormal	2.2581	-	2.4727	-
	InvGauss	2.7015	-	1.8440	-
SS002 (Off-Peak)	GEV	1.9955	-	0.9607	0.6768
	Burr	0.0612	0.6968	1.4518	2.5137
	Log Logistic	1.8795	-	1.6546	-
	InvGauss	3.6236	-	1.8267	-
	Lognormal	2.9602	-	3.8738	-

As shown in Table 6.9, the distributions fitted to the time headways revealed varied estimated parameters. Amongst these distributions, only the Lognormal, Inverse Gaussian, and Log-logistic have two parameters (shape and scale). The Burr distribution has all four parameters (two shape parameters, 1 scale, and 1 location), while the GEV distribution has three which are the shape, scale, and location parameters. Each of the parameters of the distributions varied in different proportions and they revealed the expected outcomes. Their magnitudes and differentials are significant.

Step 7: Comparison of the average time headways of the without (empirical data) and with BRT scenarios vis a vis level of capacity Utilization. Table 6.10 shows the summary of the comparison between the average time headway of the 'with' and 'without' BRT scenarios.

Table 6. 10: Summary of Probability Distribution Parameters – SS002

Location	Mean Time Headway T_h (Without BRT)	Mean Time Headway T_h (With BRT)	LCU
SS002 (Off-Peak)	3.6	1.8	C

6.4.3 Statistical Modelling of Time Headway Data for Site SS003

Step 1: Determination of Descriptive Statistics of Peak Traffic Headway Distribution Data

Recall the extracted empirical hourly traffic volume data shown in Table 4.8, chapter 4. Table 6.11 shows the descriptive statistics of the observed time headways for site SS003 at peak.

Table 6. 11: Descriptive Statistics of the Time Headways – SS003 (Peak)

Descriptive Statistics	SS003
Mean	2.163394
Standard Error	0.113701
Median	1.5
Mode	1
Standard Deviation	3.480445
Coefficient of Variation	1.66
Sample Variance	12.1135
Kurtosis	120.2194
Skewness	9.773481
Range	58
Minimum	0.1
Maximum	58.1
Sum	2027.1
Sample Size	937

Step 2: Fitting of continuous probability distribution models to headway data. Figures 6.18, 6.19, 6.20, 6.21 show the PDF, P-P, CDF, and P-value plots respectively.

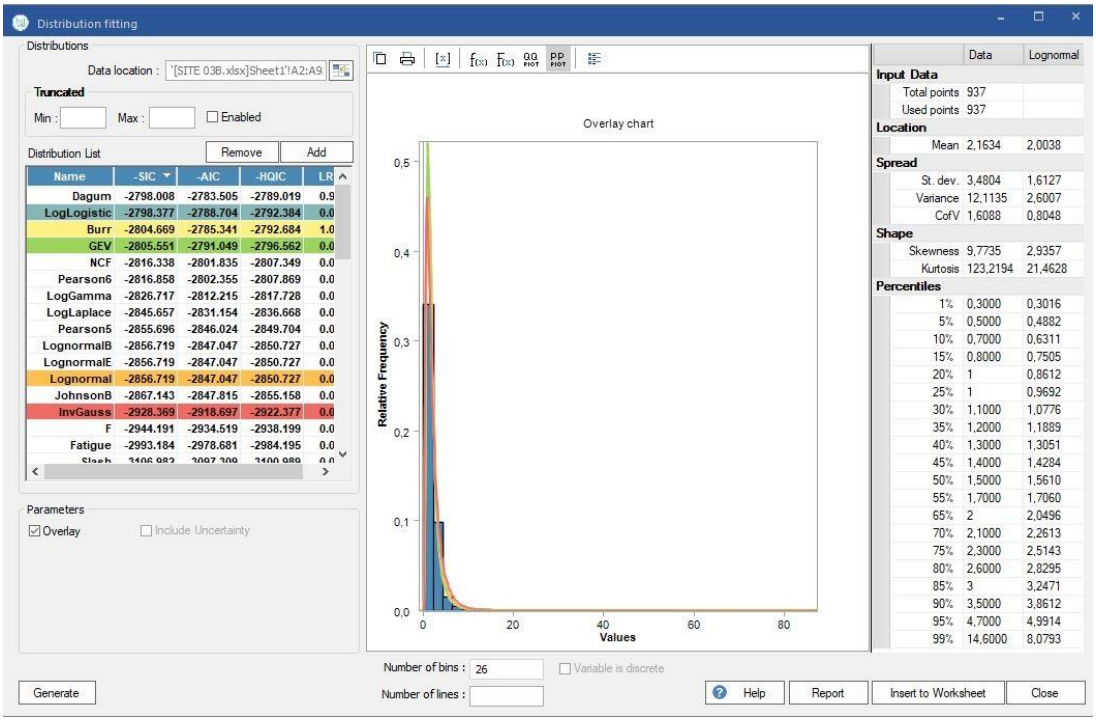

Figure 6. 18: PDF Plot for SS003 (Peak)

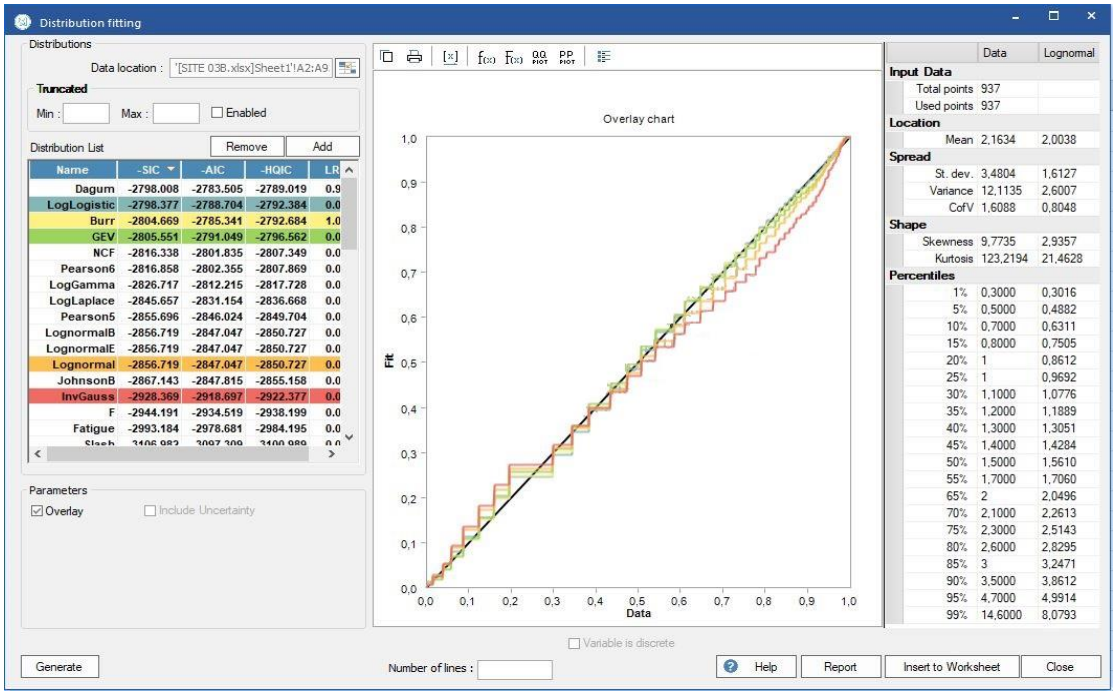

Figure 6. 19: P-P Plot for SS003 (Peak)

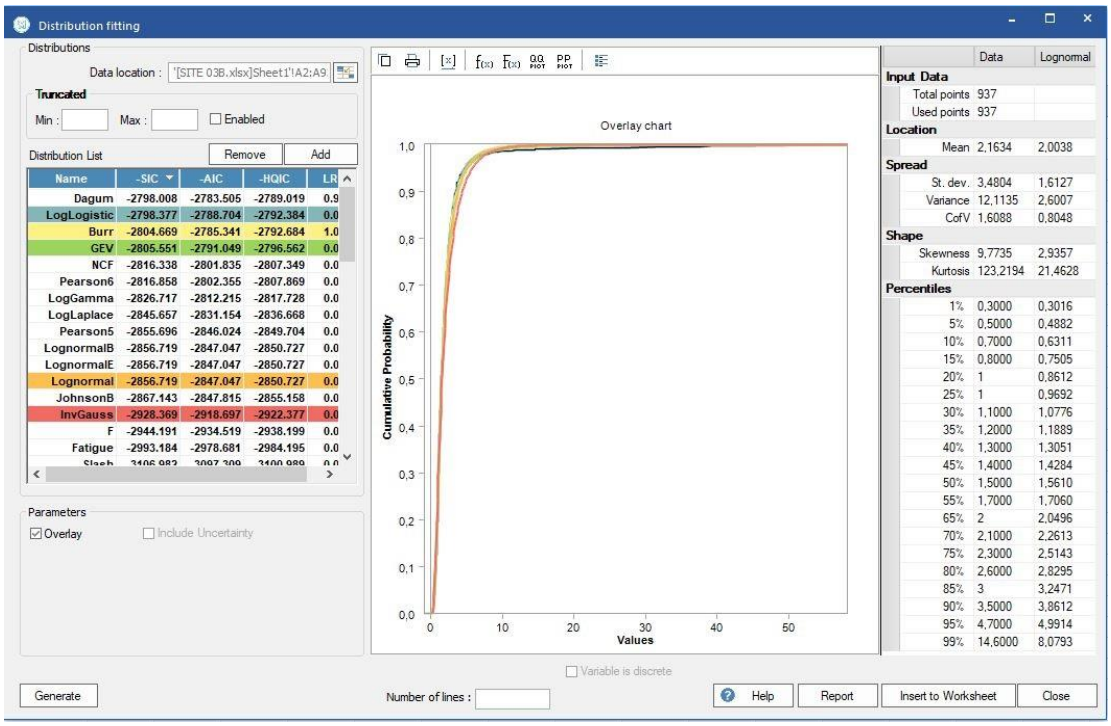

Figure 6. 20: CDF Plot for SS003 (Peak)

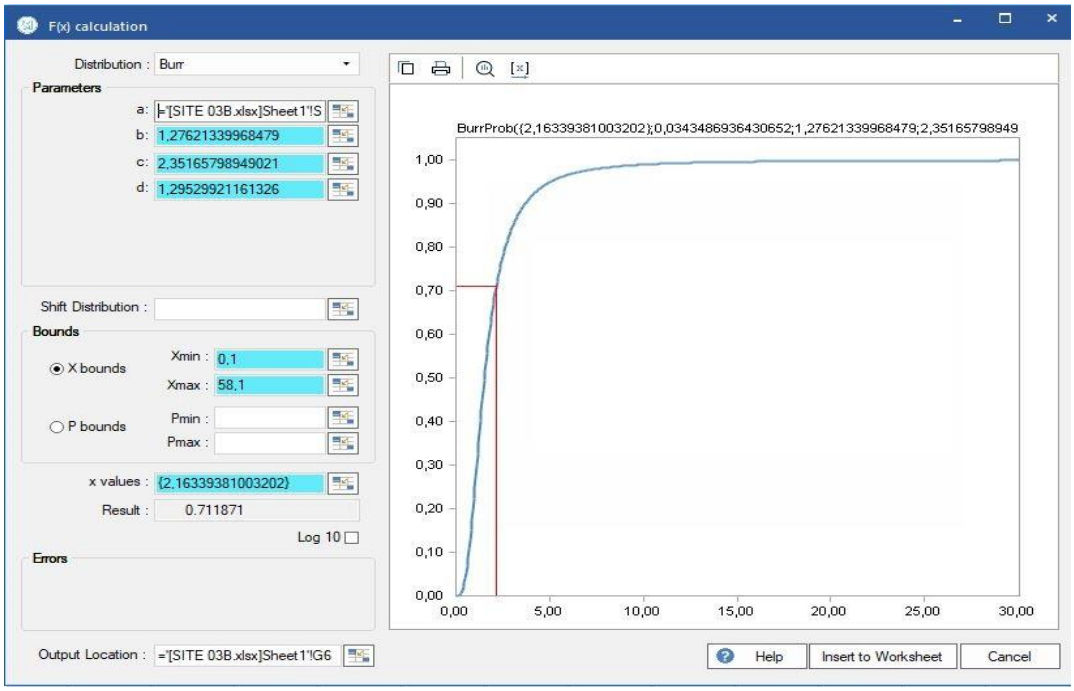

Figure 6. 21: P-Value Plot for SS003 (Peak)

Step 3: Analysis of **Off- Peak** Traffic Headway Distribution Data

Recall the extracted empirical hourly traffic volume data shown in Table 4.9, chapter 4. Table 6.12 shows the descriptive statistics of the observed time headways for site SS003 at off-peak.

Table 6. 12: Descriptive Statistics of the Time Headways – SS003 (Off-Peak)

Descriptive Statistics	SS003
Mean	2.951245552
Standard Error	0.17342949
Median	1.5
Mode	1
Standard Deviation	5.81441604
Coefficient of Variation	1.99
Sample Variance	33.80743389
Kurtosis	34.07863634
Skewness	5.561391265
Range	56.2
Minimum	0.2
Maximum	56.4
Sum	3317.2
Sample Size	1124

Step 4: Fitting of continuous probability distribution models to headway data

Using the Model Risk software, probability models were fitted to the headway data, and the PDF, CDF, P-P plots, and the P-value with its plot of the best-fitted distribution were generated from the software. Figures 6.22, 6.23, 6.24, and 6.25 show the PDF, P-P, CDF, and P-Value plots respectively.

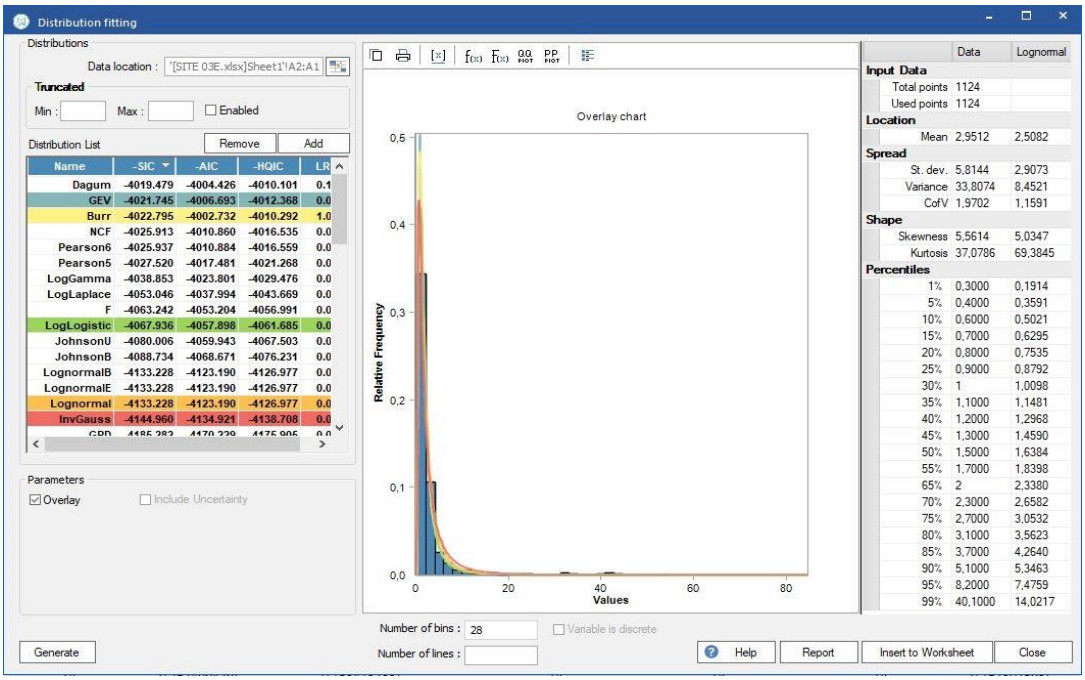

Figure 6. 22: PDF Plot for SS003 (Off-Peak)

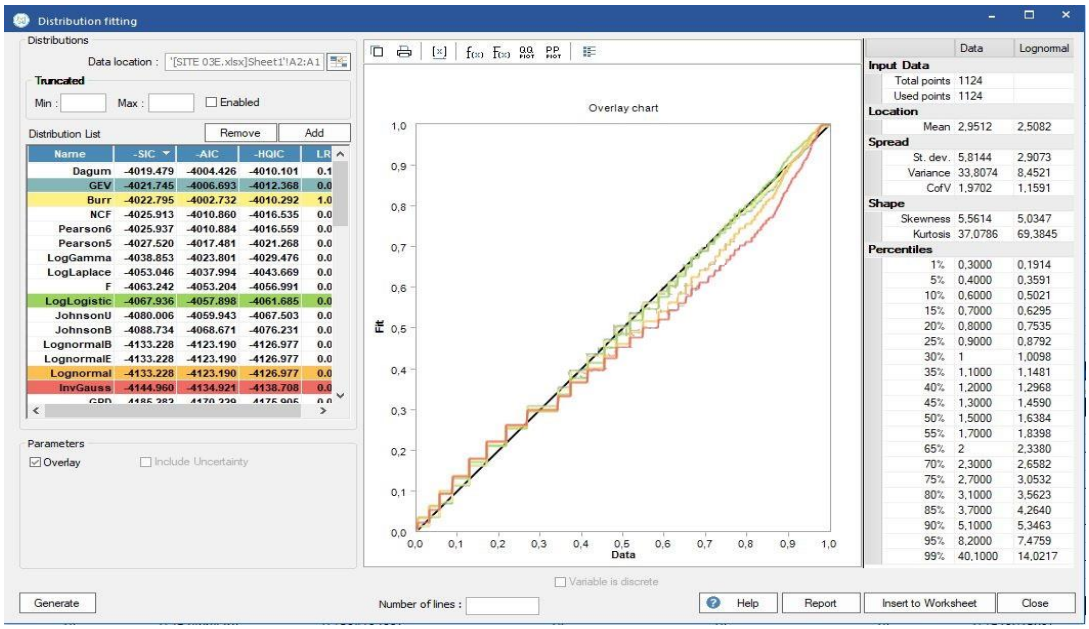

Figure 6. 23: P-P Plot for SS003 (Off-Peak)

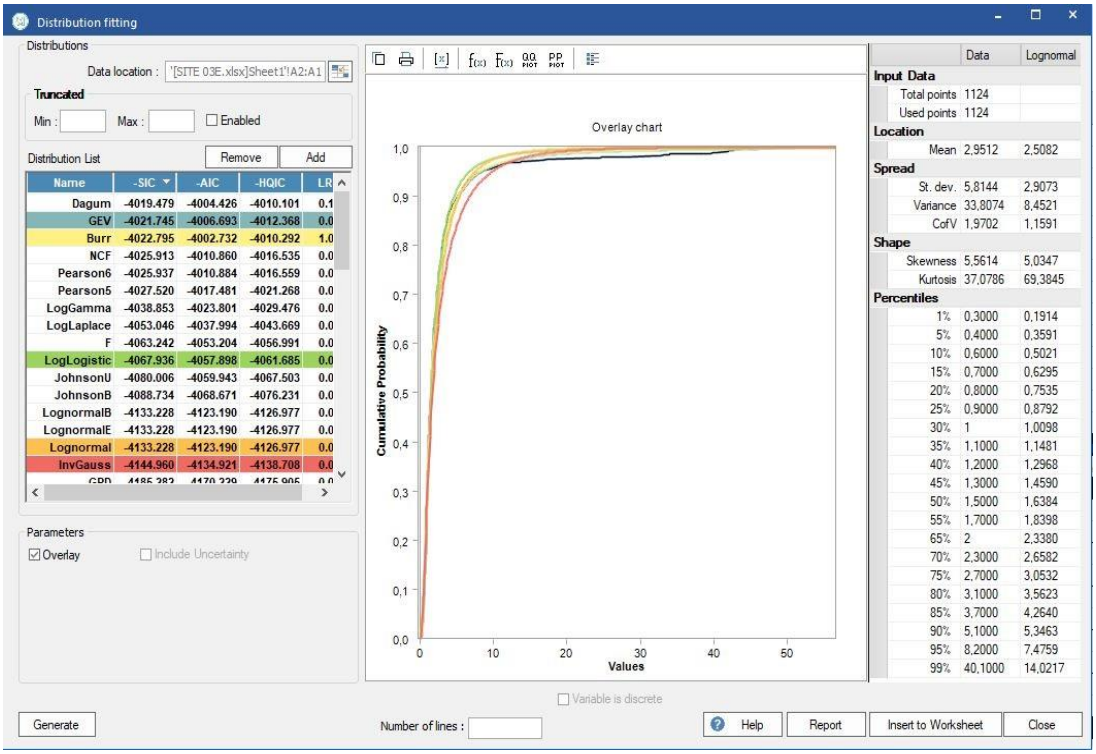

Figure 6. 24: CDF Plot for SS003 (Off-Peak)

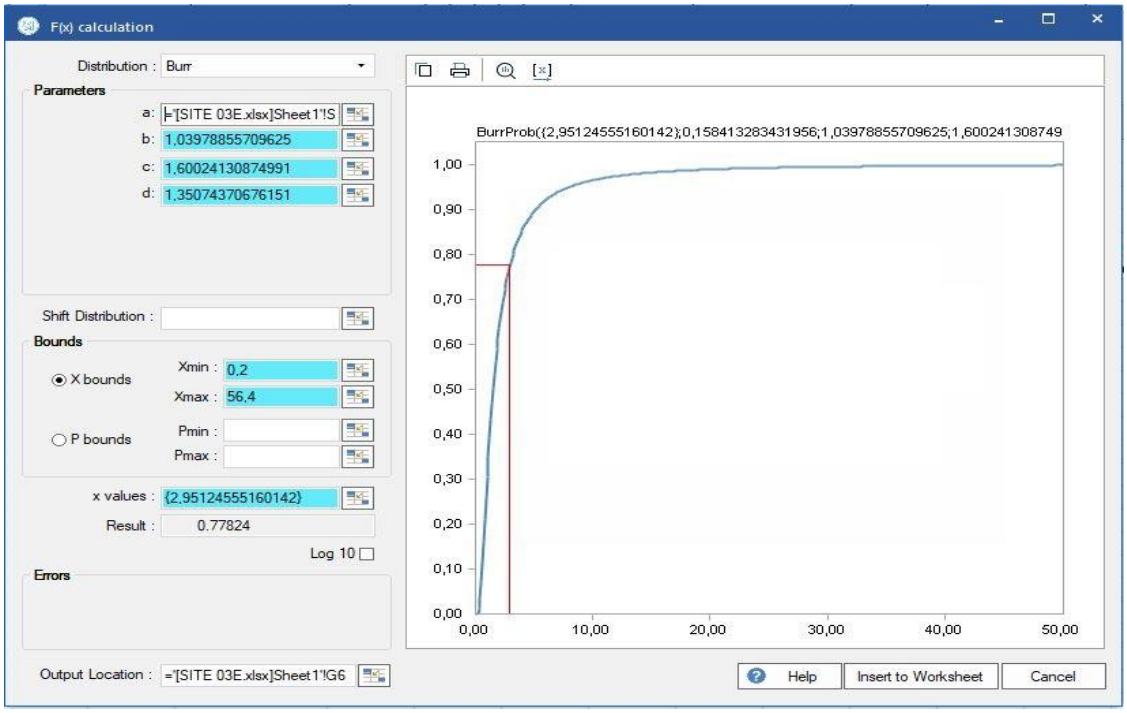

Figure 6. 25: P-Value Plot for SS003 (Off-Peak)

Step 5: Hypothesis testing of the fitted distribution models using the AIC, SIC, and HQIC. A summary of how the fitted distribution models performed is presented in Table 6.13.

Table 6. 13: Goodness of Fit and Model Performance Summary – SS003

Location	Rank	Prob. Model	SIC	AIC	HQIC	LLH	Sig. Level	P Value	Hyp. Test	Best Fit
SS003 (Peak)	2ND	Log Logistic	2798.38	2788.70	2792.38	-1392.35	0.05	0.71	Accept	Burr
	1ST	Burr	2804.67	**2785.34**	2792.68	**-1388.65**	0.05	0.71	Accept	
	3RD	GEV	2805.55	2791.05	2796.56	-1392.51	0.05	0.70	Accept	
	4TH	Lognormal	2856.72	2847.05	2850.73	-1421.52	0.05	0.68	Accept	
	5TH	InvGauss	2928.37	2918.70	2922.38	-1457.34	0.05	0.65	Accept	
SS003 (Off-Peak)	2ND	GEV	4021.75	4006.69	4012.37	-2000.34	0.05	0.77	Accept	Burr
	1ST	Burr	4022.80	**4002.73**	4010.29	**-1997.35**	0.05	0.78	Accept	
	3RD	Log Logistic	4067.94	4057.90	4061.69	-2026.94	0.05	0.78	Accept	
	4TH	Lognormal	4133.23	4123.19	4126.98	-2059.59	0.05	0.74	Accept	
	5TH	InvGauss	4144.96	4134.92	4138.71	-2065.46	0.05	0.70	Accept	

*SIC ~ Schwarz Information Criterion; AIC ~ Akaike Information Criterion; HQIC ~ Hannan Quinn Information Criterion; LLH ~ Log likelihood; P ~ Probability *IC used for Ranking - AIC*

As shown in table 6.13, it can be observed that five continuous probability distribution models were fitted to the empirical time headway data viz: Lognormal, Inverse Gaussian, Generalized Extreme Value (GEV), Log-logistic, and Burr. The models were ranked according to performance using the AIC, SIC, and HQIC criteria as mentioned earlier. Sequel to ranking and comparison with the SIC and HQIC, the smallest AIC value determines the overall best-performed model. Although at peak traffic period, the Burr distribution was the best-performed model, with the lowest AIC value of 2785.34, and the largest Log-likelihood (LLH) value of -1388.65. However, the off-peak traffic is the concern of this analysis under the steady flow condition considered. The Burr distribution performed the best with the lowest AIC value of 4002.73 and the largest LLH value of -1997.35. The P-values were acceptable and within the range of 0.65 and 0.78.

Step 6: Determination of, and comparison of the model parameters.

A summary of the probability distribution model parameters is shown in Table 6.14.

Table 6. 14: Summary of Probability Distribution Parameters – SS003

Location	Probability Distribution	Shape Parameters		Scale Parameter	Location Parameter
SS003 (Peak)	Log Logistic	2.6184	-	1.5315	-
	Burr	0.0343	1.2762	2.3517	1.2953
	GEV	1.2168	-	0.7450	0.3529
	Lognormal	2.0038	-	1.6127	-
	InvGauss	2.1634	-	2.8957	-
SS003 (Off-Peak)	GEV	1.1312	-	0.8564	0.6145
	Burr	0.5184	1.0398	1.6002	1.3507
	Log Logistic	2.0092	-	1.5423	-
	Lognormal	2.5082	-	2.9073	-
	InvGauss	2.9512	-	1.9038	-

As shown in Table 6.14, the distributions fitted to the time headways revealed varied estimated parameters. Amongst these distributions, only the Lognormal, Inverse Gaussian, and Log-logistic have two parameters (shape and scale). The Burr distribution has all four parameters (two shape parameters, 1 scale, and 1 location), while the GEV distribution has three which are the shape, scale, and location parameters. Each of the parameters of the distributions varied in different proportions and they revealed the expected outcomes. Their magnitudes and differentials are significant.

Step 7: Comparison of the average time headways of the without (empirical data) and with BRT scenarios vis a vis level of capacity Utilization. Table 6.15 shows the summary of the comparison between the average time headway of the BRT scenarios.

Table 6. 15: Summary of Probability Distribution Parameters – SS003

Location	Mean Time Headway T_h (Without BRT)	Mean Time Headway T_h (With BRT)	LCU
SS003 (Off-Peak)	2.95	1.79	C

6.4.4 Statistical Modelling of Time Headway Data for Site SS004

Step 1: Determination of Descriptive Statistics of Peak Traffic Headway Distribution Data

Recall the extracted empirical hourly traffic volume data shown in Table 4.11 of chapter 4. Table 6.16 shows the descriptive statistics of the observed time headways for site SS004 at peak.

Table 6. 16: Descriptive Statistics of the Time Headways – SS004 (Peak)

Descriptive Statistics	SS004
Mean	2.096094
Standard Error	0.090892
Median	1.4
Mode	1
Standard Deviation	3.650436
Coefficient of Variation	1.79
Sample Variance	13.32569
Kurtosis	68.44363
Skewness	7.671382
Range	44.2
Minimum	0.1
Maximum	44.3
Sum	3381
Sample Size	1613

Step 2: Fitting of continuous probability distribution models to headway data. Figures 6.26, 6.27, 6.28, 6.29 show the PDF, P-P, CDF, and P-value plots respectively.

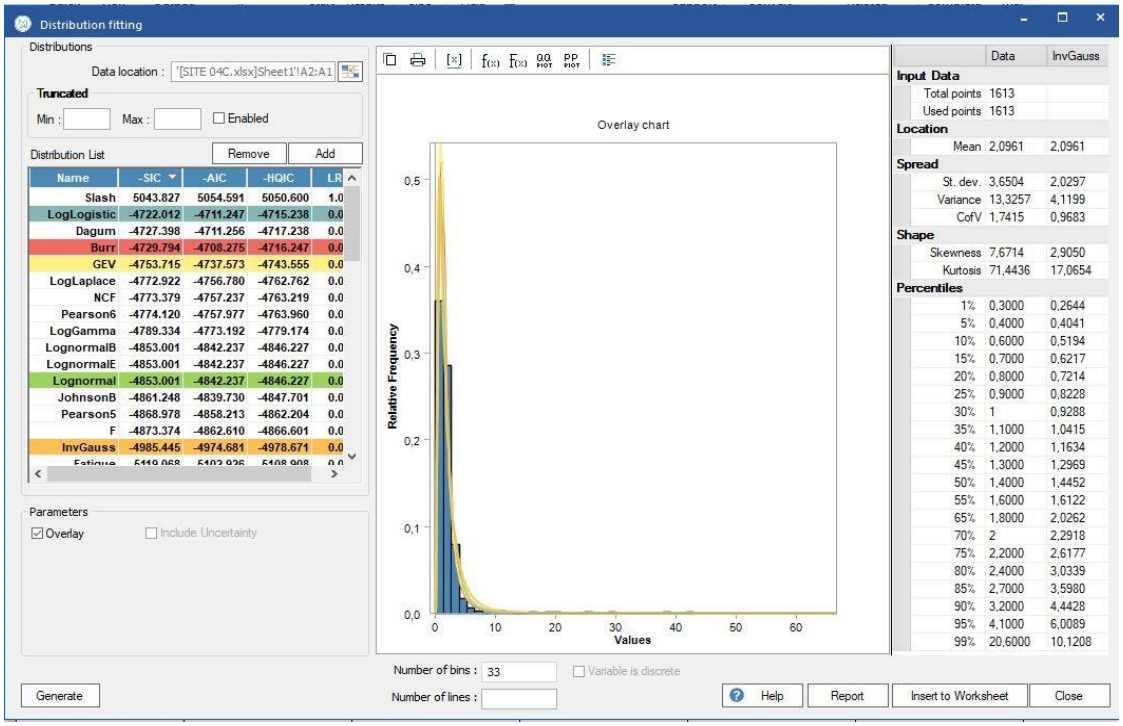

Figure 6. 26: PDF Plot for SS004 (Peak)

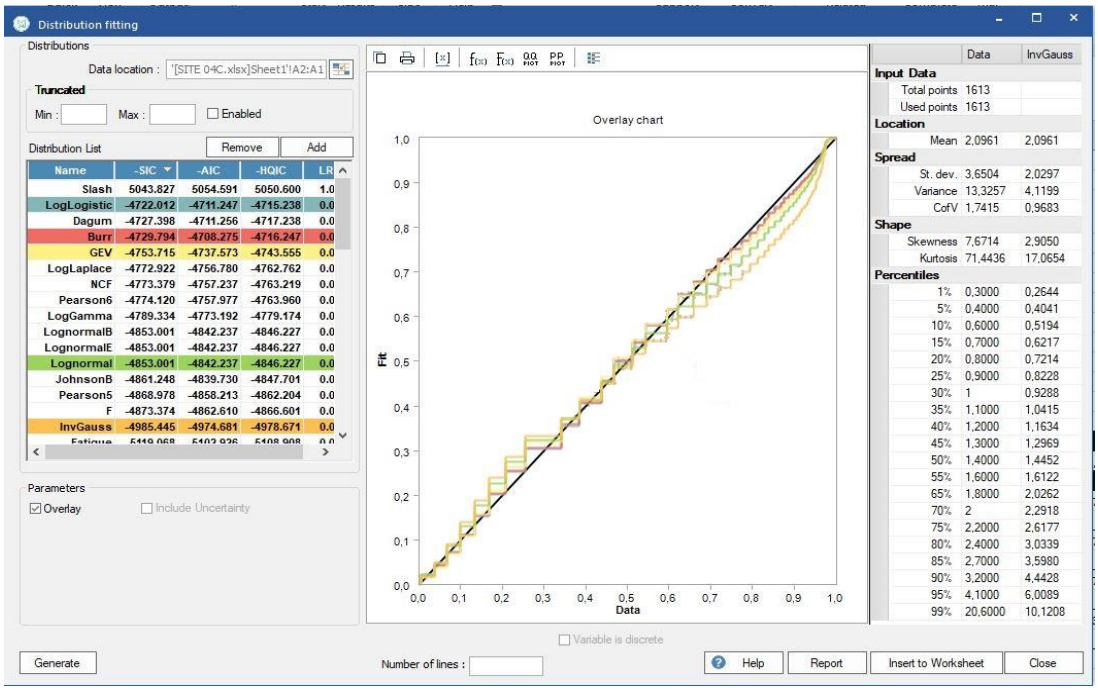

Figure 6. 27: P-P Plot for SS004 (Peak)

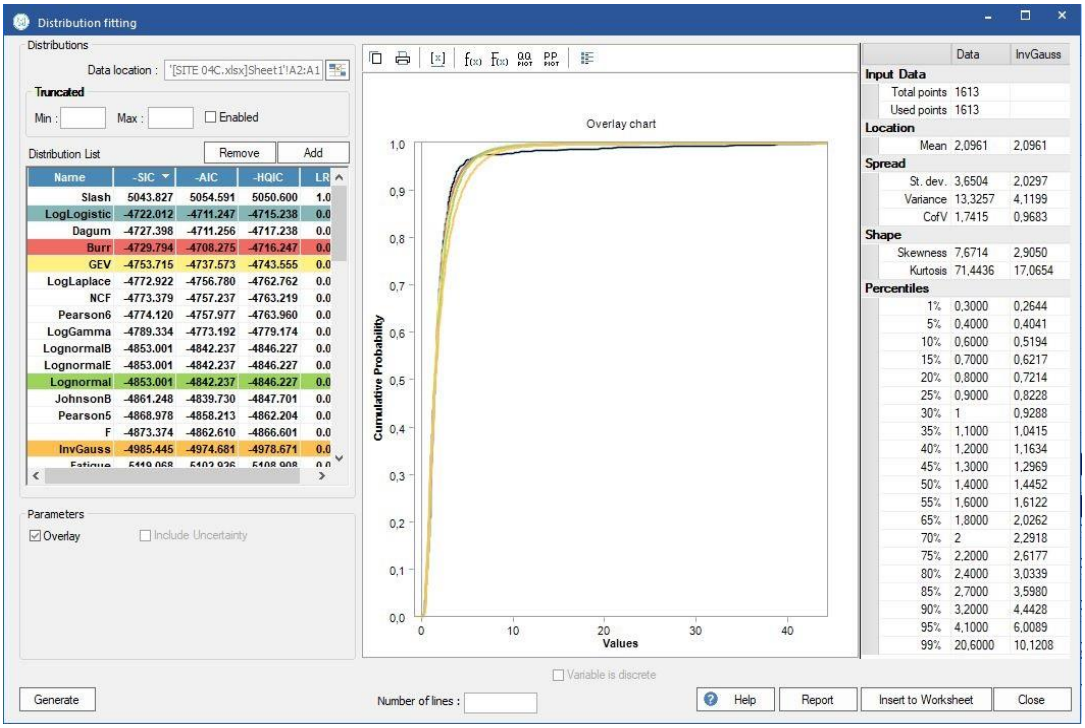

Figure 6. 28: CDF Plot for SS004 (Peak)

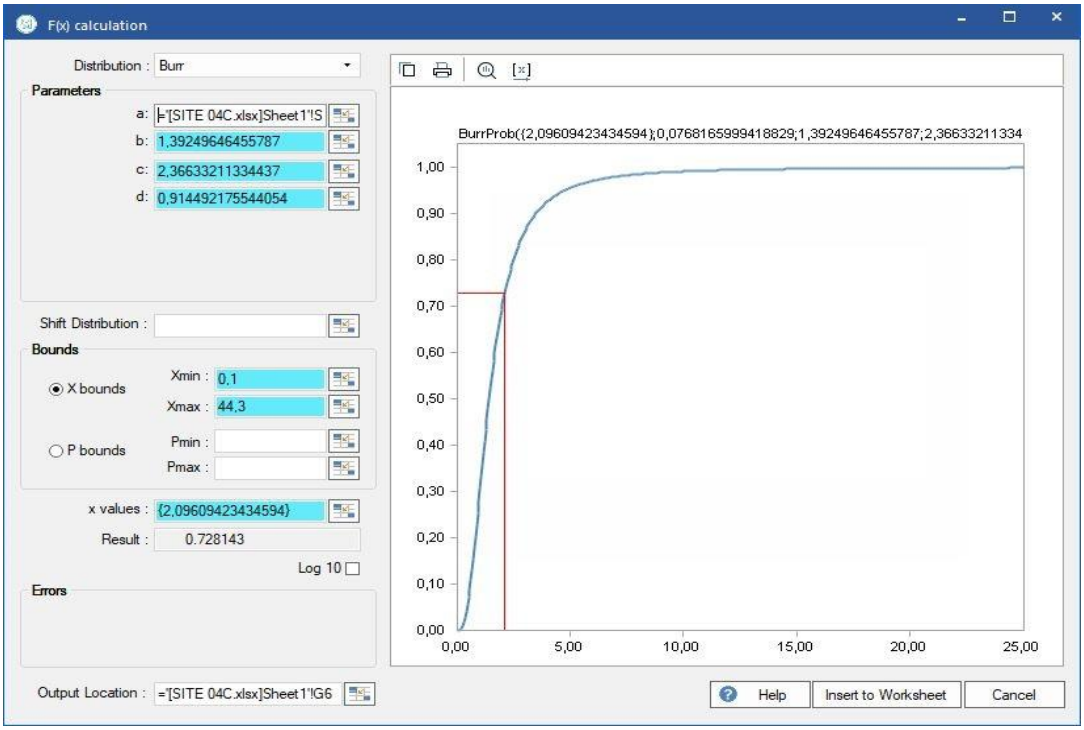

Figure 6. 29: P-Value Plot for SS004 (Peak)

Step 3: Analysis of **Off – Peak** Traffic Headway Distribution Data

Recall the extracted empirical hourly traffic volume data shown in Table 4.12 of chapter 4. Table 6.17 shows the descriptive statistics of the observed time headways for site SS004 at off-peak.

Table 6. 17: Descriptive Statistics of the Time Headways – SS004 (Off-Peak)

Descriptive Statistics	SS004
Mean	3.022636
Standard Error	0.184298
Median	1.5
Mode	1
Standard Deviation	6.112469
Coefficient of Variation	2.04
Sample Variance	37.36228
Kurtosis	29.56445
Skewness	5.228683
Range	51.9
Minimum	0.1
Maximum	52
Sum	3324.9
Sample Size	1100

Step 4: Fitting of continuous probability distribution models to headway data

Using the Model Risk software, probability models were fitted to the headway data, and the PDF, CDF, P-P plots and the P-value with its plot of the best-fitted distribution were generated from the software. Figures 6.30, 6.31, 6.32, and 6.33 show the PDF, P-P, CDF, and P-Value plots respectively.

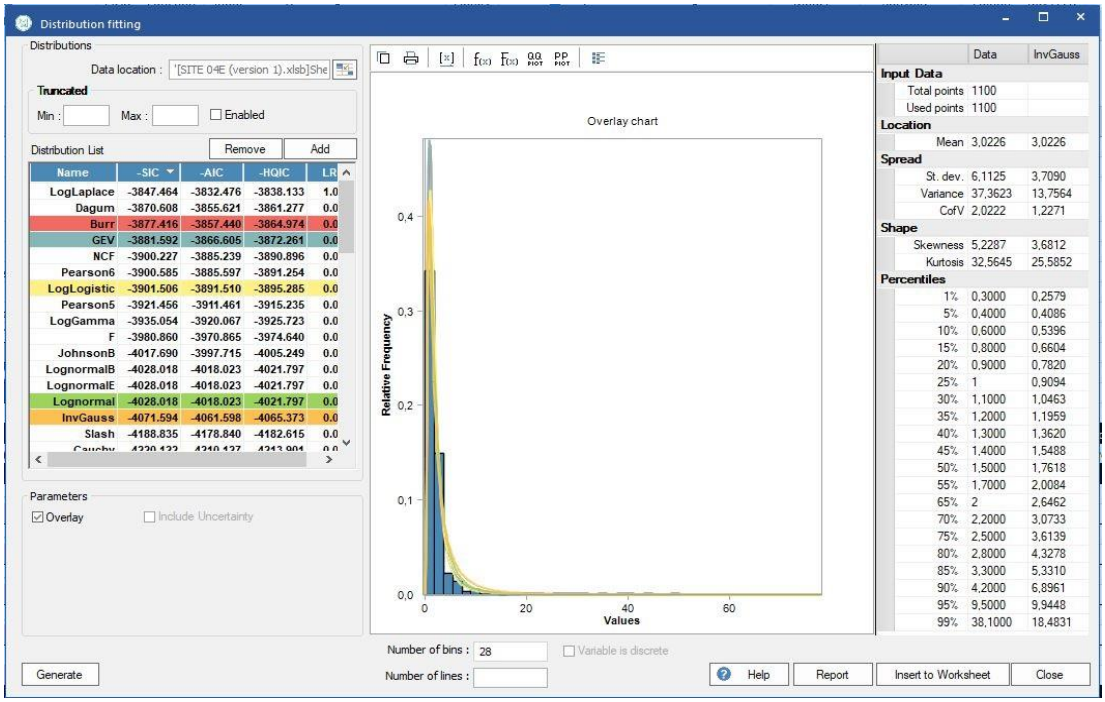

Figure 6. 30: PDF Plot for SS004 (Off-Peak)

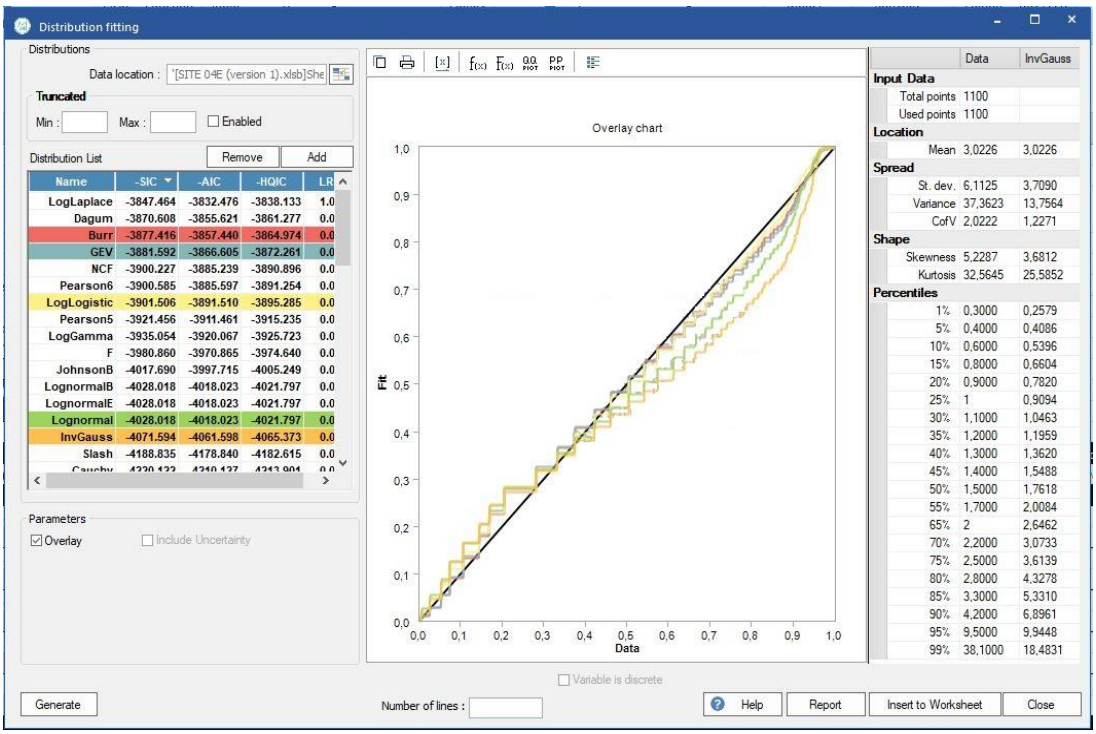

Figure 6. 31: P-P Plot for SS004(Off-Peak)

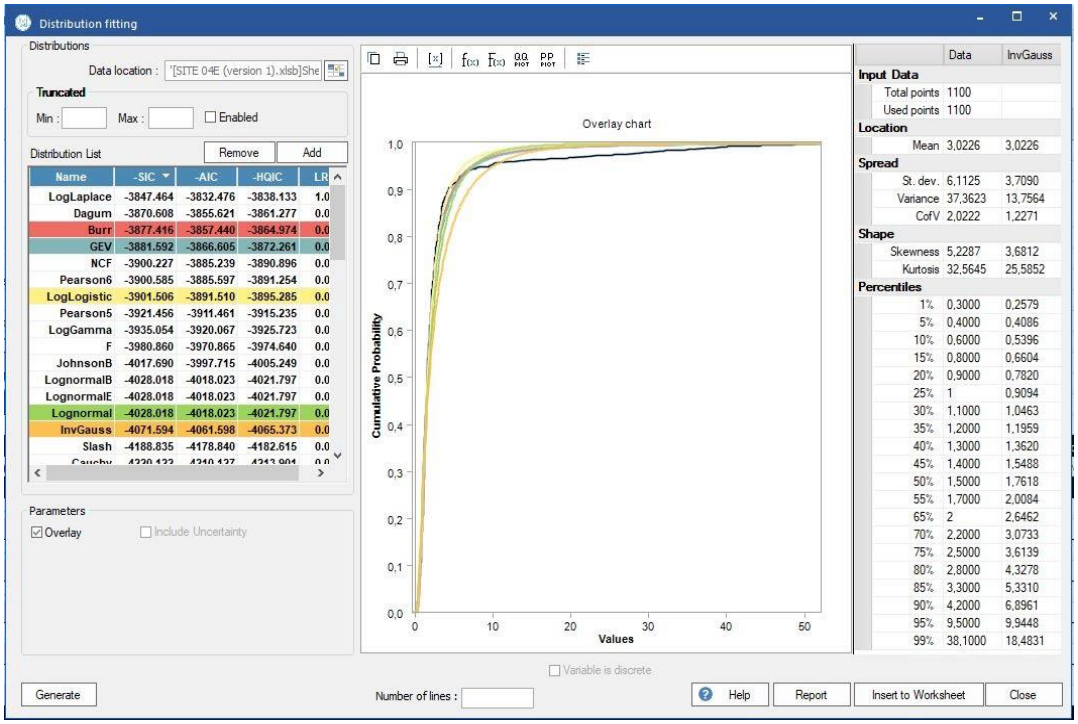

Figure 6. 32: CDF Plot for SS004 (Off-Peak)

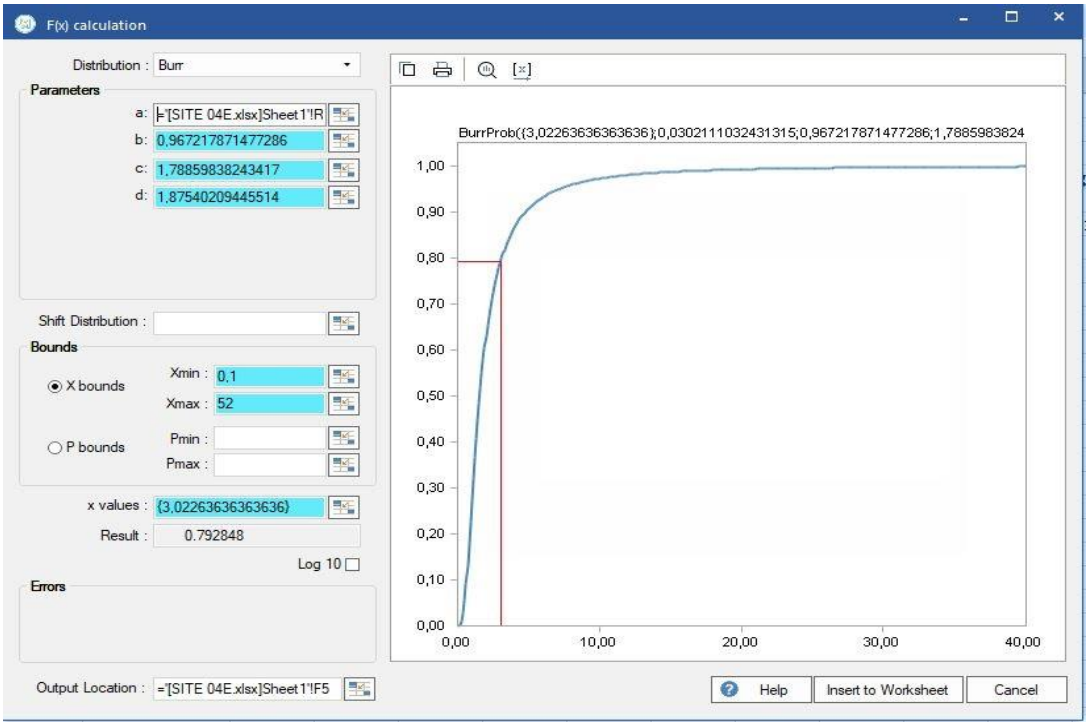

Figure 6. 33: P-Value Plot for SS004 (Off-Peak)

Step 5: Hypothesis testing of the fitted distribution models using the AIC, SIC, and HQIC. A summary of how the fitted distribution models performed is presented in Table 6.18.

Table 6. 18: Goodness of Fit and Model Performance Summary – SS004

Location	Rank	Prob. Model	SIC	AIC	HQIC	LLH	Sig. Level	P Value	Hyp. Test	Best Fit
SS004 (Peak)	2ND	Log Logistic	4722.01	4711.25	4715.24	-2353.62	0.05	0.73	Accept	Burr
	1ST	Burr	4729.79	**4708.28**	4716.25	**-2350.13**	0.05	0.73	Accept	
	3RD	GEV	4753.72	4737.57	4743.56	-2365.78	0.05	0.72	Accept	
	4TH	Lognormal	4853.00	4842.24	4846.23	-2419.11	0.05	0.70	Accept	
	5TH	InvGauss	4985.45	4974.68	4978.67	-2485.34	0.05	0.66	Accept	
SS004 (Off-Peak)	1ST	Burr	3877.44	**3857.44**	3864.97	**-1924.70**	0.05	0.79	Accept	Burr
	2ND	GEV	3881.59	3866.61	3872.26	-1930.29	0.05	0.78	Accept	
	3RD	Log Logistic	3901.51	3891.51	3895.29	-1943.75	0.05	0.81	Accept	
	4TH	Lognormal	4028.02	4018.02	4021.80	2007.01	0.05	0.74	Accept	
	5TH	InvGauss	4071.59	4061.60	4065.37	-2028.79	0.05	0.69	Accept	

*SIC ~ Schwarz Information Criterion; AIC ~ Akaike Information Criterion; HQIC ~ Hannan Quinn Information Criterion; LLH ~ Log likelihood; P ~ Probability *IC used for Ranking - AIC*

As shown in Table 6.18, it can be observed that five continuous probability distribution models were fitted to the empirical time headway data viz: Lognormal, Inverse Gaussian, Generalized Extreme Value (GEV), Log-logistic, and Burr. The models were ranked according to performance using the AIC, SIC, and HQIC criteria as mentioned earlier. Sequel to ranking and comparison with the SIC and HQIC, the smallest AIC value determines the overall best-performed model. Although at peak traffic period, the Burr distribution was the best-performed model, with the lowest AIC value of 4708.28, and the largest Log-likelihood (LLH) value of -2350.13. However, the off-peak traffic is the concern of this analysis under the steady flow condition considered. The Burr distribution performed the best with the lowest AIC value of 3857.44 and the largest LLH value of -1924.70. The P-values, taken directly from the p-value plot are acceptable and within the range of 0.66 and 0.81.

Step 6: Determination of, and comparison of the model parameters.

A summary of the probability distribution model parameters is shown in Table 6.19.

Table 6. 19: Summary of Probability Distribution Parameters – SS004

Location	Probability Distribution	Shape Parameters		Scale Parameter	Location Parameter
SS004 (Peak)	Log Logistic	2.4604	-	1.4014	
	Burr	0.0768	1.3925	2.3663	0.9145
	GEV	1.0954	-	0.7220	0.3746
	Lognormal	1.8995	-	1.6925	-
	InvGauss	2.0961	-	2.2354	-
SS004 (Off-Peak)	Burr	0.0302	0.9672	1.7886	1.8754
	GEV	1.1975	-	0.8663	0.5389
	Log Logistic	2.1681	-	1.5755	-
	Lognormal	2.5016	-	2.7745	-
	InvGauss	3.0226	-	2.0075	-

As shown in Table 6.19, the distributions fitted to the time headways revealed varied estimated parameters. Amongst these distributions, only the Lognormal, Inverse Gaussian, and Log-logistic have two parameters (shape and scale). The Burr distribution has all four parameters (two shape parameters, 1 scale, and 1 location), while the GEV distribution has three which are the shape, scale, and location parameters. Each of the parameters of the distributions varied in different proportions and they revealed the expected outcomes. Their magnitudes and differentials are significant.

Step 7: Comparison of the average time headways of the without (empirical data) and with BRT scenarios vis a vis level of capacity Utilization. Table 6.20 shows the summary of the comparison between the average time headway of the BRT scenarios.

Table 6. 20: Summary of Probability Distribution Parameters – SS004

Location	Mean Time Headway T_h (Without BRT)	Mean Time Headway T_h (With BRT)	LCU
SS004 (Off-Peak)	3.02	1.7	C

6.5 Comments on Descriptive Statistics of the Time Headway Data

Tables 6.1, 6.2, 6.6, 6.7, 6.11, 6.12, 6.16, and 6.17 have presented a summary of the statistical characteristics of the headways collected from each of the four sites surveyed. Between SS001 and SS003, the mean headway decreased, while there was a significant increase at SS004 during the morning peak period. This is due to the low traffic volumes observed at SS004 at that period. This explanation for this is that traffic volumes are higher only during the evening

peaks, especially when commuters are returning from their places of work. The standard deviation exhibited similar behaviour. The trend in the coefficient of variation indicates that there is a cluster of headways on the roadway segments, particularly at sections near intersections where long queues at morning or evening peak traffic flows quickly form because the constraints caused by the introduction of BRT dedicated lanes have eliminated one of the three previously available lanes, causing long queues to quickly build up. This was physically observed during the survey period. The time headway variable's positive skewness and kurtosis all indicate that most of the distribution's headways are to the left of the mean value, which suggests that the road segment may have smaller headways or isolated clusters.

6.6 Comments on Fitted Probability Distribution Models

The probability density function $f(x)$ or (PDF), P-P plots, CDF, and P-value plots for each site, as displayed in figures 6.2 to 6.31 indicate how well each distribution fitted the observed time headways for each flow scenario. The best-performed distribution was determined from the report of the distribution fit software and ranked by the lowest value of AIC, SIC, and HQIC respectively. The AIC value was used to determine the best-fitted distribution. All the other distributions were ranked accordingly based on the magnitude of the three information criteria. All the distributions fitted the headway data well by visual inspection as shown by the PDF and P-P plots which clearly show the time headway distribution resting on the line of best fit. However, hypothesis testing was required to properly evaluate the performance of the models with respect to the determined values of AIC, SIC, and HQIC from the ModelRisk software.

6.7 Comments on the Hypothesis Testing and Performance of the Probability Distribution Models

At SS001, it would be observed from the results of the ModelRisk software displayed in Table 6.3 that the continuous probability distributions were ranked based on their performance from 1 to 5, where 1 represents the best fitted and performed model, while 5 indicates the least performed model. The Generalized Extreme Value (GEV) distribution best fitted the headway distribution at peak traffic, while the Inverse Gaussian distribution best fitted the off-peak traffic data, having each emerged with rank number 1. Besides, the large loglikelihood values of the models also confirmed this. The P-Values, which ranged between 0.69 and 0.74, showed the likelihood of the occurrence of the data sets under the null hypothesis.

At SS002, it can be observed from the results of the ModelRisk software displayed in Table 6.8 that the Burr distribution had the overall best performance, having emerged with rank number 1 at both the peak and off-peak traffic. It was closely followed by the Generalized Extreme Value (GEV) distribution which perform. The Burr distribution also returned as the distribution with the largest log-likelihood value as shown. The P-Values, which ranged between 0.69 and 0.81, showed the likelihood of the occurrence of the data sets under the null hypothesis.

At SS003, it would be observed from the results of the ModelRisk software displayed in Table 6.13 that the Burr distribution also had the overall best performance, having emerged with rank number 1 at both the peak and off-peak traffic. It was closely followed by log-logistic and Generalized Extreme Value (GEV) distributions. The Burr distribution also returned as the distribution with the largest log-likelihood value as shown. The P-Values, which ranged between 0.65 and 0.78, showed the likelihood of the occurrence of the data sets under the null hypothesis.

At SS004, it would be observed from the results of the ModelRisk software displayed in Table 6.18 that the Burr distribution again had the overall best performance, having emerged with rank number 1 at both the peak and off-peak traffic. It was closely followed by Inverse Gaussian and log-logistic distributions. The Burr distribution also returned as the distribution with the largest log-likelihood value as shown. The P-Values, which ranged between 0.66 and 0.82, showed the likelihood of the occurrence of the data sets under the null hypothesis.

6.8 Comments on the Model Parameters

The distributions fitted to the time headways revealed varied model parameters. Amongst these distributions, only the Lognormal, Inverse Gaussian, and Log logistic distributions have two parameters (shape and scale). The Burr distribution has four parameters i.e., two shape parameters, one scale, and one location parameter, while the GEV distribution has three which are the shape, scale, and location parameters. Each of the parameters of the distributions varied in different proportions across the four sites. Their magnitudes and differentials are significant in all the sites investigated. A similar, yet anomalous increase and decrease in the magnitudes of the four parameters associated with each probability distribution was observed for each flow scenario investigated in all the sites. For instance, the shape and scale parameters of the Lognormal, log-logistic, and Inverse Gaussian, increased and decreased steadily across the four sites. The first shape parameter of the Burr distribution was also observed to be negative in all

the sites and for each flow scenario. The only explanation for these variabilities as well as the observed increase and decrease is that all the sites have different traffic characteristics with respect to flow, free flow speed, density, and of course, the vehicle time headways.

6.9 Summary

This chapter presented the implications of BRT on time headways. The time headways analyzed were the empirical or observed headway data extracted from the ATC. They were fitted to continuous probability distribution models and found to be continuously distributed. The stochastic nature of the time headway distributions from the descriptive statistics also showed the attendant erratic behaviour of the drivers due to the cluster of headways from the skewness values. The fitted probability distributions were lognormal, log logistic, Generalized Extreme Value (GEV), Inverse Gaussian, and Burr. The fitted distributions were subjected to hypothesis testing using the Akaike Information Criterion (AIC), Schwarz Information Criterion (SIC), and Hannan Quinn Information Criterion (HQIC) performance indicators and measures of goodness of fit. The AIC value was used as the determining criterion to identify the distribution that provided the best fit. Besides the distribution with the lowest value of AIC and largest Log likelihood values were selected as the best-fitted models. The analysis through the ModelRisk software also revealed model parameters whose values conformed with the expected values for the traffic flows investigated. In summary, this analysis has revealed that BRT dedicated lanes cause bottle neck flows on the adjoining lanes due to speed reduction, characterized by erratic, stochastic, and unsafe time headways which can easily lead to traffic congestion, especially from queues that quickly build up near intersections. Other concerns of reduced time headways are the safety of commuters waiting at the curb side to cross to the BRT station at the median of the carriage way. The safety of other pedestrians that may want to cross the roadway at some other points along the segment is also threatened. However, the overarching and expected implications from this study are for capacity utilization to be enhanced through minimized time headways, which has been shown by this study, as the with BRT scenario showed a reduction in time headway from the without BRT scenario, and the LCU improved to C as revealed by the criteria table developed. Consequently, this is the reason why consideration of mixed traffic flow with BRT is necessary, and secondly for easy accessibility of BRT buses at the curbside which would be a solution to the safety concerns. The next chapter 7 draws conclusions and recommendations based on the study findings.

CHAPTER 7

CONCLUSIONS

This study has attempted to assess the influence of Bus Rapid Transit (BRT) on roadway capacity utilization and their implications for time headways in Cape Town, South Africa. It investigated roadway capacity utilization for road link sections 'with and without' BRT influence and road capacity utilization of BRT dedicated lanes. Roadway capacity was the number of vehicles per hour per road section per carriageway lane. BRT was taken as physical constraints on roadways significant enough to act as impediments to an otherwise free traffic flow by significantly reducing vehicles' speed. Also, the contribution of BRT to traffic flows, vehicle speeds, and densities was established.

The study was based on the hypothesis that roadway capacity utilization differentials resulting from Bus Rapid Transit (BRT) are significant. It was conducted at four selected locations in Cape Town, South Africa. Roadway capacity was estimated using the quadratic function and the fundamental relationship between flow, speed, and density. The empirical results obtained from the capacity analysis were further investigated in light of evidence obtained from examining survey data. Based on the synthesis of evidence obtained from the relationship between roadway capacity utilization and BRT, it is correct to conclude that road capacity utilization from BRT fully dedicated lane suggests that no lasting solution to traffic flow challenges will be found unless that solution addresses the issue of roadway capacity utilization loss resulting from BRT dedicated lanes. In summary, the study has:

1. Developed a functional Level of Capacity Utilization (LCU) criteria table for the assessment of road capacity utilization.
2. Shown that a dedicated BRT lane would induce significant negative road capacity utilization.
3. Shown that BRT influence on roadway capacity utilization under off-peak traffic conditions is not significant.
4. Shown that the time headway distributions are stochastic in nature and uncertain in the traffic streams.

Speed changes mainly cause anomalous capacity utilization. Other affected traffic characteristics were the time headways which directly reflect the abnormal behaviour of drivers

on the adjoining lanes with bottlenecks and long queues during peak hours. The speed changes are usually a reduction, occasioned by erratic manoeuvres, resulting in travel time increase and service quality deterioration, and level of capacity utilization (LCU) anomalies. Although service quality implication was not part of this investigation, the potential effect of BRT dedicated lanes on service quality was revealed. The findings on the speed and travel time differentials, which are the performance indicators used by service providers and road users, point to the possibility of service quality reduction.

In light of the discussion so far, the remainder of this chapter is organized as follows: Section 7.1 presents the summary of findings based on BRT dedicated lane capacity utilization; Section 7.2 summarizes the findings based on LCU without BRT influence, while Section 7.3 summarizes the findings based on LCU with BRT influence. Section 7.4 presents the summary of findings based on estimated capacity utilization rates. In section 7.5, the findings from the time headway distribution modelling are summarized, while in section 7.6, the way forward is presented.

7.1 Summary of Findings Based on BRT Dedicated Lane Capacity Utilization.

According to the developed LCU criteria table, the capacity utilization on the BRT dedicated lanes across the four sites was at level E, all characterized by low BRT vehicle volumes, high BRT speeds, and reduced travel time. The LCU E implies poor capacity utilization on the BRT dedicated lane when compared to the expected maximum LCU A (control), as shown on the criteria tables developed for each site. At SS001 with LCU E according to the criteria table, the other associated parameters were a density of 3veh/km and a speed of 125km/hr. The corresponding parameters with a LCU E, at site SS002 were a density of 6veh/km and a speed of 100km/hr. Similarly, at site SS003, the attendant LCU parameters were a density of 7veh/km, and a speed of 95km/hr, while at site SS004, the associated LCU parameters from the criteria table were a density of 21veh/km and a speed of 80km/hr. These results have clearly shown that capacity utilization is a function of the number of BRT vehicles on the dedicated lane, hence with LCU E, this implies that the provided BRT dedicated lane width of 4.3m is not wide enough to accommodate more BRT vehicular movements side by side, with the width of each bus being 3.1m. Besides, the lane is dedicated solely for BRT buses, and not shared with other vehicle classes, hence it is logical to conclude from objective (ii) that the BRT dedicated lanes are significantly underutilized.

7.2 Summary of Findings Based on LCU 'without BRT' Influence

Findings based on roadway capacity analysis show that off-peak period maximum capacity utilization of the surveyed roads was seldom reached even though the roads play a significant role in promoting socio-economic growth. Speed distribution fluctuates on the road section without BRT influence, suggesting that drivers are not constrained and hence can choose speed. It is apparent from the distribution of traffic volume and speed on road sections 'with' and 'without' BRT that roadway capacity utilization is a constituent of volume, speed, and density. According to the developed LCU criteria table, the level of capacity utilization analysis without the influence of BRT revealed LCU at C across the four sites investigated. This shows an improvement from the LCU E of the BRT dedicated lane. With the LCU at C, at site SS001, the other associated performance parameters from the table were density of 13veh/km and speed of 95km/hr. At SS002, the corresponding LCU parameters were a density of 21veh/km and a speed of 80km/hr. At SS003, the LCU parameters were a density of 28veh/km, and a speed of 75km/hr, while at site SS004, the associated LCU parameters were a density of 23veh/km, speed of 80km/hr, and travel time of 45s. From these findings, it can be observed that capacity utilization, caused by speed changes is directly proportional to density and travel time, and inversely proportional to speed and time headways. The estimated capacity values were found to be highest at SS003, which had the highest traffic volume. Site SS004 had the second largest capacity estimate, followed by SS002 and SS001 had the least. The difference in estimated capacities was influenced mainly by the frequency of activities around the roadway segments and the type of dwelling or zones around the area. For instance, contributing factor to the high traffic volume at site SS003 is the link between the road segment and densely populated residential and recreational zones. For example, shopping malls like Bayside Mall is located very close to site SS003. Traffic was observed physically to be extremely high at the early morning peaks during the time of the survey. Based on the findings, and from objective (iii), the adjoining lanes carrying mixed traffic without BRT influence are underutilized.

7.3 Summary of Findings Based on LCU 'with BRT' Influence

From the underutilization outcome of the without BRT influence scenario, summarized in section 7.3, it became necessary to consider a mixed traffic situation 'with BRT' influence. The estimated mixed traffic capacity values with BRT influence were seen to be higher than the without BRT scenario. Consequently, the level of capacity utilization analysis with BRT influence has revealed a LCU at C across the four sites investigated. This also shows an improvement from the LCU E of the BRT dedicated lane. With the LCU C, at site SS001, the

other associated performance parameters from the criteria table were a density of 13veh/km and a speed of 95km/hr. At SS002, the corresponding LCU parameters were a density of 21veh/km and a speed of 80km/hr. At SS003, the LCU parameters were a density of 23veh/km, and a speed of 80km/hr, while at site SS004, the associated LCU parameters were a density of 23veh/km and a speed of 80km/hr. From these findings, it can be observed that capacity utilization, caused by speed changes is directly proportional to density, and inversely proportional to speed and time headways. There was no significant difference between the LCU 'without' BRT influence and LCU with BRT influence. This may be due to the possibility of an insufficient number of BRT vehicles in the MyCiTi BRT transit scheme. However, based on the findings, and from objective (iv), the mixed traffic 'with BRT' influence that is considered in this study has a slight improvement in capacity utilization as some of the 5mins flows almost showed improvement in capacity utilization to level B as the estimated capacity utilization rates which are discussed in the next section revealed.

7.4 Summary of Findings Based on Capacity Utilization Rates

Capacity utilization rates had been defined as the ratio of actual periodic (5mins) vehicular flows to the maximum (capacity) allowable flow (1hr). The estimated capacity utilization rates showed significant underutilization ranging from 37% and 79% across all four sites, under the traffic flow scenario without BRT. Besides, traffic characteristics for each site viz the speed, density, and time headways were also estimated for the 'without BRT' traffic scenario during both peak and off-peak periods, as well as the mixed traffic 'with BRT' conditions considered. From the calibrated flow-density model equations, vehicles were observed to be moving at free-flow speeds higher than the posted speed of 70km/hr. The calibrated flow-density models showed that the off-peak traffic free-flow speeds, which are considered the 85^{th} percentile speeds, at which the vehicles were moving on the roadway segments were 145.18km/hr at SS001, 102.17km/hr at SS002, 106.07km/hr at SS003, and 110.11km/hr at SS004. This is also an indication that capacity was indeed underutilized and traffic flow was at the unconstrained free and steady flow region of the flow-density curve. In order words the estimated lane capacities were below the 85 percent threshold capacity. The summary of the mixed traffic capacity utilization with BRT is discussed in the next section.

Results also showed that capacity utilization rates ranged between 40% and 75%, across all four sites under the traffic flow scenario with BRT. Besides, traffic characteristics for each site viz the speed, density, and time headways were also estimated for the 'with BRT' traffic scenario during both peak and off-peak periods. The flow density models showed a drop in

free-flow speeds under the 'with BRT' scenario. The off-peak free-flow speed drops were 137.93km/hr at SS001, 99.33km/hr at SS002, 104.4km/hr at SS003, and 107.94km/hr at SS004. This is also an indication that capacity was indeed underutilized and traffic flow was still at the unconstrained free and steady flow region of the flow-density curve. In other words, the estimated lane capacities were below the threshold capacity ($0.85Q_{max(with\ BRT)}$). Overall, there was no significant difference between the LCU 'without BRT' influence and LCU 'with BRT' influence. This may also be due to the possibility of an insufficient number of BRT vehicles in the MyCiTi BRT transit scheme. However, some of the 5mins flows almost showed improvement in capacity utilization to level B. This is a confirmation that capacity is stochastic and fluctuates from one spot to the other on a roadway.

7.5 Summary of Findings Based on Time Headway Distribution

As aforementioned, the time headway distribution was fitted to probability distribution models. The models fitted the headway data of the 'without BRT' flow scenarios well, at each site by visual inspection of the attendant Probability Density Function (PDF) plots, Cumulative Density Function (CDF) plots, and the Probability plots (P-P). Based on the postulated hypothesis 3, which states that the compatibility of observed time headway distribution with fitted probability distribution model is rejected if ($P - value\ < \alpha$) or accepted ($P - value\ > \alpha$), the Burr distribution from the pilot study was the best-fitted distribution with the largest log likelihood value of -2008 lowest AIC value of 4025.99.

Similarly for the main study, the time headway distribution data were extracted for both peak and off-peak traffic periods, vis-à-vis the traffic volume data generated in Chapter 4. During the peak traffic period at site SS001, the GEV distribution was the best-performed model, with the lowest AIC value of 4350.38, and the largest Log-likelihood (LLH) value of -2175.18. However, at off-peak, the inverse Gaussian distribution performed the best with the lowest AIC value of 4356.01 and the largest LLH value of -2176.00. The P-values were acceptable and within the range of 0.69 and 0.74.

Concerning the model parameters, only the Lognormal, Inverse Gaussian, and Log logistic have two parameters (shape and scale). The Burr distribution has all four parameters (two shape parameters, 1 scale, and 1 location), while the GEV distribution has three which are the shape, scale, and location parameters. Each of the parameters of the distributions varied in different proportions and they revealed the expected outcomes. Their magnitudes and differentials are significant.

At SS002 during the peak traffic period, the Burr distribution was the best-performed model, with the lowest AIC value of 4022.73, and the largest Log-likelihood (LLH) value of -2007.35. However, the off-peak traffic is the concern of this analysis under the steady flow condition considered. The Burr distribution performed the best with the lowest AIC value of 3623.33 and the largest LLH value of -1807.64. The P-values were acceptable and within the range of 0.71 and 0.81.

At SS003 during the peak traffic period, the Burr distribution was the best-performed model, with the lowest AIC value of 2785.34, and the largest Log-likelihood (LLH) value of -1388.65. However, the off-peak traffic is the concern of this analysis under the steady flow condition considered. The Burr distribution performed the best with the lowest AIC value of 4002.73 and the largest LLH value of -1997.35. The P-values were acceptable and within the range of 0.65 and 0.78.

At SS004 during the peak traffic period, the Burr distribution was the best-performed model, with the lowest AIC value of 4708.28, and the largest Log-likelihood (LLH) value of -2350.13. However, the off-peak traffic is the concern of this analysis under the steady flow condition considered. The Burr distribution performed the best with the lowest AIC value of 3857.44 and the largest LLH value of -1924.70. The P-values, taken directly from the p-value plot are acceptable and within the range of 0.66 and 0.81.

Overall, across the sites SS001, SS002, SS003, and SS004, the Burr distribution provided the best fit as it was rated 1st, by all the goodness of fit tests, and performed well by the ratings. The vehicle time headway fitting has shown that the headway distribution data is stochastic and hence needs to be analyzed as such. It has also shown the behaviour of drivers in mixed traffic flows ‘without BRT’ influence, and there was a reduction in the mean time headway of mixed traffic ‘with BRT’ influence as shown in the previous chapter, which implies that capacity utilization will be enhanced if the mean time headway is maintained.

7.6 The Way Forward

The research has clearly shown that capacity underutilization on BRT corridors is primarily caused by the presence of the BRT dedicated lanes and the adopted median configuration design and concludes that the determined capacity utilization levels from this study, benchmarked by the developed LCU criteria tables for each site are the true reflections of the present traffic performance at the study sites investigated. The outcome has however undermined or contradicted the overarching common purpose for which governments of

developing countries approve funds for the design and construction of BRT infrastructure, which is to provide fast and safe mobility of commuters similar to the speed of a fast-moving train or modern tram. While it is true that the speeds at which BRT buses operate can reduce the travel time of commuters or users, another germane purpose for implementing BRT corridors, which governments should consider before giving approvals is capacity utilization.

With respect to capacity utilization, and as stated in chapter 2 of this thesis, it had been erroneously argued that BRT carries more people per lane than mixed vehicular traffic. However, road carriageways are designed for mixed vehicular traffic volumes or capacities and not people per lane. This implies that currently the primary purpose for the introduction of BRT in most countries is centered on improving person or passenger capacity. Thus, it can be argued that there are more passenger movements in a mixed vehicular traffic design consideration, as shown in this study than in operating BRT buses only on the median BRT dedicated lane.

In order words, when the roadway capacity is maximized, under mixed traffic conditions, more people are transported. Contrary to the assumption that a BRT bus, carrying 100 passengers who own a private vehicle each, means that the 100 vehicles have been taken away from the roadway, it can be argued that this assumption cannot hold, as it is uncertain that all the commuters with different demographics and income status, that use BRT buses would own private cars. Therefore, given these shortcomings, and by way of proffering a solution to the problem, the consideration and implementation of mixed traffic configuration design 'with BRT' for future BRT infrastructural developments will be the way to go. The findings from this study have shown that perhaps the introduction of BRT with dedicated lanes was solely for the transportation of persons, especially populations like the one generated by the 2010 World Cup, and not vehicles. The mixed traffic roadway design, therefore, may be considered or incorporated in the design of future BRT infrastructure. This is because the longer this problem lingers, the greater will be the loss in daily GDP, as well as safety concerns due to the high risk of accidents as any pedestrian attempts to cross the adjoining lanes to access BRT and return to the curbside from the BRT station after a trip.

Concerning the fair capacity utilization findings caused by the adopted median configuration design which becomes insignificant during off-peak periods, the recommended mixed traffic consideration from the findings from this study if implemented has the potential to ameliorate any traffic flow burden, besides enhancing capacity utilization. For instance, if a BRT bus breaks down on the dedicated lane, a mixed traffic design 'with BRT' and without dedicated

lanes, would allow the continuous movement of the buses which ought to have been trapped behind the broken-down vehicle. This is possible because with the LCU of the BRT dedicated lane scenario at E, under steady flow conditions and during off-peak periods, the adjoining lanes to BRT dedicated lane would be able to accommodate the trapped vehicle from the BRT dedicated lane. The design can be implemented at sections prone to traffic congestion or at intersections, while median configuration can be maintained at other sections where there is free flow. This would reduce the cost of construction, as it avoids having to construct BRT all through the entire length of a corridor. Alternatively, the curbside configuration design can be adopted. This is a situation where a BRT dedicated lane is constructed on the left-hand side of the roadway. It has the potential capacity to attract more commuters as well as the physically challenged and elderly, hence improving accessibility. This design is currently used in England where BRT buses move on the curbside and to maximize capacity, other vehicles are allowed to use the BRT dedicated lanes at certain times of the day, usually after working hours. At the moment, the BRT system in South Africa is still very young and still needs to be introduced in all the provinces for a fully integrated system as planned. In view of the mixed traffic scenarios considered with and without BRT, it is hereby recommended for future research to consider the evaluation of traffic operations through the development and application of microscopic fundamental diagrams. This approach will provide understanding of the impact of individual vehicles and their relationships with one another in a traffic stream. Furthermore, a simulation of the time headway distribution of the proposed 'with BRT' mixed traffic scenario using transport modelling software such as VISSIM, AIMSUN, etc can also be looked into in order to visualize the traffic flow pattern. In traffic engineering practice, the curbside and mixed traffic designs are therefore recommended for implementation in future BRT infrastructure as the way forward for the South African BRT system for enhanced capacity utilization and sustainable mobility.

REFERENCES

Abtahi, S. M., Tamannaei, M., & Haghshenash, H. (2012). Analysis and Modeling Time Headway Distributions Under Heavy Traffic Flow Conditions in the Urban Highways: Case of Isfahan. *TRANSPORT*, *26*(4), 375-382. https://doi.org/10.3846/16484142.2011.635694

Acai, J., & Amadi-Echendu, J. (2018, 19-23 August 2018). Pavement Infrastructure Sustainability Assessment: A Systematic Review. Portland International Conference on Management of Engineering and Technology (PICMET),

Adams, C. A., Zambang, M. A. M., & Opoku–Boahen, R. (2014). Passenger Car Unit values for urban mixed traffic flow at signalised intersections on two lane dual carriageways in the Tamale Metropolis, Ghana. *International Refereed Journal of Engineering and Science*, *3*(4), 41-49.

Aderinlewo, O. O., Akinyemi, G. A., Afolayan, A., & Modupe, A. E. (2020). Analysis of the Operational Data of a Public Transportion System: A Case Study of the Bus Rapid Transit (BRT), Lagos State, Nigeria. *Journal of Urban and Environmental Engineering*, *14*(1), 87-97.

Adewumi, E. O., & Allopi, D. (2014a). An Appropriate Bus Rapid Transit System. *International journal of science and technology (Wallsend)*.

Adewumi, E. O., & Allopi, D. (2014b). Determining the best BRT for eThekwini. *IMIESA. Institution of Municipal Engineers of Southern Africa*.

Agarbattiwala, T. V., & Bhatt, B. V. (2016). Performance Analysis of BRT System Surat. *International Journal of Engineering Research*, *5*(6), 519-523.

Ahmed, U. (2010). *Passenger car equivalent factors for level freeway segments operating under moderate and congested conditions*. Marquette University.

Akaike, H. (1974). A new look at the statistical model identification. *IEEE transactions on automatic control*, *19*(6), 716-723.

Al-Ghamdi, A. S. (2001). Analysis of time headways on urban roads: case study from Riyadh. *Journal of Transportation Engineering*, *127*(4), 289-294.

Alhassan, H. M., & Ben-Edigbe, J. (2010). *Impact of Rainfall Intensity on Traffic Flow Rates Modelling Techniques* 3rd International Graduate Conference on Engineering, Science and Humanities (IGCESH), School of Graduate Studies, University Teknologi Malaysia.

Alhassan, H. M., & Ben-Edigbe, J. (2012a). Effect of rain on probability distributions fitted to vehicle time headways. *International Journal on Advanced Science, Engineering and Information Technology*, *2*(2), 31-37.

Alhassan, H. M., & Ben-Edigbe, J. (2012b). Effect of Rain on Probability Distributions Fitted to Vehicle Time Headways. *International Journal on Advanced Science, Engineering and Information Technology*, *2*(2), 144. https://doi.org/10.18517/ijaseit.2.2.173

Alhassan, H. M., & Ben-Edigbe, J. (2012c). Extent of highway capacity loss due to rainfall. *International Journal of Civil and Environmental Engineering*, *6*(12), 1154-1161.

Alhassan, H. M., & Ben-Edigbe, J. (2014). Effect of rainfall on traffic flow shock wave propagation. *Journal of Applied Sciences*, *14*(1), 54-59.

Alhassan, H. M., Parameswaren, S., & Johnnie, B.-E. (2012a). Discriminate Modelling of Peak and Off-Peak Motorway Capacity. *International Journal of Integrated Engineering*, *4*(3), 53-58.

Alhassan, H. M., Parameswaren, S., & Johnnie, B.-E. (2012b). Discriminate Modelling of Peak and Off-Peak Motorway Capacity. *International Journal of Integrated Engineering*, *4*(4). https://penerbit.uthm.edu.my/ojs/index.php/ijie/article/view/587

Aropet, R. (2017). Southern African solutions to public transport challenges.

Atkinson, D. (2007). Taking to the streets: Has developmental local government failed in South Africa. *State of the nation: South Africa, 2007*, 53-77.

Ben-Edigbe, Nordiana, M., & Rahman, R. (2014). Effect of Road Lighting on the Quality of Dual Carriageway Road Service. *Research Journal of Applied Sciences, Engineering and Technology*, *7*(5), 950-956.

Ben-Edigbe, J. (2003). Modeling road use for capacity loss resulting from pavement distress. International Conference on Highway Pavement Data, Analysis and Mechanistic Design Applications, 2003, Columbus, Ohio, USA,

Ben-Edigbe, J. (2009). Application of PCE Values in Highway Capacity and LOS Analysis. 13th REAAA Conference Korea,

Ben-Edigbe, J. (2010). Assessment of speed-flow-density functions under adverse pavement condition. *International Journal of Sustainable Development and Planning*, *5*(3), 238-252. https://doi.org/10.2495/sdp-v5-n3-238-252

Ben-Edigbe, J. (2016). Estimation of Midblock Median Opening U-Turn Roadway Capacity Based on Sectioning Method. *Discrete Dynamics in Nature and Society*, *2016*, 1-6. https://doi.org/10.1155/2016/8293240

Ben-Edigbe, J., Alhassan, H., & Aminu, S. (2013). Selective estimations of empirical roadway capacity. *Journal of Engineering & Applied Sciences*, *8*(1), 71-76.

Ben-Edigbe, J., & Ferguson, N. (2005). Extent of capacity loss resulting from pavement distress. Proceedings of the Institution of Civil Engineers-Transport,

Ben-Edigbe, J., & Ibijola, S. O. (2020). Anomalous capacity shrinkage at multi-lane roundabouts due to rainfall. Proceedings of the Institution of Civil Engineers-Transport,

Ben-Edigbe, J., & Johnson, O. (2014). Traffic kinematic waves at road hump zone: Perceptions and analysis. *British Journal of Applied Science & Technology*, *4*(7), 1109-1118.

Ben-Edigbe, J., & Mashros, N. (2012). Extent of highway capacity loss resulting from road humps. *International Journal of Engineering and Technology*, *4*(2), 121.

Ben-Edigbe, J., Rahman, R., & Mashros, N. (2014). Headway distributions based on empirical Erlang and Pearson type III time methods compared. *Research Journal of Applied Sciences, Engineering and Technology*, *7*(21), 4410-4414.

Berechman, J. (1984). Highway-capacity utilization and investment in transportation corridors. *Environment and Planning A*, *16*(11), 1475-1488.

Biswas, S., Chandra, S., & Ghosh, I. (2021). Side friction parameters and their influences on capacity of Indian undivided urban streets. *International Journal of Transportation Science and Technology*, *10*(1), 1-19.

BPR. (1964). *Traffic Assignments Manual* (Vol. 2). Bureau of Public Records, Washington DC, USA.

Brilon, W., Geistefeldt, J., & Regler, M. (2005). Reliability of freeway traffic flow: a stochastic concept of capacity. Proceedings of the 16th International symposium on transportation and traffic theory,

Budhkar, A. K., & Maurya, A. K. (2012). Review of Passenger Car Equivalence Studies inIndian Context.

Cervero, R., & Kang, C. D. (2011). Bus rapid transit impacts on land uses and land values in Seoul, Korea. *Transport Policy*, *18*(1), 102-116. https://doi.org/10.1016/j.tranpol.2010.06.005

Chandra, S., & Sikdar, P. (2000). Factors affecting PCU in mixed traffic situations on urban roads. *Road and transport research*, *9*(3), 40-50.

Chen, X. M., Li, Z., Jiang, H., & Li, M. (2015). Investigations of interactions between bus rapid transit and general traffic flows. *Journal of Advanced Transportation*, *49*(3), 326-340. https://doi.org/10.1002/atr.1268

Chengula, D., & Kombe, K. (2017). Assessment of the Effectiveness of Dar Es Salaam Bus Rapid Transit (DBRT) System in Tanzania. *Int. J. Sci*, *36*, 10-30.

Das, S., & Maurya, A. K. (2017). Time headway analysis for four-lane and two-lane roads. *Transportation in developing economies*, *3*(1), 9.

Das, S., & Maurya, A. K. (2018). Multivariate analysis of microscopic traffic variables using copulas in staggered car-following conditions. *Transportmetrica A: Transport Science*, *14*(10), 829-854. https://doi.org/10.1080/23249935.2018.1441200

Das, S., & Maurya, A. K. (2020). Bivariate modeling of time headways in mixed traffic streams: a copula approach. *Transportation Letters*, *12*(2), 138-148. https://doi.org/10.1080/19427867.2018.1537209

Das, S., Maurya, A. K., & Budhkar, A. K. (2019). Determinants of time headway in staggered car-following conditions. *Transportation Letters*, *11*(8), 447-457. https://doi.org/10.1080/19427867.2017.1386872

De Jongh, F., & Bruwer, M. (2017). Quantification of the natural variation in traffic flow on selected national roads in South Africa.

Devasurendra, K. W., Wirasinghe, S., & Kattan, L. (2020). A critical review of transit level of service measures and an overview of a proposed new approach. International Conference on Transportation and Development 2020,

Dowling, R., & Skabardonis, A. (1993). Improving average travel speeds estimated by planning models. *Transportation research record*, 68-68.

Dowling, R., Skabardonis, A., & Alexiadis, V. (2004). *Traffic analysis toolbox, volume III: Guidelines for applying traffic microsimulation modeling software*.

Duy-Hung, H. M., Aron Simon, Cohen. (2012). Time headway variable and probabilistic modeling. *Transportation Research Part C: Emerging Technologies*, *25*, 181-201. https://doi.org/http://dx.doi.org/10.1016/j.trc.2012.06.002

Edie, L. C. (1961). Car-following and steady-state theory for noncongested traffic. *Operations research*, *9*(1), 66-76.

Ehsan, R.-K., Fereidoon, M. N., & Masoud, T. (2020). A Study on Following Behavior Based on the Time Headway. *Jurnal Kejuruteraan*, *32*(2), 187-195, Article 2. https://doi.org/https://doi.org/10.17576/jkukm-2020-32(2)-02

Elefteriadou, L., & Lertworawanich, P. (2003). Defining, measuring and estimating freeway capacity. 82nd Annual Meeting of the Transportation Research Board, Washington, DC,

Falkner, J. (2012). South African Numbered Route Description and Destination Analysis (Report). *National Department of Transport.*, 1-6.

Fedderke, J., & Garlick, R. (2008). Infrastructure development and economic growth in South Africa: A review of the accumulated evidence. *Policy paper*, *12*.

Gartner, N. H., Messer, C. J., & Rathi, A. (2002). Traffic flow theory-A state-of-the-art report: revised monograph on traffic flow theory.

Gauthier, A., & Weinstock, A. (2010). Africa Transforming Paratransit into BRT. *Built Environment*, *36*(3), 317-327. https://doi.org/10.2148/benv.36.3.317

Gibreel, G. M., El-Dimeery, I. A., Hassan, Y., & Easa, S. M. (1999). Impact of highway consistency on capacity utilization of two-lane rural highways. *Canadian Journal of Civil Engineering*, *26*(6), 789-798.

Goodall, N. J., Smith, B. L., & Park, B. (2013). Traffic Signal Control with Connected Vehicles. *Transportation Research Record: Journal of the Transportation Research Board*, *2381*(1), 65-72. https://doi.org/10.3141/2381-08

Greenshields, B., Bibbins, J., Channing, W., & Miller, H. (1935). A study of traffic capacity. Highway research board proceedings,

Gulivindala, P., & Mehar, A. (2018). Analysis of side friction on urban arterials. *Transport and Telecommunication*, *19*(1), 21-30.

Hall, F. L., & Agyemang-Duah, K. (1991). Freeway capacity drop and the definition of capacity. *Transportation research record*(1320).

Hannan, E. J., & Quinn, B. G. (1979). The determination of the order of an autoregression. *Journal of the Royal Statistical Society: Series B (Methodological)*, *41*(2), 190-195.

Hashem, I. A. A., Kalbouneh, J. N. F., & Amoudi, S. A. S. (2016). Bus Rapid Transit (BRT) System: Nablus Case study.

HCM7. (2022). *Highway Capacity Manual 7th Edition: A Guide for Multimodal Mobility Analysis*. The National Academies Press. https://doi.org/doi:10.17226/26432

HCM. (2010). Concepts. *Transportation Research Board, National Research Council, Washington, DC*, *1207*.

HCMTRB. (2012). Transportation Research Board of the National Academies. *Washington, DC*, *2010*, 20.

Heggie, I. G. (1995). Management and financing of roads. *World Bank technical paper*(275).

Heydecker, B., & Addison, J. D. (2011). Analysis and modelling of traffic flow under variable speed limits. *Transportation Research Part C: Emerging Technologies*, *19*(2), 206-217.

Homan, T. C. (2012). *Freeway work zone capacity: empirical research on work zone capacity in the Netherlands* University of Twente].

Jang, J. (2012). Analysis of time headway distribution on suburban arterial. *KSCE Journal of Civil Engineering*, *16*(4), 644-649.

Jia, Z., Varaiya, P., Chen, C., Petty, K., & Skabardonis, A. (2000). Congestion, excess demand, and effective capacity in California freeways. *Online at pems. eecs. berkeley. edu*.

Jinhwan, J. (2012). Analysis of Time Headway Distribution on Suburban Arterial. *KSCE Journal of Civil Engineering*, *16*(4), 644-649. https://doi.org/DOI 10.1007/s12205-012-1214-4

Kaplan, E. L., & Meier, P. (1958). Nonparametric estimation from incomplete observations. *Journal of the American statistical association*, *53*(282), 457-481.

Keller, E. L., & Saklas, J. G. (1984). Passenger car equivalents from network simulation. *Journal of Transportation Engineering*, *110*(4), 397-411.

Khan, S. I., & Maini, P. (1999). Modeling Heterogeneous Traffic Flow. *Transportation Research Record: Journal of the Transportation Research Board*, *1678*(1), 234-241. https://doi.org/10.3141/1678-28

Khanorkar, A., Ghodmare, S., & Khode, B. (2014). Impact of lane width of road on passenger car unit capacity under mix traffic condition in cities on congested highways. *International Journal of Engineering*, *4*(5), 180-184.

Kimber, R., McDonald, M., & Hounsell, N. (1985). Passenger car units in saturation flows: concept, definition, derivation. *Transportation Research Part B: Methodological*, *19*(1), 39-61.

Koorey, G. (2007). Passing opportunities at slow-vehicle bays. *Journal of Transportation Engineering*, *133*(2), 129-137.

Krüger, F., Titz, A., Arndt, R., Groß, F., Mehrbach, F., Pajung, V., Suda, L., Wadenstorfer, M., & Wimmer, L. (2021). The Bus Rapid Transit (BRT) in Dar es Salaam: A Pilot Study on Critical Infrastructure, Sustainable Urban Development and Livelihoods. *Sustainability*, *13*(3), 1058. https://doi.org/10.3390/su13031058

Kutz, M. (2011). *Handbook of Transportation Engineering, Volume II: Applications and Technologies*. McGraw-Hill Education.

Lawless, J. F. (2011). *Statistical models and methods for lifetime data*. John Wiley & Sons.

Lay, M. G. (2009). *Handbook of road technology*. CRC Press.

Levinson, H. S., Zimmerman, S., Clinger, J., Bast, J., Rutherford, S., & Bruhn, E. (2003). *Bus rapid transit, volume 2: Implementation guidelines*.

Levinson, H. S., Zimmerman, S., Clinger, J., & Gast, J. (2003). Bus rapid transit: Synthesis of case studies. *Transportation research record*, *1841*(1), 1-11.

Lieu, H. (1999). Traffic-flow theory. *Public Roads*, *62*(4).

Lilley, M. (2012). The NZ Transport Agency Highways and Network Operations Traffic Control Devices Trials Update. Australasian Road Safety Research Policing Education Conference, 2012, Wellington, New Zealand,

Makinde, O., & Ben-Edigbe, J. (2019). Night-Time Rainfall Effect on Road Service and Travel Time Loss: A Case Study of Roadway without Light. *International Journal of Applied Engineering Research*, *14*(11), 2773-2781. http://www.ripublication.com

Mallikarjuna, C. (2007). *Analysis and modeling of heterogeneous traffic* IIT Delhi].

Marais, K. (2015). *Traffic Impact Study*. K. C. Engineers.

Mashros, N., & Ben-Edigbe, J. (2014). Determining the quality of highway service caused by rainfall. Proceedings of the Institution of Civil Engineers-Transport,

Maurya, A., Dey, S., & Das, S. (2015). Speed and time headway distribution under mixed traffic condition. *Journal of the Eastern Asia Society for Transportation Studies*, *11*, 1774-1792.

Mehar, A., Chandra, S., & Velmurugan, S. (2014). Passenger car units at different levels of service for capacity analysis of multilane interurban highways in India. *Journal of Transportation Engineering*, *140*(1), 81-88.

Minderhoud, M., Botma, H., & Bovy, P. (1996). An Assessment of Roadway Capacity Estimation Methods. Transportation and Traffic Engineering Section, Report No. VK 2201. 302/LVV 0920-0592. *Delft University of Technology, Delft*.

Minderhoud, M., Botma, H., & Bovy, P. (1998). Roadway capacity using the product-limit approach. 77th Annual Meeting of the Transportation Research Board, Washington DC,

Minderhoud, M. M., Botma, H., & Bovy, P. H. (1997). Assessment of roadway capacity estimation methods. *Transportation research record*, *1572*(1), 59-67.

Mitchell, M. (2014). A brief history of transport infrastructure in South Africa up to the end of the 20th century Chapter 8: the development of a national road system during the second half of the 20th century: infrastructure. *Civil Engineering= Siviele Ingenieurswese*, *2014*(8), 55-59.

Modupe, A., & Ben-Edigbe, J. (2022). Influence of Bus Rapid Transit (BRT) on Anomalous Road Capacity Utilization. International Conference on Transportation and Development 2022,

Modupe, A., & Ben-Edigbe, J. (2023). Modelling Mixed Traffic Time Headway Distribution Induced by Bus Rapid Transit (BRT) in Cape Town, South Africa. *The Open Transportation Journal*, *17*(1). https://doi.org/10.2174/18744478-v17-230811-2023-4

Mohan, R., & Ramadurai, G. (2013). Heterogeneous traffic flow modelling using macroscopic continuum model. *Procedia-Social and Behavioral Sciences*, *104*, 402-411.

Moridpour, S. (2014). Evaluating the time headway distributions in congested highways. *Journal of Traffic and Logistics Engineering Vol*, *2*(3). https://doi.org/DOI:10.13140/2.1.1638.3682

Neena, M. J. B., Jolly, Gayathry, N. P. H., S. Joseph, Roy, & Salini, P. N. (2018). Link Volume And Capacity Utilisation Of Roads in Kondotty Town. *International Research Journal of Engineering and Technology (IRJET)*, *5*(2), 1576 - 1580.

Oyaro, J., & Ben-Edigbe, J. (2020). The extent of capacity loss caused by rainfall at signalised intersections. *The Open Transportation Journal*, *14*(1).

Pasindu, H., Gamage, D., & Bandara, J. (2020). Framework for selecting pavement type for low volume roads. *Transportation research procedia*, *48*, 3924-3938.

Patel, C. R., & Joshi, G. (2012). Capacity and LOS for urban arterial road in Indian mixed traffic condition. *Procedia-Social and Behavioral Sciences*, *48*, 527-534.

Rao, A. M., Velmurugan, S., & Lakshmi, K. (2017). Evaluation of influence of roadside frictions on the capacity of roads in Delhi, India. *Transportation research procedia*, *25*, 4771-4782.

Riccardo, R., & Massimiliano, G. (2012). An empirical analysis of vehicle time headways on rural two-lane two-way roads. *Procedia-Social and Behavioral Sciences*, *54*, 865-874.

Ross, D., & Townshend, M. (2018). An economics-based road classification system for South Africa. 37th Annual Southern African Transport Conference (SATC 2018),

Roy, R., & Saha, P. (2018). Headway distribution models of two-lane roads under mixed traffic conditions: a case study from India. *European Transport Research Review*, *10*(1), 1-12.

Salisu, U. O., Oyesiku, O. O., & Odufuwa, B. O. (2020a). Highway Development and Capacity Utilisation in Ogun State, Nigeria. *LOGI – Scientific Journal on Transport and Logistics*, *11*(1), 66-77. https://doi.org/10.2478/logi-2020-0007

Salisu, U. O., Oyesiku, O. O., & Odufuwa, B. O. (2020b). Highway Development and Capacity Utilisation in Ogun State, Nigeria. *LOGI–Scientific Journal on Transport and Logistics*, *11*(1), 66-77.

SANDoT. (2007). Southern African Development Community road traffic signs manual. In: National Department of Transport Pretoria.

Schwarz, G. (1978). Estimating the dimension of a model. *The annals of statistics*, 461-464.

Scorcia, H., & Munoz-Raskin, R. (2019). Why South African cities are different? Comparing Johannesburg's Rea Vaya bus rapid transit system with its Latin American siblings. *Case studies on transport policy*, *7*(2), 395-403. https://doi.org/https://doi.org/10.1016/j.cstp.2019.01.010

Shalini, K., & Kumar, B. (2014). Estimation of the passenger car equivalent: a review. *International Journal of Emerging Technology and Advanced Engineering*, *4*(6), 97-102.

Shao, C. F., Xiao, C. Z., Wang, B. B., & Meng, M. (2015). Speed-density relation model of congested traffic flow under minimum safety distance constraint. *Jiaotong Yunshu Gongcheng Xuebao/Journal of Traffic and Transportation Engineering*, *15*(1), 92-99.

Sharma, S., Redhu, P., & Gupta, A. (2021). Analyses of lattice traffic flow model on a gradient highway.

Sipos, A. A.-D. T. (2019). Performance evaluation of bus rapid transit (BRT) operation in New Delhi using microscopic traffic simulation model.

Smith, A., & Visser, A. (2001). A South African road network classification based on traffic loading. *M Eng project report, University of Pretoria*.

Stone, T. (2009). There's nothing like BRRRRT: transport. *IMIESA*, *34*(4), 62-65.

Sugiarto, S., & Saleh, S. M. (2015). An assessment of The Capacity Drops at The Bottleneck Segments: A review on the existing methodologies. *Aceh International Journal of Science and Technology*, *4*(2), 64-77.

Suhas Vijay Patil, P. (2015). Development of passenger car units (pcu), case study-nal stop, pune. *International Journal of Science and Engineering*, *pg-89-95*.

Sun, D., Lv, J., & Paul, L. (2007). Calibrating passenger car equivalent (PCE) for highway work zones using speed and percentage of trucks. *World*.

Tanyel, S., Çalişkanelli, S. P., Aydin, M. M., & Utku, S. B. (2013). An investigation of heavy vehicle effect on traffic circles. *Teknik Dergi*, *24*(120).

Tchanche, B. (2019). A view of road transport in Africa. *African Journal of Environmental Science and Technology*, *13*(8), 296-302. https://doi.org/10.5897/ajest2018.2575

TCQSM. (2013). *Transit capacity and quality of service manual* (978-0-309-28344-1). http://nap.edu/24766

Technote10. (2013). *Technical note 10-what is the capacity of the road network for private motorised traffic and how has this changed over time* (Transport for London)

Thamizh Arasan, V., & Koshy, R. (2003). Headway distribution of heterogeneous traffic on urban arterials. *Journal of the Institution of Engineers. India. Civil Engineering Division*, *84*(nov), 210-215.

Umadevi, G., & Suresh, V. (2014). Empirical methods of capacity estimation of urban roads. *Global Journals of Research in Engineering*, *14*(J3), 9-23.

van Arem, B., Van Der Vlist, M., De Ruiter, J., Muste, M., & Smulders, S. (1994). Design of the Procedures for Current Capacity Estimation and Travel Time and Congestion Monitoring.

van Rensburg, J., & Krygsman, S. (2020). Funding for roads in South Africa: Understanding the principles of fair and efficient road user charges. *Transportation research procedia*, *48*, 1835-1847.

Van Toorenburg, J. (1986). Praktijwaarden voor de capaciteit. *Rijkswaterstaat dienst Verkeerskunde, Rotterdam*.

Venter, C. (2013). The lurch towards formalisation: Lessons from the implementation of BRT in Johannesburg, South Africa. *Research in Transportation Economics*, *39*(1), 114-120.

Veramoothea, P., Breytenbach, A., & Baloyi, E. (2015). Functional classification of the Gauteng provincial road network using the South African Road Classification and Access Management Manual (TRH26). *South African Journal of Geomatics*, *4*(3), 264-272.

Verma, A. (2016). Review of studies on mixed traffic flow: perspective of developing economies. *Transportation in developing economies*, *2*(1), 1-16.

Vilakazi, A., & Govender, P. (2014). Commuters' perceptions of public transport service in South Africa. *Journal of Social Sciences (COES&RJ-JSS)*, *3*(1), 258-270. http://www.centreofexcellence.net/J/JSS/JSS

Wang, H., Li, J., Chen, Q.-Y., & Ni, D. (2011). Logistic modeling of the equilibrium speed–density relationship. *Transportation research part A: policy and practice*, *45*(6), 554-566.

Williams, K. M. (2003). NEW TRB REPORT: ACCESS MANAGEMENT MANUAL: TRB COMMITTEE DOCUMENTS THE STATE OF THE ART. *TR News*(228).

Wirasinghe, S. C., Kattan, L., Rahman, M. M., Hubbell, J., Thilakaratne, R., & Anowar, S. (2013). Bus rapid transit – a review. *International Journal of Urban Sciences*, *17*(1), 1-31. https://doi.org/10.1080/12265934.2013.777514

Wood, A. (2014a). Learning through Policy Tourism: Circulating Bus Rapid Transit from South America to South Africa. *Environment and Planning A: Economy and Space*, *46*(11), 2654-2669. https://doi.org/10.1068/a140016p

Wood, A. (2014b). Moving policy: global and local characters circulating bus rapid transit through South African cities. *Urban Geography*, *35*(8), 1238-1254. https://doi.org/10.1080/02723638.2014.954459

Xiao-long, M., Dong-fang, M., Dian-hai, W., & Shan, L. (2015). Modeling of speed-density relationship in traffic flow based on logistic curve. *China Journal of Highway and Transport*, *28*(4), 94.

Yin, S., Li, Z., Zhang, Y., Yao, D., Su, Y., & Li, L. (2009). Headway distribution modeling with regard to traffic status. 2009 IEEE intelligent vehicles symposium,

APPENDIX

APPENDIX I

Publications, Conferences and Training

[redacted]
To: Abayomi Modupe (219091761)

Sun 1/23/2022 7:28 PM

Dear Abayomi Modupe,

On behalf of the Steering Committee of the ASCE International Conference on Transportation & Development (ICTD 2022), I am pleased to notify you that your submission was selected for inclusion in the conference program. **Although originally submitted as a POWERPOINT Presentation, your submission has been accepted as a POSTER Presentation.** ASCE is excited to be hosting ICTD 2022 in-person at the Hyatt Regency in Downtown Seattle, Washington, May 31 – June 3, 2022. The exact date and time of your poster presentation session will be provided in the coming weeks.

Your Presentation:

ID: 1926361

Title: Influence of Bus Rapid Transit (BRT) on Anomalous Road Capacity Utilization

ACCEPTANCE

Confirmation of your acceptance to present at ICTD 2022 is required by Tuesday, February 1, 2022. Email Leanne Shroeder at [redacted] to accept or decline your presentation assignment. Please include your Name, presentation ID#, and title of your email confirmation.

YOUR PRESENTATION MUST BE PRESENTED IN PERSON

All presenters are required to register by the ***speaker registration deadline, March 3rd***, attend and present their presentation in person. If you or someone else from your submission group is not able to attend the conference to present in person, please contact Leanne Shroeder [redacted] and request that your presentation be withdrawn from the program.

Speaker registration codes and instructions will be forthcoming.

For your convenience, the link and your personalized Access Key are available below. Please log in and complete the required tasks today and retain your login information for future access.

ICTD 2022 Presentation Notification

URL: https://www.conferenceharvester.com/harvester2/login.asp?EventKey=NFMDPAKR

Username: 219091761@stu.ukzn.ac.za

Password (Access Key): X U A E Y X G X

All presenters & attendees must agree to comply with all safety procedures established by ASCE as well as any other protocols put in place by the host sites, travel facilities, or any other applicable authorities. We look forward to welcoming you to ICTD 2022 in Seattle. In the meantime, should you have any questions or need assistance, please contact Leanne Shroeder ([redacted]).

Sincerely,

Leanne Shroeder, CMP
American Society of Civil Engineers
Amer, Muhammad [redacted]>

To:
Abayomi Modupe (219091761)
Tue 3/8/2022 3:42 AM
Dear Abayomi Modupe,

On behalf of the Steering Committee of ASCE International Conference on Transportation & Development (ICTD 2022), I am sending this email to notify you that the reviewers did not have any comments or suggested changes to your paper titled, "Influence of Bus Rapid Transit (BRT) on Anomalous Road Capacity Utilization" (ID 1926361). It looks good as submitted. You do not need to submit a revised final paper.

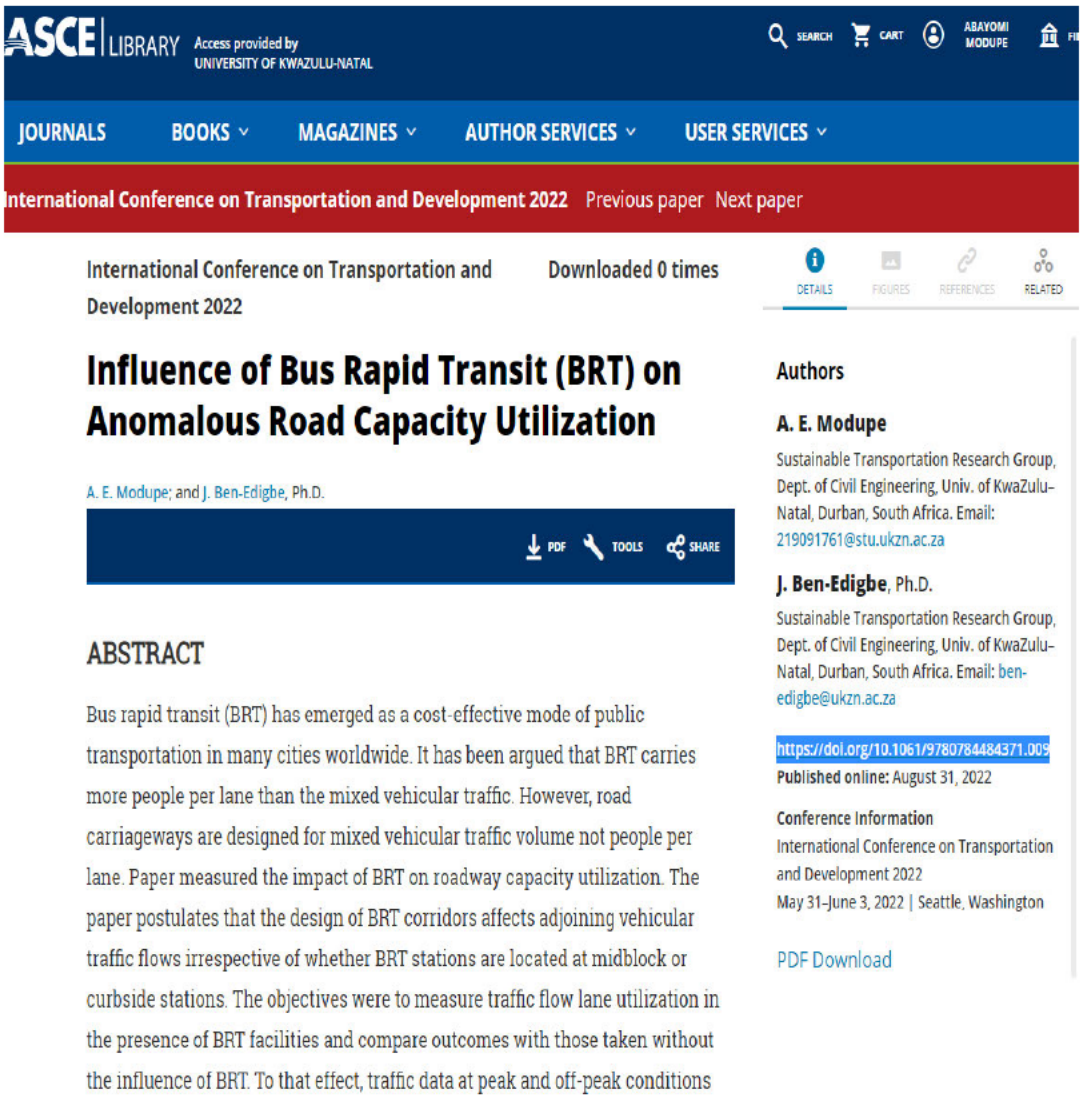

From: The Open Transportation Journal <admin@bentham.manuscriptpoint.com>
To: "[redacted]" <[redacted]>
Cc: [redacted]" <a[redacted]>
Sent: Friday, 9 June 2023 at 05:23:37 BST
Subject: Manuscript Provisional Acceptance letter | BMS-TOTJ-2023-4

Dear Dr. Johnnie Ben-Edigbe,

I am pleased to inform you that your article Reference No. BMS-TOTJ-2023-4, entitled **"Modelling Mixed Traffic Time Headway Distribution Induced by Bus Rapid Transit (BRT) in Cape Town, South Africa."** has been provisionally approved for publication in "**The Open Transportation Journal**" journal.

You will now need to pay the processing fee, either via the online payment link in the invoice sent to you or, via a bank transfer (evidence of which would need to be sent to us), before your article is published.

Please note that the final acceptance of your article is subject to a detailed scrutiny and approval of the following:

We wish to thank you for submission of the manuscript to "**The Open Transportation Journal**" and look forward to continued collaboration in the future.

With warm regards,

Ambreen Irshad

Senior Editor

Bentham Open

[redacted]

Note: For complaints contact: complaint@benthamopen.net

To unsubscribe from MPS and stop receiving emails further. **Please Click Here**

Powered by Bentham Manuscript Processing System

CSCE2023-General Conference <C[redacted]g>

- Abayomi Modupe (219091761)

Fri 4/14/2023 5:39 PM

Re: Paper 6523 - EXTENT OF BUS RAPID TRANSIT (BRT) TRAVEL TIME DIFFERENTIALS CAUSED BY MIXED TRAFFIC FLOW IN CAPE TOWN SOUTH AFRICA

Dear Abayomi Modupe,

On behalf of the Technical Committee for the Canadian Society for Civil Engineering (CSCE) 2023 Annual Conference, we are delighted to inform you that after a final review, the paper you submitted has been ACCEPTED for presentation at the conference and for publication in the proceedings.

Please note that at least one of the co-authors must be registered by April 26, 2023, for the paper to be considered for inclusion in the conference technical program and in the published proceedings. A registered delegate is limited to a maximum of two in-person paper presentations during the conference. Please follow this link to register for the conference: https://www.csce2023moncton.ca/registration.

Presenter information will be provided to registered delegates by the end of April.

Additional travel, accommodation, program and activities details can be found on the conference website : https://www.csce2023moncton.ca/

If you have any questions, you may contact the Technical Committee at [redacted]. Thank you for your interest in presenting at CSCE Moncton 2023. We look forward to seeing you in Moncton!

Serge Desjardins, Gérard J. Poitras, Catherine LeBlanc
CSCE2023-General Conference
Canadian Society for Civil Engineering 2023 Annual Conference - Moncton, NB

2023-General Conference [redacted]>

MODUPE ABAYOMI E.
SUSTAINABLE TRANSPORTATION RESEARCH GROUP
UNIVERSITY OF KWAZULU-NATAL,
DURBAN, SOUTH AFRICA
E: 219091761@STU.UKZN.AC.ZA ; [redacted]
T: [redacted]

Gothenburg, 2022-09-29

DECISION REGARDING THE APPLICATION FOR MOBILITY VISIT GRANT, MVG-2022-13

Dear Applicant,

On behalf of Henrik Nolmark, Director of the Volvo Research and Educational Foundations, we have the pleasure to inform you that the Mobility Visit Grant Application MVG-2022-13 was preliminarily approved with a grant of **30000 SEK.**

Please, find attached the requisition form for you to complete and sign. The amount will be transferred once all the criteria are fulfilled.

This visit is planned to take place as below:

Host for the visit:	Prof. Samuel ODEWUMI F5FX+P63, Lagos State University, Ojo 102101, Lagos, Nigeria E: [redacted]
Period planned for the visit:	221101-221130

The amount calculated according to the requested amount reported in your application, can be paid directly on a private account in order to avoid unnecessary overhead expenses.

Please, also specify which currency you wish to have the payment made in otherwise the grant will be paid in SEK.

Be so kind to return the form via e-mail to secretariat@vref.se for payment transfer.

Please, also find below the guidelines for post-visit reporting to be sent to us on word format (or pdf if preferred).

On 18 Nov 2022 05:08, CONFER CONFER <[redacted]> wrote:

Dear Abayomi,

Thank you for registering for the 32nd Annual International Course on Road Safety, Road Safety Audit, Vehicle Safety Technology, Pre-Hospital care and Trauma. The Course will be held at the Indian Institute of Technology, Delhi from 5th December to 19th December 2022.

As you have opted for the following module, you have been selected to participate in the course. The committee has agreed to waive off your registration fee and offer local hospitality.

Module 1A (without IRC Certificate)
International participants - US$ 750

Please confirm your participation ASAP, so that we can book your accommodation.

For updates on the course, please click on our website : Transportation Research and Injury Prevention Programme (ernet.in)

Looking forward to your participation in this Course.

Thanking you,
Kind regards
Diya Walia
TRIPP Course Secretariat

Diya Walia
D-1, Kalindi Colony
New Delhi - 110065
T: [redacted]

APPENDIX II
Statistical Tables and Charts

Table for Determining Sample Size from a Given Population

N	*S*	*N*	*S*	*N*	*S*
10	10	220	140	1200	291
15	14	230	144	1300	297
20	19	240	148	1400	302
25	24	250	152	1500	306
30	28	260	155	1600	310
35	32	270	159	1700	313
40	36	280	162	1800	317
45	40	290	165	1900	320
50	44	300	169	2000	322
55	48	320	175	2200	327
60	52	340	181	2400	331
65	56	360	186	2600	335
70	59	380	191	2800	338
75	63	400	196	3000	341
80	66	420	201	3500	346
85	70	440	ρ05	4000	351
90	73	460	210	4500	354
95	76	480	214	5000	357
100	80	500	217	6000	361
110	86	550	226	7000	364
120	92	600	234	8000	367
130	97	650	242	9000	368
140	103	700	248	10000	370
150	108	750	254	15000	375
160	113	800	260	20000	377
170	118	850	265	30000	379
180	123	900	269	40000	380
190	127	950	274	50000	381
200	132	1000	278	75000	382
210	136	1100	285	1000000	384

Note. - *N* is population size. *S* is sample size.

Source: Krejcie, R.V. and Morgan, D. W. (1970). Determining sample size for research activities, Educational and Psychological Measurement, 30, 607-610

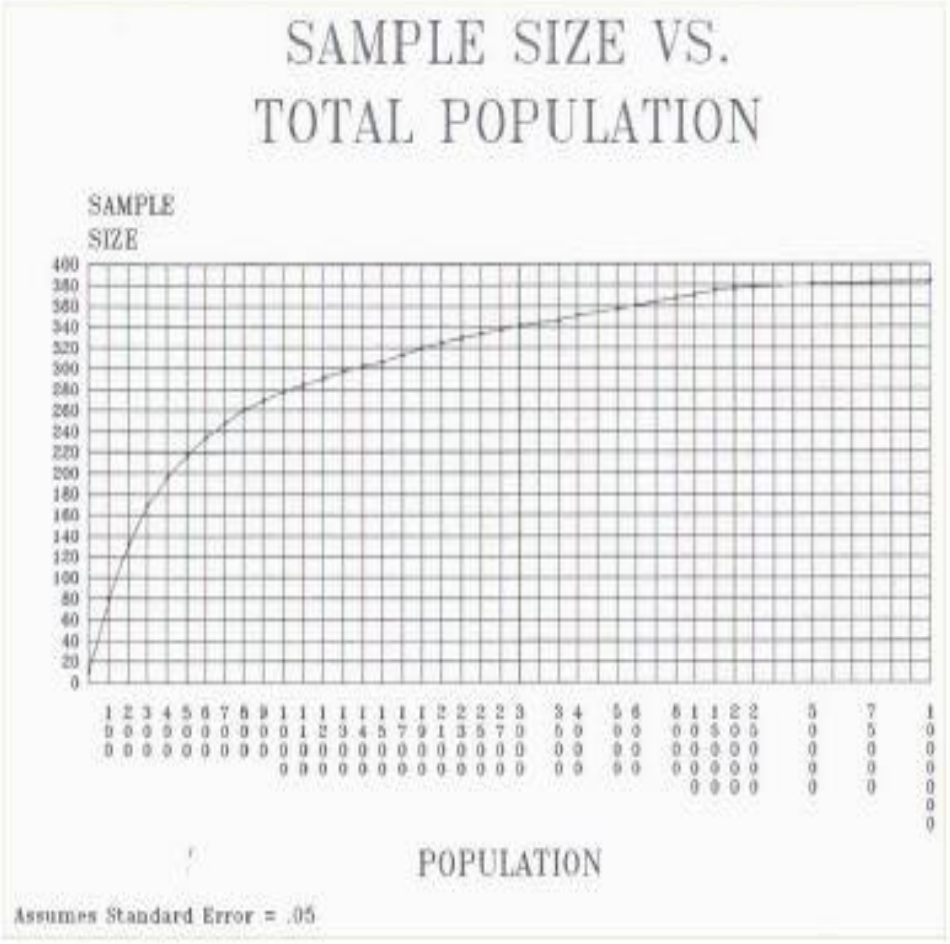

Source: Krejcie, R.V. and Morgan, D. W. (1970). Determining sample size for research activities, Educational and Psychological Measurement, 30, 607-610

Chi-square Distribution Table

d.f.	.995	.99	.975	.95	.9	.1	.05	.025	.01
1	0.00	0.00	0.00	0.00	0.02	2.71	3.84	5.02	6.63
2	0.01	0.02	0.05	0.10	0.21	4.61	5.99	7.38	9.21
3	0.07	0.11	0.22	0.35	0.58	6.25	7.81	9.35	11.34
4	0.21	0.30	0.48	0.71	1.06	7.78	9.49	11.14	13.28
5	0.41	0.55	0.83	1.15	1.61	9.24	11.07	12.83	15.09
6	0.68	0.87	1.24	1.64	2.20	10.64	12.59	14.45	16.81
7	0.99	1.24	1.69	2.17	2.83	12.02	14.07	16.01	18.48
8	1.34	1.65	2.18	2.73	3.49	13.36	15.51	17.53	20.09
9	1.73	2.09	2.70	3.33	4.17	14.68	16.92	19.02	21.67
10	2.16	2.56	3.25	3.94	4.87	15.99	18.31	20.48	23.21
11	2.60	3.05	3.82	4.57	5.58	17.28	19.68	21.92	24.72
12	3.07	3.57	4.40	5.23	6.30	18.55	21.03	23.34	26.22
13	3.57	4.11	5.01	5.89	7.04	19.81	22.36	24.74	27.69
14	4.07	4.66	5.63	6.57	7.79	21.06	23.68	26.12	29.14
15	4.60	5.23	6.26	7.26	8.55	22.31	25.00	27.49	30.58
16	5.14	5.81	6.91	7.96	9.31	23.54	26.30	28.85	32.00
17	5.70	6.41	7.56	8.67	10.09	24.77	27.59	30.19	33.41
18	6.26	7.01	8.23	9.39	10.86	25.99	28.87	31.53	34.81
19	6.84	7.63	8.91	10.12	11.65	27.20	30.14	32.85	36.19
20	7.43	8.26	9.59	10.85	12.44	28.41	31.41	34.17	37.57
22	8.64	9.54	10.98	12.34	14.04	30.81	33.92	36.78	40.29
24	9.89	10.86	12.40	13.85	15.66	33.20	36.42	39.36	42.98
26	11.16	12.20	13.84	15.38	17.29	35.56	38.89	41.92	45.64
28	12.46	13.56	15.31	16.93	18.94	37.92	41.34	44.46	48.28
30	13.79	14.95	16.79	18.49	20.60	40.26	43.77	46.98	50.89
32	15.13	16.36	18.29	20.07	22.27	42.58	46.19	49.48	53.49
34	16.50	17.79	19.81	21.66	23.95	44.90	48.60	51.97	56.06
38	19.29	20.69	22.88	24.88	27.34	49.51	53.38	56.90	61.16
42	22.14	23.65	26.00	28.14	30.77	54.09	58.12	61.78	66.21
46	25.04	26.66	29.16	31.44	34.22	58.64	62.83	66.62	71.20
50	27.99	29.71	32.36	34.76	37.69	63.17	67.50	71.42	76.15
55	31.73	33.57	36.40	38.96	42.06	68.80	73.31	77.38	82.29
60	35.53	37.48	40.48	43.19	46.46	74.40	79.08	83.30	88.38
65	39.38	41.44	44.60	47.45	50.88	79.97	84.82	89.18	94.42
70	43.28	45.44	48.76	51.74	55.33	85.53	90.53	95.02	100.43
75	47.21	49.48	52.94	56.05	59.79	91.06	96.22	100.84	106.39
80	51.17	53.54	57.15	60.39	64.28	96.58	101.88	106.63	112.33
85	55.17	57.63	61.39	64.75	68.78	102.08	107.52	112.39	118.24
90	59.20	61.75	65.65	69.13	73.29	107.57	113.15	118.14	124.12
95	63.25	65.90	69.92	73.52	77.82	113.04	118.75	123.86	129.97
100	67.33	70.06	74.22	77.93	82.36	118.50	124.34	129.56	135.81

APPENDIX III

Other Survey data and Charts from the ATC

SS001 – Sandown Station – Porterfield Station

Flow Clustered by Speed Bins

SpeedCluster-34 (Metric) Site: 00001 Lane 1.0.0N
Description: Portafield BRT Station - Sundown BRT Station
Filter time: 11:06 Saturday, November 6, 2021 => 11:22 Wednesday, November 10, 2021
Filter: Cls(1-12) Dir(NESW) Sp(10,160) Headway(>0) Span(0 - 100) Lane(0-16)
Scheme: Vehicle classification (ARX)

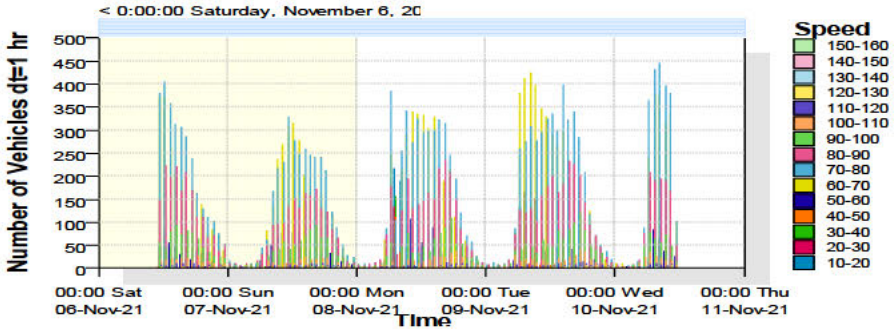

Flow Clustered by Class

ClassCluster-37 (Metric) Site: 00001 Lane 1.0.0N
Description: Portafield BRT Station - Sundown BRT Station
Filter time: 11:06 Saturday, November 6, 2021 => 11:22 Wednesday, November 10, 2021
Filter: Cls(1-12) Dir(NESW) Sp(10,160) Headway(>0) Span(0 - 100) Lane(0-16)
Scheme: Vehicle classification (ARX)

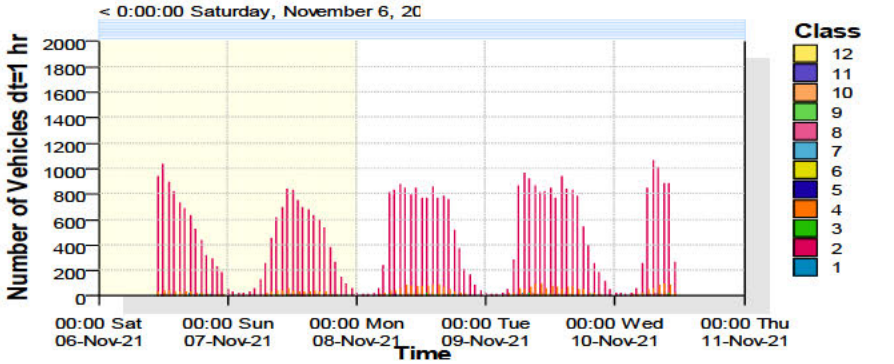

Speed Histogram

SpeedHist-38 (Metric) Site: 00001 Lane 1.0.0N
Description: Portafield BRT Station - Sundown BRT Station
Filter time: 11:06 Saturday, November 6, 2021 => 11:22 Wednesday, November 10, 2021
Filter: Cls(1-12) Dir(NESW) Sp(10,160) Headway(>0) Span(0 - 100) Lane(0-16)
Scheme: Vehicle classification (ARX)

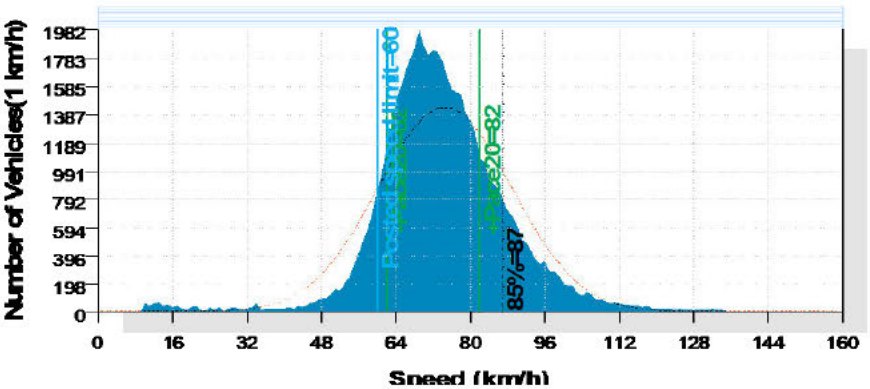

Speed Bin Chart

SpeedBin-39 (Metric) Site: 00001 Lane 1.0.0N
Description: Portafield BRT Station - Sundown BRT Station
Filter time: 11:06 Saturday, November 6, 2021 => 11:22 Wednesday, November 10, 2021
Filter: Cls(1-12) Dir(NESW) Sp(10,160) Headway(>0) Span(0 - 100) Lane(0-16)
Scheme: Vehicle classification (ARX)
Total=51727

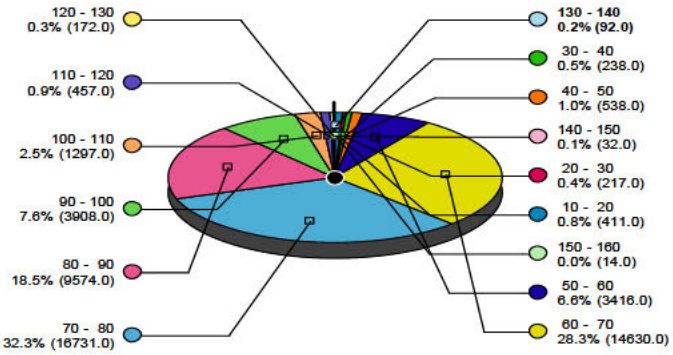

Separation Histogram

SepHist-40 (Metric) Site: 00001 Lane 1.0.0N
Description: Portafield BRT Station - Sundown BRT Station
Filter time: 11:06 Saturday, November 6, 2021 => 11:22 Wednesday, November 10, 2021
Filter: Cls(1-12) Dir(NESW) Sp(10,160) Headway(>0) Span(0 - 100) Lane(0-16)
Scheme: Vehicle classification (ARX)

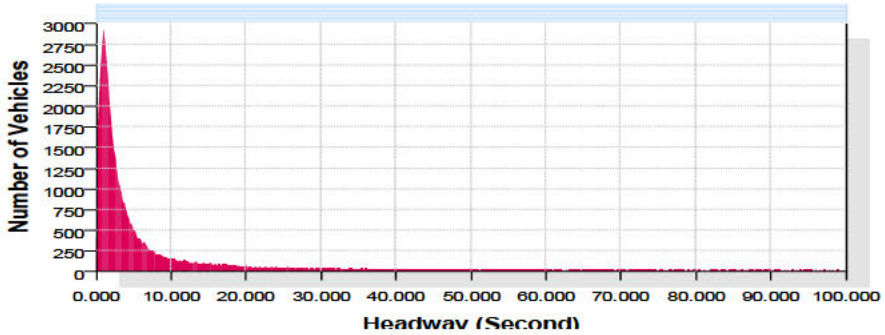

Velocity Dispersion

VelDisp-41 (Metric) Site: 00001 Lane 1.0.0N
Description: Portafield BRT Station - Sundown BRT Station
Filter time: 11:06 Saturday, November 6, 2021 => 11:22 Wednesday, November 10, 2021
Filter: Cls(1-12) Dir(NESW) Sp(10,160) Headway(>0) Span(0 - 100) Lane(0-16)
Scheme: Vehicle classification (ARX)

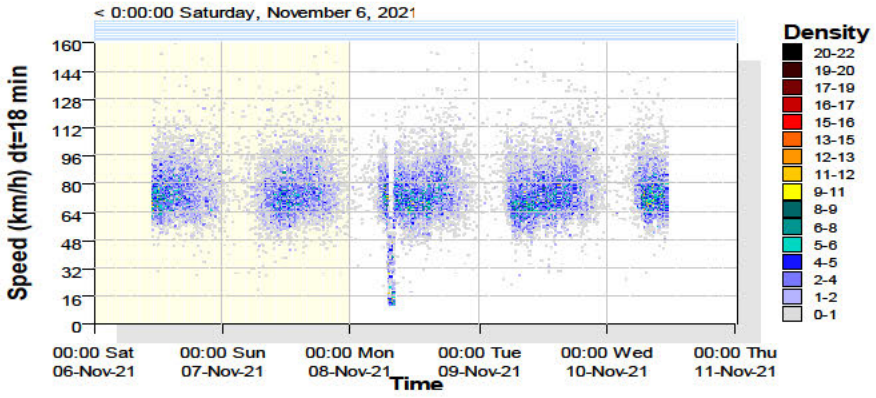

Volume vs Speed

VolSpeed-44 (Metric) **Site:** 00001 Lane 1.0.0N
Description: Portafield BRT Station - Sundown BRT Station
Filter time: 11:06 Saturday, November 6, 2021 => 11:22 Wednesday, November 10, 202
Filter: Cls(1-12) Dir(NESW) Sp(10,160) Headway(>0) Span(0 - 100) Lane(0-16)
Scheme: Vehicle classification (ARX)

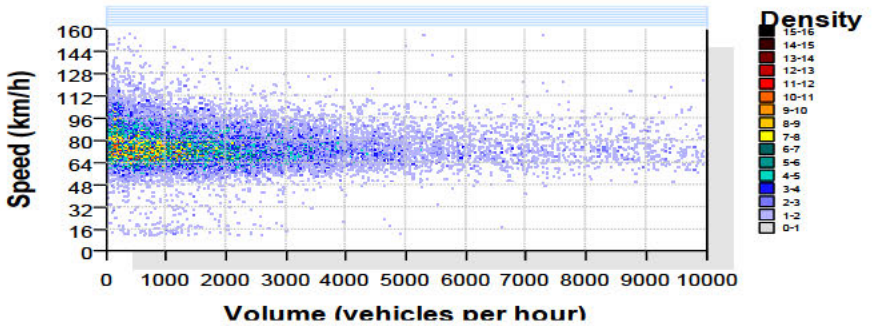

Speed vs Separation

SpeedSep-47 (Metric) **Site:** 00001 Lane 1.0.0N
Description: Portafield BRT Station - Sundown BRT Station
Filter time: 11:06 Saturday, November 6, 2021 => 11:22 Wednesday, November 10, 202
Filter: Cls(1-12) Dir(NESW) Sp(10,160) Headway(>0) Span(0 - 100) Lane(0-16)
Scheme: Vehicle classification (ARX)

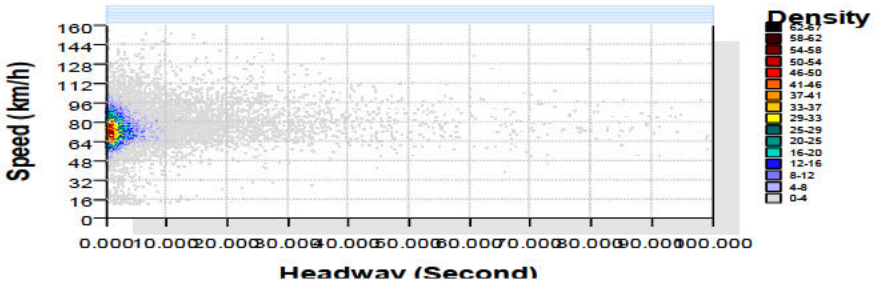

SS002 – Porterfield Station – Sandown Station

Flow Clustered by Speed Bins

SpeedCluster-18 (Metric) **Site:** 00002 Adjoining Lanes.0.0N
Description: Portafield BRT Station - Sundown BRT Station
Filter time: 12:47 Wednesday, 10 November 2021 => 09:37 Monday, 15 November 2021
Filter: Cls(1-12) Dir(NESW) Sp(10,160) Headway(>0) Span(0 - 100) Lane(0-16)
Scheme: Vehicle classification (ARX)

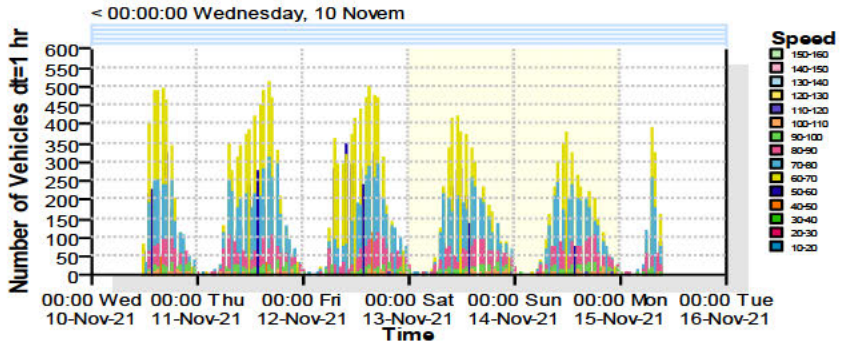

Flow Clustered by Class

ClassCluster-17 (Metric) Site: 00002 Adjoining Lanes.0.0N
Description: Portafield BRT Station - Sundown BRT Station
Filter time: 12:47 Wednesday, 10 November 2021 => 09:37 Monday, 15 November 2021
Filter: Cls(1-12) Dir(NESW) Sp(10,160) Headway(>0) Span(0 - 100) Lane(0-16)
Scheme: Vehicle classification (ARX)

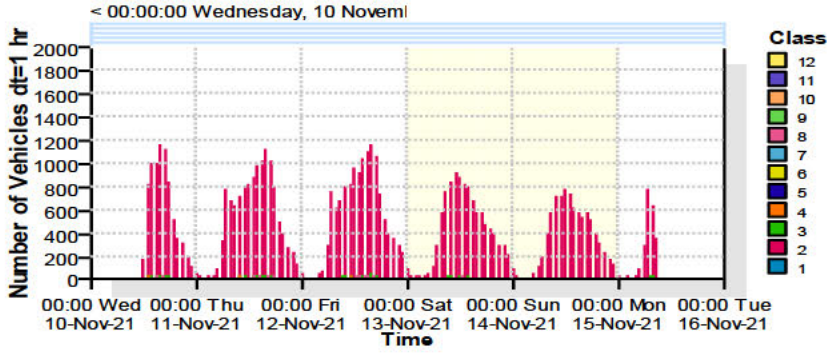

Speed Histogram

SpeedHist-23 (Metric) Site: 00002 Adjoining Lanes.0.0N
Description: Portafield BRT Station - Sundown BRT Station
Filter time: 12:47 Wednesday, 10 November 2021 => 09:37 Monday, 15 November 2021
Filter: Cls(1-12) Dir(NESW) Sp(10,160) Headway(>0) Span(0 - 100) Lane(0-16)
Scheme: Vehicle classification (ARX)

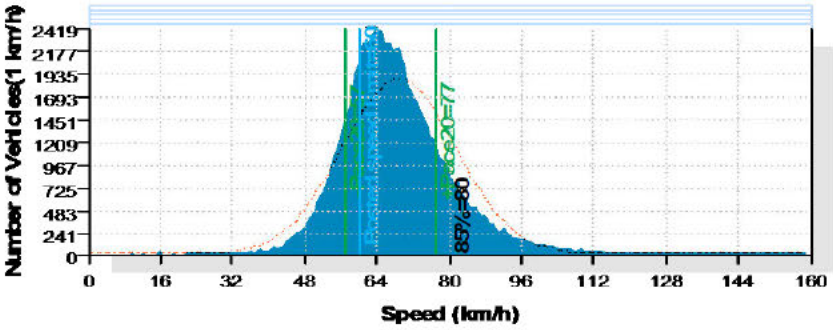

Speed Bin Chart

SpeedBin-25 (Metric) Site: 00002 Adjoining Lanes.0.0N
Description: Portafield BRT Station - Sundown BRT Station
Filter time: 12:47 Wednesday, 10 November 2021 => 09:37 Monday, 15 November 2021
Filter: Cls(1-12) Dir(NESW) Sp(10,160) Headway(>0) Span(0 - 100) Lane(0-16)
Scheme: Vehicle classification (ARX)

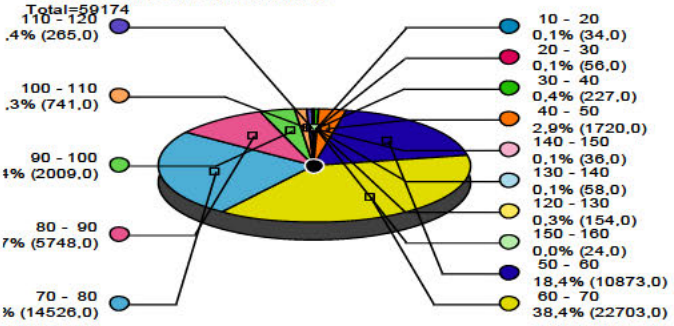

Separation Histogram

SepHist-24 (Metric) **Site:** 00002 Adjoining Lanes.0.0N
Description: Portafield BRT Station - Sundown BRT Station
Filter time: 12:47 Wednesday, 10 November 2021 => 09:37 Monday, 15 November 2021
Filter: Cls(1-12) Dir(NESW) Sp(10,160) Headway(>0) Span(0 - 100) Lane(0-16)
Scheme: Vehicle classification (ARX)

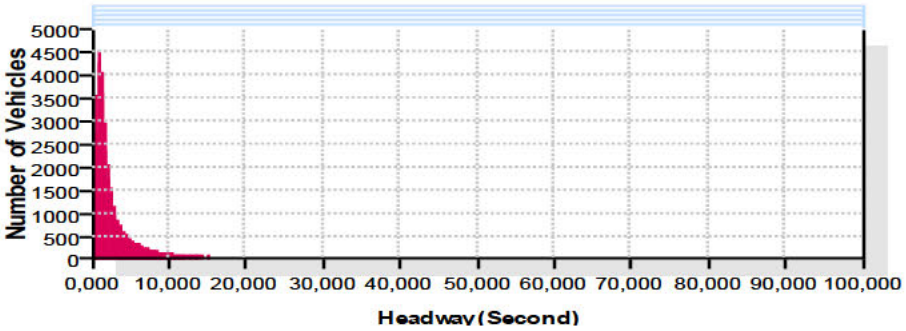

Velocity Dispersion

VelDisp-15 (Metric) **Site:** 00002 Adjoining Lanes.0.0N
Description: Portafield BRT Station - Sundown BRT Station
Filter time: 12:47 Wednesday, 10 November 2021 => 09:37 Monday, 15 November 2021
Filter: Cls(1-12) Dir(NESW) Sp(10,160) Headway(>0) Span(0 - 100) Lane(0-16)
Scheme: Vehicle classification (ARX)

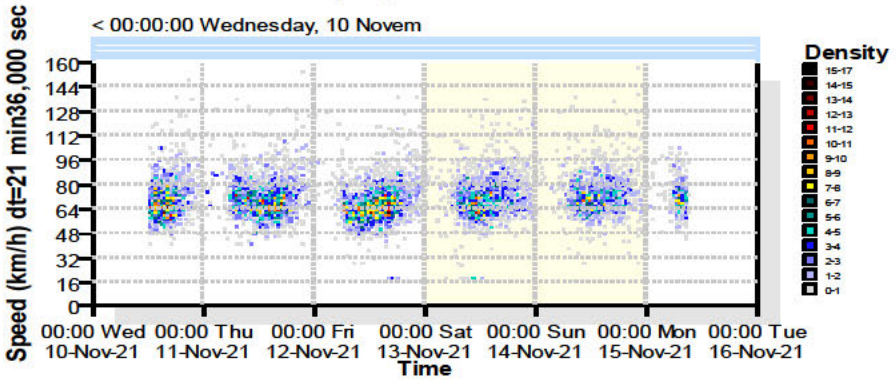

Volume vs Speed

VolSpeed-20 (Metric) **Site:** 00002 Adjoining Lanes.0.0N
Description: Portafield BRT Station - Sundown BRT Station
Filter time: 12:47 Wednesday, 10 November 2021 => 09:37 Monday, 15 November 2021
Filter: Cls(1-12) Dir(NESW) Sp(10,160) Headway(>0) Span(0 - 100) Lane(0-16)
Scheme: Vehicle classification (ARX)

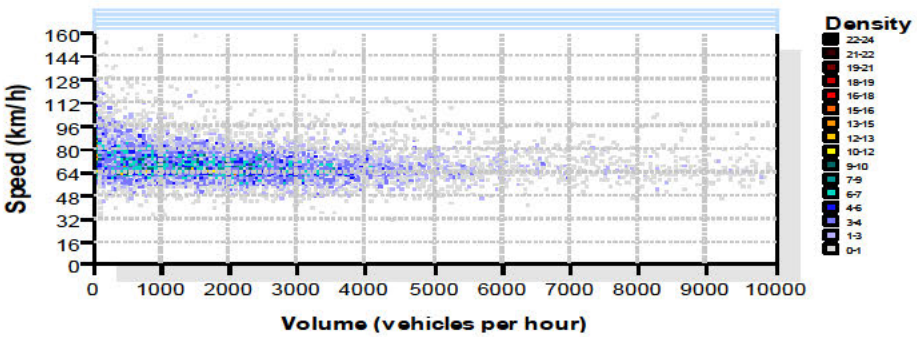

Speed vs Separation

SpeedSep-19 (Metric) Site: 00002 Adjoining Lanes.0.0N
Description: Portafield BRT Station - Sundown BRT Station
Filter time: 12:47 Wednesday, 10 November 2021 => 09:37 Monday, 15 November 2021
Filter: Cls(1-12) Dir(NESW) Sp(10,160) Headway(>0) Span(0 - 100) Lane(0-16)
Scheme: Vehicle classification (ARX)

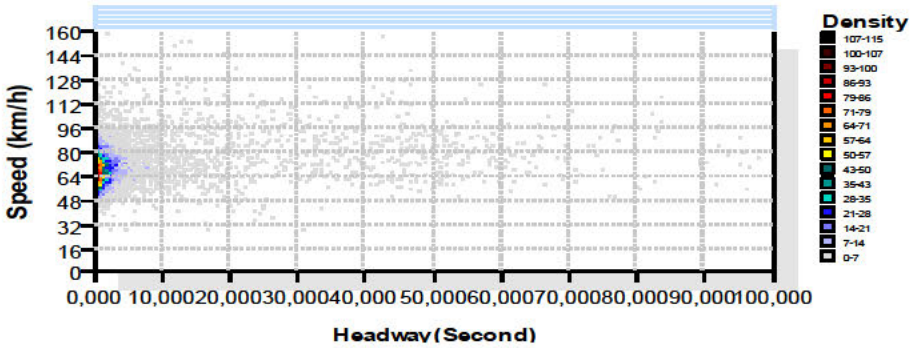

SS003 – Table View Station – Sunset City Junction

Flow Clustered by Speed Bins

SpeedCluster-88 (Metric) Site: 00003 Adjoining Lanes.0.0N
Description: Table View BRT Station - Sunset Beach
Filter time: 11:37 Friday, November 19, 2021 => 11:11 Wednesday, November 24, 2021
Filter: Cls(1-12) Dir(NESW) Sp(10,160) Headway(>0) Span(0 - 100) Lane(0-16)
Scheme: Vehicle classification (ARX)

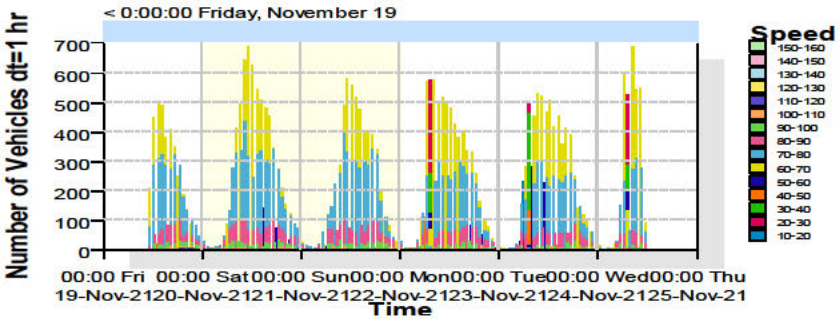

Flow Clustered by Class

ClassCluster-89 (Metric) Site: 00003 Adjoining Lanes.0.0N
Description: Table View BRT Station - Sunset Beach
Filter time: 11:37 Friday, November 19, 2021 => 11:11 Wednesday, November 24, 2021
Filter: Cls(1-12) Dir(NESW) Sp(10,160) Headway(>0) Span(0 - 100) Lane(0-16)
Scheme: Vehicle classification (ARX)

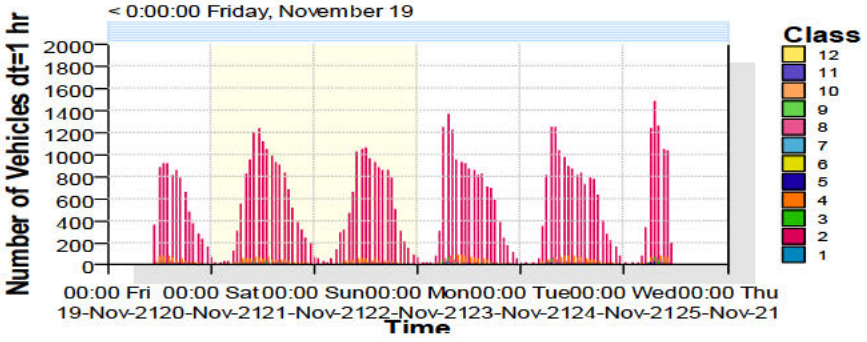

Speed Histogram

SpeedHist-93 (Metric) Site: 00003 Adjoining Lanes.0.0N
Description: Table View BRT Station - Sunset Beach
Filter time: 11:37 Friday, November 19, 2021 => 11:11 Wednesday, November 24, 2021
Filter: Cls(1-12) Dir(NESW) Sp(10,160) Headway(>0) Span(0 - 100) Lane(0-16)
Scheme: Vehicle classification (ARX)

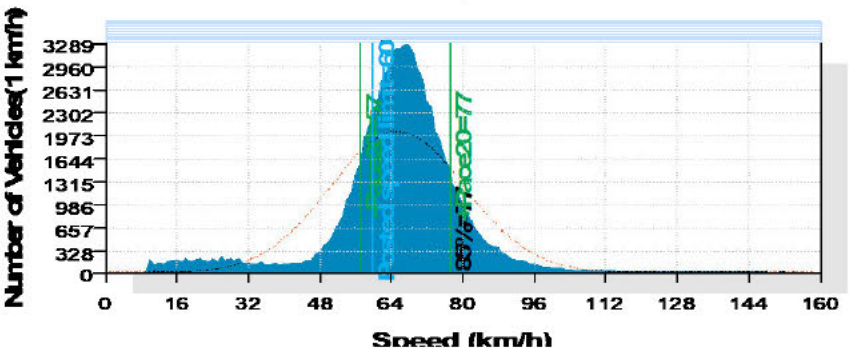

Speed Bin Chart

SpeedBin-92 (Metric) Site: 00003 Adjoining Lanes.0.0N
Description: Table View BRT Station - Sunset Beach
Filter time: 11:37 Friday, November 19, 2021 => 11:11 Wednesday, November 24, 2021
Filter: Cls(1-12) Dir(NESW) Sp(10,160) Headway(>0) Span(0 - 100) Lane(0-16)
Scheme: Vehicle classification (ARX)
Total=76372

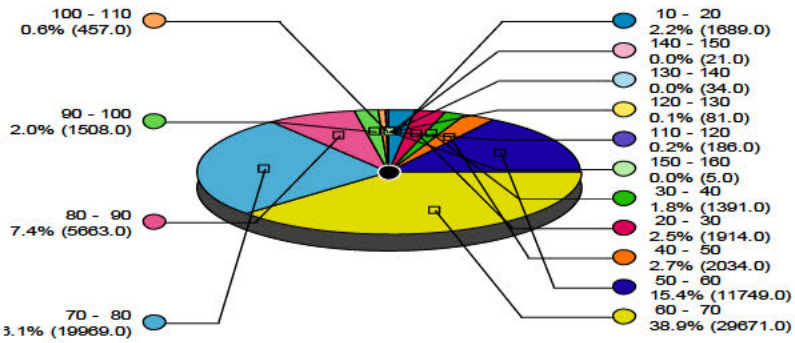

Separation Histogram

SepHist-94 (Metric) **Site:** 00003 Adjoining Lanes.0.0N
Description: Table View BRT Station - Sunset Beach
Filter time: 11:37 Friday, November 19, 2021 => 11:11 Wednesday, November 24, 2021
Filter: Cls(1-12) Dir(NESW) Sp(10,160) Headway(>0) Span(0 - 100) Lane(0-16)
Scheme: Vehicle classification (ARX)

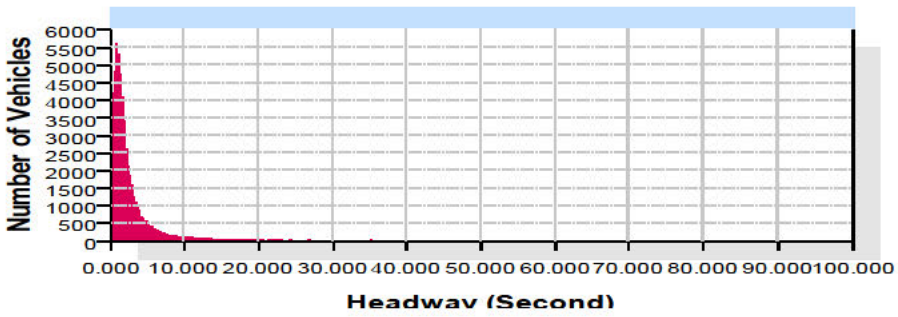

Velocity Dispersion

VelDisp-87 (Metric) **Site:** 00003 Adjoining Lanes.0.0N
Description: Table View BRT Station - Sunset Beach
Filter time: 11:37 Friday, November 19, 2021 => 11:11 Wednesday, November 24, 2021
Filter: Cls(1-12) Dir(NESW) Sp(10,160) Headway(>0) Span(0 - 100) Lane(0-16)
Scheme: Vehicle classification (ARX)

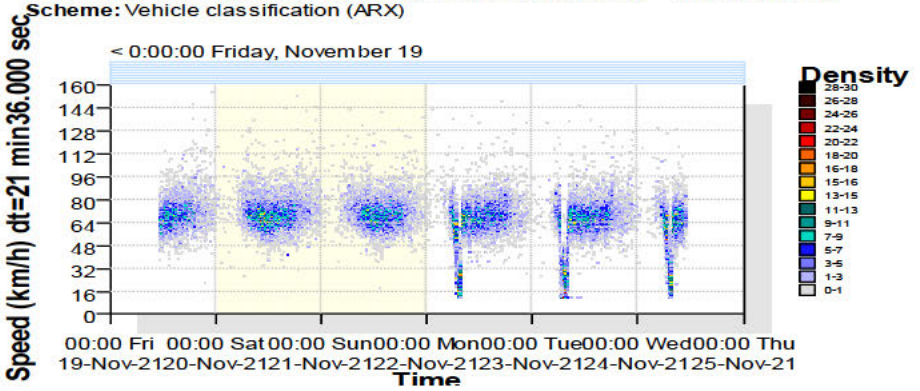

Volume vs Speed

VolSpeed-96 (Metric) **Site:** 00003 Adjoining Lanes.0.0N
Description: Table View BRT Station - Sunset Beach
Filter time: 11:37 Friday, November 19, 2021 => 11:11 Wednesday, November 24, 2021
Filter: Cls(1-12) Dir(NESW) Sp(10,160) Headway(>0) Span(0 - 100) Lane(0-16)
Scheme: Vehicle classification (ARX)

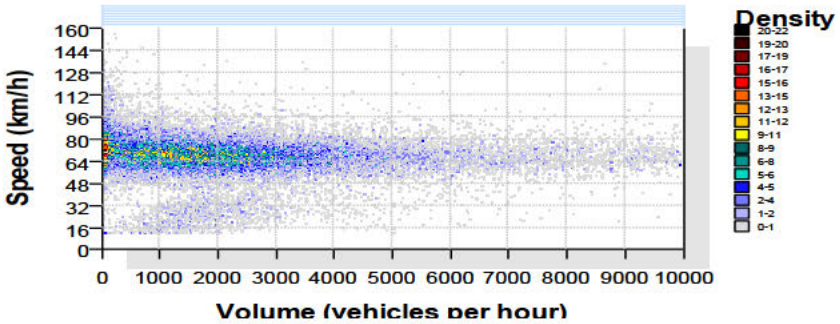

Speed vs Separation

SpeedSep-95 (Metric) **Site:** 00003 Adjoining Lanes.0.0N
Description: Table View BRT Station - Sunset Beach
Filter time: 11:37 Friday, November 19, 2021 => 11:11 Wednesday, November 24, 2021
Filter: Cls(1-12) Dir(NESW) Sp(10,160) Headway(>0) Span(0 - 100) Lane(0-16)
Scheme: Vehicle classification (ARX)

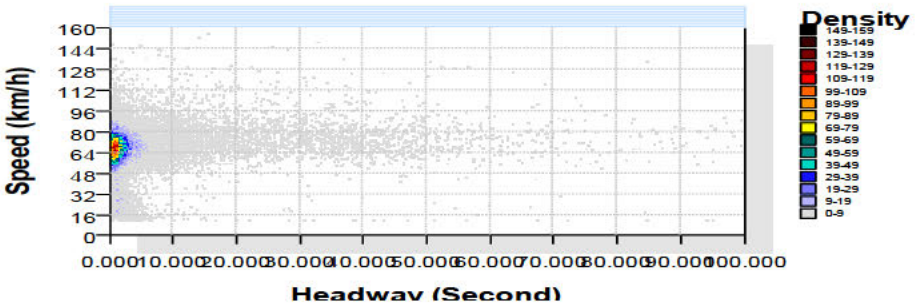

SS004 – Sunset City Junction – Table View Station

Flow Clustered by Speed Bins

SpeedCluster-130 (Metric) **Site:** 00004 Adjoining Lanes.0.0N
Description: Sunset Beach - Table View BRT Station
Filter time: 14:14 Wednesday, November 24, 2021 => 16:23 Tuesday, November 30, 202
Filter: Cls(1-12) Dir(NESW) Sp(10,160) Headway(>0) Span(0 - 100) Lane(0-16)
Scheme: Vehicle classification (ARX)

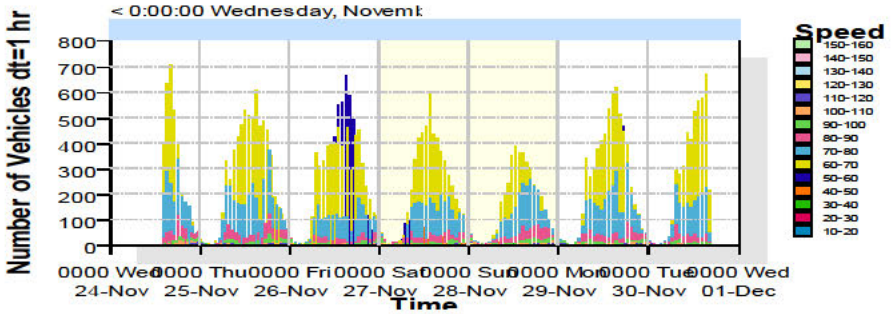

Flow Clustered by Class

ClassCluster-131 (Metric) **Site:** 00004 Adjoining Lanes.0.0N
Description: Sunset Beach - Table View BRT Station
Filter time: 14:14 Wednesday, November 24, 2021 => 16:23 Tuesday, November 30, 202
Filter: Cls(1-12) Dir(NESW) Sp(10,160) Headway(>0) Span(0 - 100) Lane(0-16)
Scheme: Vehicle classification (ARX)

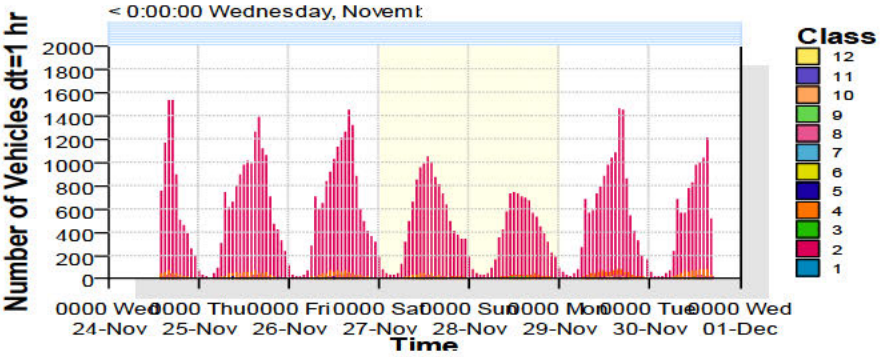

Speed Histogram

SpeedHist-138 (Metric) **Site:** 00004 Adjoining Lanes.0.0N
Description: Sunset Beach - Table View BRT Station
Filter time: 14:14 Wednesday, November 24, 2021 => 16:23 Tuesday, November 30, 2021
Filter: Cls(1-12) Dir(NESW) Sp(10,160) Headway(>0) Span(0 - 100) Lane(0-16)
Scheme: Vehicle classification (ARX)

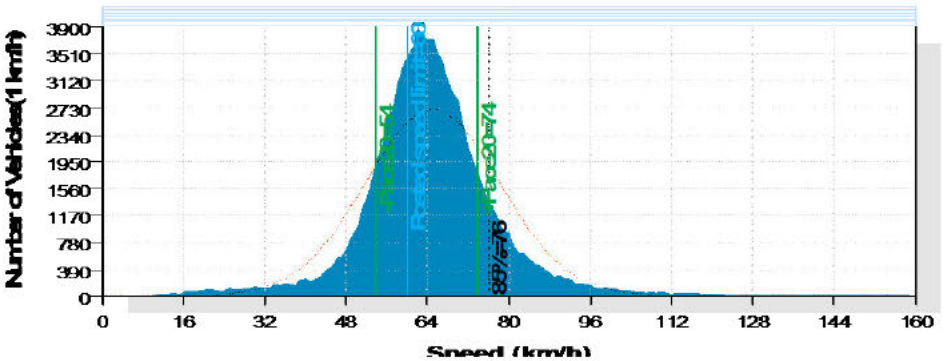

Speed Bin Chart

SpeedBin-137 (Metric) Site: 00004 Adjoining Lanes.0.0N
Description: Sunset Beach - Table View BRT Station
Filter time: 14:14 Wednesday, November 24, 2021 => 16:23 Tuesday, November 30, 2021
Filter: Cls(1-12) Dir(NESW) Sp(10,160) Headway(>0) Span(0 - 100) Lane(0-16)
Scheme: Vehicle classification (ARX)
Total=89289

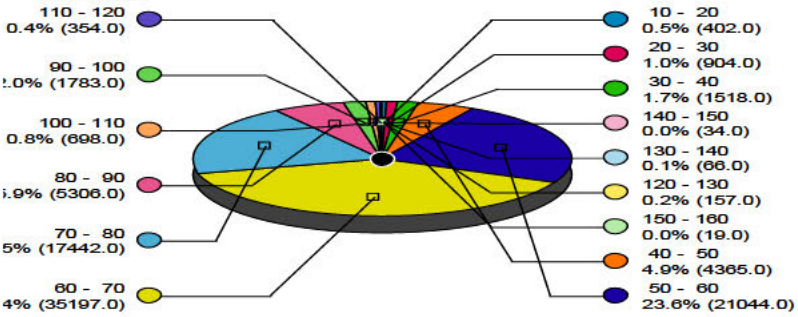

Separation Histogram

SepHist-139 (Metric) Site: 00004 Adjoining Lanes.0.0N
Description: Sunset Beach - Table View BRT Station
Filter time: 14:14 Wednesday, November 24, 2021 => 16:23 Tuesday, November 30, 2021
Filter: Cls(1-12) Dir(NESW) Sp(10,160) Headway(>0) Span(0 - 100) Lane(0-16)
Scheme: Vehicle classification (ARX)

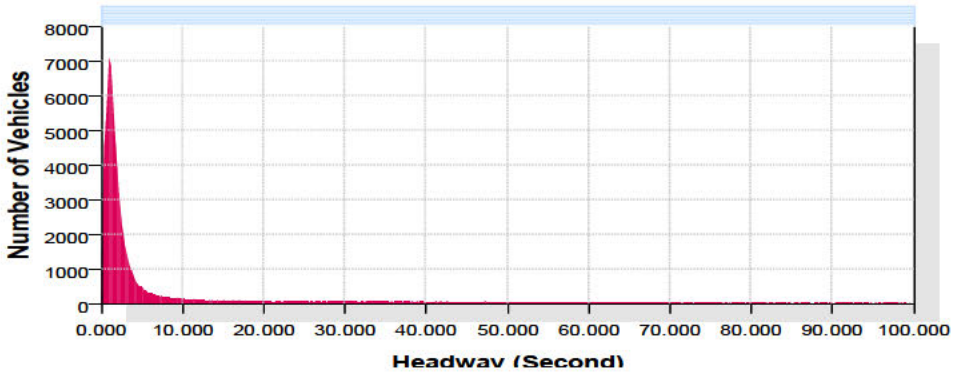

Velocity Dispersion

VelDisp-128 (Metric) Site: 00004 Adjoining Lanes.0.0N
Description: Sunset Beach - Table View BRT Station
Filter time: 14:14 Wednesday, November 24, 2021 => 16:23 Tuesday, November 30, 202
Filter: Cls(1-12) Dir(NESW) Sp(10,160) Headway(>0) Span(0 - 100) Lane(0-16)
Scheme: Vehicle classification (ARX)

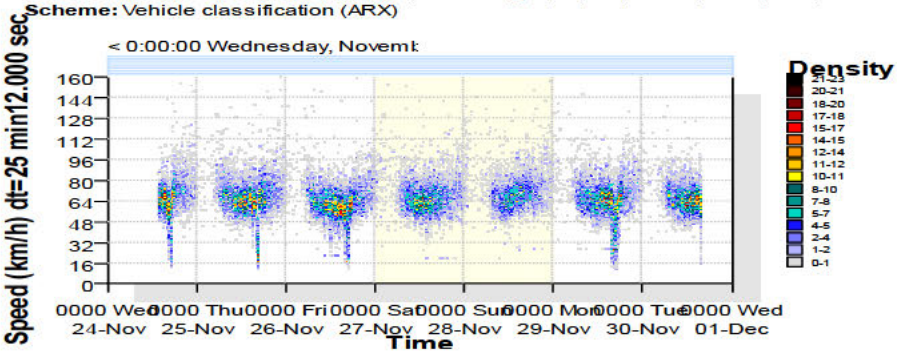

Volume vs Speed

VolSpeed-133 (Metric) **Site:** 00004 Adjoining Lanes.0.0N
Description: Sunset Beach - Table View BRT Station
Filter time: 14:14 Wednesday, November 24, 2021 => 16:23 Tuesday, November 30, 202
Filter: Cls(1-12) Dir(NESW) Sp(10,160) Headway(>0) Span(0 - 100) Lane(0-16)
Scheme: Vehicle classification (ARX)

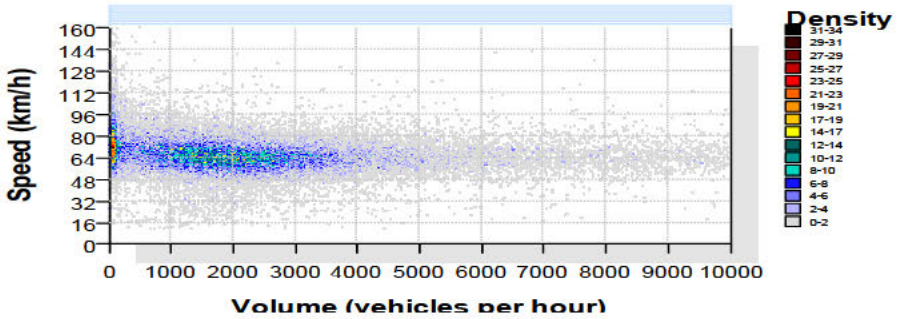

Speed vs Separation

SpeedSep-132 (Metric) **Site:** 00004 Adjoining Lanes.0.0N
Description: Sunset Beach - Table View BRT Station
Filter time: 14:14 Wednesday, November 24, 2021 => 16:23 Tuesday, November 30, 202
Filter: Cls(1-12) Dir(NESW) Sp(10,160) Headway(>0) Span(0 - 100) Lane(0-16)
Scheme: Vehicle classification (ARX)

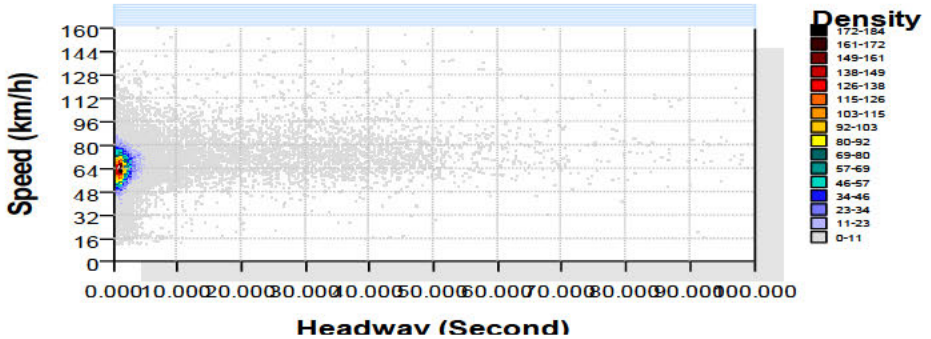

APPENDIX IV
Other Site Photos

PILOT STUDY

Researcher taking Speed and Volume Samples During Pilot Study

Researcher Observing the Geometric Features of the Roadway

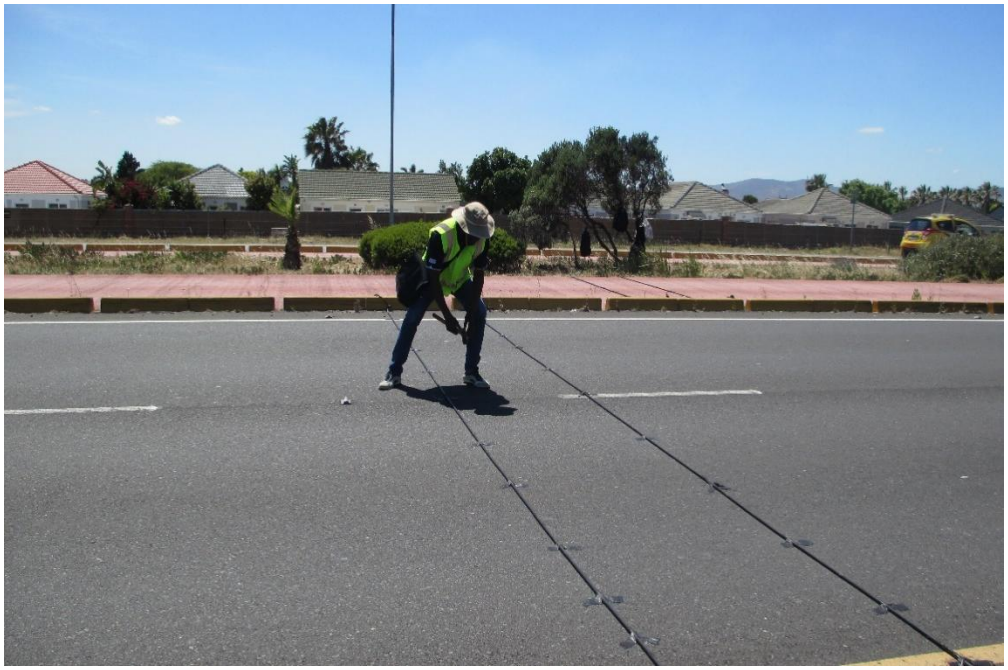

Member of the Research Team

Pilot Site

Regional Road Classification (R27) Signpost

R27 Posted Speed Limit

Researcher Measuring Roadway Segment Length

MAIN STUDY – SS001

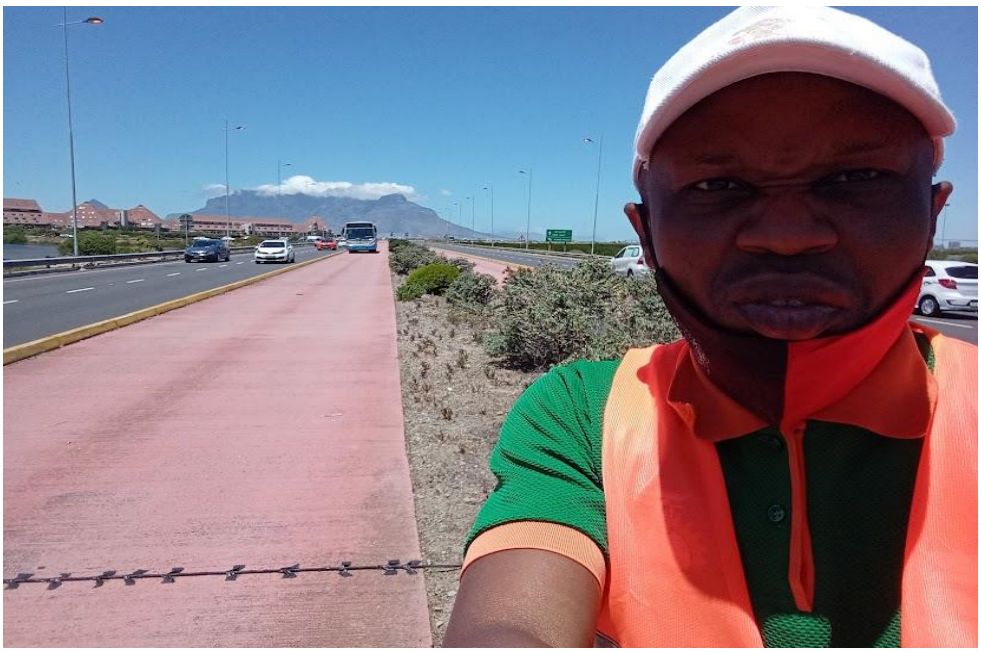

Researcher Observing Data Logging by ATC

Installation of ATCs and Pneumatic Tubes at SS001

On-Going Traffic Flow and Data Logging at SS001

MAIN STUDY – SS002

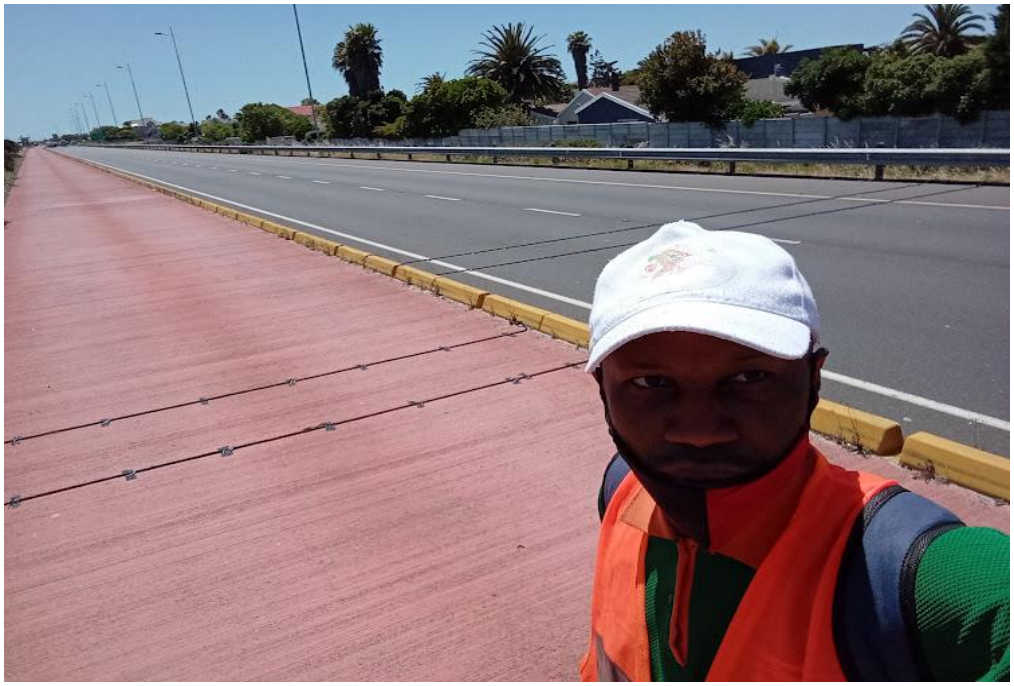

Installed Pneumatic Tubes and ATCs at SS002

Researcher Setting Up the ATCs Prior to Data Logging at SS002

Researcher Unloading Data from ATCs at SS002

Researcher Setting up ATCs at SS002

MAIN STUDY – SS003

Researcher Setting Up the ATCs Prior to Data Logging at SS003

Installed Pneumatic Tubes and ATCs at SS003

SS003

SS003

MAIN STUDY – SS004

Installation of ATCs and Pneumatic Tubes at SS004